ISSN 1007-9327 (print)
ISSN 2219-2840 (online)

World Journal of *Gastroenterology*

World J Gastroenterol 2021 April 21; 27(15): 1524-1663

Published by Baishideng Publishing Group Inc

World Journal of Gastroenterology

Contents

Weekly Volume 27 Number 15 April 21, 2021

EDITORIAL

REVIEW

MINIREVIEWS

ORIGINAL ARTICLE

Basic Study

Retrospective Cohort Study

World Journal of Gastroenterology

Weekly Volume 27 Number 15 April 21, 2021

Contents

ABOUT COVER

Editorial Board Member of *World Journal of Gastroenterology*, Halina Cichoż-Lach, MD, PhD, Professor, Department of Gastroenterology with Endoscopic Unit, Medical University of Lublin, Jaczewskiego 8, Lublin 20814, Poland. halina.lach@umlub.pl

AIMS AND SCOPE

The primary aim of *World Journal of Gastroenterology* (*WJG*, *World J Gastroenterol*) is to provide scholars and readers from various fields of gastroenterology and hepatology with a platform to publish high-quality basic and clinical research articles and communicate their research findings online. *WJG* mainly publishes articles reporting research results and findings obtained in the field of gastroenterology and hepatology and covering a wide range of topics including gastroenterology, hepatology, gastrointestinal endoscopy, gastrointestinal surgery, gastrointestinal oncology, and pediatric gastroenterology.

INDEXING/ABSTRACTING

The *WJG* is now indexed in Current Contents®/Clinical Medicine, Science Citation Index Expanded (also known as SciSearch®), Journal Citation Reports®, Index Medicus, MEDLINE, PubMed, PubMed Central, and Scopus. The 2020 edition of Journal Citation Report® cites the 2019 impact factor (IF) for *WJG* as 3.665; IF without journal self cites: 3.534; 5-year IF: 4.048; Ranking: 35 among 88 journals in gastroenterology and hepatology; and Quartile category: Q2. The *WJG*'s CiteScore for 2019 is 7.1 and Scopus CiteScore rank 2019: Gastroenterology is 17/137.

RESPONSIBLE EDITORS FOR THIS ISSUE

Production Editor: *Yu-Jie Ma*; **Production Department Director:** *Xiang Li*; **Editorial Office Director:** *Ze-Mao Gong*.

NAME OF JOURNAL
World Journal of Gastroenterology

ISSN
ISSN 1007-9327 (print) ISSN 2219-2840 (online)

LAUNCH DATE
October 1, 1995

FREQUENCY
Weekly

EDITORS-IN-CHIEF
Andrzej S Tarnawski, Subrata Ghosh

EDITORIAL BOARD MEMBERS
http://www.wjgnet.com/1007-9327/editorialboard.htm

PUBLICATION DATE
April 21, 2021

INSTRUCTIONS TO AUTHORS
https://www.wjgnet.com/bpg/gerinfo/204

GUIDELINES FOR ETHICS DOCUMENTS
https://www.wjgnet.com/bpg/GerInfo/287

GUIDELINES FOR NON-NATIVE SPEAKERS OF ENGLISH
https://www.wjgnet.com/bpg/gerinfo/240

PUBLICATION ETHICS
https://www.wjgnet.com/bpg/GerInfo/288

PUBLICATION MISCONDUCT
https://www.wjgnet.com/bpg/gerinfo/208

ARTICLE PROCESSING CHARGE
https://www.wjgnet.com/bpg/gerinfo/242

STEPS FOR SUBMITTING MANUSCRIPTS
https://www.wjgnet.com/bpg/GerInfo/239

ONLINE SUBMISSION
https://www.f6publishing.com

World Journal of Gastroenterology

Submit a Manuscript: https://www.f6publishing.com

World J Gastroenterol 2021 April 21; 27(15): 1524-1530

DOI: 10.3748/wjg.v27.i15.1524

ISSN 1007-9327 (print) ISSN 2219-2840 (online)

EDITORIAL

Textbook outcomes in hepatobiliary and pancreatic surgery

Diamantis I Tsilimigras, Timothy Michael Pawlik, Dimitrios Moris

ORCID number: Diamantis I Tsilimigras 0000-0002-3676-9263; Timothy Michael Pawlik 0000-0002-4828-8096; Dimitrios Moris 0000-0002-5276-0699.

Author contributions: Tsilimigras DI and Moris D designed the work; Tsilimigras DI conducted analysis and interpretation of working data; Pawlik TM and Moris D drafted the work, and strictly revised the important knowledge content; all authors made the final approval of this version.

Conflict-of-interest statement: There has nothing to disclose.

Manuscript source: Invited manuscript

Specialty type: Gastroenterology and hepatology

Diamantis I Tsilimigras, Timothy Michael Pawlik, Department of Surgery, Ohio State University, Columbus, OH 43210, United States

Dimitrios Moris, Department of Surgery, Duke University Medical Center, Duke University, Durham, NC 27710, United States

Corresponding author: Dimitrios Moris, MD, MSc, PhD, Surgeon, Department of Surgery, Duke University Medical Center, Duke University, 2310 Erwin Road, Durham, NC 27710, United States. dimmoris@yahoo.com

Abstract

The concept of textbook outcome (TO) has recently gained popularity in surgical research and has been used to evaluate the quality or success of different surgical procedures, including hepatopancreatobiliary (HPB) operations. TO consists of individual outcome parameters that each reflect different domains of care including structure, process, and individual outcomes; in turn, the composite TO metric represents the optimal course after a surgical episode. TO can be used to assess patient-level outcomes, hospital performance, center designation and quality metrics. In addition to being an outcome measurement, TO may also be linked to healthcare costs. Future efforts should be directed towards establishing a universal definition of TO in HPB surgery so that surgeons and hospitals can assess and compare outcomes, identify shortcomings and improve real world patient outcomes.

Key Words: Textbook; Outcome; Hepatopancreatobiliary; Surgery

Core Tip: The concept of textbook outcome (TO) has recently gained popularity in surgical research and has been used to evaluate the quality or success of different surgical procedures, including hepatopancreatobiliary (HPB) operations. TO can be used to assess patient-level outcomes, hospital performance, center designation and quality metrics. Future efforts should be directed towards establishing a universal definition of TO in HPB surgery so that surgeons and hospitals can assess and compare outcomes, identify shortcomings and improve real world patient outcomes.

Citation: Tsilimigras DI, Pawlik TM, Moris D. Textbook outcomes in hepatobiliary and

Country/Territory of origin: United States

Peer-review report's scientific quality classification
Grade A (Excellent): A
Grade B (Very good): 0
Grade C (Good): 0
Grade D (Fair): 0
Grade E (Poor): 0

Received: January 19, 2021
Peer-review started: January 19, 2021
First decision: February 10, 2021
Revised: February 12, 2021
Accepted: March 29, 2021
Article in press: March 29, 2021
Published online: April 21, 2021

P-Reviewer: Piardi T
S-Editor: Fan JR
L-Editor: A
P-Editor: Ma YJ

pancreatic surgery. *World J Gastroenterol* 2021; 27(15): 1524-1530
URL: https://www.wjgnet.com/1007-9327/full/v27/i15/1524.htm
DOI: https://dx.doi.org/10.3748/wjg.v27.i15.1524

INTRODUCTION

Traditionally, quality assessment of complex surgery has focused on analyzing and evaluating individual outcome parameters, mainly complications, length of stay (LOS), in-hospital mortality, as well as 30-, 90-d mortality and readmission[1]. More recently, there has been a shift in quality assessment from individual outcome parameters to composite outcomes, which have been considered superior to assess patient outcomes and hospital performance[2-5]. A recently introduced concept, "textbook outcome" (TO) represents the optimal course following surgery that is better aligned with patient expectations around "optimal" care[2-5]. TO uses an "all-or-none" approach in which the optimal or "textbook" outcome is not achieved unless patients achieve all of the individual parameters comprising a TO[2-5].

The concept of TO has gained popularity in surgical clinical research and has been advocated as a measure to assess quality or success of complex surgical procedures, including abdominal aortic aneurysm repair, as well as hepatopancreatic, esophageal, gastric, sarcoma, colon cancer resection and transplantation[2-10]. Specifically, TO is a composite measure that aggregates various clinically important perioperative outcomes included in the definition of an "optimal" surgical episode. Such a composite measure encompasses determinants of quality of care from different domains including structure, process, and individual outcomes[2]. Indeed, each individual outcome may capture different domains of quality (*e.g.*, perioperative mortality might be related to operative volume, failure-to-rescue may be related to structure or processes of perioperative care, while LOS or readmissions may be related to discharge planning processes in place for each institution)[5]. In turn, TO is particularly relevant in the care of complex cancers, including hepatopancreatobiliary (HPB) malignancies, which require coordination across a number of specialties and through various phases of multidisciplinary treatment to achieve the best possible outcome[3,5,11]. In addition, TO can be used as a "benchmark" to track the quality of care delivered to patients and compare hospital performance across different institutions or health systems[12-14]. In this article, we highlight the existing and emerging literature on TOs in HPB surgery.

ASSESSING PATIENT-LEVEL OUTCOMES USING TO

Although the concept of TO was initially described in 2013 by a group of colorectal surgeons in Netherlands[2], it was used for the first time to assess outcomes of patients undergoing hepatopancreatic surgery in 2018[4]. Merath *et al*[4] first assessed TO rates after hepatopancreatic surgery among Medicare beneficiaries from 2013 to 2015[4]. TO was defined no postoperative complications, no prolonged LOS (*i.e.*, ≤ 75th percentile), no 90-d readmission and no 90-d postoperative mortality[4]. The study analyzed patients with all surgical indications (*i.e.*, both benign and malignant diseases) and demonstrated that TO was achieved in 44% of individuals undergoing hepatopancreatic surgery[4]. Of note, among patients who underwent pancreatic resection, TO was achieved in 47.8% following minor pancreatic resection (*i.e.*, distal pancreatectomy or other partial pancreatectomy) and 24.7% following major pancreatic resection (*i.e.*, proximal pancreatectomy, pancrea-ticoduodenectomy, total pancreatectomy)[4]. Similarly, while TO was achieved in 46.8% of patients undergoing minor hepatectomy, the incidence of TO decreased to 33.3% among patients who had undergone a major liver resection[4]. These data highlighted the fact that less than one-half of patients overall experienced an optimal or "textbook" outcome after hepatopancreatic surgery; in particular, achievement of TO was markedly lower among patients undergoing major pancreatic or liver resections.

Due to the inherent limitations of administrative billing databases, several important perioperative outcomes were not captured and assessed in the initial study by Merath *et al*[4]. Rather, the use single- or multi-center institutional databases that contain more granular data to provide more clinically important information and allow for a more thorough assessment of postoperative outcomes was needed. To this

end, Merath *et al*[3] published a subsequent study that assessed the incidence of TO following resection of intrahepatic cholangiocarcinoma (ICC) using a multi-institutional database that incorporated data from 15 major HPB centers[3]. In this study, the authors defined TO as R0 resection, no perioperative transfusion, no postoperative complications, no prolonged LOS, no 30-d readmission and no 30-d mortality[3]. Among 687 patients analyzed, TO was achieved only in 25.5% of patients undergoing curative-intent resection for ICC. Younger patient age (age < 60 years), absence of preoperative jaundice, earlier T-category disease (*i.e.*, T1a, T1b), node-negative disease, and no bile duct resection were independent predictors of TO[3]. Although 30-d mortality was less than 5%, a TO was achieved in only one-fourth of patients largely due to high rates of complications and LOS, highlighting the need for further improvements in managing patients undergoing complex HPB procedures[3].

Another study examined TO after curative-intent resection of hepatocellular carcinoma (HCC)[5]. TO was defined as R0 resection, no reoperation, no severe postoperative complications (Clavien-Dindo ≥ III), no prolonged LOS, no 90-d readmission and no 90-d mortality[5]. In analyzing 605 patients, the incidence of TO was 62.3% after curative-intent resection of HCC[5]. Patients with BCLC-0 HCC and albumin-bilirubin grade grade 1 (*i.e.*, good liver function) had higher odds of achieving a TO[5]. In addition to examining perioperative outcomes, the impact of TO on long-term outcomes was also assessed. Of note, patients who experienced a TO had a better 5-year overall survival (OS) of 69.6% compared with a 5-year OS of 56.9% among individuals who did not achieve a TO[5], which was in line with previous studies on esophageal and gastric cancer[6]. Similarly, Heidsma *et al*[15] reported an incidence of TO that was 49.3% among patients undergoing resection for pancreatic neuroendocrine tumors; the odds of TO varied based on the type of procedure performed[15]. In fact, the highest TO rates were noted among individuals undergoing distal pancreatectomy (56.7%) followed by those undergoing enucleation (52.0%) and then pancreatoduodenectomy (32.5%)[15]. TO was also an independent predictor of long-term outcomes, with 3-year disease-free survival ranging from 91.7% among patients who achieved a TO to 85.2% among patients who did not[15]. These data validated the clinical relevance of TO among cancer patients, aligning the importance of surgical quality (and outcomes) with the primary goal of achieving a potentially curative operation. As more investigators integrate TO into the field of surgical oncology, TO may evolve to incorporate other variables representing domains of multidisciplinary care delivery (*i.e.*, negative margin resection, adequate lymph node sampling, receipt of neoadjuvant/adjuvant chemotherapy) to create an oncologic composite outcome measure [*i.e.*, textbook oncologic outcome (TOO)][16,17]. Although consensus as to which individual components should define a TOO has not been reached (Table 1), the use of a TOO might be a better way to characterize patient and hospital-level outcomes among cancer patients.

ASSESSING HOSPITAL PERFORMANCE, DESIGNATIONS AND QUALITY METRICS USING TOs

Hospital performance remains an important topic among patients and stakeholders, such as insurance and pharmaceutical companies as well as the government. To date, different designations and ranking systems are available to evaluate hospital performance. Of note, teaching hospitals have been assigned with the mission to teach the next generation of physicians, support research and provide excellent patient care[18,19]. Previous studies had demonstrated contradictory results when examining individual outcome parameters (*i.e.*, mortality, morbidity, readmissions) relative to teaching hospital status[18,19]. To this point, Mehta *et al*[12] investigated the impact of teaching status on TO among Medicare beneficiaries undergoing hepatopancreatic surgery[12]. Of note, patients undergoing surgery for pancreatic cancer at a major teaching hospital were more likely to achieve a TO *vs* patients treated at a minor teaching hospital[12]. When assessing only high volume hospitals, the odds of a TO were comparable among patients treated at major *vs* minor teaching centers, highlighting that the beneficial effect of teaching hospital status was largely mediated by procedural volume and not necessarily by teaching status itself[12].

Another study investigated a commonly used ranking system, the United States News & World Report (USNWR) Best Hospital rankings, relative to TO[13]. Although the USNWR rankings are commonly used by patients and are thought to influence patient decision-making and choice of hospital to undergo treatment, a recent study demonstrated similar odds of achieving a TO among patients undergoing complex

Table 1 Existing literature around textbook outcome in hepatopancreatobiliary surgery

Ref.	Study period	Database	Indication	Components of TO	TO rates
Merath *et al*[3], 2019	2013-2015	Medicare	Benign and malignant hepatopancreatic lesions	No complications. No prolonged LOS. No 90-d mortality. No 90-d readmission	44.0%
Merath *et al*[4], 2020	1993-2015	Multi-institutional ICC database	Intrahepatic cholangiocarcinoma	R0 resection No transfusion. No complications. No prolonged LOS. No 30-d mortality. No 30-d readmission	25.5%
Tsilimigras *et al*[5], 2020	2000-2015	Multi-institutional HCC database	Hepatocellular carcinoma	R0 resection No reoperation. No complications (Clavien-Dindo ≥ III) No prolonged LOS. No 90-d mortality. No 90-d readmission	62.3%
Heidsma *et al*[15], 2020	2000-2016	US Neuroendocrine Tumor Study Group database	Pancreatic neuroendocrine tumors	R0 resection No complications (Clavien-Dindo ≥ III). No prolonged LOS. No 90-d mortality. No 90-d readmission	49.3%

TO: Textbook outcome; LOS: Length of stay; ICC: Intrahepatic cholangiocarcinoma; US: Ultrasonography; HCC: Hepatocellular carcinoma.

cancer surgery (*i.e.*, lung, colorectal, esophageal, liver and pancreatic resections) at honor roll (top 20 institutions) *vs* non-honor roll hospitals[13]. These data suggested that the USNWR ranking had only a minor impact on the likelihood of achieving a TO and, thus, should not necessarily been used to choose institutions to undergo complex cancer surgery. In addition, these data suggested that composite outcomes such as TO should perhaps been taken into consideration among policymakers to establish the methodology of hospital ranking systems for complex cancer surgery.

For oncologic patients, quality of care is of particular importance as patients seek a holistic, multidisciplinary care in the battle against cancer. To date, there are only 10 dedicated cancer centers (DCCs) that provide care to cancer patients[20]. Another important designation for hospitals providing cancer care is the National Cancer Institute cancer center (NCI-CC) designation, which approximately 70 institutions in the United States hold for outstanding efforts related to prevention, diagnosis and treatment of cancer[21]. In another study by Mehta *et al*[20], the authors compared outcomes of patients undergoing hepatopancreatic surgery at DCC *vs* NCI-CC for cancer[20]. Of note, patients who underwent hepatopancreatic surgery had increased odds of achieving a TO when treated at a DCC *vs* NCI-CC (pancreatic resections: 22% higher chance of a TO; liver resection: 31% higher chance of a TO), despite the fact that DCCs more frequently cared for patients with multiple comorbidities[20]. Higher TO rates translated into reduced Medicare expenditures at DCCs, which suggested a higher value proposition of DCC *vs* NCI-CC in the treatment of patients with hepatopancreatic malignancies[20].

Several other national quality metrics have been proposed to assess quality of care provided to patients. For example, hospital magnet recognition, established by the American Nurses Credentialing Center has been used to identify institutions with a focus on improving nursing care and, in turn, quality of care delivered to patients[22]. In addition, the Leapfrog Group has set a minimum annual hospital surgical volume for certain operations–including pancreatic resection (*i.e.*, > 20 pancreatic resections)–associated with improved outcomes[23]. Another quality indicator made available by the Leapfrog group is the Leapfrog safety grade which is solely focused on patient safety[23,24]. In analyzing data from 4853 Medicare beneficiaries, Merath *et al*[14] examined all 3 quality indicators (*i.e.*, leapfrog minimum volume standards, safety grade and magnet status) relative to TO following hepatopancreatic resections[14]. Of note, patients undergoing pancreatectomy at hospitals meeting all 3 quality metrics (*i.e.*, quality trifactor) had 28% higher odds of experiencing a TO compared with individuals undergoing pancreatectomy at non-trifactor hospitals[14]. When examining each of the quality indicators separately, magnet status and safety grade A were alone not enough to confer high TO rates. Rather, the positive effect of the quality trifactor was largely mediated by the compliance with the Leapfrog minimum volume standards that were associated with lower odds of mortality and serious complications and, in turn, greater odds of TO[14].

ASSESSING TRENDS IN TOs OVER TIME

TO has also been assessed relative to changes in practice and outcomes in HPB surgery over time. By analyzing the American College of Surgeons National Surgical Quality Improvement Program database, Beane *et al*[25] reported an increase in optimal or "textbook" outcomes after pancreatic surgery in North America[25]. There was a decrease in postoperative morbidity, mortality and LOS between 2013-2017 that resulted in an increase in the incidence of TO by 3% to 5% after pancreatic surgery on a nationwide level[25]. A number of reasons might be responsible for this improvement. First, there was a decrease in superficial and deep surgical site infections, and a decrease in the rates of shock/sepsis after pancreatic resection[25]. In addition, an increase in minimally invasive pancreatic resection was noted over time (mainly robotic resection) that may have contributed to a decrease in LOS. The broad dissemination and implementation of enhanced recovery after surgery protocols over the past 5 to 10 years likely also contributed to the observed reduction in LOS[26,27]. Furthermore, the increase in TO incidence over time may also have been to centralization of pancreatic cancer care at specialized centers and increased access to multidisciplinary oncologic teams. In turn, the modest improvement in the incidence of TO noted over time may be a reflection of the varied distribution of pancreatic cancer cases, and not an actual improvement in the majority of centers throughout the nation[25].

Indeed, by combining two multi-institutional datasets, Tsilimigras *et al*[11] analyzed the trends in TO rates after curative-intent resection of primary liver malignancies (*i.e.*, ICC and HCC) at major HPB centers over a 12-year period[11]. Overall, 62.0% of patients achieved a TO after ICC or HCC resection at major HPB centers. In assessing the trends of TO over the years, no significant improvement was noted over the study period examined (2005-2017) (P_{trend} = 0.90)[11]. When analyzing the individual components comprising TO, no specific factor demonstrated an increasing trend over time (all P_{trend} > 0.05). Perhaps more surprisingly, no increasing trends in TO rates were noted among patients undergoing either major (2005 to 2009: 49%; 2014 to 2017: 48%) or minor liver resection (2005 to 2009: 71%, 2014 to 2017: 71%) over the study period (both P_{trend} > 0.05)[11]. Apart from TO itself, the year of surgery was also not associated with improved long-term outcomes among patients with either ICC or HCC[11]. These data highlight the fact that despite advances in surgical techniques and perioperative care, only modest improvements in the outcomes of HCC and ICC patients occurred over the last decade. In turn, there is still a long way to optimize real world outcomes among patients with HPB malignancies.

FINANCIAL IMPACT OF TOs

Besides representing a quality outcome measure, TO may also have financial implications. In fact, the financial impact of TO has been investigated and data have suggested that a disproportionate amount of money is spent on patients who do not achieve a TO after hepatopancreatic surgery. For example, Merath *et al*[4] noted that among patients who achieved a TO, Medicare payments were approximately $11000 less following minor hepatopancreatic resections and $14000 less for patients undergoing major resection when compared with individuals who did not achieve a TO[4]. Similarly, Mehta *et al*[12] suggested that TO resulted in an average of $5000 less in Medicare expenditures after hepatopancreatic surgery at teaching hospitals (TO: $19191, *vs* no TO: $24165, $P < 0.001$)[12]. The association of decreased overall costs with the achievement of a TO was consistent across major and minor teaching hospitals, as well as among high and low volume institutions, highlighting that TO has financial implications irrespective of the hospital setting[12]. Collectively, the data suggest that TO might be a composite metric that reflects value—*i.e.*, high quality combined with lower costs. In turn, improving TO rates after hepatopancreatic surgery may not only optimize the quality of care provided to patients, but also decrease health care costs and lead to cost-effective and high-value care.

ADVOCATING FOR WIDER IMPLEMENTATION OF TO IN HPB SURGERY

Advocates of TO note that this composite metric provides a more comprehensive estimate of quality of perioperative care[28]. However, a primary criticism of TO is that there is no consensus in the literature as to what should be considered an "optimal"

outcome after a specific operation. Moreover, patient risk factors strongly influence outcomes and require comprehensive risk adjustment in order to make valid comparisons. With the thoughtful implementation of composite quality metrics in HPB surgery, surgeons and centers will hopefully gain a better understanding of the perioperative processes of care and develop insights to improve patient outcomes. Moreover, the optimization of expectation management will be facilitated, especially in high-risk patients. Improved understanding of these gaps through the use of TO can allow systems to identify patients who are high risk of failure to achieve optimal short- and long-term outcomes after surgery and redirect resources accordingly. Thus, fundamentally the concept of TO aligns with the patient best interest, which is the ideal outcome after surgery.

CONCLUSION

TO provides a more realistic assessment of patient-centered perioperative care and represents the optimal experience around a surgical episode. TO should be the ideal outcome that surgeons should strive to achieve for their patients. The use of TO in cancer populations is of paramount importance as a measure of both short- and long-term outcomes. TO can be used to assess performance across different institutions as well as assess quality metrics or hospital designations. Future efforts should be directed towards establishing a universal definition of TO in HPB surgery so that surgeons and hospitals can assess and compare outcomes, as well as identify shortcomings and improve real-world patient outcomes.

REFERENCES

1 **Dimick JB**, Staiger DO, Baser O, Birkmeyer JD. Composite measures for predicting surgical mortality in the hospital. *Health Aff (Millwood)* 2009; **28**: 1189-1198 [PMID: 19597221 DOI: 10.1377/hlthaff.28.4.1189]

2 **Kolfschoten NE**, Kievit J, Gooiker GA, van Leersum NJ, Snijders HS, Eddes EH, Tollenaar RA, Wouters MW, Marang-van de Mheen PJ. Focusing on desired outcomes of care after colon cancer resections; hospital variations in 'textbook outcome'. *Eur J Surg Oncol* 2013; **39**: 156-163 [PMID: 23102705 DOI: 10.1016/j.ejso.2012.10.007]

3 **Merath K**, Chen Q, Bagante F, Alexandrescu S, Marques HP, Aldrighetti L, Maithel SK, Pulitano C, Weiss MJ, Bauer TW, Shen F, Poultsides GA, Soubrane O, Martel G, Koerkamp BG, Guglielmi A, Itaru E, Cloyd JM, Pawlik TM. A Multi-institutional International Analysis of Textbook Outcomes Among Patients Undergoing Curative-Intent Resection of Intrahepatic Cholangiocarcinoma. *JAMA Surg* 2019; **154**: e190571 [PMID: 31017645 DOI: 10.1001/jamasurg.2019.0571]

4 **Merath K**, Chen Q, Bagante F, Beal E, Akgul O, Dillhoff M, Cloyd JM, Pawlik TM. Textbook Outcomes Among Medicare Patients Undergoing Hepatopancreatic Surgery. *Ann Surg* 2020; **271**: 1116-1123 [PMID: 30499800 DOI: 10.1097/SLA.0000000000003105]

5 **Tsilimigras DI**, Mehta R, Merath K, Bagante F, Paredes AZ, Farooq A, Ratti F, Marques HP, Silva S, Soubrane O, Lam V, Poultsides GA, Popescu I, Grigorie R, Alexandrescu S, Martel G, Workneh A, Guglielmi A, Hugh T, Aldrighetti L, Endo I, Pawlik TM. Hospital variation in Textbook Outcomes following curative-intent resection of hepatocellular carcinoma: an international multi-institutional analysis. *HPB (Oxford)* 2020; **22**: 1305-1313 [PMID: 31889626 DOI: 10.1016/j.hpb.2019.12.005]

6 **van der Kaaij RT**, de Rooij MV, van Coevorden F, Voncken FEM, Snaebjornsson P, Boot H, van Sandick JW. Using textbook outcome as a measure of quality of care in oesophagogastric cancer surgery. *Br J Surg* 2018; **105**: 561-569 [PMID: 29465746 DOI: 10.1002/bjs.10729]

7 **Karthaus EG**, Lijftogt N, Busweiler LAD, Elsman BHP, Wouters MWJM, Vahl AC, Hamming JF; Dutch Society of Vascular Surgery, the Steering Committee of the Dutch Surgical Aneurysm Audit, the Dutch Institute for Clinical Auditing. Textbook Outcome: A Composite Measure for Quality of Elective Aneurysm Surgery. *Ann Surg* 2017; **266**: 898-904 [PMID: 28746156 DOI: 10.1097/SLA.0000000000002388]

8 **Moris D**, Shaw BI, Gloria J, Kesseli SJ, Samoylova ML, Schmitz R, Manook M, McElroy LM, Patel Y, Berg CL, Knechtle SJ, Sudan DL, Barbas AS. Textbook Outcomes in Liver Transplantation. *World J Surg* 2020; **44**: 3470-3477 [PMID: 32488663 DOI: 10.1007/s00268-020-05625-9]

9 **Moris D**, Cerullo M, Nussbaum DP, Blazer DG 3rd. Textbook Outcomes Among Patients Undergoing Retroperitoneal Sarcoma Resection. *Anticancer Res* 2020; **40**: 2107-2115 [PMID: 32234903 DOI: 10.21873/anticanres.14169]

10 **Wiseman JT**, Ethun CG, Cloyd JM, Shelby R, Suarez-Kelly L, Tran T, Poultsides G, Mogal H, Clarke C, Tseng J, Roggin KK, Chouliaras K, Votanopoulos K, Krasnick B, Fields R, Walle KV, Ronnekleiv-Kelly S, Howard JH, Cardona K, Grignol V. Analysis of textbook outcomes among patients undergoing resection of retroperitoneal sarcoma: A multi-institutional analysis of the US

Sarcoma Collaborative. *J Surg Oncol* 2020; **122**: 1189-1198 [PMID: 32696475 DOI: 10.1002/jso.26136]

11 **Tsilimigras DI**, Sahara K, Moris D, Mehta R, Paredes AZ, Ratti F, Marques HP, Soubrane O, Lam V, Poultsides GA, Popescu I, Alexandrescu S, Martel G, Workneh A, Guglielmi A, Hugh T, Aldrighetti L, Weiss M, Bauer TW, Maithel SK, Pulitano C, Shen F, Koerkamp BG, Endo I, Pawlik TM. Assessing Textbook Outcomes Following Liver Surgery for Primary Liver Cancer Over a 12-Year Time Period at Major Hepatobiliary Centers. *Ann Surg Oncol* 2020; **27**: 3318-3327 [PMID: 32388742 DOI: 10.1245/s10434-020-08548-w]

12 **Mehta R**, Paredes AZ, Tsilimigras DI, Moro A, Sahara K, Farooq A, Dillhoff M, Cloyd JM, Tsung A, Ejaz A, Pawlik TM. Influence of hospital teaching status on the chance to achieve a textbook outcome after hepatopancreatic surgery for cancer among Medicare beneficiaries. *Surgery* 2020; **168**: 92-100 [PMID: 32303348 DOI: 10.1016/j.surg.2020.02.024]

13 **Mehta R**, Tsilimigras DI, Paredes AZ, Sahara K, Moro A, Farooq A, White S, Ejaz A, Tsung A, Dillhoff M, Cloyd JM, Pawlik TM. Comparing textbook outcomes among patients undergoing surgery for cancer at U. S. News & World Report ranked hospitals. *J Surg Oncol* 2020; **121**: 927-935 [PMID: 32124433 DOI: 10.1002/jso.25833]

14 **Merath K**, Mehta R, Tsilimigras DI, Farooq A, Sahara K, Paredes AZ, Wu L, Moro A, Ejaz A, Dillhoff M, Cloyd J, Tsung A, Pawlik TM. Quality of Care Among Medicare Patients Undergoing Pancreatic Surgery: Safety Grade, Magnet Recognition, and Leapfrog Minimum Volume Standards-Which Quality Benchmark Matters? *J Gastrointest Surg* 2021; **25**: 269-277 [PMID: 32040811 DOI: 10.1007/s11605-019-04504-6]

15 **Heidsma CM**, Hyer M, Tsilimigras DI, Rocha F, Abbott DE, Fields R, Smith PM, Poultsides GA, Cho C, Maithel SK, Pawlik TM; Other Members of the US Neuroendocrine Tumor Study Group. Incidence and impact of Textbook Outcome among patients undergoing resection of pancreatic neuroendocrine tumors: Results of the US Neuroendocrine Tumor Study Group. *J Surg Oncol* 2020; **121**: 1201-1208 [PMID: 32185804 DOI: 10.1002/jso.25900]

16 **Nicholas E**, van Roessel S, de Burlet K, Hore T, Besselink MG, Connor S. Using Textbook Outcomes to benchmark practice in pancreatic surgery. *ANZ J Surg* 2021; **91**: 361-366 [PMID: 33475226 DOI: 10.1111/ans.16555]

17 **van Roessel S**, Mackay TM, van Dieren S, van der Schelling GP, Nieuwenhuijs VB, Bosscha K, van der Harst E, van Dam RM, Liem MSL, Festen S, Stommel MWJ, Roos D, Wit F, Molenaar IQ, de Meijer VE, Kazemier G, de Hingh IHJT, van Santvoort HC, Bonsing BA, Busch OR, Groot Koerkamp B, Besselink MG; Dutch Pancreatic Cancer Group. Textbook Outcome: Nationwide Analysis of a Novel Quality Measure in Pancreatic Surgery. *Ann Surg* 2020; **271**: 155-162 [PMID: 31274651 DOI: 10.1097/SLA.0000000000003451]

18 **Shahian DM**, Nordberg P, Meyer GS, Blanchfield BB, Mort EA, Torchiana DF, Normand SL. Contemporary performance of U.S. teaching and nonteaching hospitals. *Acad Med* 2012; **87**: 701-708 [PMID: 22534588 DOI: 10.1097/ACM.0b013e318253676a]

19 **Taylor DH Jr**, Whellan DJ, Sloan FA. Effects of admission to a teaching hospital on the cost and quality of care for Medicare beneficiaries. *N Engl J Med* 1999; **340**: 293-299 [PMID: 9920955 DOI: 10.1056/NEJM199901283400408]

20 **Mehta R**, Tsilimigras DI, Paredes AZ, Sahara K, Dillhoff M, Cloyd JM, Ejaz A, White S, Pawlik TM. Dedicated Cancer Centers are More Likely to Achieve a Textbook Outcome Following Hepatopancreatic Surgery. *Ann Surg Oncol* 2020; **27**: 1889-1897 [PMID: 32108924 DOI: 10.1245/s10434-020-08279-y]

21 **National cancer Institute**. Office of Cancer Centers. Cancer centers program. [cited 14 January 2021]. Available from: https://imaging.nci.nih.gov/nbia-search-cover/

22 **Friese CR**, Xia R, Ghaferi A, Birkmeyer JD, Banerjee M. Hospitals In 'Magnet' Program Show Better Patient Outcomes On Mortality Measures Compared To Non-'Magnet' Hospitals. *Health Aff (Millwood)* 2015; **34**: 986-992 [PMID: 26056204 DOI: 10.1377/hlthaff.2014.0793]

23 **Leapfrog Group**. Proposed changes to the 2019 leapfrog hospital survey. [cited 14 January 2021]. Available from: https://www.leapfroggroup.org/sites/default/files/Files/LeapfrogHospitalSurvey_ProposedChanges_2019_Final.pdf

24 **Hota B**, Webb T, Chatrathi A, McAninch E, Lateef O. Disagreement Between Hospital Rating Systems: Measuring the Correlation of Multiple Benchmarks and Developing a Quality Composite Rank. *Am J Med Qual* 2020; **35**: 222-230 [PMID: 31253048 DOI: 10.1177/1062860619860250]

25 **Beane JD**, Borrebach JD, Zureikat AH, Kilbane EM, Thompson VM, Pitt HA. Optimal Pancreatic Surgery: Are We Making Progress in North America? *Ann Surg* 2019 [PMID: 31663969 DOI: 10.1097/SLA.0000000000003628]

26 **Morgan KA**, Lancaster WP, Walters ML, Owczarski SM, Clark CA, McSwain JR, Adams DB. Enhanced Recovery After Surgery Protocols Are Valuable in Pancreas Surgery Patients. *J Am Coll Surg* 2016; **222**: 658-664 [PMID: 26916130 DOI: 10.1016/j.jamcollsurg.2015.12.036]

27 **Agarwal V**, Thomas MJ, Joshi R, Chaudhari V, Bhandare M, Mitra A, deSouza A, Ambulkar R, Shrikhande SV. Improved Outcomes in 394 Pancreatic Cancer Resections: the Impact of Enhanced Recovery Pathway. *J Gastrointest Surg* 2018; **22**: 1732-1742 [PMID: 29777454 DOI: 10.1007/s11605-018-3809-7]

28 **Fong Y**. Textbook Outcome Nomograms as Multivariate Clinical Tools for Building Cancer Treatment Pathways and Prognosticating Outcomes. *JAMA Surg* 2019; **154**: e190572 [PMID: 31017642 DOI: 10.1001/jamasurg.2019.0572]

World Journal of Gastroenterology

Submit a Manuscript: https://www.f6publishing.com

World J Gastroenterol 2021 April 21; 27(15): 1531-1552

DOI: 10.3748/wjg.v27.i15.1531

ISSN 1007-9327 (print) ISSN 2219-2840 (online)

REVIEW

Impact of cytokine storm and systemic inflammation on liver impairment patients infected by SARS-CoV-2: Prospective therapeutic challenges

Fares E M Ali, Zuhair M Mohammedsaleh, Mahmoud M Ali, Osama M Ghogar

ORCID number: Fares E M Ali 0000-0001-8341-7458; Zuhair M Mohammedsaleh 0000-0002-7391-0529; Mahmoud M Ali 0000-0001-6173-1876; Osama M Ghogar 0000-0002-2003-1408.

Author contributions: Ali FEM designed and critical wrote the manuscript; Mohammedsaleh ZM performed the manuscript proof editing and revision; Ali MM and Ghogar OM collected data and drafting the manuscript.

Conflict-of-interest statement: No potential conflicts of interest and financial support for this work.

Manuscript source: Invited

Fares E M Ali, Department of Pharmacology and Toxicology, Faculty of Pharmacy, Al-Azhar University, Assiut Branch, Assiut 71524, Egypt

Zuhair M Mohammedsaleh, Department of Medical Laboratory Technology, Faculty of Applied Medical Sciences, University of Tabuk, Tabuk 71491, Saudi Arabia

Mahmoud M Ali, Osama M Ghogar, Pre-graduated students, Faculty of Pharmacy, Al-Azhar University, Assiut Branch, Assiut 71524, Egypt

Corresponding author: Fares E M Ali, MSc, PhD, Lecturer, Research Scientist, Department of Pharmacology and Toxicology, Faculty of Pharmacy, Al-Azhar University, Assiut Branch, Al-Azhar University Street, Assiut 71524, Egypt. faresali@azhar.edu.eg

Abstract

Coronavirus disease 2019 (COVID-19) is a devastating worldwide pandemic infection caused by a severe acute respiratory syndrome namely coronavirus 2 (SARS-CoV-2) that is associated with a high spreading and mortality rate. On the date this review was written, SARS-CoV-2 infected about 96 million people and killed about 2 million people. Several arguments disclosed the high mortality of COVID-19 due to acute respiratory distress syndrome or change in the amount of angiotensin-converting enzyme 2 (ACE2) receptor expression or cytokine storm strength production. In a similar pattern, hepatic impairment patients co-infected with SARS-CoV-2 exhibited overexpression of ACE2 receptors and cytokine storm overwhelming, which worsens the hepatic impairment and increases the mortality rate. In this review, the impact of SARS-CoV-2 on hepatic impairment conditions we overviewed. Besides, we focused on the recent studies that indicated cytokine storm as well as ACE2 as the main factors for high COVID-19 spreading and mortality while hinting at the potential therapeutic strategies.

Key Words: COVID-19; Hepatic impairment; SARS-CoV-2; Cytokine storm; Immuno-modulators receptors

manuscript

Specialty type: Gastroenterology and hepatology

Country/Territory of origin: Egypt

Peer-review report's scientific quality classification

Grade A (Excellent): 0
Grade B (Very good): 0
Grade C (Good): C
Grade D (Fair): 0
Grade E (Poor): 0

Received: January 26, 2021
Peer-review started: January 27, 2021
First decision: February 10, 2021
Revised: February 17, 2021
Accepted: March 29, 2021
Article in press: March 29, 2021
Published online: April 21, 2021

P-Reviewer: Pawlowska M
S-Editor: Fan JR
L-Editor: A
P-Editor: Liu JH

Core Tip: Implications of fast coronavirus disease 2019 (COVID-19) outbreak are huge annoying problems that affected countries' health and economies around the world. Patients associated with hepatic impairment are considered at a high-risk target for severe acute respiratory syndrome namely coronavirus 2 severity and mortality. A good understanding of virus machinery provides excellent ideas about how to combat this monster. We provide detailed information about the recent mechanisms of COVID-19 pathogenesis, implications on several hepatic disorders, and potential therapeutic strategies.

Citation: Ali FEM, Mohammedsaleh ZM, Ali MM, Ghogar OM. Impact of cytokine storm and systemic inflammation on liver impairment patients infected by SARS-CoV-2: Prospective therapeutic challenges. *World J Gastroenterol* 2021; 27(15): 1531-1552
URL: https://www.wjgnet.com/1007-9327/full/v27/i15/1531.htm
DOI: https://dx.doi.org/10.3748/wjg.v27.i15.1531

INTRODUCTION

Coronaviruses are classified into four categories, namely α, β, γ, and δ type. The α- and β-coronaviruses could infect mammals, while γ- and δ- coronaviruses appear to infect birds[1]. Six coronaviruses reported as human-affected viruses include α-coronaviruses NL63 and 229E, low-pathogenic β-coronaviruses OC43 and HKU1, these viruses cause mild respiratory symptoms as common cold[2]. The remaining two types were identified as β-coronavirus, which unusually induced fatal respiratory tract infections[3]. Between 2002 and 2003, severe acute respiratory syndrome (SARS) resulted in the outbreak of SARS0[4]. In 2012 the Middle East respiratory syndrome (MERS) originated and circulated in camels[5].

In 2019, a newly discovered coronavirus is a SARS coronavirus 2 (SARS-CoV-2), which induces a contagious disease coronavirus disease 2019 (COVID-19) and is currently spreading nationwide[6]. Consequently, the third identified zoonotic coronavirus detected after SARS and MERS cause potentially fatal respiratory tract infections[7,8]. The early cases of COVID-19 were linked to the Huanan seafood market, Wuhan, China[9,10].

On January 12, 2020, the World Health Organization (WHO) temporarily named this new virus the 2019 novel coronavirus (2019-nCoV)[11]. On January 30, 2020, the WHO declared the 2019-nCoV epidemic a public health emergency of international burden[11]. After that February 11, 2020, the WHO formally named the disease caused by 2019-nCoV as COVID-19[12]. On the same day, the international committee of taxonomy named this virus as SARS-CoV-2 and classified it as coronavirus under the family Coronaviridae, subfamily Orthocoronavirinae, based on the genotypic and serological characterization[11,13,14].

SARS-CoV-2 is a new generation of β-coronavirus which shares 79% and 50% genome sequencing with SARS and MERS, respectively[15]. This information confirmed some of the available evidence that SARS-CoV-2 was generated from bats and pangolins[14]. Other studies suggest that SARS-CoV-2 was a chimeric virus obtained from the fusion of a bat's coronavirus and a coronavirus of unknown origin[16]. In the same context, the study conducted by Sun *et al*[17] showed that the structure of SARS-CoV-2 was similar to the coronavirus isolated from Chinese chrysanthemum-headed bats in 2015. So far, no confirmation has been made of the zoonotic source of SARS-CoV-2 yet[18].

SARS-CoV-2 has a 29891-nucleotide genome (encoding 9860 amino acids)[19] with a diameter of about 50-200 nm[20]. Two-thirds of viral RNA, primarily in the first open reading frames (ORFs) (ORF1a/b), converts into two non-structural polyproteins pp1a, pp1ab, and encodes 16 non-structural proteins (NSP). In contrast, the remaining ORFs encode structural and accessory proteins[21,22]. Six ORFs of functions are arranged between 5′ to 3′ (ORF1a/ORF1b), spike glycoprotein (S), a small envelope protein (E), matrix protein (M), and nucleocapsid protein (N)[21]. Moreover, seven putative ORFs encoding accessory proteins are disseminated between the structural genes[23,24]. The glycoprotein S is responsible for the receptor-binding site and membrane fusion[25]. The envelope protein E has essential roles in releasing and accumulating viruses[26], besides protein M[27]. Additionally, a NSP plays many functions during the viral cycle[28].

SARS-CoV-2 AND ANGIOTENSIN-CONVERTING ENZYME 2

Only specific and permissive cells inside the host may be infected. Specifically, cells that generate proteins and viral factors which are required for virus replication. As soon as the virus enters the cell, the virus recruits cells to produce essential viral encoded proteins involved in replicating the virus's genetic material[29]. The viral replication process generally known as cytopathic effects, could induce biochemical changes resulting in cellular damage. Interestingly, SARS-CoV-2 relies on specific cellular receptors to invade the cells that carry these factors like other types of coronaviruses[30].

The surface of SARS-CoV-2 is covered by several types of glycosylated S proteins that facilitate the virus's attachment to the host angiotensin-converting enzyme 2 (ACE2), hence mediating the entry of the virus into the host cells[31]. This action could activate S protein by a specific type of serine protease located on the host cell membrane called TM protease serine 2. After the virus recruited the host cell, it releases its RNA and uses the host cells to replicate and synthesize its functional proteins[32].

SARS-CoV-2 is predicted to have organ tropism beyond the respiratory tract, also including the kidney, heart, skeletal muscle, central nervous system, liver, and gastrointestinal tract. The spread of infection through the body is reasonable for developing COVID-19 systemic symptoms and exacerbating pre-existing disorders[33,34]. Therefore, patients with severe COVID-19 illness show multiple organ damage, such as acute kidney injury, acute pulmonary injury, heart injury, and liver injury[35].

SARS-CoV-2 may induce liver injury *via* a similar mechanism. Furthermore, we cannot neglect angiotensin II's action; once SARS-CoV-2 binds to ACE2 receptors it stimulates angiotensin II to mediate the tissue injury[36]. These findings confirm that angiotensin II levels are increased in healthy patients with COVID-19 and are directly correlated with viral load[37].

Hepatic sharing of ACE2 receptors is unreasonable; it is widely distributed in the endothelial layer but not in the sinusoidal endothelium[38]. On the surface of cholangiocytes, ACE2 receptors have more significant expressions than hepatocytes[39]. Cholangiocytes ACE2 receptors expression was close to that of type II alveoli cells in the lungs, indicating that the liver may be a strong candidate for SARS-CoV-2[40]. In Contrast, Immunohistochemical stains for Kupffer cells and lymphocytes T and B for ACE2 are negative[41]. In fact, in patients with COVID-19, SARS-CoV-2 has been detected in their liver and can induce liver injury through different pathways[42]. The general mechanism of ACE2 mediated SARS-CoV-2 infection is outlined in Figure 1.

SARS-CoV-2 and devastating cytokine storm

Cytokine storm is an augmented cytokine output attributable to an irregular immune response to various stimuli like viral infections, rheumatic disorders, cancer, sepsis, multiple organ failure, and drugs that contribute to unnecessary immune cell activation[43]. Consequently, the rising aggressive systemic hyperinflammatory reaction is associated with the release of many pro-inflammatory cytokines responsible for critical illness[43,44]. Cytokine storm has been found in various viral infections, including influenza H5N1, H1N1 viruses, and two SARS-CoV and MERS-CoV coronaviruses[45-48]. Recent data reported that patients infected by SARS-CoV-2 show massive levels of cytokines and chemokines and are implicated with COVID-19 severity and high mortality rate[49].

The growing cytokine storm results in the continuous activation and expansion of innate and adaptive immune cells to produce a harmonized cascade of inflammatory responses, resulting in a devastating cytokine storm[50]. Indeed, the result of a mixture of several immune active molecules is the cytokine storm's product. The main components involved in forming the cytokine storm are interferons (IFNs) and interleukins (ILs)[51]. However, other inflammatory biomarkers such as c-reactive protein (CRP), fibroblast growth factor, macrophage-colony stimulating factor (M-CSF), interferon gamma-induced protein 10, monocyte chemoattractant protein-1 (MCP-1), macrophage inflammatory proteins-1α and 1β, platelet-derived growth factor, tumor necrosis factor-alpha (TNF-α), and vascular endothelial growth factor (VEGF) are markedly detected in the COVID-19 sever case-patients[52-54]. Hence, the uncontrolled response in severe COVID-19 patients is correlated with unfavorable clinicopathological consequences.

During COVID-19 illness, several pathological factors have been reported to participate in the initiation and propagation of SARS-CoV-2-induced cytokine storm (Figure 2).

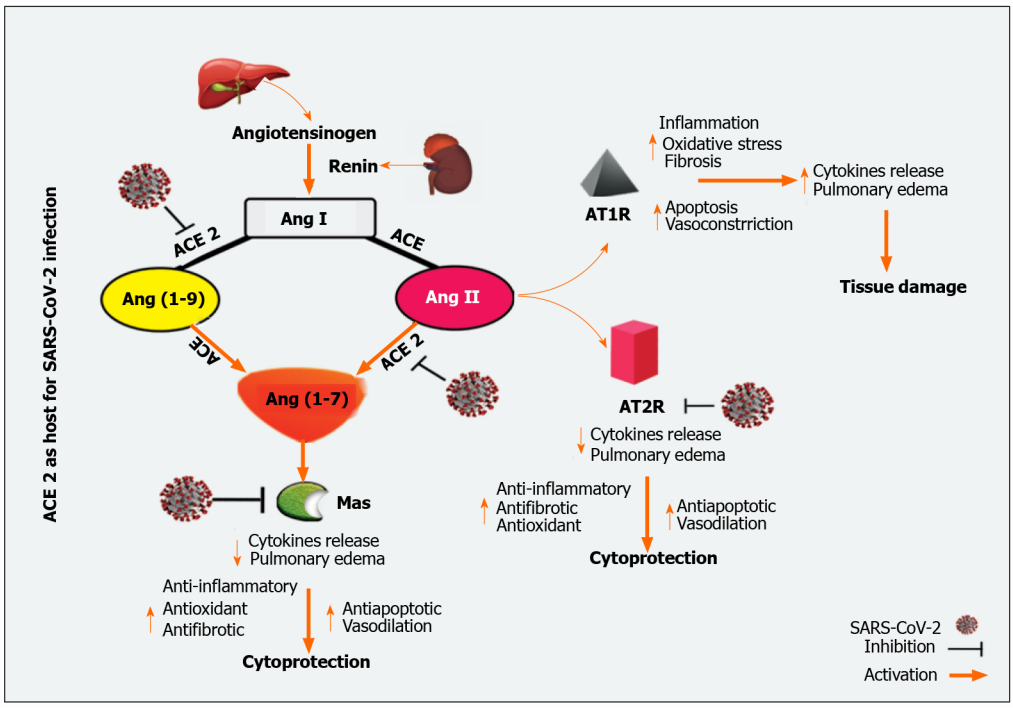

Figure 1 Angiotensin-converting enzyme 2 as a host for severe acute respiratory syndrome coronavirus 2 infection. SARS-CoV-2: Severe acute respiratory syndrome coronavirus 2; ACE: Angiotensin-converting enzyme; Ang: angiotensin; ATR: Angiotensin receptors type.

Renin angiotensin-aldosterone system

The Renin-angiotensin-aldosterone system (RAAS) is a significant regulator of several physiology and pathophysiology conditions such as maintenance of fluid and electrolyte homeostasis with the maintenance of vascular tone[55,56]. Recent evidence implies that RAAS has autocrine and paracrine effects in addition to the classical circulating endocrine effects. Hence, RAAS plays pivotal roles in cellular growth, migration, differentiation, apoptosis, inflammation, thrombosis, and fibrosis[11,57-59].

When renin is secreted directly into the bloodstream by juxtaglomerular cells, this secreted renin cleaves the liver-released substrate, angiotensinogen, to generate the inactive peptide, angiotensin (Ang) I, which is then converted by endothelial ACE to Ang II[56,60]. On the other hand, ACE2 cleaves Ang I to produce Ang (1-9) peptide. Besides, Ang II and Ang (1-9) can metabolize by ACE or other peptidases to form Ang 1-7[61,62].

The RAAS is a double-edged sword that acts through two distinct opposing arms: the ACE/Ang II/AT1 receptor axis, which is responsible for main actions, and the ACE-2/Ang-(1-7) /Mas receptor axis, the counter-regulatory arm[63,64]. The ACE catalytic activity contributes to an increase of Ang II levels and an increase in Ang-(1-7) catabolism, while ACE2 catalytic activity is primarily based on Ang I and Ang II and leads to the formation of Ang (1-7)[64,65]. Ang II plays a central role in the RAAS *via* angiotensin II type 1 and 2 receptors (AT1R and AT2R); thus, stimulating the ACE/Ang II/AT1 receptor axis which results in regulating vasoconstriction, fibrotic remodeling, inflammatory response, and production of reactive oxygen species (ROS)[66]. Ang II itself will directly activate the nuclear factor-kappaB (NF-κB) pathway through the phosphorylation of the p65 subunit of NF-κB; therefore, increases the output of IL-6, IL-1β, TNF-α, and IL-10[67,68]. Ang II also affects mitogen-activated protein kinases (MAPKs; extracellular signal-regulated kinases 1/2, c-Jun N-terminal kinases, p38-MAPK), which have a high impact on pro-inflammatory cytokines release[68,69]. Besides, a spontaneous association of Ang II with host immune cells, *e.g.*, neutrophils, T and B lymphocytes, and tissue-resident cells results in the release of pro-inflammatory cytokines, including prostaglandins, IL-6, IL-1β, TNF-α, VEGF, and IFN-γ, as well as the activation of kinase plethora [*e.g.*, Janus kinase (JAK) and p38 MAPK][70,71].

As soon as the SARS-CoV-2 spike (S)-protein binds to ACE2[72], the serum level of Ang II was significantly increased, which in turn mediated trans-signaling of the IL-6/soluble IL-6 receptor-a complex in to finally activate of signal transducer and activator of transcription 3 (STAT3)[73]. STAT-3 has been reported to up-regulated

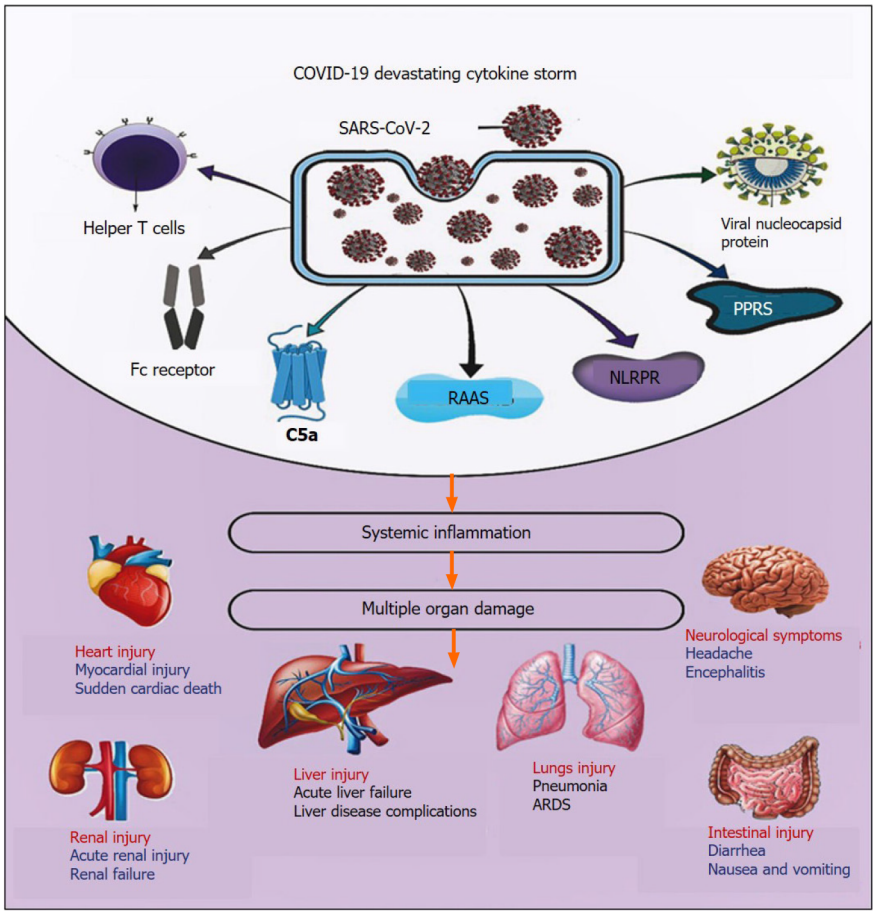

Figure 2 Coronavirus disease 2019 and devastating cytokine storm. COVID-19: Coronavirus disease 2019; SARS-CoV-2: Severe acute respiratory syndrome coronavirus 2; C5a: Complement component 5a; RAAS: Renin-angiotensin-aldosterone system; NLRPR: Nucleotide-binding oligomerization domain, Leucine-rich repeat and pyrin domain-containing receptor; PPRs: Pattern recognition receptors; ARDS: Acute respiratory distress syndrome.

several inflammatory genes like NF-κB. Besides activation of NF-κB by SARS-CoV-2 mediated STAT3 activation, SARS-CoV-2 itself can activate NF-κB by binding with pattern recognition receptors (PRRs). The net results trigger a cytokine storm accompanied by acute respiratory distress syndrome (ARDS) and multiple organ damage[68,74]. During COVID-19, ACE2 depletion and ACE/Ang II/AT1R axis activity are highly augmented[75]. Therefore, a therapeutic modality by administering exogenous ACE2 to patients with COVID-19 can potentially impact COVID-19 severity[76]. On the other hand, targeting the ACE/Ang-II/AT1R axis downstream, such as the IL-6/STAT3 axis, should be considered to avoid ARDS inflammation and end-organ damage induced by cytokine storm[68,76].

In contrast to the ACE/Ang II/AT1R pathway, the Ang (1-7) interacts with the Mas receptor to provide vasodilation and antiproliferative effects[77]. Indeed, activating Mas receptors induce activation of phospholipase A, phosphoinositide 3 kinases/protein kinase B axis, endothelial nitric oxide synthase, and intracellular calcium accumulation[78]. Additionally, Ang (1-7) down-regulates p38 MAPK and NF-κB expression harmony with the suppression of inflammatory markers such as IL-6, IL-8, and TNF-α[68]. Furthermore, Ang (1-7) *via* the Mas receptor activation attenuated Ang II-induced intercellular adhesion molecule-1, vascular cell adhesion molecule-1, and MCP-1[68,79]. Together, activation of these pathways suggests that Ang (1-7) has antiproliferative, anti-thrombotic, and anti-inflammatory functions and ameliorates tissue damages[70,78].

Interestingly, down-regulation of the ACE-2/Ang (1-7)/Mas receptors axis was proposed to be increased during COVID-19; since the virus uses the enzyme's peptidase domain to enter into the cells, there is a down-regulation of ACE-2 with ACE up-regulation[63]. Thus, it contributes to a massive release of cytokines and inflammatory responses. Since Ang (1-7) plays a critical role in counteracting the pro-inflammatory activity of RAAS, it has been proposed that Ang (1-7) or one of its associated agents could be administered to patients with COVID-19 since it protects against activation of inflammatory mediators in a cytokine outbreak[68]. Additionally,

Ang (1-7) was previously reported to inhibit liver fibrogenesis[80]. Thus, it may be helpful to attenuate liver injury in patients with liver impairments infected with SARS-CoV-2.

Fc receptor

SARS-CoV-2 is a specific antibody with the Fc receptor. Indeed, SARS-CoV-2 recruits several immune cells, *e.g.*, granulocytes, monocytes, and macrophages, and activates the complement cascade, resulting in high virus reproduction and violent infection[81,82]. Since the liver includes several cells related to the immune response, so, antibody-dependent, ACE2-independent pathway was activated[83]. As a result, SARS-CoV-2 infection overactivated and secreted excessive amounts of cytokines and chemokines such as TNF-α, IFN-γ, IL-6, IL-8[82].

Viral nucleocapsid proteins

Viral nucleocapsid proteins fused with the infected cells' host cell membrane, which permits the viral nucleocapsid protein to stay on the surface of the cell membrane[84]. This fusion makes the proteins easily recognizable by antigen-presenting cells that activate the immune response[83]. The normal antigen-presenting cells are dendritic cells, macrophage cells, monocytes, plasma cells, *etc.*, introduced to viral particles CD8+ cytotoxic and CD4+ regulatory T lymphocytes, the major histocompatibility complexes[85].

PRRs

Several PRRs are the first line receptors that detect pathogenic infection like SARS-CoV-2. After the virus enters the body, it produces pathogen-associated molecular patterns (PAMPs), which recognizes by PRRs and fires the standard innate immune system[86]. The membrane-bound toll-like receptor (TLR) family among PRRs, predominantly recognizes PAMPs in the extracellular system and to a lesser degree in the intracellular milieu[87]. Activation of this signal contributes to increasing the expression of transcription factors that induce pro-inflammatory cytokine production, such as NF-κB, and activate immune defense against viral infection *via* the IFN type I pathway[85,88].

Nucleotide-binding oligomerization domain, Leucine-rich Repeat and Pyrin domain-containing (nod-like receptor protein) receptor

Another family of pathogenic detecting receptors is nod-like receptor protein (NLRP) receptors (NLRP1, NLRP3, NLRP7, and NLRC4), which are the cytosol of endogenous danger-associated molecular patterns expressed inside the cell[89,90]. The activation of these receptors by SARS-CoV-2 has been reported to associate with the adhesion of molecules' activation, inflammatory response, and triggering innate immune cells[91]. This reaction contributes to the activation of pro-inflammatory mediators cytokines production such as TNF-α, IL-1, IL-6, IL-10, or type 1 interferons[92,93].

T-helper type 1 cell

The T-helper type 1 (Th1) cell response can be triggered by the elevation of inflammatory cytokines, which plays a significant role in providing a memory response against the virus and adaptive immunity. It is essential to coordinate humoral and cytotoxic T cell responses during viral infections[94]. Besides, elevated levels of Th2 cells secrete cytokines in patients with COVID-19, *e.g.*, IL-4 and IL-10, which inhibit inflammatory responses[95]. Furthermore, there was a significant increase in cytokines secreted by Th1 and Th2 cells, such as TNF-α, IL-6, IL-18, IL-4, and IL-10. Additionally, IL-2 and IL-6 are significantly elevated in patients with COVID-19 and correlate with the disease's seriousness[96]. Interestingly, hepatocytes, Kupffer cell, and hepatic stellate cells after being infected with SARS-CoV-2 immune cells after overactivation and secretion of excessive cytokines, *e.g.*, IL-6, IL-8, TNF-α, IFN-γ, which are involved in severe cytokine storm and causes tissue damage[85,97]. Compared to a reduced level of naive B cells, plasma B cells significantly increased in COVID-19 patients, several naive B-cell receptor isotypes [immunoglobulin heavy chain (IGHV) 3-15, IGHV3-30, and IGHV3-11] were previously used in the manufacture of other virus vaccines which were also reported and identified in patients[98]. Furthermore, the novel target genes in cytokine storm are IL-1β, IL-6, and the granulocyte-macrophage colony-stimulating factor (GM-CSF), while TNFSF13, IL-18, IL-2, and IL-4 seemed to help patients' recovery from COVID-19[99].

Complement activation

Viral infection has been reported to stimulate the complement cascade and consequently, initiate specific inflammatory responses[100]. Among these complements, complement factor 5a (C5a) is the most potent inflammatory peptide in the complement cascade, which increases the production of pro-inflammatory cytokines such as IL-6, IL-1, and TNF-α from macrophages under the effect of TLR-2, TLR-4, and TLR-9[101,102]. Terminal complement variable C5b-9 stimulates the release of IL-6 from vascular smooth muscle cells by stimulating the redox-sensitive transcription factor NF-κB, activator protein 1, and MCP-1[68,100]. Besides, C3a overexpression results in increased production of IL-1, IL-6, and TNF-α[103].

The complement cascade plays aberrant pivotal roles in the pathogenesis of SARS-CoV-2. It promotes viral nucleocapsid protein-mediated auto-activation of mannan-binding lectin serine peptidase-2 (MASP-2)[104]. Indeed, MASP-2 is considered the main serine protease in the lectin pathway. It binds to the mannose-binding lectin pathway to induce the downstream complement cascade, which in turn accelerates inflammatory responses. In two patients with COVID-19 who received an anti-C5a antibody, a positive clinical response was improved as evidence by enhancing lung oxygenation and alleviating systemic inflammation[105,106]. Hence anti-C5a antibodies could be a new therapeutic option for combating COVID-19 severity.

COVID-19 and hepatic dysfunction

Patients with digestive issues and co-infected with SARS-CoV-2 show a higher risk of mortality than patients without digestive problems. In severe cases of COVID-19, liver dysfunction was observed and associated with extensive activation of coagulative and fibrinolytic pathways as well as alteration of platelets, neutrophils, and lymphocytes profiles[8]. In parallel, patients with chronic liver disease (CLD), hepatitis viruses [hepatitis B virus (HBV), hepatitis C virus (HCV), hepatitis D virus, and hepatitis E virus], hepatotropic viruses infection, non-alcoholic fatty liver disease, and non-alcoholic steatohepatitis are more susceptible to COVID-19 and may present worse outcomes from ARDS compared with the other critically ill patients[82,107]. Alqahtani *et al*[108] performed a meta-analysis that showed that patients with a previous history of liver disease have a 57.33% chance of severing COVID-19 infection and a 17.65 % higher mortality rate than other patients[108]. A recent multicenter cohort study showed that hepatic decompensation was positively associated with COVID-19 disease, which increasing the risk of death from 26.2% to 63.2%[109]. This rate could be related to low platelets and lymphocytes in those patients or due to cirrhosis-related immune dysfunction[97]. Besides, COVID-19 is markedly distinguished by an increase in cytokine secretion, which induces hepatocytes injury, contributing to the loss of hepatic regeneration and worse clinical outcome, especially in patients with CLD[97,110]. In contrast, Lippi *et al*[111] indicated that CLD plays a minor role in affecting patients' progression, severity, or mortality[111].

The pattern of liver damage in COVID-19 is essentially considered during COVID-19. The liver injury can be associated with the virus's immediate cytopathic effect, unregulated immune response, sepsis, hypoxia, and drug-inducing liver injury[112,113]. Also, COVID-19 causes underlying chronic hepatic disorders to exacerbate and contributes to liver decompensation with higher mortality[114]. Recent general studies show that about 2%-11% of COVID-19 patients have underlying CLD, and 14%-53% developed hepatic dysfunction with COVID-19[8,14,115,116]. In patients with severe COVID-19, the ratio of hepatic injury is highly set in contrast to mild patients' rate. Hence, hepatic injury frequency can represent 58.06%, 51%, and 78% in patients' death from COVID-19[14]. Cai *et al*[117] conducted a study on 417 patients with COVID-19 which showed that about 76.3% of patients had abnormal liver test results and 21.5% exhibited liver injury during hospitalization[117]. Li *et al*[118] indicated that patients with abnormal liver activity (58.8% and 66.7%) could be more likely to have moderate to severe COVID-19[118].

It is understood that cholangiocytes play an essential role in liver regeneration and immune response, and cholangiocytes ACE2 expression is greater than that of hepatocytes[38,116,119]. Thus, it was proposed that the liver injury that resulted in SARS-CoV-2 infection could be due to the damage caused by virus infection to bile duct cells and not liver cells[113]. The expression of ACE2 in cholangiocytes was also observed, it is about 20 times higher than in hepatocytes[13]. Additionally, gamma-glutamyl transferase, a diagnostic biomarker for cholangiocyte injury, has also been identified to be highly up-regulated in severe cases of COVID-19[120,121]. However, aspartate aminotransferase (AST) and alanine aminotransferase (ALT) are elevated predominantly in COVID-19. Generally, it is 1-2 times more than the normal range,

which averages to modestly elevated total bilirubin (TBIL) levels early in the disease process[112,115,116]. On the contrary, the study conducted by Chen *et al*[122] showed an elevation of ALT and AST serum levels to 7590 U/L and 1445 U/L, respectively, in patients with severe COVID-19[122].

Several studies have found that AST, ALT, and TBIL were substantially higher in the intensive care unit (ICU) patients than in non-ICU patients[123,124]. A retrospective cohort study performed by Hundt *et al*[125] reported abnormal liver tests [AST, ALT, Alkaline phosphatase (ALP), and TBIL] in the patients with COVID-19. Most patients with abnormal liver tests had an elevation limit of 1-2 times more than the normal limits. It has also been reported that abnormal liver tests were directly proportionated with poorer clinical outcomes[125].

Hypothesizes of hepatic injury during COVID-19 illness

Hepatic injury in COVID-19 patients could result from a cytokine storm rather than direct cytopathic effects of the virus itself[112,113,126]. The direct cytopathic effects of SARS-CoV-2 can induce stress on endoplasmic reticulum and mitochondrial dysfunction[127]. Moreover, the human body can initiate immune-mediated inflammation, such as cytokine storm resulting in liver damage or hepatic failure in critical COVID-19 patients[128-130]. Hypoxia is also a common characteristic of extreme COVID-19 illness that promotes ROS production and initiates the release of multiple pro-inflammatory factors to induce more liver damage[82]. Electron microscope examination of liver obtained from patients infected with SARS-CoV-2 revealed that SARS-CoV-2 causes endoplasmic reticulum tension that induces de novo lipogenesis. Lipogenesis could also contribute to the production of non-specific inflammatory changes, including hepatocyte swelling and steatosis, mild hepatic sinus cell proliferation, and Kupffer cell hyperplasia[82].

Effect of SARS-CoV-2 on several types of liver disorders

As we mentioned before, SARS-CoV-2 is remarkably impactful on patients with chronic diseases, including chronic hepatic impairments. The impact of SARS-CoV-2 on several types of liver disorders is outlined in Table 1.

Non-alcoholic fatty liver disease and COVID-19

Several studies have documented that obesity is a significant mortality factor in COVID-19 patients. The need for overall survival and mechanical ventilation correlated with obesity[131]. Typically the ACE2 expression level in adipose tissue is greater than that of lung tissue[97]. These clarify adipose tissue's susceptibility to invasion by SARS-CoV-2, and then the virus can spread to other organs[132]. Obese patients are at high risk for non-alcoholic fatty liver disease (NAFLD), which in turn has a higher chance of developing severe COVID-19 with a higher probability of abnormal liver function and a more extended viral shedding period[133]. NAFLD is associated with the development and severity of COVID-19[97,133]. NAFLD patients also elevate cytokine levels, rendering them more vulnerable to COVID-19 related to excessive cytokine production[134]. Experimentally, it has been shown that ACE2 expression increases in chronic liver damage and NAFLD[135]. Patients with COVID-19 exhibit increased serum levels of MCP-1, which exacerbate steatohepatitis; thus, the virus can increase NAFLD progression to Non-alcoholic steatohepatitis (NASH)[136]. Multicenter retrospective by Hashemi *et al*[137] study the clinical outcome of COVID-19 and CLD. Patients with high NAFLD require ICU admission and mechanical ventilation. There is no overall mortality among CLD patients mainly due to NAFLD[137]. According to the evidence available, NAFLD is an independent risk factor for extreme COVID-19, but most studies did not separate NAFLD from its more extreme NASH[138].

Liver cirrhosis and COVID-19

Patients with liver cirrhosis have a potentially higher risk of SARS-CoV-2 infection, a higher risk of a severe condition, and a higher risk of liver decompensation[139]. Liver cirrhosis in SARS-CoV-2 infected patients is described as a predictor of mortality[140,141]. A decrease in ACE2 *via* SARS-CoV-2 induced internalization is predicted to exacerbate liver fibrosis and augment the disease's severity, especially in the long term. Therefore, the impact of COVID-19 on long-term liver-related outcomes is also worth considering in patients with cirrhosis[142]. A multicenter matched cohort study by Kushner and Cafardi[139] patients with cirrhosis plus COVID-19 were observed to have mortality equal to cirrhosis patients alone higher than those with COVID-19 alone[139]. Sarin *et al*[143] The APCOLIS study of pre-existing liver disease indicated that in CLD patients,

Table 1 Implication of severe acute respiratory syndrome coronavirus 2 on patients with hepatic disorders

Hepatic disorders	Main findings of the study	Ref.
NAFLD	NAFLD is associated with a higher risk of symptomatic, severe, and progressive COVID-19	Hashemi *et al*[137], 2020
	SARS-CoV-2 infection in patients with NAFLD required ICU admission and mechanical ventilation concomitant with increased NAFLD progression to NASH	Sachdeva *et al*[212], 2020
Liver cirrhosis	Patients with liver cirrhosis and COVID-19 are related to worse clinical outcomes and a high mortality rate than patients with COVID-19 alone	Kushner and Cafardi[139], 2020
	SARS-CoV-2 co-infection augmented liver injury as evidenced by worsens decompensated clinical status	Sarin *et al*[143], 2020
	Cirrhotic patients with COVID-19 had a higher risk of mortality than COVID-19 patients alone, but they are equally mortality rate with cirrhosis patients without COVID-19	Bajaj *et al*[144], 2021
HCC	Patients with HCC consider a risk group, and HCC is positively related to deterioration symptoms and bad outcomes in COVID-19	Zhang *et al*[213], 2020
	Patients with cancer are more susceptible to infection and poorer prognosis of COVID-19	Liang *et al*[147], 2020
Hepatitis B	Patients infected with HBV tend to have a more severe form of COVID-19	Chen *et al*[150], 2020
	SARS-CoV-2 and HBV co-infection showed monocytopenia, lymphopenia, and thrombocytopenia, as well as metabolic disorders	Liu *et al*[151], 2021
	COVID-19 may induce HBV reactivation, but it rarely occurs	Aldhaleei *et al*[152], 2020
Hepatitis C	Patients infected with HBV or HCV showed a high risk of mortality and morbidity if co-morbid with COVID-19	Mirzaie *et al*[155], 2020
	Patient with hepatic c and COVID-19 has an undesirable clinical outcome	Mostardeiro *et al*[156], 2020
	HCV pre-existing was associated with high mortality	Mangia *et al*[157], 2020

NAFLD: Non-alcoholic fatty liver disease; HCC: Hepatocellular carcinoma; NASH: Non-alcoholic steatohepatitis; SARS-CoV-2: Severe acute respiratory syndrome coronavirus 2; COVID-19: Coronavirus disease 2019; HBV: Hepatitis B virus; HCV: Hepatitis C virus; ICU: Intensive care units.

SARS-CoV-2 infection causes severe liver damage, decompensating one-fifth of the cirrhosis and worsening the already decompensated clinical status[143]. Bajaj *et al*[144] multicenter North American contemporaneously enrolled study, compared to patients with cirrhosis alone or cirrhosis and COVID-19 patients had similar mortality rate, but higher than patients with COVID-19 alone[144].

Hepatocellular carcinoma and COVID-19

In general, cancer patients, especially those who have recently received cancer treatment, have a greater chance of infection and a worse outcome. Besides, epidemiological data suggest that patients with cancer are more vulnerable to SARS-CoV-2 infection[145]. Hepatocellular carcinoma (HCC) is the sixth most prevalent cancer globally, accounting for about 6% of all cancer incidences[146]. HCC patients are more susceptible than other cancers to the consequences of the COVID-19 pandemic since the liver damage caused by SARS-CoV-2 could complicate current hepatitis in most HCC patients[146]. A retrospective cohort study by Yang *et al*[96] confirmed that cancer patients had deteriorating symptoms and bad results from SARS-CoV-2 infection[96]. Besides, these patients have poor nutritional status-related anemia and hypoproteinemia that impair their immunity, rendering them more vulnerable to severe disease[96].

A prospective nationwide cohort study in China on cancer patients, including HCC patents and COVID-19, was more vulnerable to severe disease. They had an increased chance of mortality and ICU admission. Recent chemotherapy within a month also increased the risk of severe disease[147]. Most HCC and CLD patients fall into a high-risk group and are expected to have worse outcomes[114]. Vigorous screening for COVID-19 disease should be prescribed in cancer patients undergoing antitumor therapy, and medications that induce suppression of immunity should be stopped, or their dosages decreased in the event of COVID-19[148].

Hepatitis B and COVID-19

For patients with chronic hepatitis B and are in the immune tolerance phase, further tests are required to confirm whether these patients have active viral replication and repeated liver damage after co-infection with SARS-CoV-2[82]. Several Chinese clinical

trials have found patients with hepatitis B infection are also present among patients with severe COVID-19 cases. That suggests that patients infected with HBV tend to have a more severe form of SARS-CoV-2[85,149]. Chen *et al*[150] found that 47% of patients with HBV are observed with severe COVID-19 cases[150]. However, other studies have shown that chronic viral hepatitis does not seem to be proportional to the severity of COVID-19[115]. Liu *et al*[151] retrospective study reported that COVID-19 was not substantially affected by co-infection with HBV. However, at the onset of COVID-19, patients co-infected with SARS-CoV-2 and HBV showed more severe monocytopenia, thrombocytopenia, hypoalbuminemia, and hepatic deficiency in lipid metabolism[151]. SARS-CoV-2 and HBV co-infection produces lymphopenia that can cause HBV reactivation. However, it has been reported just in one case of a patient with potential HBV reactivation, which seems to be an unusual event[152]. Chinese medical association and Chinese society of hepatology indicated that patients with hepatitis B administrated antiviral therapy, discontinuation of anti-HBV drugs, or failure to receive anti-HBV treatment can lead to the reactivation of HBV, especially during SRSA-CoV-2 infection following high-dose hormone therapy[82].

Hepatitis C and COVID-19

HCV infection is a dominant factor for liver diseases, including liver cirrhosis, hepatocellular carcinoma, and a common liver transplantation cause[153]. All over the world, HCV infection is the primary cause of liver-related mortality and morbidity[154]. Similarly, the symptoms of hepatic impairments are widespread among patients with COVID-19 and HCV[155]. Therefore, the American associations of liver disease evaluated the underline liver diseases' status, *e.g.*, hepatitis A, hepatitis B, and hepatitis C, in COVID-19 patients and found that co-infection between HCV and SARS Cov-2 increased liver enzyme levels, especially in pediatric[112]. Besides, a systematic preprint review by Mirzaie *et al*[155] suggested that patients with hepatitis B and/or hepatitis C present a high risk of morbidity to COVID-19 and require further investigation to overcome a significant marker of mortality due to co-infection[155]. Mostardeiro *et al*[156] reported that in a case study patient with hepatitis C and COVID-19 co-morbidity has an undesirable clinical outcome[156]. Correspondingly, a cohort study by Mangia *et al*[157] has been elucidated that HCV pre-existing associated with high mortality; meanwhile, HCV antibodies suggestive as a protective agent against COVID-19[157].

On the other hand, countries co-operated and adapted to develop a screening model to detect HCV as a hepatitis elimination program[158]. Nowadays, due to the spreading of the COVID-19 pandemic, it extends beyond the direct morbidity and mortality associated with coinfection COVID-19 may act as a barrier to reduce hepatitis C care, result in a decrease in HCV serological testing and identification[159]. Hence, Blach *et al*[160] based on their mathematical models, predicted scenario of the 1-year delay which resulted in an additional 44800 liver cancers and 72300 deaths from HCV globally by 2030[160]. Thus, rapid HCV testing in the context of SARS-CoV-2 screening programs may be the only solution for achieving the WHO's 2030 HCV elimination target[161].

Therapeutic approaches for aborting COVID-19 cytokine storm

As mentioned before, SARS-CoV-2 infections may cause cytokine storm to result in hyperactivation of T lymphocytes and release massive amounts of cytokines such as IL-6, IL-1β, TNF-α, and others[162]. Neutralization of these cytokines offer an excellent therapeutic avenue in combating the COVID-19 outbreak. Here, several therapeutic options can be used for terminating SARS-CoV-2-induced cytokine storm.

IL-6 inhibitors

IL-6 acts as a critical catalyst during cytokine storm, specifically during COVID-19[163]. Hence, IL-6 may be the main accused acute phase response, including fever, the elevation of CRP and ferritinemia, ARDS, multiorgan damage in cases of severe COVID-19[90,164]. Anti-IL-6 biologics targeted the IL-6 receptor or IL-6 itself with anti-inflammatory properties[44]. So, anti-IL-6 agents like tocilizumab, siltuximab, and sarilumab are all humanized monoclonal antibodies that are generated to the IL-6 receptor[165,166]. Currently, tocilizumab (TCZ) is used in active rheumatoid arthritis, juvenile idiopathic arthritis, autoimmune rheumatic diseases[165,167], temporal arteritis, and giant-cell arteritis[168]. Recently, TCZ is used to attenuate the adverse effects of the cytokine storm-induced by chimeric antigen receptor T cell treatment[169,170]. Giving TCZ a potential therapeutic option for critically ill patients with COVID-19 who have a significant elevation in the level of IL-6[171]. However, the treatment of COVID-19 with TCZ is an off-label use[172]. However, based on existing evidence, it could be a right and

safe choice to compete with cytokine storm during COVID-19. A retrospective study by Nasonov and Samsonov[172] indicated that tocilizumab directly enhances clinical outcomes in severe and critical COVID-19 patients, no noticeable adverse reactions were observed, and it is effectively reducing mortality[172]. Another retrospective study by Luo *et al*[173] reported that in COVID-19 patients with a risk of cytokine storm, TCZ is an excellent treatment choice. They are also recommended a repeat dose of TCZ for severe COVID-19 patients with elevated IL-6[173]. Because of its common uses in rheumatoid arthritis and other auto-inflammatory disorders, TCZ hepatic side effect is well known. Typically mild elevations of serum aminotransferase are observed[174]. In contrast, TCZ may be correlated with HBV reactivation. Hence, HBV serological test could be a part of routine pretreatment work-up[175].

IL-1 inhibitors

IL-1 is an active pro-inflammatory cytokine secreted during cytokine storm[49]. It can lower pain thresholds, on the other hand it is one of the cytokines playing a dominant role in tissue damage[176,177]. The IL-1 receptor antagonist, anakinra, canakinumab, and Rilonacept are already indicated in conditions characterized by sustained fevers and systemic inflammatory response such as rheumatoid arthritis, familial Mediterranean fever, and cryopyrin-associated periodic syndrome[169]. Anakinra is the first biologic recombinant IL-1R antagonist. Anakinra inhibits both IL-1α and IL-1β *via* competitively IL-1R binding[178]. As previously reported, anakinra is effective in attenuating cytokine storm[169,178]. These promising results suggest the role of anakinra in combating CS in patients with COVID-19[179]. A retrospective cohort study by Huet *et al*[180] showed that in patients with COVID-19, anakinra decreased both the need for invasive mechanical ventilation in the ICU and mortality rate without significant side effects[180]. Anakinra is not a hepatotoxic agent but is more likely to indirectly trigger acute liver damage through activity against IL-1 or the immune system. Moreover, it has not been related to hepatitis B reactivation[181].

TNF-α inhibitors

The viral spike protein of SARS-Cov2 induced a TNF-α converting enzyme-dependent shedding of the ACE2 ectodomain, facilitating viral penetration into cells and promoting tissue injury *via* increased TNF-α production[90,182]. TNF-α is a crucial cytokine produced in all inflammatory conditions, and autoimmune diseases stimulate inflammation and oxidative stress production. TNF-α is mainly produced by monocytes, macrophages, B cells, and other tissues[93,183]. Activation of TNF-α increases IL-1 and IL-6 release[49]. TNF-α inhibitors such as adalimumab, etanercept, and infliximab are used to manage several conditions like rheumatoid arthritis, ankylosing spondylitis, psoriatic arthritis, and inflammatory bowel disease[88,169]. Consequently, attenuate IL-6, IL-1, and VEGF levels as well as adhesion molecules and angiogenic factors. In patients with COVID-19, both plasma and tissues show an excessive amount of TNF-α[184]. Therefore, the anti-TNF-α antibody markedly reduces TNF-α in the blood, indicating that anti-TNF-α antibody could have potential anti-inflammatory benefits during COVID-19[185]. Additionally, it may cause downregulation of ACE2 expression and shedding[186,187]. So far, in treating patients with COVID-19, TNF-α blockers have not been proposed, but TNF-α blockers' effectiveness in treating patients with COVID-19 needs more priority[188,189].

JAK/STAT inhibitors

The JAK family and the adaptor-associated protein kinase 1 (AAK1) is a member of the numb-associated kinase family that plays a role in viral particles endocytosis, which act as a regulator of clathrin-mediated endocytosis[190,191]. Inhibitors of AAK1 can prevent viral particles entry into the cell[40,50]. Phosphorylated cytokine receptors recruit STAT transcription factors that modulate gene transcription. Furthermore, inhibiting activated cytokine receptors' phosphorylation through Janus kinase inhibitors, which could suppress cytokine signaling pathways[165]. Thus, AAK1 inhibitors have been suggested as possible candidates for the treatment of COVID-19. By inhibiting the JAK-STAT pathway, and cellular viral entry in COVID-19[192,193]. Janus kinase inhibitors such as baricitinib, filgotinib, fostamatinib, peficitinib, tofacitinib, and upadacitinib are previously indicated in managing the treatment of rheumatoid arthritis and autoimmune diseases[194,195]. Baricitinib is a JAK inhibitor with an extreme affinity to AAK1-binding[190]. Therefore, it inhibits the JAK-STAT pathway, that is used to suppress pro-inflammatory cytokine and attenuate the risk of cytokine storm[191,196]. Baricitinib is supposed to have dual effects in COVID 19 patients *via* reducing viral cell entry and inflammation[190]. One consideration related to the use of Baricitinib could be

superior to other JAK-STAT signaling inhibitors, as it is relatively safe[190,197]. However, baricitinib is in harmony with increased thromboembolic events, which affect the risk of developing these events in patients with COVID-19[198]. However, it is also probable that the JAK inhibitors might affect the activity of numerous cytokines, *e.g.*, INF-α, a potent mediator of antiviral response, may be impaired by JAK inhibitors[199]. Data by Bronte *et al*[200] suggests that baricitinib prevented the progression of COVID-19 by regulating patients' immune response, accordingly improving clinical outcomes[200].

Corticosteroids

Corticosteroids have a broad spectrum of cellular immune responses, different pharmacological activity, and wide therapeutic applications[201,202]. Glucocorticoids can inhibit innate and adaptive immune responses which are significantly used in inflammatory conditions and autoimmune disorders[203]. These anti-inflammatory and immunosuppressive effects occur in different mechanisms through direct actions on gene expression, transcription factors, and glucocorticoids' receptors' second messenger cascades[203]. Corticosteroids receptor complex induces gene transcription of many anti-inflammatory genes, involving IκB, which have immunosuppressive effects by inhibiting the activation of NF-κB signaling resulting in downregulation of IL-1β, IL-4, IL-10, IL-13, GM-CSF, TNF-α, and transforming growth factor-β[165,204,205].

Additionally, Corticosteroids reduce T cells and macrophages proliferation, activation, differentiation, and survival. Corticosteroids diminishes Th1 and macrophage pro-inflammatory cytokines IL-1β, IL-2, IL-6, TNF-α, and IL-17[206,207]. The uses of corticosteroids suppress the immune response, reduce viral clearance, and provoke viral replication[202]. Corticosteroids are widely used in critically ill patients with SARS and MERS infections[44]. Evidence has shown that corticosteroids' delayed their viral clearance[201]. The controversy on the use of corticosteroids remains far from definitive in COVID-19 patients. Corticosteroids decrease the pro-inflammatory cytokine's transcription, thus avoiding prolonged cytokine reaction and cytokine storm[208]. It allows corticosteroids in low doses and short duration and specific conditions with COVID-19 and requiring respiratory support the wat to survive[209]. In patients with COVID-19, trials indicated that dexamethasone in low dose, *i.e.*, 6 mg once daily orally for ten days reduced the death rate by one-third in patients who undergo ventilation and one-fifth in patients with oxygen supplementation[210]. Today, dexamethasone is widely used in severe COVID-19, including in patients with pre-existing CLD[211].

CONCLUSION

The outbreak of COVID-19 disease is the most annoying problem all over the world. This situation was developed due to a mutant version of the SARS virus called the SARS-CoV-2 virus. Studying the virus structure, mode of infection, and pathogenesis mechanism provided excellent hints about how we can fight it. In this review, we concluded that the most destructive power of the virus is the generation of violent cytokine storm, which is probably the cause of high mortality rates in hepatic and non-hepatic patients. Moreover, this review concluded that the possible ways to combat aggressive cytokine chaos might be a potential therapy for the COVID-19 patient co-morbid with liver disorders. Finally, this review encourages the scientists to study the SARS-CoV-2 virus cytokine storm in deep to find more effective and promising therapy for COVID-19 illness.

REFERENCES

1 **Yin Y**, Wunderink RG. MERS, SARS and other coronaviruses as causes of pneumonia. *Respirology* 2018; **23**: 130-137 [PMID: 29052924 DOI: 10.1111/resp.13196]

2 **Zheng J**. SARS-CoV-2: an Emerging Coronavirus that Causes a Global Threat. *Int J Biol Sci* 2020; **16**: 1678-1685 [PMID: 32226285 DOI: 10.7150/ijbs.45053]

3 **Páramo JA**. [Coagulopathy and thrombosis: similarities and differences among pathogenic coronaviruses]. *An Sist Sanit Navar* 2020; **43**: 245-249 [PMID: 32814926 DOI: 10.23938/ASSN.0885]

4 **Zhong NS**, Zheng BJ, Li YM, Poon, Xie ZH, Chan KH, Li PH, Tan SY, Chang Q, Xie JP, Liu XQ, Xu J, Li DX, Yuen KY, Peiris, Guan Y. Epidemiology and cause of severe acute respiratory syndrome (SARS) in Guangdong, People's Republic of China, in February, 2003. *Lancet* 2003; **362**: 1353-1358 [PMID: 14585636 DOI: 10.1016/s0140-6736(03)14630-2]

5 **Zaki AM**, van Boheemen S, Bestebroer TM, Osterhaus AD, Fouchier RA. Isolation of a novel coronavirus from a man with pneumonia in Saudi Arabia. *N Engl J Med* 2012; **367**: 1814-1820 [PMID: 23075143 DOI: 10.1056/NEJMoa1211721]

6 **Morens DM**, Fauci AS. Emerging Pandemic Diseases: How We Got to COVID-19. *Cell* 2020; **182**: 1077-1092 [PMID: 32846157 DOI: 10.1016/j.cell.2020.08.021]

7 **Li H**, Liu SM, Yu XH, Tang SL, Tang CK. Coronavirus disease 2019 (COVID-19): current status and future perspectives. *Int J Antimicrob Agents* 2020; **55**: 105951 [PMID: 32234466 DOI: 10.1016/j.ijantimicag.2020.105951]

8 **Wang D**, Hu B, Hu C, Zhu F, Liu X, Zhang J, Wang B, Xiang H, Cheng Z, Xiong Y, Zhao Y, Li Y, Wang X, Peng Z. Clinical Characteristics of 138 Hospitalized Patients With 2019 Novel Coronavirus-Infected Pneumonia in Wuhan, China. *JAMA* 2020; **323**: 1061-1069 [PMID: 32031570 DOI: 10.1001/jama.2020.1585]

9 **Singhal T**. A Review of Coronavirus Disease-2019 (COVID-19). *Indian J Pediatr* 2020; **87**: 281-286 [PMID: 32166607 DOI: 10.1007/s12098-020-03263-6]

10 **Guo YR**, Cao QD, Hong ZS, Tan YY, Chen SD, Jin HJ, Tan KS, Wang DY, Yan Y. The origin, transmission and clinical therapies on coronavirus disease 2019 (COVID-19) outbreak - an update on the status. *Mil Med Res* 2020; **7**: 11 [PMID: 32169119 DOI: 10.1186/s40779-020-00240-0]

11 **Wrapp D**, Wang N, Corbett KS, Goldsmith JA, Hsieh CL, Abiona O, Graham BS, McLellan JS. Cryo-EM structure of the 2019-nCoV spike in the prefusion conformation. *Science* 2020; **367**: 1260-1263 [PMID: 32075877 DOI: 10.1126/science.abb2507]

12 **Tang X**, Du R, Wang R, Cao T, Guan L, Shi H. Comparison of hospitalized patients with acute respiratory distress syndrome caused by covid-19 and H1N1. *Chest* 2020; 158 [DOI: 10.1016/j.chest.2020.03.032]

13 **Ahn JY**, Sohn Y, Lee SH, Cho Y, Hyun JH, Baek YJ, Jeong SJ, Kim JH, Ku NS, Yeom JS, Roh J, Ahn MY, Chin BS, Kim YS, Lee H, Yong D, Kim HO, Kim S, Choi JY. Use of Convalescent Plasma Therapy in Two COVID-19 Patients with Acute Respiratory Distress Syndrome in Korea. *J Korean Med Sci* 2020; **35**: e149 [PMID: 32281317 DOI: 10.3346/jkms.2020.35.e149]

14 **Cai Q**, Huang D, Ou P, Yu H, Zhu Z, Xia Z, Su Y, Ma Z, Zhang Y, Li Z, He Q, Liu L, Fu Y, Chen J. COVID-19 in a designated infectious diseases hospital outside Hubei Province, China. *Allergy* 2020; **75**: 1742-1752 [PMID: 32239761 DOI: 10.1111/all.14309]

15 **Fani M**, Teimoori A, Ghafari S. Comparison of the COVID-2019 (SARS-CoV-2) pathogenesis with SARS-CoV and MERS-CoV infections. *Future Virol* 2020; 15 [DOI: 10.2217/fvl-2020-0050]

16 **Segreto R**, Deigin Y. The genetic structure of SARS-CoV-2 does not rule out a laboratory origin: SARS-CoV-2 chimeric structure and furin cleavage site might be the result of genetic manipulation. *Bioessays* 2021; **43**: e2000240 [PMID: 33200842 DOI: 10.1002/bies.202000240]

17 **Sun P**, Lu X, Xu C, Sun W, Pan B. Understanding of COVID-19 based on current evidence. *J Med Virol* 2020; **92**: 548-551 [PMID: 32096567 DOI: 10.1002/jmv.25722]

18 **Khan S**, Siddique R, Shereen MA, Ali A, Liu J, Bai Q, Bashir N, Xue M. Emergence of a Novel Coronavirus, Severe Acute Respiratory Syndrome Coronavirus 2: Biology and Therapeutic Options. *J Clin Microbiol* 2020; **58** [PMID: 32161092 DOI: 10.1128/jcm.00187-20]

19 **Zhou P**, Yang XL, Wang XG, Hu B, Zhang L, Zhang W, Si HR, Zhu Y, Li B, Huang CL, Chen HD, Chen J, Luo Y, Guo H, Jiang RD, Liu MQ, Chen Y, Shen XR, Wang X, Zheng XS, Zhao K, Chen QJ, Deng F, Liu LL, Yan B, Zhan FX, Wang YY, Xiao GF, Shi ZL. A pneumonia outbreak associated with a new coronavirus of probable bat origin. *Nature* 2020; **579**: 270-273 [PMID: 32015507 DOI: 10.1038/s41586-020-2012-7]

20 **Bar-On YM**, Flamholz A, Phillips R, Milo R. SARS-CoV-2 (COVID-19) by the numbers. *Elife* 2020; **9** [PMID: 32228860 DOI: 10.7554/eLife.57309]

21 **Cui J**, Li F, Shi ZL. Origin and evolution of pathogenic coronaviruses. *Nat Rev Microbiol* 2019; **17**: 181-192 [PMID: 30531947 DOI: 10.1038/s41579-018-0118-9]

22 **Chan JF**, Kok KH, Zhu Z, Chu H, To KK, Yuan S, Yuen KY. Genomic characterization of the 2019 novel human-pathogenic coronavirus isolated from a patient with atypical pneumonia after visiting Wuhan. *Emerg Microbes Infect* 2020; **9**: 221-236 [PMID: 31987001 DOI: 10.1080/22221751.2020.1719902]

23 **Wan Y**, Shang J, Graham R, Baric RS, Li F. Receptor Recognition by the Novel Coronavirus from Wuhan: an Analysis Based on Decade-Long Structural Studies of SARS Coronavirus. *J Virol* 2020; **94**: e00127-20 [PMID: 31996437 DOI: 10.1128/JVI.00127-20]

24 **Lu R**, Zhao X, Li J, Niu P, Yang B, Wu H, Wang W, Song H, Huang B, Zhu N, Bi Y, Ma X, Zhan F, Wang L, Hu T, Zhou H, Hu Z, Zhou W, Zhao L, Chen J, Meng Y, Wang J, Lin Y, Yuan J, Xie Z, Ma J, Liu WJ, Wang D, Xu W, Holmes EC, Gao GF, Wu G, Chen W, Shi W, Tan W. Genomic characterisation and epidemiology of 2019 novel coronavirus: implications for virus origins and receptor binding. *Lancet* 2020; **395**: 565-574 [PMID: 32007145 DOI: 10.1016/S0140-6736(20)30251-8]

25 **Belouzard S**, Millet JK, Licitra BN, Whittaker GR. Mechanisms of coronavirus cell entry mediated by the viral spike protein. *Viruses* 2012; **4**: 1011-1033 [PMID: 22816037 DOI: 10.3390/v4061011]

26 **Vennema H**, Godeke GJ, Rossen JW, Voorhout WF, Horzinek MC, Opstelten DJ, Rottier PJ. Nucleocapsid-independent assembly of coronavirus-like particles by co-expression of viral envelope protein genes. *EMBO J* 1996; **15**: 2020-2028 [PMID: 8617249]

27 **Neuman BW**, Kiss G, Kunding AH, Bhella D, Baksh MF, Connelly S, Droese B, Klaus JP, Makino S, Sawicki SG, Siddell SG, Stamou DG, Wilson IA, Kuhn P, Buchmeier MJ. A structural analysis of

M protein in coronavirus assembly and morphology. *J Struct Biol* 2011; **174**: 11-22 [PMID: 21130884 DOI: 10.1016/j.jsb.2010.11.021]

28 **van der Hoeven B**, Oudshoorn D, Koster AJ, Snijder EJ, Kikkert M, Bárcena M. Biogenesis and architecture of arterivirus replication organelles. *Virus Res* 2016; **220**: 70-90 [PMID: 27071852 DOI: 10.1016/j.virusres.2016.04.001]

29 **Cohen FS**. How Viruses Invade Cells. *Biophys J* 2016; **110**: 1028-1032 [PMID: 26958878 DOI: 10.1016/j.bpj.2016.02.006]

30 **Li W**, Moore MJ, Vasilieva N, Sui J, Wong SK, Berne MA, Somasundaran M, Sullivan JL, Luzuriaga K, Greenough TC, Choe H, Farzan M. Angiotensin-converting enzyme 2 is a functional receptor for the SARS coronavirus. *Nature* 2003; **426**: 450-454 [PMID: 14647384 DOI: 10.1038/nature02145]

31 **Letko M**, Marzi A, Munster V. Functional assessment of cell entry and receptor usage for SARS-CoV-2 and other lineage B betacoronaviruses. *Nat Microbiol* 2020; **5**: 562-569 [PMID: 32094589 DOI: 10.1038/s41564-020-0688-y]

32 **Fehr AR**, Perlman S. Coronaviruses: an overview of their replication and pathogenesis. *Methods Mol Biol* 2015; **1282**: 1-23 [PMID: 25720466 DOI: 10.1007/978-1-4939-2438-7_1]

33 **Xu H**, Zhong L, Deng J, Peng J, Dan H, Zeng X, Li T, Chen Q. High expression of ACE2 receptor of 2019-nCoV on the epithelial cells of oral mucosa. *Int J Oral Sci* 2020; **12**: 8 [PMID: 32094336 DOI: 10.1038/s41368-020-0074-x]

34 **Hamming I**, Timens W, Bulthuis ML, Lely AT, Navis G, van Goor H. Tissue distribution of ACE2 protein, the functional receptor for SARS coronavirus. A first step in understanding SARS pathogenesis. *J Pathol* 2004; **203**: 631-637 [PMID: 15141377 DOI: 10.1002/path.1570]

35 **Serafim RB**, Póvoa P, Souza-Dantas V, Kalil AC, Salluh JIF. Clinical course and outcomes of critically ill patients with COVID-19 infection: a systematic review. *Clin Microbiol Infect* 2021; **27**: 47-54 [PMID: 33190794 DOI: 10.1016/j.cmi.2020.10.017]

36 **Sparks MA**, South A, Welling P, Luther JM, Cohen J, Byrd JB, Burrell LM, Batlle D, Tomlinson L, Bhalla V, Rheault MN, Soler MJ, Swaminathan S, Hiremath S. Sound Science before Quick Judgement Regarding RAS Blockade in COVID-19. *Clin J Am Soc Nephrol* 2020; **15**: 714-716 [PMID: 32220930 DOI: 10.2215/CJN.03530320]

37 **Liu Y**, Yang Y, Zhang C, Huang F, Wang F, Yuan J, Wang Z, Li J, Feng C, Zhang Z, Wang L, Peng L, Chen L, Qin Y, Zhao D, Tan S, Yin L, Xu J, Zhou C, Jiang C, Liu L. Clinical and biochemical indexes from 2019-nCoV infected patients linked to viral loads and lung injury. *Sci China Life Sci* 2020; **63**: 364-374 [PMID: 32048163 DOI: 10.1007/s11427-020-1643-8]

38 **Chai X**, Hu L, Zhang Y, Han W, Lu Z, Ke A, Zhou J, Shi G, Fang N, Fan J, Cai J, Lan F. Specific ACE2 Expression in Cholangiocytes May Cause Liver Damage After 2019-nCoV Infection. 2020 Preprint. Available from: bioRxiv:2020.2002.2003.931766 [DOI: 10.1101/2020.02.03.931766]

39 **Kumar P**, Sharma M, Kulkarni A, Rao PN. Pathogenesis of Liver Injury in Coronavirus Disease 2019. *J Clin Exp Hepatol* 2020; **10**: 641-642 [PMID: 32837092 DOI: 10.1016/j.jceh.2020.05.006]

40 **Salamanna F**, Maglio M, Landini MP, Fini M. Body Localization of ACE-2: On the Trail of the Keyhole of SARS-CoV-2. *Front Med (Lausanne)* 2020; **7**: 594495 [PMID: 33344479 DOI: 10.3389/fmed.2020.594495]

41 **Zhao S**, Lin Q, Ran J, Musa SS, Yang G, Wang W, Lou Y, Gao D, Yang L, He D, Wang MH. Preliminary estimation of the basic reproduction number of novel coronavirus (2019-nCoV) in China, from 2019 to 2020: A data-driven analysis in the early phase of the outbreak. *Int J Infect Dis* 2020; **92**: 214-217 [PMID: 32007643 DOI: 10.1016/j.ijid.2020.01.050]

42 **Garrido I**, Liberal R, Macedo G. Review article: COVID-19 and liver disease-what we know on 1st May 2020. *Aliment Pharmacol Ther* 2020; **52**: 267-275 [PMID: 32402090 DOI: 10.1111/apt.15813]

43 **Tisoncik JR**, Korth MJ, Simmons CP, Farrar J, Martin TR, Katze MG. Into the eye of the cytokine storm. *Microbiol Mol Biol Rev* 2012; **76**: 16-32 [PMID: 22390970 DOI: 10.1128/MMBR.05015-11]

44 **Tang Y**, Liu J, Zhang D, Xu Z, Ji J, Wen C. Cytokine Storm in COVID-19: The Current Evidence and Treatment Strategies. *Front Immunol* 2020; **11**: 1708 [PMID: 32754163 DOI: 10.3389/fimmu.2020.01708]

45 **Kalaiyarasu S**, Kumar M, Senthil Kumar D, Bhatia S, Dash SK, Bhat S, Khetan RK, Nagarajan S. Highly pathogenic avian influenza H5N1 virus induces cytokine dysregulation with suppressed maturation of chicken monocyte-derived dendritic cells. *Microbiol Immunol* 2016; **60**: 687-693 [PMID: 27730669 DOI: 10.1111/1348-0421.12443]

46 **Lau SKP**, Lau CCY, Chan KH, Li CPY, Chen H, Jin DY, Chan JFW, Woo PCY, Yuen KY. Delayed induction of proinflammatory cytokines and suppression of innate antiviral response by the novel Middle East respiratory syndrome coronavirus: implications for pathogenesis and treatment. *J Gen Virol* 2013; **94**: 2679-2690 [PMID: 24077366 DOI: 10.1099/vir.0.055533-0]

47 **Woo PC**, Tung ET, Chan KH, Lau CC, Lau SK, Yuen KY. Cytokine profiles induced by the novel swine-origin influenza A/H1N1 virus: implications for treatment strategies. *J Infect Dis* 2010; **201**: 346-353 [PMID: 20030555 DOI: 10.1086/649785]

48 **Channappanavar R**, Perlman S. Pathogenic human coronavirus infections: causes and consequences of cytokine storm and immunopathology. *Semin Immunopathol* 2017; **39**: 529-539 [PMID: 28466096 DOI: 10.1007/s00281-017-0629-x]

49 **Costela-Ruiz VJ**, Illescas-Montes R, Puerta-Puerta JM, Ruiz C, Melguizo-Rodríguez L. SARS-CoV-2 infection: The role of cytokines in COVID-19 disease. *Cytokine Growth Factor Rev* 2020; **54**: 62-75 [PMID: 32513566 DOI: 10.1016/j.cytogfr.2020.06.001]

50 **Ragab D**, Salah Eldin H, Taeimah M, Khattab R, Salem R. The COVID-19 Cytokine Storm; What We Know So Far. *Front Immunol* 2020; **11**: 1446 [PMID: 32612617 DOI: 10.3389/fimmu.2020.01446]

51 **Coperchini F**, Chiovato L, Croce L, Magri F, Rotondi M. The cytokine storm in COVID-19: An overview of the involvement of the chemokine/chemokine-receptor system. *Cytokine Growth Factor Rev* 2020; **53**: 25-32 [PMID: 32446778 DOI: 10.1016/j.cytogfr.2020.05.003]

52 **Zhou F**, Yu T, Du R, Fan G, Liu Y, Liu Z, Xiang J, Wang Y, Song B, Gu X, Guan L, Wei Y, Li H, Wu X, Xu J, Tu S, Zhang Y, Chen H, Cao B. Clinical course and risk factors for mortality of adult inpatients with COVID-19 in Wuhan, China: a retrospective cohort study. *Lancet* 2020; **395**: 1054-1062 [PMID: 32171076 DOI: 10.1016/S0140-6736(20)30566-3]

53 **Herold T**, Jurinovic V, Arnreich C, Hellmuth JC, von Bergwelt-Baildon M, Klein M, Weinberger T. Level of IL-6 predicts respiratory failure in hospitalized symptomatic COVID-19 patients. 2020 Preprint. Available from: medRxiv:2020.2004.2001.20047381 [DOI: 10.1101/2020.04.01.20047381]

54 **Miao Y**, Fan L, Li JY. Potential Treatments for COVID-19 Related Cytokine Storm - Beyond Corticosteroids. *Front Immunol* 2020; **11**: 1445 [PMID: 32612616 DOI: 10.3389/fimmu.2020.01445]

55 **Kuba K**, Imai Y, Rao S, Gao H, Guo F, Guan B, Huan Y, Yang P, Zhang Y, Deng W, Bao L, Zhang B, Liu G, Wang Z, Chappell M, Liu Y, Zheng D, Leibbrandt A, Wada T, Slutsky AS, Liu D, Qin C, Jiang C, Penninger JM. A crucial role of angiotensin converting enzyme 2 (ACE2) in SARS coronavirus-induced lung injury. *Nat Med* 2005; **11**: 875-879 [PMID: 16007097 DOI: 10.1038/nm1267]

56 **Oudit GY**, Kassiri Z, Jiang C, Liu PP, Poutanen SM, Penninger JM, Butany J. SARS-coronavirus modulation of myocardial ACE2 expression and inflammation in patients with SARS. *Eur J Clin Invest* 2009; **39**: 618-625 [PMID: 19453650 DOI: 10.1111/j.1365-2362.2009.02153.x]

57 **Border WA**, Noble NA. Interactions of transforming growth factor-beta and angiotensin II in renal fibrosis. *Hypertension* 1998; **31**: 181-188 [PMID: 9453300 DOI: 10.1161/01.HYP.31.1.181]

58 **Perlman S**, Netland J. Coronaviruses post-SARS: update on replication and pathogenesis. *Nat Rev Microbiol* 2009; **7**: 439-450 [PMID: 19430490 DOI: 10.1038/nrmicro2147]

59 **Santos RA**, Simoes e Silva AC, Maric C, Silva DM, Machado RP, de Buhr I, Heringer-Walther S, Pinheiro SV, Lopes MT, Bader M, Mendes EP, Lemos VS, Campagnole-Santos MJ, Schultheiss HP, Speth R, Walther T. Angiotensin-(1-7) is an endogenous ligand for the G protein-coupled receptor Mas. *Proc Natl Acad Sci USA* 2003; **100**: 8258-8263 [PMID: 12829792 DOI: 10.1073/pnas.1432869100]

60 **Imai Y**, Kuba K, Rao S, Huan Y, Guo F, Guan B, Yang P, Sarao R, Wada T, Leong-Poi H, Crackower MA, Fukamizu A, Hui CC, Hein L, Uhlig S, Slutsky AS, Jiang C, Penninger JM. Angiotensin-converting enzyme 2 protects from severe acute lung failure. *Nature* 2005; **436**: 112-116 [PMID: 16001071 DOI: 10.1038/nature03712]

61 **Donoghue M**, Hsieh F, Baronas E, Godbout K, Gosselin M, Stagliano N, Donovan M, Woolf B, Robison K, Jeyaseelan R, Breitbart RE, Acton S. A novel angiotensin-converting enzyme-related carboxypeptidase (ACE2) converts angiotensin I to angiotensin 1-9. *Circ Res* 2000; **87**: E1-E9 [PMID: 10969042 DOI: 10.1161/01.res.87.5.e1]

62 **Tipnis SR**, Hooper NM, Hyde R, Karran E, Christie G, Turner AJ. A human homolog of angiotensin-converting enzyme. Cloning and functional expression as a captopril-insensitive carboxypeptidase. *J Biol Chem* 2000; **275**: 33238-33243 [PMID: 10924499 DOI: 10.1074/jbc.M002615200]

63 **Dalan R**, Bornstein SR, El-Armouche A, Rodionov RN, Markov A, Wielockx B, Beuschlein F, Boehm BO. The ACE-2 in COVID-19: Foe or Friend? *Horm Metab Res* 2020; **52**: 257-263 [PMID: 32340044 DOI: 10.1055/a-1155-0501]

64 **Simões e Silva AC**, Silveira KD, Ferreira AJ, Teixeira MM. ACE2, angiotensin-(1-7) and Mas receptor axis in inflammation and fibrosis. *Br J Pharmacol* 2013; **169**: 477-492 [PMID: 23488800 DOI: 10.1111/bph.12159]

65 **Tikellis C**, Thomas MC. Angiotensin-Converting Enzyme 2 (ACE2) Is a Key Modulator of the Renin Angiotensin System in Health and Disease. *Int J Pept* 2012; **2012**: 256294 [PMID: 22536270 DOI: 10.1155/2012/256294]

66 **Fyhrquist F**, Saijonmaa O. Renin-angiotensin system revisited. *J Intern Med* 2008; **264**: 224-236 [PMID: 18793332 DOI: 10.1111/j.1365-2796.2008.01981.x]

67 **Mancini L**, Quinzi V, Mummolo S, Marzo G, Marchetti EJAS. Angiotensin-Converting Enzyme 2 as a Possible Correlation between COVID-19 and Periodontal Disease. *Appl Sci* 2020; **10**: 6224 [DOI: 10.3390/app10186224]

68 **Mahmudpour M**, Roozbeh J, Keshavarz M, Farrokhi S, Nabipour I. COVID-19 cytokine storm: The anger of inflammation. *Cytokine* 2020; **133**: 155151 [PMID: 32544563 DOI: 10.1016/j.cyto.2020.155151]

69 **Mehta PK**, Griendling KK. Angiotensin II cell signaling: physiological and pathological effects in the cardiovascular system. *Am J Physiol Cell Physiol* 2007; **292**: C82-C97 [PMID: 16870827 DOI: 10.1152/ajpcell.00287.2006]

70 **Iwasaki M**, Saito J, Zhao H, Sakamoto A, Hirota K, Ma D. Inflammation Triggered by SARS-CoV-2 and ACE2 Augment Drives Multiple Organ Failure of Severe COVID-19: Molecular Mechanisms and Implications. *Inflammation* 2021; **44**: 13-34 [PMID: 33029758 DOI:

10.1007/s10753-020-01337-3]
71 **Ji Y**, Liu J, Wang Z, Liu N. Angiotensin II induces inflammatory response partly *via* toll-like receptor 4-dependent signaling pathway in vascular smooth muscle cells. *Cell Physiol Biochem* 2009; **23**: 265-276 [PMID: 19471094 DOI: 10.1159/000218173]
72 **Chaudhary M**. COVID-19 susceptibility: potential of ACE2 polymorphisms. *Egyp J Med Hum Genet* 2020; **21**: 54 [DOI: 10.1186/s43042-020-00099-9]
73 **Gheblawi M**, Wang K, Viveiros A, Nguyen Q, Zhong JC, Turner AJ, Raizada MK, Grant MB, Oudit GY. Angiotensin-Converting Enzyme 2: SARS-CoV-2 Receptor and Regulator of the Renin-Angiotensin System: Celebrating the 20th Anniversary of the Discovery of ACE2. *Circ Res* 2020; **126**: 1456-1474 [PMID: 32264791 DOI: 10.1161/CIRCRESAHA.120.317015]
74 **Mustafa MI**, Abdelmoneim AH, Mahmoud EM, Makhawi AM. Cytokine Storm in COVID-19 Patients, Its Impact on Organs and Potential Treatment by QTY Code-Designed Detergent-Free Chemokine Receptors. *Mediators Inflamm* 2020; **2020**: 8198963 [PMID: 33029105 DOI: 10.1155/2020/8198963]
75 **Saba L**, Gerosa C, Fanni D, Marongiu F, La Nasa G, Caocci G, Barcellona D, Balestrieri A, Coghe F, Orru G, Coni P, Piras M, Ledda F, Suri JS, Ronchi A, D'Andrea F, Cau R, Castagnola M, Faa G. Molecular pathways triggered by COVID-19 in different organs: ACE2 receptor-expressing cells under attack? *Eur Rev Med Pharmacol Sci* 2020; **24**: 12609-12622 [PMID: 33336781 DOI: 10.26355/eurrev_202012_24058]
76 **Hirano T**, Murakami M. COVID-19: A New Virus, but a Familiar Receptor and Cytokine Release Syndrome. *Immunity* 2020; **52**: 731-733 [PMID: 32325025 DOI: 10.1016/j.immuni.2020.04.003]
77 **Fan Z**, Chen L, Li J, Cheng X, Yang J, Tian C, Zhang Y, Huang S, Liu Z, Cheng J. Clinical Features of COVID-19-Related Liver Functional Abnormality. *Clin Gastroenterol Hepatol* 2020; **18**: 1561-1566 [PMID: 32283325 DOI: 10.1016/j.cgh.2020.04.002]
78 **Amraei R**, Rahimi N. COVID-19, Renin-Angiotensin System and Endothelial Dysfunction. *Cells* 2020; **9** [PMID: 32660065 DOI: 10.3390/cells9071652]
79 **Medina-Enríquez MM**, Lopez-León S, Carlos-Escalante JA, Aponte-Torres Z, Cuapio A, Wegman-Ostrosky T. ACE2: the molecular doorway to SARS-CoV-2. *Cell Biosci* 2020; **10**: 148 [PMID: 33380340 DOI: 10.1186/s13578-020-00519-8]
80 **Sansoè G**, Aragno M, Wong F. Pathways of hepatic and renal damage through non-classical activation of the renin-angiotensin system in chronic liver disease. *Liver Int* 2020; **40**: 18-31 [PMID: 31580514 DOI: 10.1111/liv.14272]
81 **Liu C**, Jiang ZC, Shao CX, Zhang HG, Yue HM, Chen ZH, Ma BY, Liu WY, Huang HH, Yang J, Wang Y, Liu HY, Xu D, Wang JT, Yang JY, Pan HQ, Zou SQ, Li FJ, Lei JQ, Li X, He Q, Gu Y, Qi XL. [Preliminary study of the relationship between novel coronavirus pneumonia and liver function damage: a multicenter study]. *Zhonghua Gan Zang Bing Za Zhi* 2020; **28**: 107-111 [PMID: 32077660 DOI: 10.3760/cma.j.issn.1007-3418.2020.02.003]
82 **Tian D**, Ye Q. Hepatic complications of COVID-19 and its treatment. *J Med Virol* 2020; **92**: 1818-1824 [PMID: 32437004 DOI: 10.1002/jmv.26036]
83 **Shah VK**, Firmal P, Alam A, Ganguly D, Chattopadhyay S. Overview of Immune Response During SARS-CoV-2 Infection: Lessons From the Past. *Front Immunol* 2020; **11**: 1949 [PMID: 32849654 DOI: 10.3389/fimmu.2020.01949]
84 **Tang T**, Bidon M, Jaimes JA, Whittaker GR, Daniel S. Coronavirus membrane fusion mechanism offers a potential target for antiviral development. *Antiviral Res* 2020; **178**: 104792 [PMID: 32272173 DOI: 10.1016/j.antiviral.2020.104792]
85 **Sahin TT**, Akbulut S, Yilmaz S. COVID-19 pandemic: Its impact on liver disease and liver transplantation. *World J Gastroenterol* 2020; **26**: 2987-2999 [PMID: 32587443 DOI: 10.3748/wjg.v26.i22.2987]
86 **Mogensen TH**. Pathogen recognition and inflammatory signaling in innate immune defenses. *Clin Microbiol Rev* 2009; **22**: 240-273, Table of Contents [PMID: 19366914 DOI: 10.1128/CMR.00046-08]
87 **Iqbal MS**, Sardar N, Akmal W, Sultan R, Abdullah H, Qindeel M, Dhama K, Bila M. Role of toll-like receptors in coronavirus infection and immune response. *J Exp Biol Agric Sci* 2020; **8**: S66-S78 [DOI: 10.18006/2020.8(Spl-1-SARS-CoV-2).S66.S78]
88 **Soy M**, Keser G, Atagündüz P, Tabak F, Atagündüz I, Kayhan S. Cytokine storm in COVID-19: pathogenesis and overview of anti-inflammatory agents used in treatment. *Clin Rheumatol* 2020; **39**: 2085-2094 [PMID: 32474885 DOI: 10.1007/s10067-020-05190-5]
89 **Jamilloux Y**, Henry T, Belot A, Viel S, Fauter M, El Jammal T, Walzer T, François B, Sève P. Should we stimulate or suppress immune responses in COVID-19? *Autoimmun Rev* 2020; **19**: 102567 [PMID: 32376392 DOI: 10.1016/j.autrev.2020.102567]
90 **Iannaccone G**, Scacciavillani R, Del Buono MG, Camilli M, Ronco C, Lavie CJ, Abbate A, Crea F, Massetti M, Aspromonte N. Weathering the Cytokine Storm in COVID-19: Therapeutic Implications. *Cardiorenal Med* 2020; **10**: 277-287 [PMID: 32599589 DOI: 10.1159/000509483]
91 **Franchi L**, Warner N, Viani K, Nuñez G. Function of Nod-like receptors in microbial recognition and host defense. *Immunol Rev* 2009; **227**: 106-128 [PMID: 19120480 DOI: 10.1111/j.1600-065X.2008.00734.x]
92 **Kawai T**, Akira S. TLR signaling. *Cell Death Differ* 2006; **13**: 816-825 [PMID: 16410796 DOI: 10.1038/sj.cdd.4401850]
93 **Kany S**, Vollrath JT, Relja B. Cytokines in Inflammatory Disease. *Int J Mol Sci* 2019; **20** [PMID:

31795299 DOI: 10.3390/ijms20236008]
94 **Marchingo JM**, Sinclair LV, Howden AJ, Cantrell DA. Quantitative analysis of how Myc controls T cell proteomes and metabolic pathways during T cell activation. *Elife* 2020; **9** [PMID: 32022686 DOI: 10.7554/eLife.53725]
95 **Ye Q**, Wang B, Mao J. The pathogenesis and treatment of the `Cytokine Storm' in COVID-19. *J Infect* 2020; **80**: 607-613 [PMID: 32283152 DOI: 10.1016/j.jinf.2020.03.037]
96 **Yang X**, Yu Y, Xu J, Shu H, Xia J, Liu H, Wu Y, Zhang L, Yu Z, Fang M, Yu T, Wang Y, Pan S, Zou X, Yuan S, Shang Y. Clinical course and outcomes of critically ill patients with SARS-CoV-2 pneumonia in Wuhan, China: a single-centered, retrospective, observational study. *Lancet Respir Med* 2020; **8**: 475-481 [PMID: 32105632 DOI: 10.1016/S2213-2600(20)30079-5]
97 **Metawea MI**, Yousif WI, Moheb I. COVID 19 and liver: An A-Z literature review. *Dig Liver Dis* 2021; **53**: 146-152 [PMID: 32988758 DOI: 10.1016/j.dld.2020.09.010]
98 **Wen W**, Su W, Tang H, Le W, Zhang X, Zheng Y, Liu X, Xie L, Li J, Ye J, Dong L, Cui X, Miao Y, Wang D, Dong J, Xiao C, Chen W, Wang H. Immune cell profiling of COVID-19 patients in the recovery stage by single-cell sequencing. *Cell Discov* 2020; **6**: 31 [PMID: 32377375 DOI: 10.1038/s41421-020-0168-9]
99 **Parvez MK**. COVID-19 and coronaviral hepatitis: evidence of collateral damage. *Future Virol* 2020; **15**: 325-329 [DOI: 10.2217/fvl-2020-0065]
100 **Mellors J**, Tipton T, Longet S, Carroll M. Viral Evasion of the Complement System and Its Importance for Vaccines and Therapeutics. *Front Immunol* 2020; **11**: 1450 [PMID: 32733480 DOI: 10.3389/fimmu.2020.01450]
101 **Hawlisch H**, Belkaid Y, Baelder R, Hildeman D, Gerard C, Köhl J. C5a negatively regulates toll-like receptor 4-induced immune responses. *Immunity* 2005; **22**: 415-426 [PMID: 15845447 DOI: 10.1016/j.immuni.2005.02.006]
102 **Zhang X**, Kimura Y, Fang C, Zhou L, Sfyroera G, Lambris JD, Wetsel RA, Miwa T, Song WC. Regulation of Toll-like receptor-mediated inflammatory response by complement in vivo. *Blood* 2007; **110**: 228-236 [PMID: 17363730 DOI: 10.1182/blood-2006-12-063636]
103 **Laudisi F**, Spreafico R, Evrard M, Hughes TR, Mandriani B, Kandasamy M, Morgan BP, Sivasankar B, Mortellaro A. Cutting edge: the NLRP3 inflammasome links complement-mediated inflammation and IL-1β release. *J Immunol* 2013; **191**: 1006-1010 [PMID: 23817414 DOI: 10.4049/jimmunol.1300489]
104 **Noris M**, Benigni A, Remuzzi G. The case of complement activation in COVID-19 multiorgan impact. *Kidney Int* 2020; **98**: 314-322 [PMID: 32461141 DOI: 10.1016/j.kint.2020.05.013]
105 **Vlaar APJ**, de Bruin S, Busch M, Timmermans SAMEG, van Zeggeren IE, Koning R, Ter Horst L, Bulle EB, van Baarle FEHP, van de Poll MCG, Kemper EM, van der Horst ICC, Schultz MJ, Horn J, Paulus F, Bos LD, Wiersinga WJ, Witzenrath M, Rueckinger S, Pilz K, Brouwer MC, Guo RF, Heunks L, van Paassen P, Riedemann NC, van de Beek D. Anti-C5a antibody IFX-1 (vilobelimab) treatment *vs* best supportive care for patients with severe COVID-19 (PANAMO): an exploratory, open-label, phase 2 randomised controlled trial. *Lancet Rheumatol* 2020; **2**: e764-e773 [PMID: 33015643 DOI: 10.1016/S2665-9913(20)30341-6]
106 **Annane D**, Heming N, Grimaldi-Bensouda L, Frémeaux-Bacchi V, Vigan M, Roux AL, Marchal A, Michelon H, Rottman M, Moine P; Garches COVID 19 Collaborative Group. Eculizumab as an emergency treatment for adult patients with severe COVID-19 in the intensive care unit: A proof-of-concept study. *EClinicalMedicine* 2020; **28**: 100590 [PMID: 33173853 DOI: 10.1016/j.eclinm.2020.100590]
107 **Kudaravalli P**, Saleem SA, Ibeche B, John S. Case series and review of liver dysfunction in covid-19 patients. *Eur J Gastroenterol Hepat* 2020 [DOI: 10.1097/MEG.0000000000001806]
108 **Alqahtani JS**, Oyelade T, Aldhahir AM, Alghamdi SM, Almehmadi M, Alqahtani AS, Quaderi S, Mandal S, Hurst JR. Prevalence, Severity and Mortality associated with COPD and Smoking in patients with COVID-19: A Rapid Systematic Review and Meta-Analysis. *PLoS One* 2020; **15**: e0233147 [PMID: 32392262 DOI: 10.1371/journal.pone.0233147]
109 **Moon AM**, Webb GJ, Aloman C, Armstrong MJ, Cargill T, Dhanasekaran R, Genescà J, Gill US, James TW, Jones PD, Marshall A, Mells G, Perumalswami PV, Qi X, Su F, Ufere NN, Barnes E, Barritt AS, Marjot T. High mortality rates for SARS-CoV-2 infection in patients with pre-existing chronic liver disease and cirrhosis: Preliminary results from an international registry. *J Hepatol* 2020; **73**: 705-708 [PMID: 32446714 DOI: 10.1016/j.jhep.2020.05.013]
110 **Bonnel AR**, Bunchorntavakul C, Reddy KR. Immune dysfunction and infections in patients with cirrhosis. *Clin Gastroenterol Hepatol* 2011; **9**: 727-738 [PMID: 21397731 DOI: 10.1016/j.cgh.2011.02.031]
111 **Lippi G**, de Oliveira MHS, Henry BM. Chronic liver disease is not associated with severity or mortality in Coronavirus disease 2019 (COVID-19): a pooled analysis. *Eur J Gastroenterol Hepatol* 2021; **33**: 114-115 [PMID: 32282549 DOI: 10.1097/MEG.0000000000001742]
112 **Fix OK**, Hameed B, Fontana RJ, Kwok RM, McGuire BM, Mulligan DC, Pratt DS, Russo MW, Schilsky ML, Verna EC, Loomba R, Cohen DE, Bezerra JA, Reddy KR, Chung RT. Clinical Best Practice Advice for Hepatology and Liver Transplant Providers During the COVID-19 Pandemic: AASLD Expert Panel Consensus Statement. *Hepatology* 2020; **72**: 287-304 [PMID: 32298473 DOI: 10.1002/hep.31281]
113 **Liu J**, Li S, Liu J, Liang B, Wang X, Wang H, Li W, Tong Q, Yi J, Zhao L, Xiong L, Guo C, Tian J, Luo J, Yao J, Pang R, Shen H, Peng C, Liu T, Zhang Q, Wu J, Xu L, Lu S, Wang B, Weng Z, Han

C, Zhu H, Zhou R, Zhou H, Chen X, Ye P, Zhu B, Wang L, Zhou W, He S, He Y, Jie S, Wei P, Zhang J, Lu Y, Wang W, Zhang L, Li L, Zhou F, Wang J, Dittmer U, Lu M, Hu Y, Yang D, Zheng X. Longitudinal characteristics of lymphocyte responses and cytokine profiles in the peripheral blood of SARS-CoV-2 infected patients. *EBioMedicine* 2020; **55**: 102763 [PMID: 32361250 DOI: 10.1016/j.ebiom.2020.102763]

114 **Jothimani D**, Venugopal R, Abedin MF, Kaliamoorthy I, Rela M. COVID-19 and the liver. *J Hepatol* 2020; **73**: 1231-1240 [PMID: 32553666 DOI: 10.1016/j.jhep.2020.06.006]

115 **Zhang C**, Shi L, Wang FS. Liver injury in COVID-19: management and challenges. *Lancet Gastroenterol Hepatol* 2020; **5**: 428-430 [PMID: 32145190 DOI: 10.1016/S2468-1253(20)30057-1]

116 **APASL Covid-19 Task Force**, Lau G, Sharma M. Clinical practice guidance for hepatology and liver transplant providers during the COVID-19 pandemic: APASL expert panel consensus recommendations. *Hepatol Int* 2020; **14**: 415-428 [PMID: 32447721 DOI: 10.1007/s12072-020-10054-w]

117 **Cai Q**, Huang D, Yu H, Zhu Z, Xia Z, Su Y, Li Z, Zhou G, Gou J, Qu J, Sun Y, Liu Y, He Q, Chen J, Liu L, Xu L. COVID-19: Abnormal liver function tests. *J Hepatol* 2020; **73**: 566-574 [PMID: 32298767 DOI: 10.1016/j.jhep.2020.04.006]

118 **Li L**, Li S, Xu M, Yu P, Zheng S, Duan Z, Liu J, Chen Y, Li J. Risk factors related to hepatic injury in patients with corona virus disease 2019. 2020 Preprint. Available from: medRxiv: 2020.2002.2028.20028514 [DOI: 10.1101/2020.02.28.20028514]

119 **Banales JM**, Huebert RC, Karlsen T, Strazzabosco M, LaRusso NF, Gores GJ. Cholangiocyte pathobiology. *Nat Rev Gastroenterol Hepatol* 2019; **16**: 269-281 [PMID: 30850822 DOI: 10.1038/s41575-019-0125-y]

120 **Xu L**, Liu J, Lu M, Yang D, Zheng X. Liver injury during highly pathogenic human coronavirus infections. *Liver Int* 2020; **40**: 998-1004 [PMID: 32170806 DOI: 10.1111/liv.14435]

121 **Testino G**, Pellicano R. Alcohol consumption in the COVID-19 era. *Minerva Gastroenterol Dietol* 2020; **66**: 90-92 [PMID: 32221278 DOI: 10.23736/S1121-421X.20.02698-7]

122 **Chen N**, Zhou M, Dong X, Qu J, Gong F, Han Y, Qiu Y, Wang J, Liu Y, Wei Y, Xia J, Yu T, Zhang X, Zhang L. Epidemiological and clinical characteristics of 99 cases of 2019 novel coronavirus pneumonia in Wuhan, China: a descriptive study. *Lancet* 2020; **395**: 507-513 [PMID: 32007143 DOI: 10.1016/S0140-6736(20)30211-7]

123 **Huang C**, Wang Y, Li X, Ren L, Zhao J, Hu Y, Zhang L, Fan G, Xu J, Gu X, Cheng Z, Yu T, Xia J, Wei Y, Wu W, Xie X, Yin W, Li H, Liu M, Xiao Y, Gao H, Guo L, Xie J, Wang G, Jiang R, Gao Z, Jin Q, Wang J, Cao B. Clinical features of patients infected with 2019 novel coronavirus in Wuhan, China. *Lancet* 2020; **395**: 497-506 [PMID: 31986264 DOI: 10.1016/S0140-6736(20)30183-5]

124 **Garnier-Crussard A**, Forestier E, Gilbert T, Krolak-Salmon P. Novel Coronavirus (COVID-19) Epidemic: What Are the Risks for Older Patients? *J Am Geriatr Soc* 2020; **68**: 939-940 [PMID: 32162679 DOI: 10.1111/jgs.16407]

125 **Hundt MA**, Deng Y, Ciarleglio MM, Nathanson MH, Lim JK. Abnormal Liver Tests in COVID-19: A Retrospective Observational Cohort Study of 1,827 Patients in a Major U.S. Hospital Network. *Hepatology* 2020; **72**: 1169-1176 [PMID: 32725890 DOI: 10.1002/hep.31487]

126 **Gu J**, Han B, Wang J. COVID-19: Gastrointestinal Manifestations and Potential Fecal-Oral Transmission. *Gastroenterology* 2020; **158**: 1518-1519 [PMID: 32142785 DOI: 10.1053/j.gastro.2020.02.054]

127 **Nardo AD**, Schneeweiss-Gleixner M, Bakail M, Dixon ED, Lax SF, Trauner M. Pathophysiological mechanisms of liver injury in COVID-19. *Liver Int* 2021; **41**: 20-32 [PMID: 33190346 DOI: 10.1111/liv.14730]

128 **Alqahtani SA**, Schattenberg JM. Liver injury in COVID-19: The current evidence. *United European Gastroenterol J* 2020; **8**: 509-519 [PMID: 32450787 DOI: 10.1177/2050640620924157]

129 **Ghoda A**, Ghoda M. Liver Injury in COVID-19 Infection: A Systematic Review. *Cureus* 2020; **12**: e9487 [PMID: 32879813 DOI: 10.7759/cureus.9487]

130 **Chand N**, Sanyal AJ. Sepsis-induced cholestasis. *Hepatology* 2007; **45**: 230-241 [PMID: 17187426 DOI: 10.1002/hep.21480]

131 **Kassir R**. Risk of COVID-19 for patients with obesity. *Obes Rev* 2020; **21**: e13034 [PMID: 32281287 DOI: 10.1111/obr.13034]

132 **Bourgeois C**, Gorwood J, Barrail-Tran A, Lagathu C, Capeau J, Desjardins D, Le Grand R, Damouche A, Béréziat V, Lambotte O. Specific Biological Features of Adipose Tissue, and Their Impact on HIV Persistence. *Front Microbiol* 2019; **10**: 2837 [PMID: 31921023 DOI: 10.3389/fmicb.2019.02837]

133 **Ji D**, Qin E, Xu J, Zhang D, Cheng G, Wang Y, Lau G. Non-alcoholic fatty liver diseases in patients with COVID-19: A retrospective study. *J Hepatol* 2020; **73**: 451-453 [PMID: 32278005 DOI: 10.1016/j.jhep.2020.03.044]

134 **Prins GH**, Olinga P. Potential implications of COVID-19 in non-alcoholic fatty liver disease. *Liver Int* 2020; **40**: 2568 [PMID: 32306495 DOI: 10.1111/liv.14484]

135 **Paizis G**, Tikellis C, Cooper ME, Schembri JM, Lew RA, Smith AI, Shaw T, Warner FJ, Zuilli A, Burrell LM, Angus PW. Chronic liver injury in rats and humans upregulates the novel enzyme angiotensin converting enzyme 2. *Gut* 2005; **54**: 1790-1796 [PMID: 16166274 DOI: 10.1136/gut.2004.062398]

136 **Boeckmans J**, Rodrigues RM, Demuyser T, Piérard D, Vanhaecke T, Rogiers V. COVID-19 and drug-induced liver injury: a problem of plenty or a petty point? *Arch Toxicol* 2020; **94**: 1367-1369

[PMID: 32266419 DOI: 10.1007/s00204-020-02734-1]

137 **Hashemi N**, Viveiros K, Redd WD, Zhou JC, McCarty TR, Bazarbashi AN, Hathorn KE, Wong D, Njie C, Shen L, Chan WW. Impact of chronic liver disease on outcomes of hospitalized patients with COVID-19: A multicentre United States experience. *Liver Int* 2020; **40**: 2515-2521 [PMID: 32585065 DOI: 10.1111/liv.14583]

138 **Saviano A**, Wrensch F, Ghany MG, Baumert TF. Liver disease and COVID-19: from Pathogenesis to Clinical Care. *Hepatology* 2020 [PMID: 33332624 DOI: 10.1002/hep.31684]

139 **Kushner T**, Cafardi J. Chronic Liver Disease and COVID-19: Alcohol Use Disorder/Alcohol-Associated Liver Disease, Nonalcoholic Fatty Liver Disease/Nonalcoholic Steatohepatitis, Autoimmune Liver Disease, and Compensated Cirrhosis. *Clin Liver Dis (Hoboken)* 2020; **15**: 195-199 [PMID: 32537135 DOI: 10.1002/cld.974]

140 **Lei HY**, Ding YH, Nie K, Dong YM, Xu JH, Yang ML, Liu MQ, Wei L, Nasser MI, Xu LY, Zhu P, Zhao MY. Potential effects of SARS-CoV-2 on the gastrointestinal tract and liver. *Biomed Pharmacother* 2021; **133**: 111064 [PMID: 33378966 DOI: 10.1016/j.biopha.2020.111064]

141 **Marjot T**, Moon AM, Cook JA, Abd-Elsalam S, Aloman C, Armstrong MJ, Pose E, Brenner EJ, Cargill T, Catana MA, Dhanasekaran R, Eshraghian A, García-Juárez I, Gill US, Jones PD, Kennedy J, Marshall A, Matthews C, Mells G, Mercer C, Perumalswami PV, Avitabile E, Qi X, Su F, Ufere NN, Wong YJ, Zheng MH, Barnes E, Barritt AS 4th, Webb GJ. Outcomes following SARS-CoV-2 infection in patients with chronic liver disease: An international registry study. *J Hepatol* 2021; **74**: 567-577 [PMID: 33035628 DOI: 10.1016/j.jhep.2020.09.024]

142 **Gao F**, Huang ZM. The impact of COVID-19 on the clinical outcome of patients with cirrhosis deserves more attention and research. *J Hepatol* 2020; **73**: 1568-1569 [PMID: 32574579 DOI: 10.1016/j.jhep.2020.06.024]

143 **Sarin SK**, Choudhury A, Lau GK, Zheng MH, Ji D, Abd-Elsalam S, Hwang J, Qi X, Cua IH, Suh JI, Park JG, Putcharoen O, Kaewdech A, Piratvisuth T, Treeprasertsuk S, Park S, Wejnaruemarn S, Payawal DA, Baatarkhuu O, Ahn SH, Yeo CD, Alonzo UR, Chinbayar T, Loho IM, Yokosuka O, Jafri W, Tan S, Soo LI, Tanwandee T, Gani R, Anand L, Esmail ES, Khalaf M, Alam S, Lin CY, Chuang WL, Soin AS, Garg HK, Kalista K, Batsukh B, Purnomo HD, Dara VP, Rathi P, Al Mahtab M, Shukla A, Sharma MK, Omata M; APASL COVID Task Force, APASL COVID Liver Injury Spectrum Study (APCOLIS Study-NCT 04345640). Pre-existing liver disease is associated with poor outcome in patients with SARS CoV2 infection; The APCOLIS Study (APASL COVID-19 Liver Injury Spectrum Study). *Hepatol Int* 2020; **14**: 690-700 [PMID: 32623632 DOI: 10.1007/s12072-020-10072-8]

144 **Bajaj JS**, Garcia-Tsao G, Biggins SW, Kamath PS, Wong F, McGeorge S, Shaw J, Pearson M, Chew M, Fagan A, de la Rosa Rodriguez R, Worthington J, Olofson A, Weir V, Trisolini C, Dwyer S, Reddy KR. Comparison of mortality risk in patients with cirrhosis and COVID-19 compared with patients with cirrhosis alone and COVID-19 alone: multicentre matched cohort. *Gut* 2021; **70**: 531-536 [PMID: 32660964 DOI: 10.1136/gutjnl-2020-322118]

145 **Derosa L**, Melenotte C, Griscelli F, Gachot B, Marabelle A, Kroemer G, Zitvogel L. The immuno-oncological challenge of COVID-19. *Nat Cancer* 2020; **1**: 946-964 [DOI: 10.1038/s43018-020-00122-3]

146 **Chan SL**, Kudo M. Impacts of COVID-19 on Liver Cancers: During and after the Pandemic. *Liver Cancer* 2020; **9**: 491-502 [PMID: 33078127 DOI: 10.1159/000510765]

147 **Liang W**, Guan W, Chen R, Wang W, Li J, Xu K, Li C, Ai Q, Lu W, Liang H, Li S, He J. Cancer patients in SARS-CoV-2 infection: a nationwide analysis in China. *Lancet Oncol* 2020; **21**: 335-337 [PMID: 32066541 DOI: 10.1016/S1470-2045(20)30096-6]

148 **Jyotsana N**, King MR. The Impact of COVID-19 on Cancer Risk and Treatment. *Cell Mol Bioeng* 2020; 1-7 [PMID: 32837583 DOI: 10.1007/s12195-020-00630-3]

149 **Guan WJ**, Ni ZY, Hu Y, Liang WH, Ou CQ, He JX, Liu L, Shan H, Lei CL, Hui DSC, Du B, Li LJ, Zeng G, Yuen KY, Chen RC, Tang CL, Wang T, Chen PY, Xiang J, Li SY, Wang JL, Liang ZJ, Peng YX, Wei L, Liu Y, Hu YH, Peng P, Wang JM, Liu JY, Chen Z, Li G, Zheng ZJ, Qiu SQ, Luo J, Ye CJ, Zhu SY, Zhong NS; China Medical Treatment Expert Group for Covid-19. Clinical Characteristics of Coronavirus Disease 2019 in China. *N Engl J Med* 2020; **382**: 1708-1720 [PMID: 32109013 DOI: 10.1056/NEJMoa2002032]

150 **Chen X**, Jiang Q, Ma Z, Ling J, Hu W, Cao Q, Mo P, Yao L, Yang R, Gao S, Gui X, Hou W, Xiong Y, Li J, Zhang Y. Clinical Characteristics of Hospitalized Patients with SARS-CoV-2 and Hepatitis B Virus Co-infection. *Virol Sin* 2020; **35**: 842-845 [PMID: 32839868 DOI: 10.1007/s12250-020-00276-5]

151 **Liu R**, Zhao L, Cheng X, Han H, Li C, Li D, Liu A, Gao G, Zhou F, Liu F, Jiang Y, Zhu C, Xia Y. Clinical characteristics of COVID-19 patients with hepatitis B virus infection - a retrospective study. *Liver Int* 2021; **41**: 720-730 [PMID: 33351265 DOI: 10.1111/liv.14774]

152 **Aldhaleei WA**, Alnuaimi A, Bhagavathula AS. COVID-19 Induced Hepatitis B Virus Reactivation: A Novel Case From the United Arab Emirates. *Cureus* 2020; **12**: e8645 [PMID: 32550096 DOI: 10.7759/cureus.8645]

153 **Pokorska-Śpiewak M**, Śpiewak M. Management of hepatitis C in children and adolescents during COVID-19 pandemic. *World J Hepatol* 2020; **12**: 485-492 [PMID: 32952875 DOI: 10.4254/wjh.v12.i8.485]

154 **Indolfi G**, Easterbrook P, Dusheiko G, El-Sayed MH, Jonas MM, Thorne C, Bulterys M, Siberry G, Walsh N, Chang MH, Meyers T, Giaquinto C, Wirth S, Chan PL, Penazzato M. Hepatitis C virus

infection in children and adolescents. *Lancet Gastroenterol Hepatol* 2019; **4**: 477-487 [PMID: 30982721 DOI: 10.1016/S2468-1253(19)30046-9]

155 **Mirzaie H**, Vahidi M, Shokoohi M, Darvishian M, Sharifi H, Sharafi H, Karamouzian M. COVID-19 among patients with hepatitis B or hepatitis C: A systematic review. 2020 Preprint. Available from: medRxiv: 2020.2010.2022.20216317 [DOI: 10.1101/2020.10.22.20216317]

156 **Mostardeiro LR**, Antoniolli ECA, Xavier JW. Coronavirus in a patient with hepatitis C: case report. *J Bras Patolo Med Lab* 2020; 56 [DOI: 10.5935/1676-2444.20200059]

157 **Mangia A**, Cenderello G, Verucchi G, Ciancio A, Fontana A, Piazzolla V, Minerva N, Squillante MM, Copetti M. Is positivity for hepatitis C virus antibody predictive of lower risk of death in COVID-19 patients with cirrhosis? *World J Clin Cases* 2020; **8**: 5831-5834 [PMID: 33344581 DOI: 10.12998/wjcc.v8.i22.5831]

158 **Waked I**, Esmat G, Elsharkawy A, El-Serafy M, Abdel-Razek W, Ghalab R, Elshishiney G, Salah A, Abdel Megid S, Kabil K, El-Sayed MH, Dabbous H, El Shazly Y, Abo Sliman M, Abou Hashem K, Abdel Gawad S, El Nahas N, El Sobky A, El Sonbaty S, El Tabakh H, Emad E, Gemeah H, Hashem A, Hassany M, Hefnawy N, Hemida AN, Khadary A, Labib K, Mahmoud F, Mamoun S, Marei T, Mekky S, Meshref A, Othman A, Ragab O, Ramadan E, Rehan A, Saad T, Saeed R, Sharshar M, Shawky H, Shawky M, Shehata W, Soror H, Taha M, Talha M, Tealaab A, Zein M, Hashish A, Cordie A, Omar Y, Kamal E, Ammar I, AbdAlla M, El Akel W, Doss W, Zaid H. Screening and Treatment Program to Eliminate Hepatitis C in Egypt. *N Engl J Med* 2020; **382**: 1166-1174 [PMID: 32187475 DOI: 10.1056/NEJMsr1912628]

159 **Sperring H**, Ruiz-Mercado G, Schechter-Perkins EM. Impact of the 2020 COVID-19 Pandemic on Ambulatory Hepatitis C Testing. *J Prim Care Community Health* 2020; **11**: 2150132720969554 [PMID: 33225792 DOI: 10.1177/2150132720969554]

160 **Blach S**, Kondili LA, Aghemo A, Cai Z, Dugan E, Estes C, Gamkrelidze I, Ma S, Pawlotsky JM, Razavi-Shearer D, Razavi H, Waked I, Zeuzem S, Craxi A. Impact of COVID-19 on global HCV elimination efforts. *J Hepatol* 2021; **74**: 31-36 [PMID: 32777322 DOI: 10.1016/j.jhep.2020.07.042]

161 **Giacomelli A**, Pagani G, Conti F, Bassoli C, Galli M. Detecting HCV infection by means of mass population SARS-CoV-2 screening: a pilot experience in Northern Italy. *J Hepatol* 2021 [PMID: 33453329 DOI: 10.1016/j.jhep.2020.12.026]

162 **Misra DP**, Agarwal V, Gasparyan AY, Zimba O. Rheumatologists' perspective on coronavirus disease 19 (COVID-19) and potential therapeutic targets. *Clin Rheumatol* 2020; **39**: 2055-2062 [PMID: 32277367 DOI: 10.1007/s10067-020-05073-9]

163 **Alijotas-Reig J**, Esteve-Valverde E, Belizna C, Selva-O'Callaghan A, Pardos-Gea J, Quintana A, Mekinian A, Anunciacion-Llunell A, Miró-Mur F. Immunomodulatory therapy for the management of severe COVID-19. Beyond the anti-viral therapy: A comprehensive review. *Autoimmun Rev* 2020; **19**: 102569 [PMID: 32376394 DOI: 10.1016/j.autrev.2020.102569]

164 **Rossi-Semerano L**, Hermeziu B, Fabre M, Koné-Paut I. Macrophage activation syndrome revealing familial Mediterranean fever. *Arthritis Care Res (Hoboken)* 2011; **63**: 780-783 [PMID: 21557533 DOI: 10.1002/acr.20418]

165 **Burrage DR**, Koushesh S, Sofat N. Immunomodulatory Drugs in the Management of SARS-CoV-2. *Front Immunol* 2020; **11**: 1844 [PMID: 32903555 DOI: 10.3389/fimmu.2020.01844]

166 **Lotfi M**, Hamblin MR, Rezaei N. COVID-19: Transmission, prevention, and potential therapeutic opportunities. *Clin Chim Acta* 2020; **508**: 254-266 [PMID: 32474009 DOI: 10.1016/j.cca.2020.05.044]

167 **Ding C**, Jones G. Anti-interleukin-6 receptor antibody treatment in inflammatory autoimmune diseases. *Rev Recent Clin Trials* 2006; **1**: 193-200 [PMID: 18473972 DOI: 10.2174/157488706778250168]

168 **Rouse BT**, Sehrawat S. Immunity and immunopathology to viruses: what decides the outcome? *Nat Rev Immunol* 2010; **10**: 514-526 [PMID: 20577268 DOI: 10.1038/nri2802]

169 **Rizk JG**, Kalantar-Zadeh K, Mehra MR, Lavie CJ, Rizk Y, Forthal DN. Pharmaco-Immunomodulatory Therapy in COVID-19. *Drugs* 2020; **80**: 1267-1292 [DOI: 10.1007/s40265-020-01367-z]

170 **Dholaria BR**, Bachmeier CA, Locke F. Mechanisms and Management of Chimeric Antigen Receptor T-Cell Therapy-Related Toxicities. *BioDrugs* 2019; **33**: 45-60 [PMID: 30560413 DOI: 10.1007/s40259-018-0324-z]

171 **Atal S**, Fatima Z. IL-6 Inhibitors in the Treatment of Serious COVID-19: A Promising Therapy? *Pharmaceut Med* 2020; **34**: 223-231 [PMID: 32535732 DOI: 10.1007/s40290-020-00342-z]

172 **Nasonov E**, Samsonov M. The role of Interleukin 6 inhibitors in therapy of severe COVID-19. *Biomed Pharmacother* 2020; **131**: 110698 [PMID: 32920514 DOI: 10.1016/j.biopha.2020.110698]

173 **Luo P**, Liu Y, Qiu L, Liu X, Liu D, Li J. Tocilizumab treatment in COVID-19: A single center experience. *J Med Virol* 2020; **92**: 814-818 [PMID: 32253759 DOI: 10.1002/jmv.25801]

174 **Boettler T**, Marjot T, Newsome PN, Mondelli MU, Maticic M, Cordero E, Jalan R, Moreau R, Cornberg M, Berg T. Impact of COVID-19 on the care of patients with liver disease: EASL-ESCMID position paper after 6 mo of the pandemic. *JHEP Rep* 2020; **2**: 100169 [PMID: 32835190 DOI: 10.1016/j.jhepr.2020.100169]

175 **Chen LF**, Mo YQ, Jing J, Ma JD, Zheng DH, Dai L. Short-course tocilizumab increases risk of hepatitis B virus reactivation in patients with rheumatoid arthritis: a prospective clinical observation. *Int J Rheum Dis* 2017; **20**: 859-869 [PMID: 28160426 DOI: 10.1111/1756-185X.13010]

176 **Sarzi-Puttini P**, Giorgi V, Sirotti S, Marotto D, Ardizzone S, Rizzardini G, Antinori S, Galli M.

COVID-19, cytokines and immunosuppression: what can we learn from severe acute respiratory syndrome? *Clin Exp Rheumatol* 2020; **38**: 337-342 [PMID: 32202240]

177 **Nicholls JM**, Poon LL, Lee KC, Ng WF, Lai ST, Leung CY, Chu CM, Hui PK, Mak KL, Lim W, Yan KW, Chan KH, Tsang NC, Guan Y, Yuen KY, Peiris JS. Lung pathology of fatal severe acute respiratory syndrome. *Lancet* 2003; **361**: 1773-1778 [PMID: 12781536 DOI: 10.1016/s0140-6736(03)13413-7]

178 **Monteagudo LA**, Boothby A, Gertner E. Continuous Intravenous Anakinra Infusion to Calm the Cytokine Storm in Macrophage Activation Syndrome. *ACR Open Rheumatol* 2020; **2**: 276-282 [PMID: 32267081 DOI: 10.1002/acr2.11135]

179 **Langer-Gould A**, Smith JB, Gonzales EG, Castillo RD, Figueroa JG, Ramanathan A, Li BH, Gould MK. Early identification of COVID-19 cytokine storm and treatment with anakinra or tocilizumab. *Int J Infect Dis* 2020; **99**: 291-297 [PMID: 32768693 DOI: 10.1016/j.ijid.2020.07.081]

180 **Huet T**, Beaussier H, Voisin O, Jouveshomme S, Dauriat G, Lazareth I, Sacco E, Naccache JM, Bézie Y, Laplanche S, Le Berre A, Le Pavec J, Salmeron S, Emmerich J, Mourad JJ, Chatellier G, Hayem G. Anakinra for severe forms of COVID-19: a cohort study. *Lancet Rheumatol* 2020; **2**: e393-e400 [PMID: 32835245 DOI: 10.1016/S2665-9913(20)30164-8]

181 **LiverTox: Clinical and Research Information on Drug-Induced Liver Injury [Internet]**. Bethesda (MD): National Institute of Diabetes and Digestive and Kidney Diseases, 2012 [PMID: 31643176]

182 **Brojakowska A**, Narula J, Shimony R, Bander J. Clinical Implications of SARS-CoV-2 Interaction With Renin Angiotensin System: JACC Review Topic of the Week. *J Am Coll Cardiol* 2020; **75**: 3085-3095 [PMID: 32305401 DOI: 10.1016/j.jacc.2020.04.028]

183 **Lefebvre AL**, McAuliffe L. Targeted Immunomodulatory Therapy: An Overview. *R I Med J (2013)* 2016; **99**: 19-22 [PMID: 27902994]

184 **Fara A**, Mitrev Z, Rosalia RA, Assas BM. Cytokine storm and COVID-19: a chronicle of pro-inflammatory cytokines. *Open Biol* 2020; **10**: 200160 [PMID: 32961074 DOI: 10.1098/rsob.200160]

185 **Mendoza VMM**. Interleukin-17: A potential therapeutic target in COVID-19. *J Infect* 2020; **81**: e136-e138 [PMID: 32504739 DOI: 10.1016/j.jinf.2020.05.072]

186 **Haga S**, Yamamoto N, Nakai-Murakami C, Osawa Y, Tokunaga K, Sata T, Sasazuki T, Ishizaka Y. Modulation of TNF-alpha-converting enzyme by the spike protein of SARS-CoV and ACE2 induces TNF-alpha production and facilitates viral entry. *Proc Natl Acad Sci USA* 2008; **105**: 7809-7814 [PMID: 18490652 DOI: 10.1073/pnas.0711241105]

187 **Mahase E**. Covid-19: what treatments are being investigated? *BMJ* 2020; **368**: m1252 [PMID: 32217607 DOI: 10.1136/bmj.m1252]

188 **Feldmann M**, Maini RN, Woody JN, Holgate ST, Winter G, Rowland M, Richards D, Hussell T. Trials of anti-tumour necrosis factor therapy for COVID-19 are urgently needed. *Lancet* 2020; **395**: 1407-1409 [PMID: 32278362 DOI: 10.1016/S0140-6736(20)30858-8]

189 **Robinson PC**, Richards D, Tanner HL, Feldmann M. Accumulating evidence suggests anti-TNF therapy needs to be given trial priority in COVID-19 treatment. *Lancet Rheumatol* 2020; **2**: e653-e655 [PMID: 33521660 DOI: 10.1016/S2665-9913(20)30309-X]

190 **Richardson P**, Griffin I, Tucker C, Smith D, Oechsle O, Phelan A, Rawling M, Savory E, Stebbing J. Baricitinib as potential treatment for 2019-nCoV acute respiratory disease. *Lancet* 2020; **395**: e30-e31 [PMID: 32032529 DOI: 10.1016/S0140-6736(20)30304-4]

191 **Stebbing J**, Phelan A, Griffin I, Tucker C, Oechsle O, Smith D, Richardson P. COVID-19: combining antiviral and anti-inflammatory treatments. *Lancet Infect Dis* 2020; **20**: 400-402 [PMID: 32113509 DOI: 10.1016/S1473-3099(20)30132-8]

192 **Richardson PJ**, Corbellino M, Stebbing J. Baricitinib for COVID-19: a suitable treatment? *Lancet Infect Dis* 2020; **20**: 1013-1014 [PMID: 32251639 DOI: 10.1016/S1473-3099(20)30270-X]

193 **Seif F**, Khoshmirsafa M, Aazami H, Mohsenzadegan M, Sedighi G, Bahar M. The role of JAK-STAT signaling pathway and its regulators in the fate of T helper cells. *Cell Commun Signal* 2017; **15**: 23 [PMID: 28637459 DOI: 10.1186/s12964-017-0177-y]

194 **Sepriano A**, Kerschbaumer A, Smolen JS, van der Heijde D, Dougados M, van Vollenhoven R, McInnes IB, Bijlsma JW, Burmester GR, de Wit M, Falzon L, Landewé R. Safety of synthetic and biological DMARDs: a systematic literature review informing the 2019 update of the EULAR recommendations for the management of rheumatoid arthritis. *Ann Rheum Dis* 2020; **79**: 760-770 [PMID: 32033941 DOI: 10.1136/annrheumdis-2019-216653]

195 **Zhang J**, Xie B, Hashimoto K. Current status of potential therapeutic candidates for the COVID-19 crisis. *Brain Behav Immun* 2020; **87**: 59-73 [PMID: 32334062 DOI: 10.1016/j.bbi.2020.04.046]

196 **Jamilloux Y**, El Jammal T, Vuitton L, Gerfaud-Valentin M, Kerever S, Sève P. JAK inhibitors for the treatment of autoimmune and inflammatory diseases. *Autoimmun Rev* 2019; **18**: 102390 [PMID: 31520803 DOI: 10.1016/j.autrev.2019.102390]

197 **Tanner T**, Wahezi DM. Hyperinflammation and the utility of immunomodulatory medications in children with COVID-19. *Paediatr Respir Rev* 2020; **35**: 81-87 [PMID: 32792288 DOI: 10.1016/j.prrv.2020.07.003]

198 **Jorgensen SCJ**, Tse CLY, Burry L, Dresser LD. Baricitinib: A Review of Pharmacology, Safety, and Emerging Clinical Experience in COVID-19. *Pharmacotherapy* 2020; **40**: 843-856 [PMID: 32542785 DOI: 10.1002/phar.2438]

199 **Favalli EG**, Biggioggero M, Maioli G, Caporali R. Baricitinib for COVID-19: a suitable treatment? *Lancet Infect Dis* 2020; **20**: 1012-1013 [PMID: 32251638 DOI: 10.1016/S1473-3099(20)30262-0]

200 **Bronte V**, Ugel S, Tinazzi E, Vella A, De Sanctis F, Canè S, Batani V, Trovato R, Fiore A, Petrova V, Hofer F, Barouni RM, Musiu C, Caligola S, Pinton L, Torroni L, Polati E, Donadello K, Friso S, Pizzolo F, Iezzi M, Facciotti F, Pelicci PG, Righetti D, Bazzoni P, Rampudda M, Comel A, Mosaner W, Lunardi C, Olivieri O. Baricitinib restrains the immune dysregulation in patients with severe COVID-19. *J Clin Invest* 2020; **130**: 6409-6416 [PMID: 32809969 DOI: 10.1172/JCI141772]

201 **Tufan A**, Avanoğlu Güler A, Matucci-Cerinic M. COVID-19, immune system response, hyperinflammation and repurposing antirheumatic drugs. *Turk J Med Sci* 2020; 620-632 [PMID: 32299202 DOI: 10.3906/sag-2004-168]

202 **Russell CD**, Millar JE, Baillie JK. Clinical evidence does not support corticosteroid treatment for 2019-nCoV lung injury. *Lancet* 2020; **395**: 473-475 [PMID: 32043983 DOI: 10.1016/S0140-6736(20)30317-2]

203 **Vandewalle J**, Luypaert A, De Bosscher K, Libert C. Therapeutic Mechanisms of Glucocorticoids. *Trends Endocrinol Metab* 2018; **29**: 42-54 [PMID: 29162310 DOI: 10.1016/j.tem.2017.10.010]

204 **Ristimäki A**, Narko K, Hla T. Down-regulation of cytokine-induced cyclo-oxygenase-2 transcript isoforms by dexamethasone: evidence for post-transcriptional regulation. *Biochem J* 1996; **318** (Pt 1): 325-331 [PMID: 8761489 DOI: 10.1042/bj3180325]

205 **Almawi WY**, Melemedjian OK. Negative regulation of nuclear factor-kappaB activation and function by glucocorticoids. *J Mol Endocrinol* 2002; **28**: 69-78 [PMID: 11932204 DOI: 10.1677/jme.0.0280069]

206 **Coutinho AE**, Chapman KE. The anti-inflammatory and immunosuppressive effects of glucocorticoids, recent developments and mechanistic insights. *Mol Cell Endocrinol* 2011; **335**: 2-13 [PMID: 20398732 DOI: 10.1016/j.mce.2010.04.005]

207 **Franchimont D**. Overview of the actions of glucocorticoids on the immune response: a good model to characterize new pathways of immunosuppression for new treatment strategies. *Ann N Y Acad Sci* 2004; **1024**: 124-137 [PMID: 15265777 DOI: 10.1196/annals.1321.009]

208 **Montón C**, Ewig S, Torres A, El-Ebiary M, Filella X, Rañó A, Xaubet A. Role of glucocorticoids on inflammatory response in nonimmunosuppressed patients with pneumonia: a pilot study. *Eur Respir J* 1999; **14**: 218-220 [PMID: 10489855 DOI: 10.1034/j.1399-3003.1999.14a37.x]

209 **Sharun K**, Tiwari R, Dhama J, Dhama K. Dexamethasone to combat cytokine storm in COVID-19: Clinical trials and preliminary evidence. *Int J Surg* 2020; **82**: 179-181 [PMID: 32896649 DOI: 10.1016/j.ijsu.2020.08.038]

210 **Mahase E**. Covid-19: Low dose steroid cuts death in ventilated patients by one third, trial finds. *BMJ* 2020; **369**: m2422 [PMID: 32546467 DOI: 10.1136/bmj.m2422]

211 **Boettler T**, Newsome PN, Mondelli MU, Maticic M, Cordero E, Cornberg M, Berg T. Care of patients with liver disease during the COVID-19 pandemic: EASL-ESCMID position paper. *JHEP Rep* 2020; **2**: 100113 [PMID: 32289115 DOI: 10.1016/j.jhepr.2020.100113]

212 **Sachdeva S**, Khandait H, Kopel J, Aloysius MM, Desai R, Goyal H. NAFLD and COVID-19: a Pooled Analysis. *SN Compr Clin Med* 2020: 1-4 [PMID: 33173850 DOI: 10.1007/s42399-020-00631-3]

213 **Zhang L**, Zhu F, Xie L, Wang C, Wang J, Chen R, Jia P, Guan HQ, Peng L, Chen Y, Peng P, Zhang P, Chu Q, Shen Q, Wang Y, Xu SY, Zhao JP, Zhou M. Clinical characteristics of COVID-19-infected cancer patients: a retrospective case study in three hospitals within Wuhan, China. *Ann Oncol* 2020; **31**: 894-901 [PMID: 32224151 DOI: 10.1016/j.annonc.2020.03.296]

World Journal of Gastroenterology

Submit a Manuscript: https://www.f6publishing.com

World J Gastroenterol 2021 April 21; 27(15): 1553-1562

DOI: 10.3748/wjg.v27.i15.1553

ISSN 1007-9327 (print) ISSN 2219-2840 (online)

MINIREVIEWS

Diagnostic approach to faecal incontinence: What test and when to perform?

Wisam Sbeit, Tawfik Khoury, Amir Mari

ORCID number: Wisam Sbeit 0000-0002-0921-4676; Tawfik Khoury 0000-0001-6699-8625; Amir Mari 0000-0002-6828-4738.

Author contributions: Sbeit W and Mari A contributed to the concept and design; All authors contributed to data collection and analyses; Sbeit W and Mari A wrote the first manuscript draft; Khoury T prepared the figures; All authors contributed to final writing of the manuscript and approved the final version to be published.

Conflict-of-interest statement: The authors declare no conflict of interest regarding this manuscript.

Manuscript source: Invited manuscript

Wisam Sbeit, Tawfik Khoury, Department of Gastroenterology, Galilee Medical Center, Naharia 2210001, Faculty of Medicine in the Galilee, Bar-Ilan University, Safed, Israel

Amir Mari, Gastroenterology and Endoscopy Unit, The Nazareth Hospital, EMMS, Nazareth 464000, Faculty of Medicine in the Galilee, Bar-Ilan University, Safed, Israel

Corresponding author: Tawfik Khoury, MD, Doctor, Lecturer, Senior Researcher, Department of Gastroenterology, Galilee Medical Center, Faculty of Medicine in the Galilee, Bar-Ilan University, Safed, POB 12000, Naharia 2210001, Israel. tawfikkhoury1@hotmail.com

Abstract

Faecal incontinence (FI) is a debilitating common end result of several diseases affecting the quality of life and leading to patient disability, morbidity, and increased societal burden. Given the various causes of FI, it is important to assess and identify the underlying pathomechanisms. Several investigatory tools are available including high-resolution anorectal manometry, transrectal ultrasound, magnetic resonance imaging, and electromyography. This review article provides an overview on the causes and pathophysiology of FI and the author's perspective of the stepwise investigation of patients with FI based on the available literature. Overall, high-resolution anorectal manometry should be the first investigatory tool for FI, followed by either transrectal ultrasound or magnetic resonance imaging for anal internal sphincter and external anal sphincter injury, respectively.

Key Words: Incontinence; Manometry; Ultrasound; Rectal; Magnetic resonance imaging; Faecal

Core Tip: Faecal incontinence (FI) is a debilitating symptom, which causes severe disability that deeply affect patients' quality of life. Given the various causes of FI, it is important for clinicians to recognize the available diagnostic investigatory tools and be familiar with the clinical approach for FI. Herein, we provide a concise overview of FI and recommend a stepwise algorithm for FI investigation.

Specialty type: Gastroenterology and hepatology

Country/Territory of origin: Israel

Peer-review report's scientific quality classification

Grade A (Excellent): 0
Grade B (Very good): B
Grade C (Good): 0
Grade D (Fair): 0
Grade E (Poor): 0

Received: December 7, 2020
Peer-review started: December 7, 2020
First decision: December 31, 2020
Revised: January 1, 2021
Accepted: March 17, 2021
Article in press: March 17, 2021
Published online: April 21, 2021

P-Reviewer: Gong J
S-Editor: Zhang L
L-Editor: Filipodia
P-Editor: Ma YJ

Citation: Sbeit W, Khoury T, Mari A. Diagnostic approach to faecal incontinence: What test and when to perform? *World J Gastroenterol* 2021; 27(15): 1553-1562
URL: https://www.wjgnet.com/1007-9327/full/v27/i15/1553.htm
DOI: https://dx.doi.org/10.3748/wjg.v27.i15.1553

INTRODUCTION

Faecal incontinence (FI) is defined as the recurrent involuntary passage of rectal contents (solid or liquid stool) through the anal canal, and the inability to delay evacuation until socially convenient. Crucial factors to consider when defining FI include the duration of symptoms for at least 1 mo and age of onset of at least 4 years with previously attained control[1-3]. FI is considered to be a prevalent disorder with a considerable economic burden, but due to embarrassment, it is generally underreported; hence, its true prevalence is challenging to assess[4]. The prevalence of FI in the adult population of the United States is estimated to be 0.8%-6.2%[5]. The prevalence of FI increases with age from approximately 3% in the age group of 20 to 29 years to 16% in people aged ≥ 70 years[6]. A systematic review by Sharma *et al*[7] of over 30 studies estimated a prevalence of 1.4% to 19.5%. This discrepancy was clarified by variance in data collection methods applied and FI definition. Unsurprisingly, lower rates of FI were reported in personal interviews compared with anonymous questionnaires. The prevalence of FI is similar in both males and females, while the pathogenesis is often dissimilar between sexes.

FI has important consequences on social activities and quality of life as well as significant economic burden attributable to diagnostics, medications, instruments, procedures, and reduced work ability[8]. FI is regularly classified from a clinical point of view as: urge incontinence (discharge despite active efforts to constrict anal sphincters), passive incontinence (involuntary discharge with no awareness), and faecal seepage (leakage of stool with normal continence and evacuation)[2].

Numerous causes and associated conditions are linked to FI such as anal sphincter dysfunction, rectal disorders, neurological diseases, malignant diseases, psychiatric conditions, and other disease[8]. One major challenge in the management of FI is the hitch in correlating objective with subjective parameters.

In this review article, we shed light on the clinical evaluation and workup of patients with FI, from history taking to diagnostics including high-resolution anorectal manometry (HRAM), transrectal ultrasound (TRUS), perineal ultrasound, magnetic resonance imaging (MRI) of the pelvic floor including MR proctography, and nerve studies such as anal sphincter electromyography (EMG). The purpose of the review is to provide a practical tool box for clinicians to use when evaluating patients with FI.

CAUSES AND RISK FACTORS OF FAECAL INCONTINENCE

FI represents a final pathway of several traumatic and non-traumatic disorders. The most non-traumatic causes include anal sphincters and rectal dysfunctions as well as various inflammatory, congenital, structural, metabolic, neurological, muscular, psychological and functional diseases (Table 1). Alterations in bowel habits, such as diarrhoea for any reason (including inflammatory bowel disease, irritable bowel disease) and constipation with paradoxical diarrhoea and overflow incontinence are considered to be among the most established risk factors for FI[9]. The most common anal sphincters structural traumatic causes leading to FI are related to obstetrical trauma during vaginal delivery, anorectal surgical procedures including anorectal dilation, haemorrhoidectomy, fistulotomy, fistulectomy, sphincterotomy, rectal prolapse repair, and after ileo-anal reconstructive surgeries[10-12]. Many patients with neurological disorders affecting the brain, spinal cord or peripheral nervous system have FI because of impaired anal sphincter control, reduced or absent anorectal sensibility or abnormal anorectal reflexes. Patients with diabetes may have neuropathy of the anal canal and some have chronic diarrhoea. Connective tissue diseases, remarkable scleroderma, myopathy and atrophy of the internal anal sphincter (IAS) may lead to FI. Rectal surgery may disturb the reservoir function of the rectum as seen in patients after anterior resection surgery. Additionally, pelvic radiotherapy may lead to FI.

Table 1 Organic causes of faecal incontinence

Congenital neurological	**Spina bifida**
Acquired neurological	Pudendal neuropathy; Spinal injury/surgery; Demyelinating diseases; Degenerative diseases; Neurological malignancy
Congenital structural disease	Imperforate anus; Cloacal anomalies
Acquired structural disease	Vaginal delivery; Obstetric trauma; Ano-rectal surgery; Ano-rectal trauma
Gastrointestinal diseases	Inflammatory bowel disease; Irritable bowel syndrome; Radiation proctitis; Microscopic colitis; Malabsorption
Neoplastic	Hypersecretory tumours; Colorectal cancer; Ana cancer
Psychiatric	Psychiatric diseases
Medications	Diarrheal agents; Chemotherapy

INVESTIGATION FOR FAECAL INCONTINENCE

History taking and physical examination

It is important in the early stages of FI evaluation to search for possible causes and risk factors during careful detailed history taking in order to route diagnostics accordingly. The main symptoms of faecal incontinence are the progressive loss of control of rectal contents including solids stool and liquids. Urge incontinence is specified by the patient's awareness to defecation call but inability to constrict the external anal sphincter (EAS) sufficiently until reaching the toilet, and many patients report "accidents" within a few seconds or minutes. Involuntary discharge without awareness is categorized as passive incontinence and generally caused by disturbed sensation capability of the rectum and anal canal. It is imperative to identify discrete disparities in relation to various triggers such as daytime *vs* night time, physical activity, cough, stress, stool consistency, or food intake. Other secondary symptoms of FI may arise due to stool leakage including pruritus, perianal skin irritation, and infection as well as urinary tract infections. Notably, these secondary symptoms may be the chief complaints prompting patients to seek medical care without mentioning FI. Moreover, FI may have other important related conditions, which mandates direct exploration with the patient such as urinary incontinence, vaginal bulging (rectocele, cystocele), rectal prolapse, altered bowel habits, defecation disorders, and rectal bleeding.

Physical examination of the anorectal region is of paramount importance and starts with a visual inspection to search for leaked stool, skin irritation and infections, haemorrhoids, fistulas opening, and anal fissures[13]. During digital rectal examination, the experienced index finger is capable of affording a general estimation of the anal resting and squeeze pressures. Moreover, coordinated relaxation of the pelvic floor muscles during straining can be addressed as well during Valsalva manoeuver to search for possible defecation disorders (*i.e.* functional anismus)[14-16].

HRAM

According to American College of Gastroenterology guidelines, in cases of FI, it is worth testing with AM[17]. HRAM is an important diagnostic tool for the assessment of anorectal motor and sensory function[18]. The utilization of HRAM is a necessary diagnostic key tool in the evaluation of FI, as it enhances the understanding of the underlying pathophysiological bases of FI, permitting the delivering of optimal therapy for each specific patient. HRAM, which provides a dynamic recording of the anal sphincters and intraluminal rectal pressures, is considered to be the best-established diagnostic tool that permits an objective evaluation of several factors of anal and rectal function including basal tone and contractility, recto-anal coordination, and reflex function (such as recto-anal inhibitory reflux) as well as rectal sensation thresholds[18,19], which is an important predictor of response to biofeedback training[19]. The recently established international anorectal physiology working group published a consensus guideline paper that proposes a practical standardized protocol for the performance and analysis of anorectal manometry, named the London Classification[20]. Several manometric findings may be linked to FI such as impaired anal sphincter resting pressure tone (hypotension) and impaired squeeze pressure (hypo-contractility) (Figures 1 and 2). Moreover, HRAM enables the assessment of abnormal rectal sensitivity both hypersensitivity and hyposensitivity, two conditions that may cause FI in different manners. Rectal sensation is assessed by inflating a balloon in the rectum and recording balloon volumes needed to produce the first

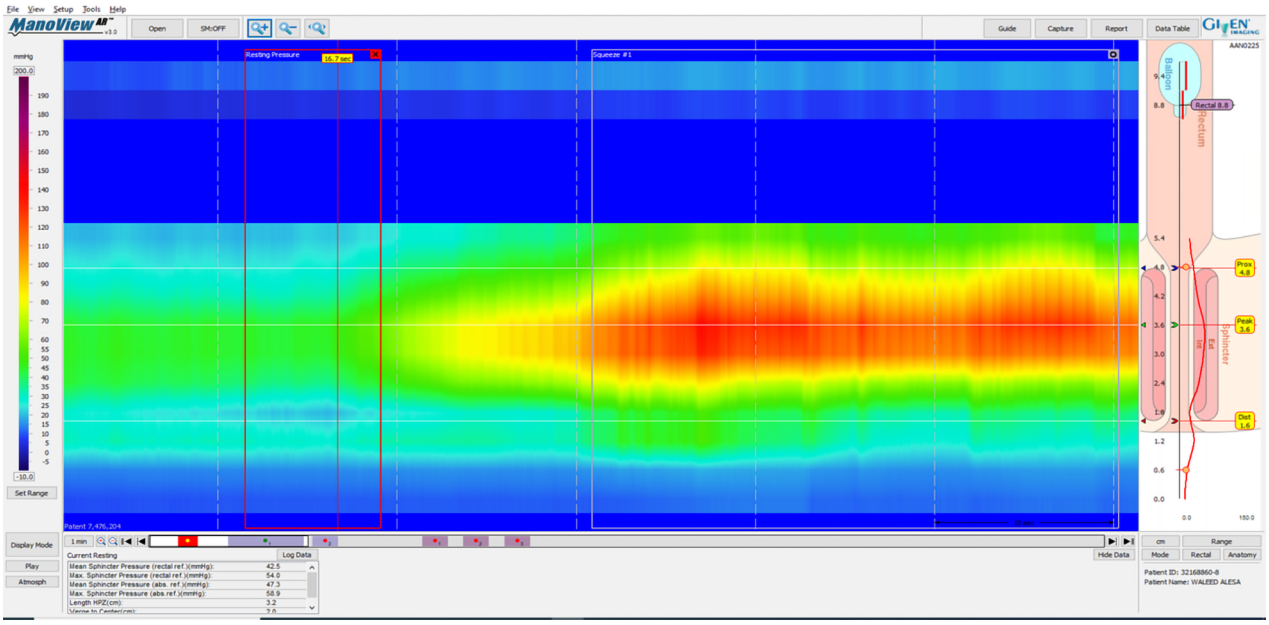

Figure 1 High-resolution anorectal manometry demonstrating normal resting and squeeze anal pressures. Supplied from the Gastroenterology and Endoscopy United, The Nazareth Hospital, EMMS, Nazareth, Israel.

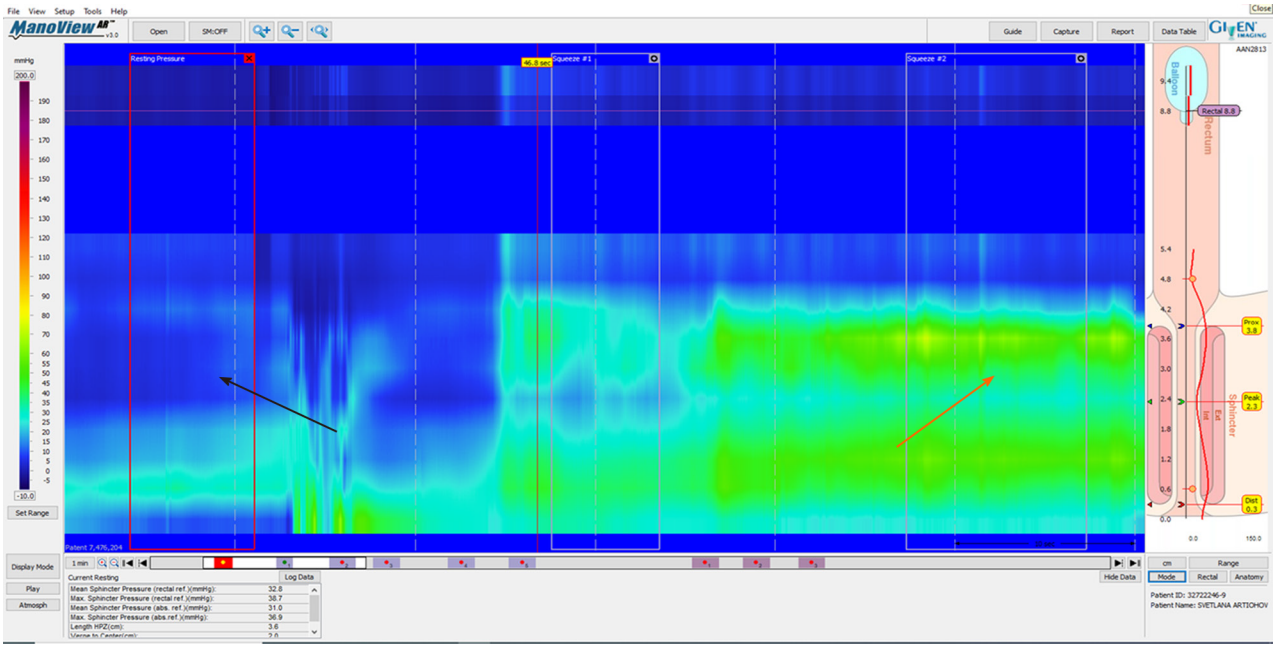

Figure 2 High-resolution anorectal manometry demonstrating low resting anal pressure (black arrow) and low squeeze pressure (orange arrow). Supplied from the Gastroenterology and Endoscopy United, The Nazareth Hospital, EMMS, Nazareth, Israel.

sensation, urge, and discomfort[20]. Rectal hyposensitivity can be caused by neuropathy, mucosal inflammation, or fibrosis and may lead to patient unawareness to the presence of stool in the rectum leading to accumulation of stool and incontinence. Rectal hypersensitivity may lead to urge incontinence and is common among patients with irritable bowel syndrome[13].

Pelvic floor and anal canal imaging

In incontinent patients with reduced anal pressures, especially when surgery is being considered, the anatomic integrity of the anal sphincters, rectal wall, and puborectalis muscle region should be evaluated by either endoscopic ultrasound or MRI[17]. Although, both tests are considered overlapping in identifying abnormalities including scars, defects, marked focal thinning or atrophy however, every test has its

uniqueness and diagnostic capabilities. While ultrasound is superior in identifying IAS tears, EAS atrophy is more identified by MRI[21,22]. Additionally, discriminating between an external anal sphincter tear and scar is better with MRI[17].

Endoscopic ultrasound: TRUS or endoanal ultrasound (EAUS) is a simple, well tolerated, widely available examination considered the gold standard in investigating the anal sphincter integrity[23,24] (Figure 3). However, its sensitivity and accuracy in identifying sphincter injuries is debated and operator-dependent[25]. Gold *et al*[26] reported that the interobserver agreement in diagnosing sphincter defects and IAS measurements by EAUS is very good, and better than EAS measurements. Common structural pathologies in patients suffering from FI that are easily identified by EAUS include IAS discontinuity (defect), IAS atrophy (identified by diffuse thinning of the sphincter to less than 1 mm thickness (Figure 4)[27], and EAS discontinuity (defect) or scar manifested as focal thinning (Figure 5)[19,28]. On the other hand, precise determination of EAS atrophy is difficult with EAUS due to its inferiority in determining the EAS boundaries and its inability to distinguish between normal muscle tissue and fatty infiltration[29]. Indeed, EAS atrophy is defined by diffuse reduction in muscle bulk on serial images below the level of the puborectalis, to the point where the muscle is barely identifiable[21]. The leading cause of FI is anal sphincter injury originating from vaginal delivery in females, and it may result from direct anal sphincter laceration or indirectly from sphincter innervation damage[29].

Two-dimensional EAUS, which allows cross sectional images only in the axial plane, remains the mainstay of sphincter inspection[24]; however it does not achieve accurate longitudinal measurements necessary for planning complete surgical intervention. On the other hand, three-dimensional EAUS enables the determination of length, thickness, area, and volume measurements by producing a digital volume that can be seen from any plane[29], and is displayed as either multiplanar images or tomographic slicing, thus allowing more accurate defect visualization[24].

MRI: MRI is expensive, not readily available, and not tolerated by claustrophobic patients and is unsuitable in patients with pacemakers, defibrillators, and other metal implants[29]. Two modalities of MRI are available in clinical practice: the invasive endoanal MRI using endoluminal coils and the non-invasive external phased-array. Both modalities are comparable in identifying EAS defects[30] and atrophy[31]. Compared to EAUS, the accuracy of endoanal MRI in diagnosing IAS defects is lower[32]. Several studies have reported that EAUS and endoanal MRI are equivalent in diagnosing EAS injuries[22,32,33]; however, endo-anal MRI allows better distinction between fat and muscle and in identifying scars[27]. This property underscores the diagnostic ability of EAUS in detecting focal EAS thinning and structural lesions[34-37]. Interestingly, only moderate agreement between EAUS and external phased-array MRI in diagnosing obstetric injuries, which represent the main aetiology for FI, has been reported[38]. Recently, magnetic resonance defecography has gradually emerged as a modern modality substituting the traditional X-ray based defecography. It is non-invasive test that uses MRI to obtain images at various stages of defecation to evaluate how well the pelvic muscles are working and provide insights into rectal function. Magnetic resonance defecography can provide important functional disorders related to the defecation process as well as various important structural abnormalities associated with FI and other pelvic floor disorders. These structural abnormalities include rectocele, enterocele, anorectal descent, and descending perineum[39]. The identification may impact the kind of surgical treatments[40].

Electromyography

A neurophysiological assessment of the anorectum includes an assessment of the conduction of the pudendal and spinal nerves using EMG examination of the sphincter. This test is of particular significance when surgery is being considered; however its availability is mainly reserved for research purposes and its clinical application has been declining recently in many countries[41,42]. However, EMG use has been advocated in patients with refractory symptoms, suspected to originate from neurogenic sphincter weakness especially when it is assumed to result from sacral root injury, it is advocated to assess rectal sensation and compliance by needle EMG of the anal sphincter[43].

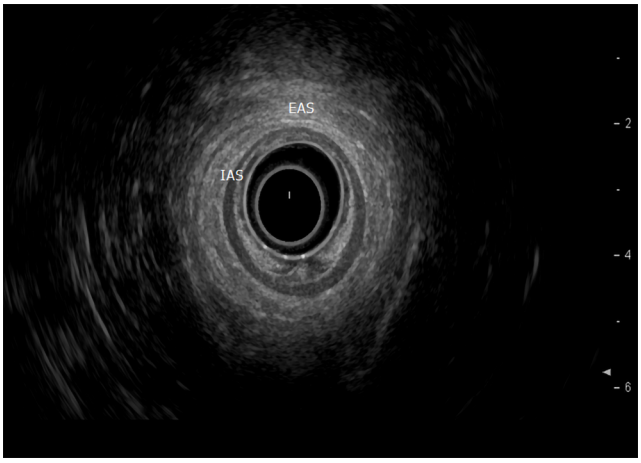

Figure 3 Normal internal and external anal sphincters (internal anal sphincter and external anal sphincter). Supplied from the Department of Gastroenterology, Galilee Medical Center, Nahariya, Israel. EAS: External anal sphincter; IAS: Internal anal sphincter.

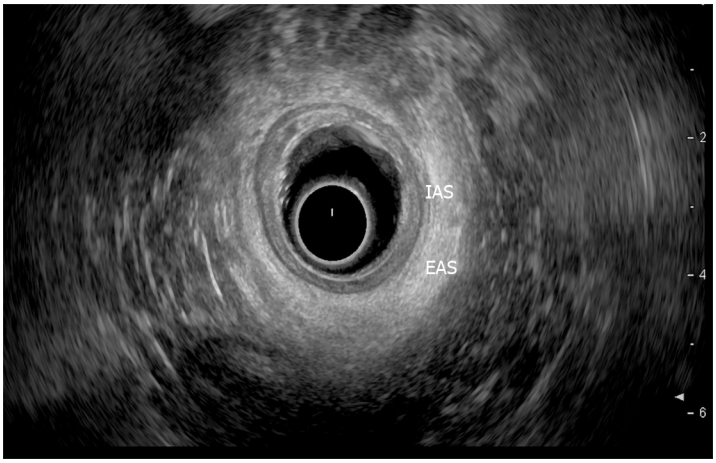

Figure 4 Internal anal sphincter atrophy manifested as sphincter thinning. Supplied from the Department of Gastroenterology, Galilee Medical Center, Nahariya, Israel. EAS: External anal sphincter; IAS: Internal anal sphincter.

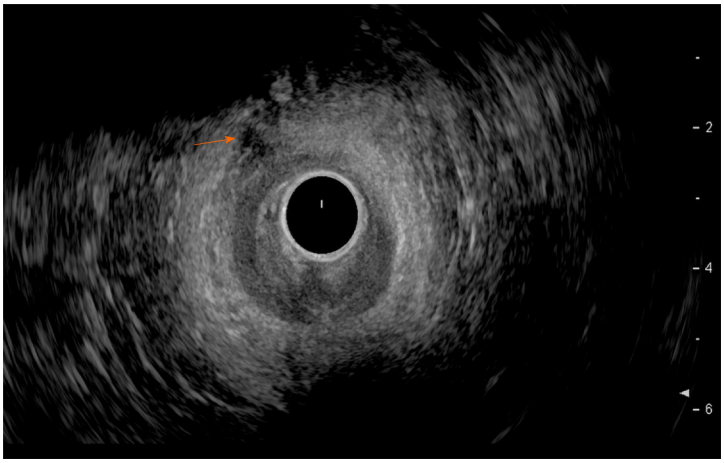

Figure 5 External anal sphincter tear. Supplied from the Department of Gastroenterology, Galilee Medical Center, Nahariya, Israel.

CONCLUSION

FI is considered to be a prevalent disorder with a considerable economic burden, but due to embarrassment it is generally underreported. FI impacts severely patients' quality of life, leading to various organic and psychological comorbidities. Detailed history taking and anamnesis by physician is mandatory to define the patient's main complaints with a focus on risk factors for FI and whether passive or urge FI is dominant. Moreover, digital rectal examination is of paramount importance to assess anorectal sensation, anal sphincter resting and importantly the squeeze pressures as well. HRAM is an important initial diagnostic modality to start with, as it can provide crucial information about the anal sphincter functions and can evaluate rectal sensation capability using balloon dilation in the rectum. The anatomic integrity of the anal sphincters, rectal wall, and puborectalis muscle region should be evaluated by either TRUS or MRI. Although, both tests are considered overlapping in identifying abnormalities including scars, defects, marked focal thinning or atrophy, every test has its own uniqueness and diagnostic capabilities. While TRUS is superior in identifying internal anal sphincter tears, external anal sphincter atrophy is more identified by MRI. Additionally, discriminating between an external anal sphincter tear and scar is better with MRI. Figure 6 demonstrates the authors' perspective of the structured, step-by-step approach for the evaluation and diagnosis of FI. Still, the place of EMG in the evaluation of FI needs to be explored. Finally, this recommended approach should aid clinicians in the stepwise management of patients with FI.

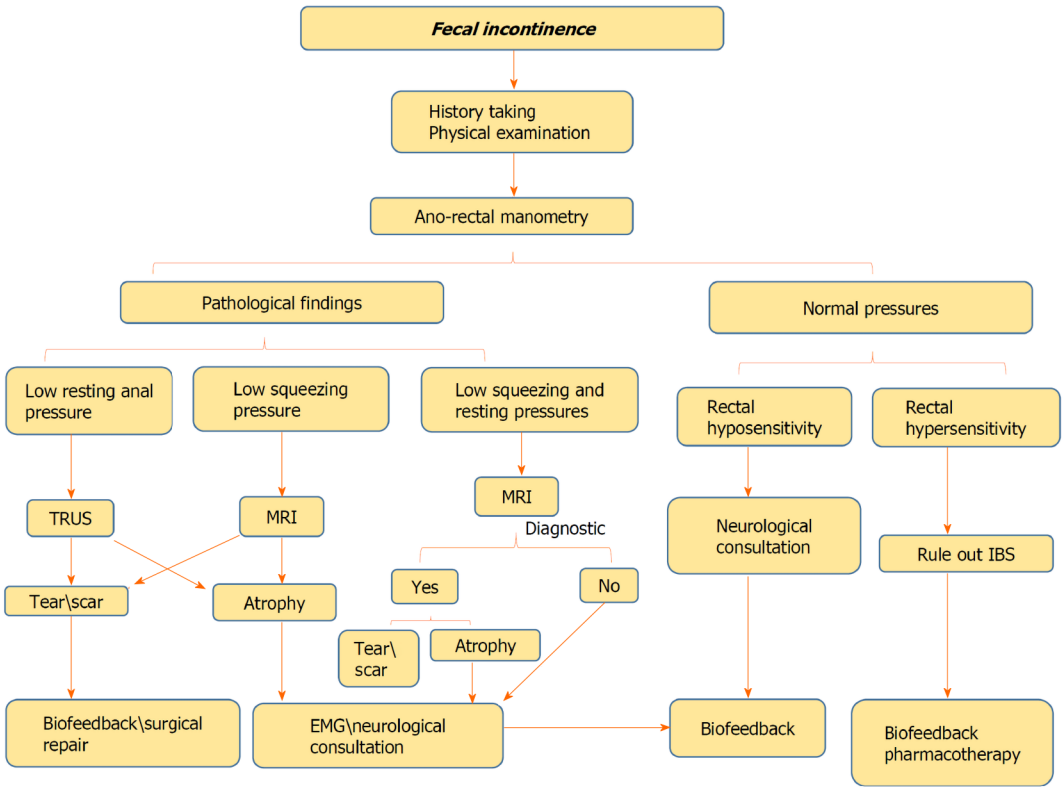

Figure 6 Stepwise approach of faecal incontinence investigation. EMG: Electromyography; MRI: Magnetic resonance imaging; TRUS: Trans-rectal ultrasound.

REFERENCES

1 **Wald A**. Clinical practice. Fecal incontinence in adults. *N Engl J Med* 2007; **356**: 1648-1655 [PMID: 17442907 DOI: 10.1056/NEJMcp067041]

2 **Rao SS**; American College of Gastroenterology Practice Parameters Committee. Diagnosis and management of fecal incontinence. American College of Gastroenterology Practice Parameters Committee. *Am J Gastroenterol* 2004; **99**: 1585-1604 [PMID: 15307881 DOI: 10.1111/j.1572-0241.2004.40105.x]

3 **Paquette IM**, Varma MG, Kaiser AM, Steele SR, Rafferty JF. The American Society of Colon and Rectal Surgeons' Clinical Practice Guideline for the Treatment of Fecal Incontinence. *Dis Colon Rectum* 2015; **58**: 623-636 [PMID: 26200676 DOI: 10.1097/DCR.0000000000000397]

4 **Bharucha AE**, Dunivan G, Goode PS, Lukacz ES, Markland AD, Matthews CA, Mott L, Rogers RG, Zinsmeister AR, Whitehead WE, Rao SS, Hamilton FA. Epidemiology, pathophysiology, and classification of fecal incontinence: state of the science summary for the National Institute of Diabetes and Digestive and Kidney Diseases (NIDDK) workshop. *Am J Gastroenterol* 2015; **110**: 127-136 [PMID: 25533002 DOI: 10.1038/ajg.2014.396]

5 **Pretlove SJ**, Radley S, Toozs-Hobson PM, Thompson PJ, Coomarasamy A, Khan KS. Prevalence of anal incontinence according to age and gender: a systematic review and meta-regression analysis. *Int Urogynecol J Pelvic Floor Dysfunct* 2006; **17**: 407-417 [PMID: 16572280 DOI: 10.1007/s00192-005-0014-5]

6 **Ditah I**, Devaki P, Luma HN, Ditah C, Njei B, Jaiyeoba C, Salami A, Ditah C, Ewelukwa O, Szarka L. Prevalence, trends, and risk factors for fecal incontinence in United States adults, 2005-2010. *Clin Gastroenterol Hepatol* 2014; **12**: 636-43.e1-2 [PMID: 23906873 DOI: 10.1016/j.cgh.2013.07.020]

7 **Sharma A**, Yuan L, Marshall RJ, Merrie AE, Bissett IP. Systematic review of the prevalence of faecal incontinence. *Br J Surg* 2016; **103**: 1589-1597 [PMID: 27704537 DOI: 10.1002/bjs.10298]

8 **Duelund-Jakobsen J**, Worsoe J, Lundby L, Christensen P, Krogh K. Management of patients with faecal incontinence. *Therap Adv Gastroenterol* 2016; **9**: 86-97 [PMID: 26770270 DOI: 10.1177/1756283X15614516]

9 **Andrews CN**, Bharucha AE. The etiology, assessment, and treatment of fecal incontinence. *Nat Clin Pract Gastroenterol Hepatol* 2005; **2**: 516-525 [PMID: 16355157 DOI: 10.1038/ncpgasthep0315]

10 **Ternent CA**, Fleming F, Welton ML, Buie WD, Steele S, Rafferty J; American Society of Colon and Rectal Surgeons. Clinical Practice Guideline for Ambulatory Anorectal Surgery. *Dis Colon Rectum* 2015; **58**: 915-922 [PMID: 26347962 DOI: 10.1097/DCR.0000000000000451]

11 **Wallenhorst T**, Bouguen G, Brochard C, Cunin D, Desfourneaux V, Ropert A, Bretagne JF, Siproudhis L. Long-term impact of full-thickness rectal prolapse treatment on fecal incontinence.

Surgery 2015; **158**: 104-111 [PMID: 25869649 DOI: 10.1016/j.surg.2015.03.005]
12 **Markland AD**, Dunivan GC, Vaughan CP, Rogers RG. Anal Intercourse and Fecal Incontinence: Evidence from the 2009-2010 National Health and Nutrition Examination Survey. *Am J Gastroenterol* 2016; **111**: 269-274 [PMID: 26753893 DOI: 10.1038/ajg.2015.419]
13 **Dobben AC**, Terra MP, Deutekom M, Gerhards MF, Bijnen AB, Felt-Bersma RJ, Janssen LW, Bossuyt PM, Stoker J. Anal inspection and digital rectal examination compared to anorectal physiology tests and endoanal ultrasonography in evaluating fecal incontinence. *Int J Colorectal Dis* 2007; **22**: 783-790 [PMID: 17096089 DOI: 10.1007/s00384-006-0217-3]
14 **Eckardt VF**, Kanzler G. How reliable is digital examination for the evaluation of anal sphincter tone? *Int J Colorectal Dis* 1993; **8**: 95-97 [PMID: 8409694 DOI: 10.1007/BF00299335]
15 **Hallan RI**, Marzouk DE, Waldron DJ, Womack NR, Williams NS. Comparison of digital and manometric assessment of anal sphincter function. *Br J Surg* 1989; **76**: 973-975 [PMID: 2679966 DOI: 10.1002/bjs.1800760934]
16 **Mimura T**, Kaminishi M, Kamm MA. Diagnostic evaluation of patients with faecal incontinence at a specialist institution. *Dig Surg* 2004; **21**: 235-41; discussion 241 [PMID: 15237257 DOI: 10.1159/000079493]
17 **Wald A**, Bharucha AE, Cosman BC, Whitehead WE. ACG clinical guideline: management of benign anorectal disorders. *Am J Gastroenterol* 2014; **109**: 1141-57; (Quiz) 1058 [PMID: 25022811 DOI: 10.1038/ajg.2014.190]
18 **Scott SM**, Carrington EV. The London Classification: Improving Characterization and Classification of Anorectal Function with Anorectal Manometry. *Curr Gastroenterol Rep* 2020; **22**: 55 [PMID: 32935278 DOI: 10.1007/s11894-020-00793-z]
19 **Carrington EV**, Scott SM, Bharucha A, Mion F, Remes-Troche JM, Malcolm A, Heinrich H, Fox M, Rao SS; International Anorectal Physiology Working Group and the International Working Group for Disorders of Gastrointestinal Motility and Function. Expert consensus document: Advances in the evaluation of anorectal function. *Nat Rev Gastroenterol Hepatol* 2018; **15**: 309-323 [PMID: 29636555 DOI: 10.1038/nrgastro.2018.27]
20 **Carrington EV**, Heinrich H, Knowles CH, Fox M, Rao S, Altomare DF, Bharucha AE, Burgell R, Chey WD, Chiarioni G, Dinning P, Emmanuel A, Farouk R, Felt-Bersma RJF, Jung KW, Lembo A, Malcolm A, Mittal RK, Mion F, Myung SJ, O'Connell PR, Pehl C, Remes-Troche JM, Reveille RM, Vaizey CJ, Vitton V, Whitehead WE, Wong RK, Scott SM; All members of the International Anorectal Physiology Working Group. The international anorectal physiology working group (IAPWG) recommendations: Standardized testing protocol and the London classification for disorders of anorectal function. *Neurogastroenterol Motil* 2020; **32**: e13679 [PMID: 31407463 DOI: 10.1111/nmo.13679]
21 **Bharucha AE**, Fletcher JG, Harper CM, Hough D, Daube JR, Stevens C, Seide B, Riederer SJ, Zinsmeister AR. Relationship between symptoms and disordered continence mechanisms in women with idiopathic faecal incontinence. *Gut* 2005; **54**: 546-555 [PMID: 15753542 DOI: 10.1136/gut.2004.047696]
22 **West RL**, Dwarkasing S, Briel JW, Hansen BE, Hussain SM, Schouten WR, Kuipers EJ. Can three-dimensional endoanal ultrasonography detect external anal sphincter atrophy? A comparison with endoanal magnetic resonance imaging. *Int J Colorectal Dis* 2005; **20**: 328-333 [PMID: 15666154 DOI: 10.1007/s00384-004-0693-2]
23 **Sultan AH**, Kamm MA, Talbot IC, Nicholls RJ, Bartram CI. Anal endosonography for identifying external sphincter defects confirmed histologically. *Br J Surg* 1994; **81**: 463-465 [PMID: 8173933 DOI: 10.1002/bjs.1800810349]
24 **Abdool Z**, Sultan AH, Thakar R. Ultrasound imaging of the anal sphincter complex: a review. *Br J Radiol* 2012; **85**: 865-875 [PMID: 22374273 DOI: 10.1259/bjr/27314678]
25 **Jiang AC**, Panara A, Yan Y, Rao SSC. Assessing Anorectal Function in Constipation and Fecal Incontinence. *Gastroenterol Clin North Am* 2020; **49**: 589-606 [PMID: 32718572 DOI: 10.1016/j.gtc.2020.04.011]
26 **Gold DM**, Halligan S, Kmiot WA, Bartram CI. Intraobserver and interobserver agreement in anal endosonography. *Br J Surg* 1999; **86**: 371-375 [PMID: 10201781 DOI: 10.1046/j.1365-2168.1999.01032.x]
27 **Engin G**. Endosonographic imaging of anorectal diseases. *J Ultrasound Med* 2006; **25**: 57-73 [PMID: 16371556 DOI: 10.7863/jum.2006.25.1.57]
28 **Dvorkin LS**, Chan CL, Knowles CH, Williams NS, Lunniss PJ, Scott SM. Anal sphincter morphology in patients with full-thickness rectal prolapse. *Dis Colon Rectum* 2004; **47**: 198-203 [PMID: 15043290 DOI: 10.1007/s10350-003-0035-4]
29 **Albuquerque A**. Endoanal ultrasonography in fecal incontinence: Current and future perspectives. *World J Gastrointest Endosc* 2015; **7**: 575-581 [PMID: 26078826 DOI: 10.4253/wjge.v7.i6.575]
30 **Terra MP**, Beets-Tan RG, van Der Hulst VP, Dijkgraaf MG, Bossuyt PM, Dobben AC, Baeten CG, Stoker J. Anal sphincter defects in patients with fecal incontinence: endoanal *vs* external phased-array MR imaging. *Radiology* 2005; **236**: 886-895 [PMID: 16014438 DOI: 10.1148/radiol.2363041162]
31 **Terra MP**, Beets-Tan RG, van der Hulst VP, Deutekom M, Dijkgraaf MG, Bossuyt PM, Dobben AC, Baeten CG, Stoker J. MRI in evaluating atrophy of the external anal sphincter in patients with fecal incontinence. *AJR Am J Roentgenol* 2006; **187**: 991-999 [PMID: 16985148 DOI: 10.2214/AJR.05.0386]
32 **Malouf AJ**, Williams AB, Halligan S, Bartram CI, Dhillon S, Kamm MA. Prospective assessment of

accuracy of endoanal MR imaging and endosonography in patients with fecal incontinence. *AJR Am J Roentgenol* 2000; **175**: 741-745 [PMID: 10954460 DOI: 10.2214/ajr.175.3.1750741]

33 **Dobben AC**, Terra MP, Slors JF, Deutekom M, Gerhards MF, Beets-Tan RG, Bossuyt PM, Stoker J. External anal sphincter defects in patients with fecal incontinence: comparison of endoanal MR imaging and endoanal US. *Radiology* 2007; **242**: 463-471 [PMID: 17255418 DOI: 10.1148/radiol.2422051575]

34 **Williams AB**, Bartram CI, Modhwadia D, Nicholls T, Halligan S, Kamm MA, Nicholls RJ, Kmiot WA. Endocoil magnetic resonance imaging quantification of external anal sphincter atrophy. *Br J Surg* 2001; **88**: 853-859 [PMID: 11412258 DOI: 10.1046/j.0007-1323.2001.01796.x]

35 **Bartram C**, Halligan S. Endoanal MR is really complementary to endoanal US. *Radiology* 2000; **216**: 918-920 [PMID: 10966734 DOI: 10.1148/radiology.216.3.r00se56918]

36 **Rociu E**, Stoker J, Zwamborn AW, Laméris JS. Endoanal MR imaging of the anal sphincter in fecal incontinence. *Radiographics* 1999; **19** Spec No: S171-S177 [PMID: 10517453 DOI: 10.1148/radiographics.19.suppl_1.g99oc02s171]

37 **Rociu E**, Stoker J, Eijkemans MJ, Schouten WR, Laméris JS. Fecal incontinence: endoanal US *vs* endoanal MR imaging. *Radiology* 1999; **212**: 453-458 [PMID: 10429703 DOI: 10.1148/radiology.212.2.r99au10453]

38 **Kirss J Jr**, Huhtinen H, Niskanen E, Ruohonen J, Kallio-Packalen M, Victorzon S, Victorzon M, Pinta T. Comparison of 3D endoanal ultrasound and external phased array magnetic resonance imaging in the diagnosis of obstetric anal sphincter injuries. *Eur Radiol* 2019; **29**: 5717-5722 [PMID: 30915565 DOI: 10.1007/s00330-019-06125-8]

39 **Piloni V**, Bergamasco M, Melara G, Garavello P. The clinical value of magnetic resonance defecography in males with obstructed defecation syndrome. *Tech Coloproctol* 2018; **22**: 179-190 [PMID: 29512048 DOI: 10.1007/s10151-018-1759-4]

40 **Thapar RB**, Patankar RV, Kamat RD, Thapar RR, Chemburkar V. MR defecography for obstructed defecation syndrome. *Indian J Radiol Imaging* 2015; **25**: 25-30 [PMID: 25709162 DOI: 10.4103/0971-3026.150134]

41 **Bharucha AE**, Daube J, Litchy W, Traue J, Edge J, Enck P, Zinsmeister AR. Anal sphincteric neurogenic injury in asymptomatic nulliparous women and fecal incontinence. *Am J Physiol Gastrointest Liver Physiol* 2012; **303**: G256-G262 [PMID: 22575218 DOI: 10.1152/ajpgi.00099.2012]

42 **Law PJ**, Kamm MA, Bartram CI. A comparison between electromyography and anal endosonography in mapping external anal sphincter defects. *Dis Colon Rectum* 1990; **33**: 370-373 [PMID: 2183977 DOI: 10.1007/BF02156260]

43 **Weledji EP**. Electrophysiological Basis of Fecal Incontinence and Its Implications for Treatment. *Ann Coloproctol* 2017; **33**: 161-168 [PMID: 29159162 DOI: 10.3393/ac.2017.33.5.161]

World Journal of Gastroenterology

Submit a Manuscript: https://www.f6publishing.com

World J Gastroenterol 2021 April 21; 27(15): 1563-1568

DOI: 10.3748/wjg.v27.i15.1563

ISSN 1007-9327 (print) ISSN 2219-2840 (online)

MINIREVIEWS

Prevention of late complications with coverage agents in endoscopic resection of colorectal lesions: Current landscape in gastrointestinal endoscopy

Vicente Lorenzo-Zúñiga, Marco Bustamante-Balén, Vicente Pons-Beltrán

ORCID number: Vicente Lorenzo-Zúñiga 0000-0002-4072-3241; Marco Bustamante-Balén 0000-0003-2019-0158; Vicente Pons-Beltrán 0000-0001-8909-8929.

Author contributions: Lorenzo-Zúñiga V wrote the paper; Bustamante-Balén M and Pons-Beltrán V reviewed the paper.

Conflict-of-interest statement: Authors declare no conflict of interest for this article.

Manuscript source: Invited manuscript

Specialty type: Gastroenterology and hepatology

Vicente Lorenzo-Zúñiga, Endoscopy Unit, Department of Gastroenterology, Hospital Universitari i Politècnic La Fe, Valencia 46026, Spain

Vicente Pons-Beltrán, Digestive Diseases Department, La Fe Polytechnic University Hospital, Valencia 46026, Spain

Corresponding author: Vicente Lorenzo-Zúñiga, MD, PhD, Associate Professor, Consultant Physician-Scientist, Endoscopy Unit, Department of Gastroenterology, Hospital Universitari i Politècnic La Fe, Avenida Fernando Abril Martorell 106, Valencia 46026, Spain. vlorenzozuniga@gmail.com

Abstract

Endoscopic removal of large (≥ 20 mm) non-pedunculated colorectal lesions (LNPCLs) may result in major adverse events, such as delayed bleeding (DB) and delayed perforation (DP), despite closure of the mucosal defects with clips. Topical application of a coverage agent refers to the creation of a shield with a biocompatible medical device (tissue or hydrogel) with proven bioactive properties. Coverage of the eschar after endoscopic resection provides shielding protection to prevent delayed complications. The aim of the present review was to systematically collect and review the currently available literature regarding the prevention of DB and DP with coverage agents after endoscopic mucosal resection or endoscopic submucosal dissection of LNPCLs.

Key Words: Large colorectal lesions; Delayed bleeding; Topical application; Endoscopic mucosal resection; Endoscopic submucosal dissection

Core Tip: The use of coverage agents is the simplest and quickest technique to protect large mucosal defects. Published data have confirmed their efficacy in the prevention of delayed adverse events in patients with non-pedunculated colorectal lesions, especially in proximal lesions with an increased risk of bleeding of at least 2-fold. There are no comparative studies that address the best treatment. We herein review the

Country/Territory of origin: Spain

Peer-review report's scientific quality classification
Grade A (Excellent): 0
Grade B (Very good): B
Grade C (Good): C, C
Grade D (Fair): 0
Grade E (Poor): 0

Received: December 27, 2020
Peer-review started: December 27, 2020
First decision: January 23, 2021
Revised: February 5, 2021
Accepted: March 9, 2021
Article in press: March 9, 2021
Published online: April 21, 2021

P-Reviewer: Chiba H, Hidaka E
S-Editor: Zhang H
L-Editor: Webster JR
P-Editor: Li JH

current landscape of the available agents in gastrointestinal endoscopy.

Citation: Lorenzo-Zúñiga V, Bustamante-Balén M, Pons-Beltrán V. Prevention of late complications with coverage agents in endoscopic resection of colorectal lesions: Current landscape in gastrointestinal endoscopy. *World J Gastroenterol* 2021; 27(15): 1563-1568
URL: https://www.wjgnet.com/1007-9327/full/v27/i15/1563.htm
DOI: https://dx.doi.org/10.3748/wjg.v27.i15.1563

INTRODUCTION

Endoscopic resection of precancerous colorectal lesions is one the most frequently performed medical interventions, which significantly decreases the risk of colorectal cancer incidence and death. Large (20 mm) non-pedunculated colorectal lesions (LNPCLs) show the highest cancer risk and their careful, complete, and timely removal is especially critical. Endoscopic removal of these lesions may result in major adverse events, such as delayed bleeding (DB) and delayed perforation (DP), especially in high-risk patients with a Spanish Endoscopy Society Endoscopic Resection Group score 6 or deep mural injury signs II-V, despite closure of the mucosal defects with clips[1-3]. Complete clip closure is not possible in 40% cases due to large size or poor accessibility[4]. The risk of DB ranges from 1% to 12% (1.5% with complete closure, 9% with partial closure and 12% with failed closure), whereas the risk of DP is around 1%[5,6]. The routine use of prophylactic clipping does not reduce the risk of post-procedural bleeding overall[7]. On the other, prophylactic endoscopic coagulation of visible vessels is not effective in the prevention of clinically significant DB[8].

Topical application of a coverage agent refers to the creation of a shield with a biocompatible medical device (tissue or hydrogel) with proven bioactive properties. Coverage of the eschar after endoscopic resection provides shielding protection to prevent delayed complications[9]. A comprehensive understanding of the pathogenic mechanisms of action involved is mandatory to address these challenges. The aim of the present review was to systematically collect and review the currently available literature regarding the prevention of DB and DP with coverage agents after endoscopic mucosal resection (EMR) or endoscopic submucosal dissection (ESD) of LNPCLs.

SEARCH STRATEGIES

A comprehensive search of PubMed was performed to identify articles in English. Search strategies and key words were as follows: (1) ("Endoscopy" [All Fields] AND ("topical application" [All Fields]); (2) ("Large colorectal lesions" [All Fields] AND "EMR" [All Fields] OR "ESD" [All Fields]); and (3) ("Delayed bleeding" [All Fields] OR "delayed perforation" [All Fields]). In addition, manually inspected relevant articles that were missed by the above search strategy were also included.

CLINICAL DATA

Following our search, 8 studies were identified with 191 patients included in case series, which are summarized in Table 1. Tested agents were: Polyglycocolic acid sheets with fibrin glue (PGA-FG), Surgicel, platelet-rich plasma (PRP), Purastat and cyanoacrylate. All these measures present biological safety after experience in clinical practice. The first report was published in 2014 to evaluate the shielding technique after ESD in 10 patients with LNPCLs, placing PGA sheets on the mucosal defect with biopsy forceps and then spraying FG through a special double-lumen tube[10]. PGA is an absorbent and hydrophilic suture reinforcement material, hydrolysed *in vivo*, with a degradation and absorption period within approximately 15 wk[11]. To perform this technique, soft and elastic PGA sheets were cut into small pieces, held with biopsy forceps, and transported to the mucosal defect through the channel of the scope.

Table 1 Outcome of coverage agents to prevent delayed bleeding and perforation after endoscopic resection of colorectal lesions

Ref.	Year	Design	*n*	Size (mm)	Agent	Primary endpoint	Follow-up	Outcomes
Tsuji *et al*[10]	2014	SA	10	39.7	PGA-FG	Prevent late complications	2 wk	0% DB/0% DP
Myung *et al*[13]	2016	SA	49	38.8	Surgicel	Prevent late complications	1 wk	0% DB/0% DP/6% PPS
Lorenzo-Zúñiga *et al*[17]	2021	SA	4	53.7	PRP	Prevent late complications	4 wk	25% DB/0% DP/79% MHR
Pioche *et al*[18]	2016	SA	22	38.5	Purastat	Prevent delayed bleeding	4 wk	6.7% DB
Subramanian *et al*[19]	2019	SA	31	44.2	Purastat	Prevent delayed bleeding	4 wk	0% DB
Soons *et al*[20]	2020	SA	17	38.4	Purastat	Prevent delayed bleeding	4 wk	11.7% DB
Subramanian *et al*[21]	2021	RCT	43	33.7	Purastat	Prevent late complications	4 wk	5.5% DB
Martines *et al*[22]	2020	TA	15	25	NBCA-MS	Prevent delayed bleeding	-	0% DB

SA: Single-arm interventional case series study; TA: Two-arm interventional case series study; RCT: Randomized clinical trial; PGA-FG: Polyglycocolic acid sheet with fibrin glue; PRP: Platelet-rich plasma; NBCA-MS: N-butyl-2-cyanoacrylate with methacrylosulfolane (Glubran 2); DB: Delayed bleeding; DP: Delayed perforation; MHR: Mucosal healing rate.

Fibrinogen first and then thrombin were sprayed with different spray tubes to fix the sheets to the ulcer and to enhance the coating effect[12]. The use of PGA-FG in LNPCLs achieved a success rate of 100%, but required a long-procedure time (a mean of 19 min). During follow-up colonoscopy, 80% of patients showed persistence of PGA sheets at 2 wk.

Surgicel Fibrillar, an oxidized regenerated cellulose that swells into a gelatinous mass, was the second substance investigated to reduce late complications in a large case-series of 49 patients with colorectal ESD[13], using one layer of this agent diluted in 10 mL of normal saline through a special spraying catheter. Surgicel aids in clot formation after blood saturation, serving as a haemostatic adjunct, and has a localized bactericidal effect due to a low pH of 3.4-3.7[14]. To assess the effectiveness of Surgicel application, a retrospective comparison with another 52 patients with LNPCLs who underwent conventional ESD was performed. All lesions were successfully covered, and the covering procedure was less time-consuming (5 min). During the follow-up period, rebleeding occurred in 0 (0%) patients and 4 (7.7% in the control group) patients. Postpolypectomy syndrome (PPS) was observed in three patients (6.1%) who were treated with Surgicel, compared with 17 (32.7%) in the non-Surgicel group. In 20 patients treated with this product, a follow-up colonoscopy was performed the next day, and Surgicel remained on the defect in all cases. Based on this, the authors speculated that the reduction in the inflammatory reaction was associated with the shielding effect and reduced endotoxemia due to the bactericidal property of this agent, which acidifies the environment.

PRP, also known as autologous platelet gel, has confirmed robust healing properties over the eschar after EMR in preclinical models[15]. Platelets play a fundamental role in haemostasis and are a natural source of growth factors. PRP fluid contains at least a 2-fold peripheral blood platelet count and a large amount of pivotal growth factors for reepithelization, which are released from the alpha granules of activated platelets[16]. The use of PRP is justified in the exponential release of multiple pleiotropic factors, which enhances the physiological and haemostatic healing processes, with a very low risk of fibrotic healing or strictures. In clinical practice, PRP was used as a coverage agent to prevent late complications in a limited number of patients with very large lesions located in the rectum (mean size 54 mm)[17]. PRP was obtained from a sample of patient's blood (18-36 mL) drawn at the time of endoscopy. DB occurred in 1 of 4 lesions with blood transfusion or endoscopic treatment not required. PRP also showed a very high mucosal healing rate after 4 wk (79%), the time to apply PRP was very quick (2 min), and the force required to pass the composition was appropriate, comparable to saline. Nevertheless, patient number is too small to draw any conclusions on efficacy, and controlled data are lacking.

PuraStat has also been tested to prevent DB after endoscopic resection of LNPCLs. This agent is a fully synthetic matrix scaffold built from a chain of three types of amino acids than bond together to form a peptide. It forms a transparent gel when it comes into contact with blood or tissue fluids, comprising a network of nanofibers that form an extracellular matrix, providing a physical barrier to stop bleeding by blocking blood vessels. Three case series (single-arm interventional studies) and one randomized clinical trial have been reported in 113 patients with LNPCLs[18-21]. Total lesion surface was completely covered with a dose of 3 mL in a median time of 2 min. Clinically significant DB occurred in 4.4% of patients (range 0%-12%). The concerns with this gel are that it has to be applied through a special catheter, it is affected by gravity, and slowly slides from the ulcer bed after covering. Exsufflation after application seems to be effective in applying the gel to the whole area with less migration.

Recently, cyanoacrylate has been evaluated in a two-arm study[22]. Two groups of fifteen patients with LNPCLs were compared to evaluate early and DB after EMR in association with a modified cyanoacrylate glue (N-butyl-2-cyanoacrylate + methacryloxysulfolane-Glubran 2®) *vs* EMR alone. Cyanoacrylate is a strong and fast-acting synthetic glue with sealing, adhesive and haemostatic properties, which rapidly polymerizes in the presence of water to form long and strong chains. Based on these properties it has been widely used in surgery, and for primary and secondary prophylaxis of bleeding from gastric varices[23]. This substance has been applied using a 7 Fr spray Teflon catheter. No case of early bleeding was reported in both groups. Two cases (13.3%) of DB with readmission to hospital and redo endoscopy with apposition of haemostatic clips were performed in patients with EMR alone, as compared with no cases of DB in the shielded group (P = 0.48).

DISCUSSION

Endoscopic shielding with coverage agents is a very promising method to prevent late complications in patients with LNPCLs, especially in proximal lesions with an increased risk of bleeding of at least 2-fold. The protective effect of clips is limited to those cases where complete closure was achieved (57% of cases), and the median number of clips to completely close the resection defect was four[4-6]. The absence of efficacy in many cases of the clipping technique, with its cost and technical difficulties, induced the appearance of new endoscopic approaches to solve this unmet need.

The use of coverage agents is the quickest and simplest technique to cover large mucosal defects, and published data seem to confirm their efficacy in the prevention of late complications. However, most of the reports are case series, without a control arm and with a relatively short follow-up. There is a lack of randomized controlled trials and of head-to-head comparative studies of shielding products. Moreover, none of the published series can incorporate blinding, with considerable bias therefore inevitable.

Regarding the type of active treatment used, there is no ideal treatment, and all have pros and cons (Table 2). As options developed to prevent DB and DP it is important to consider the cost-effectiveness of each treatment. The overall rate of delayed adverse events is assessed as 10%, and the cost for management of these complications, including admission and additional therapies, is estimated at 5000 $ per patient. The cost for an economical prophylactic measure for each patient without adding to the overall financial cost is around 500 $ per cushion. Commercially available data show the price range per 1 mL to be 10-150 $; thus, it is necessary to consider the economics, the upfront cost for the added prophylactic intervention, and the downstream cost savings for an avoided hospitalization. If the mean used volume is 3 mL, we can estimate the cost-effectiveness of each tested agent, from PRP, the cheapest, to cyanoacrylate, the most expensive.

Apart from efficacy, mucosal healing activity is another important issue to consider. All these prophylactic measures help and accelerate mucosal reepithelialisation, but the healing process has only been measured with PRP. The ideal coverage agent should have a chemical structure and physical properties showing an appropriate adhesion capacity to avoid migration against gravity and adherence failure, some refractoriness to bacterial degradation in order to increase the bioactive period and reduce the incidence of PPS, and healing activity to increase mucosal healing rate. Application should be straight with minimal force to pass the agent, ideally using standard devices accessible to all endoscopy units, inducing a small increase in the time of the resection procedure and with a short learning curve. Ideally, it should also be able to release bioactive drugs to treat specific conditions such as colorectal cancer

Table 2 Pros and cons of coverage agents based on ideal properties

Property	PGA-FG	Surgicel	PRP	Purastat	Cyanoacrylate
Appropriate adhesion capacity	+	+	+	+	+
Absence of special device	-	+	+	-	+
Not time-consuming	-	+	+	+	+
Refractory to bacterial degradation	+	+	-	-	+
Healing activity	+	+	+	+	+
Price range of 1 mL ($)	20-25	15-20	10-12	100-150	150
Drug-release	-	-	-	-	-

PGA-FG: Polyglycocolic acid sheet with fibrin glue; PRP: Platelet-rich plasma.

or inflammatory bowel disease. All these properties are still to be confirmed in proof of concept studies with robust data.

To obtain the ideal agent, larger prospective studies with control groups and a comparison of the different substances are needed.

CONCLUSION

The use of coverage agents is the quickest and simplest technique to cover large mucosal defects, and published data seem to confirm their efficacy in the prevention of late complications. However, most of the reports are case series, without a control arm and with a relatively short follow-up. There is a lack of randomized controlled trials and of head-to-head comparative studies of shielding products. Moreover, none of the published series can incorporate blinding, with considerable bias therefore inevitable.

REFERENCES

1 **Burgess NG**, Metz AJ, Williams SJ, Singh R, Tam W, Hourigan LF, Zanati SA, Brown GJ, Sonson R, Bourke MJ. Risk factors for intraprocedural and clinically significant delayed bleeding after wide-field endoscopic mucosal resection of large colonic lesions. *Clin Gastroenterol Hepatol* 2014; **12**: 651-661. e1-3 [PMID: 24090728 DOI: 10.1016/j.cgh.2013.09.049]

2 **Albéniz E**, Fraile M, Ibáñez B, Alonso-Aguirre P, Martínez-Ares D, Soto S, Gargallo CJ, Ramos Zabala F, Álvarez MA, Rodríguez-Sánchez J, Múgica F, Nogales Ó, Herreros de Tejada A, Redondo E, Pin N, León-Brito H, Pardeiro R, López-Roses L, Rodríguez-Téllez M, Jiménez A, Martínez-Alcalá F, García O, de la Peña J, Ono A, Alberca de Las Parras F, Pellisé M, Rivero L, Saperas E, Pérez-Roldán F, Pueyo Royo A, Eguaras Ros J, Zúñiga Ripa A, Concepción-Martín M, Huelin-Álvarez P, Colán-Hernández J, Cubiella J, Remedios D, Bessa I Caserras X, López-Viedma B, Cobian J, González-Haba M, Santiago J, Martínez-Cara JG, Valdivielso E, Guarner-Argente C; Endoscopic Mucosal Resection Endoscopic Spanish Society Group. A Scoring System to Determine Risk of Delayed Bleeding After Endoscopic Mucosal Resection of Large Colorectal Lesions. *Clin Gastroenterol Hepatol* 2016; **14**: 1140-1147 [PMID: 27033428 DOI: 10.1016/j.cgh.2016.03.021]

3 **Burgess NG**, Bassan MS, McLeod D, Williams SJ, Byth K, Bourke MJ. Deep mural injury and perforation after colonic endoscopic mucosal resection: a new classification and analysis of risk factors. *Gut* 2017; **66**: 1779-1789 [PMID: 27464708 DOI: 10.1136/gutjnl-2015-309848]

4 **Ortiz O**, Rex DK, Ian G, Moyer M, Hasan MK, Pleskow D, Elmunzer JB, Khashab MA, Sanaei O, Al-Kawas F, Gordon SR, Mathew A, Levenick J, Aslanian H, Antaki F, von Renteln D, Crockett S, Rastogi A, Gill J, Law RJ, Wallace MB, Elias P, MacKenzie TA, Pohl H, Pellisé M. Factors associated with complete clip closure after endoscopic mucosal resection of large colorectal polyps. *Endoscopy* 2020 [PMID: 33291159 DOI: 10.1055/a-1332-6727]

5 **Pohl H**, Grimm IS, Moyer MT, Hasan MK, Pleskow D, Elmunzer BJ, Khashab MA, Sanaei O, Al-Kawas FH, Gordon SR, Mathew A, Levenick JM, Aslanian HR, Antaki F, von Renteln D, Crockett SD, Rastogi A, Gill JA, Law RJ, Elias PA, Pellise M, Wallace MB, Mackenzie TA, Rex DK. Clip Closure Prevents Bleeding After Endoscopic Resection of Large Colon Polyps in a Randomized Trial. *Gastroenterology* 2019; **157**: 977-984. e3 [PMID: 30885778 DOI: 10.1053/j.gastro.2019.03.019]

6 **Albéniz E**, Álvarez MA, Espinós JC, Nogales O, Guarner C, Alonso P, Rodríguez-Téllez M, Herreros de Tejada A, Santiago J, Bustamante-Balén M, Rodríguez Sánchez J, Ramos-Zabala F, Valdivielso E, Martínez-Alcalá F, Fraile M, Elosua A, Guerra Veloz MF, Ibáñez Beroiz B, Capdevila F, Enguita-

Germán M. Clip Closure After Resection of Large Colorectal Lesions With Substantial Risk of Bleeding. *Gastroenterology* 2019; **157**: 1213-1221. e4 [PMID: 31362007 DOI: 10.1053/j.gastro.2019.07.037]

7 **Spadaccini M**, Albéniz E, Pohl H, Maselli R, Thoguluva Chandrasekar V, Correale L, Anderloni A, Carrara S, Fugazza A, Badalamenti M, Iwatate M, Antonelli G, Enguita-Germán M, Álvarez MA, Sharma P, Rex DK, Hassan C, Repici A. Prophylactic Clipping After Colorectal Endoscopic Resection Prevents Bleeding of Large, Proximal Polyps: Meta-analysis of Randomized Trials. *Gastroenterology* 2020; **159**: 148-158. e11 [PMID: 32247023 DOI: 10.1053/j.gastro.2020.03.051]

8 **Lee HS**, Jeon SW, Kwon YH, Nam SY, Shin S, Kim R, Ahn S. Prophylactic endoscopic coagulation to prevent delayed post-EMR bleeding in the colorectum: a prospective randomized controlled trial (with videos). *Gastrointest Endosc* 2019; **90**: 813-822 [PMID: 31175874 DOI: 10.1016/j.gie.2019.05.039]

9 **Bon I**, Bartolí R, Lorenzo-Zúñiga V. Endoscopic shielding technique, a new method in therapeutic endoscopy. *World J Gastroenterol* 2017; **23**: 3761-3764 [PMID: 28638215 DOI: 10.3748/wjg.v23.i21.3761]

10 **Tsuji Y**, Ohata K, Gunji T, Shozushima M, Hamanaka J, Ohno A, Ito T, Yamamichi N, Fujishiro M, Matsuhashi N, Koike K. Endoscopic tissue shielding method with polyglycolic acid sheets and fibrin glue to cover wounds after colorectal endoscopic submucosal dissection (with video). *Gastrointest Endosc* 2014; **79**: 151-155 [PMID: 24140128 DOI: 10.1016/j.gie.2013.08.041]

11 **Hiroyuki T**, Kohki Y, Hiroe M, Tsunehito H, Rie A, Shota T, Hiroko T, Yuki O, Takagi T, Kengo T, Takashi T, Hideyuki K, Hideki T, Akeo H. A basic study of the effect of the shielding method with polyglycolic acid fabric and fibrin glue after endoscopic submucosal dissection. *Endosc Int Open* 2016; **4**: E1298-E1304 [PMID: 27995192 DOI: 10.1055/s-0042-118208]

12 **Shinya N**, Oka S, Miyabashira S, Kaetsu H, Uchida T, Sueyoshi M, Takase K, Akuzawa M, Miyamoto A, Shigaki T. Improvement of the tissue-adhesive and sealing effect of fibrin sealant using polyglycolic acid felt. *J Invest Surg* 2009; **22**: 383-389 [PMID: 19842894 DOI: 10.1080/08941930903214743]

13 **Myung YS**, Ko BM, Han JP, Hong SJ, Jeon SR, Kim JO, Moon JH, Lee MS. Effectiveness of Surgicel® (Fibrillar) in patients with colorectal endoscopic submucosal dissection. *Surg Endosc* 2016; **30**: 1534-1541 [PMID: 26201411 DOI: 10.1007/s00464-015-4369-5]

14 **Spangler D**, Rothenburger S, Nguyen K, Jampani H, Weiss S, Bhende S. In vitro antimicrobial activity of oxidized regenerated cellulose against antibiotic-resistant microorganisms. *Surg Infect (Larchmt)* 2003; **4**: 255-262 [PMID: 14588160 DOI: 10.1089/109629603322419599]

15 **Lorenzo-Zúñiga V**, Boix J, Moreno de Vega V, Bon I, Marín I, Bartolí R. Efficacy of platelet-rich plasma as a shielding technique after endoscopic mucosal resection in rat and porcine models. *Endosc Int Open* 2016; **4**: E859-E864 [PMID: 27540573 DOI: 10.1055/s-0042-109170]

16 **Zhou B**, Ren J, Ding C, Wu Y, Chen J, Wang G, Gu G, Li J. Protection of colonic anastomosis with platelet-rich plasma gel in the open abdomen. *Injury* 2014; **45**: 864-868 [PMID: 24552769 DOI: 10.1016/j.injury.2014.01.018]

17 **Lorenzo-Zúñiga V**, Moreno de Vega V, Bartolí R. Endoscopic Shielding With Platelet-rich Plasma After Resection Of Large Colorectal Lesions. *Surg Laparosc Endosc Percutan Tech* 2021; Epub ahead of print [PMID: 33538545 DOI: 10.1097/SLE.0000000000000898]

18 **Pioche M**, Camus M, Rivory J, Leblanc S, Lienhart I, Barret M, Chaussade S, Saurin JC, Prat F, Ponchon T. A self-assembling matrix-forming gel can be easily and safely applied to prevent delayed bleeding after endoscopic resections. *Endosc Int Open* 2016; **4**: E415-E419 [PMID: 27092320 DOI: 10.1055/s-0042-102879]

19 **Subramaniam S**, Kandiah K, Thayalasekaran S, Longcroft-Wheaton G, Bhandari P. Haemostasis and prevention of bleeding related to ER: The role of a novel self-assembling peptide. *United European Gastroenterol J* 2019; **7**: 155-162 [PMID: 30788128 DOI: 10.1177/2050640618811504]

20 **Soons E**, Turan A, van Geenen E, Siersema P. Application of a novel self-assembling peptide to prevent hemorrhage after EMR, a feasibility and safety study. *Surg Endosc* 2020 [PMID: 32804267 DOI: 10.1007/s00464-020-07819-7]

21 **Subramaniam S**, Kandiah K, Chedgy F, Fogg C, Thayalasekaran S, Alkandari A, Baker-Moffatt M, Dash J, Lyons-Amos M, Longcroft-Wheaton G, Brown J, Bhandari P. A novel self-assembling peptide for hemostasis during endoscopic submucosal dissection: a randomized controlled trial. *Endoscopy* 2021; **53**: 27-35 [PMID: 32679602 DOI: 10.1055/a-1198-0558]

22 **Martines G**, Picciariello A, Dibra R, Trigiante G, Jambrenghi OC, Chetta N, Altomare DF. Efficacy of cyanoacrylate in the prevention of delayed bleeding after endoscopic mucosal resection of large colorectal polyps: a pilot study. *Int J Colorectal Dis* 2020; **35**: 2141-2144 [PMID: 32577871 DOI: 10.1007/s00384-020-03678-9]

23 **Weilert F**, Binmoeller KF. Cyanoacrylate glue for gastrointestinal bleeding. *Curr Opin Gastroenterol* 2016; **32**: 358-364 [PMID: 27380462 DOI: 10.1097/MOG.0000000000000294]

World Journal of Gastroenterology

Submit a Manuscript: https://www.f6publishing.com

World J Gastroenterol 2021 April 21; 27(15): 1569-1577

DOI: 10.3748/wjg.v27.i15.1569

ISSN 1007-9327 (print) ISSN 2219-2840 (online)

MINIREVIEWS

Current status of diagnosis and therapy for intraductal papillary neoplasm of the bile duct

Yuji Sakai, Masayuki Ohtsuka, Harutoshi Sugiyama, Rintaro Mikata, Shin Yasui, Izumi Ohno, Yotaro Iino, Jun Kato, Toshio Tsuyuguchi, Naoya Kato

ORCID number: Yuji Sakai 0000-0002-1782-4829; Masayuki Ohtsuka 0000-0002-5091-1078; Harutoshi Sugiyama 0000-0001-6995-9605; Rintaro Mikata 0000-0002-9025-8085; Shin Yasui 0000-0002-3778-0712; Izumi Ohno 0000-0001-6434-6797; Yotaro Iino 0000-0002-7084-2268; Jun Kato 0000-0002-1869-2135; Toshio Tsuyuguchi 0000-0003-4897-5635; Naoya Kato 0000-0001-5812-2818.

Author contributions: Sakai Y, Ohtsuka M, Kato J, Tsuyuguchi T, and Kato N were responsible for manuscript preparation; Sakai Y wrote the paper; Tsuyuguchi T and Kato N revised the manuscript; Sugiyama H, Mikata R, Yasui S, Ohno I, and Iino Y collected the references.

Conflict-of-interest statement: The authors have no other disclosures.

Yuji Sakai, Harutoshi Sugiyama, Rintaro Mikata, Shin Yasui, Izumi Ohno, Yotaro Iino, Jun Kato, Toshio Tsuyuguchi, Naoya Kato, Department of Gastroenterology and Nephrology, Graduate School of Medicine, Chiba University, Chiba 260-8670, Japan

Masayuki Ohtsuka, Department of General Surgery, Graduate School of Medicine, Chiba University, Chiba 260-8670, Japan

Corresponding author: Yuji Sakai, MD, Doctor, Department of Gastroenterology and Nephrology, Graduate School of Medicine, Chiba University, Inohana 1-8-1, Chuou-ku, Chiba 260-8670, Japan. sakai4754@yahoo.co.jp

Abstract

Bile duct epithelial tumours showing papillary neoplasm in the bile duct lumen are present in the intrahepatic and extrahepatic bile ducts. Clinicopathological images of these tumours are distinctive and diverse, including histological images with a low to high grade dysplasia, infiltrating and noninfiltrating characteristics, excessive mucus production, and similarity to intraductal papillary mucinous neoplasm (IPMN) of the pancreas. The World Health Organization Classification of Tumours of the Digestive System in 2010 named these features, intraductal papillary neoplasm of the bile duct (IPNB), as precancerous lesion of biliary carcinoma. IPNB is currently classified into type 1 that is similar to IPMN, and type 2 that is not similar to IPMN. Many of IPNB spreads superficially, and diagnosis with cholangioscopy is considered mandatory to identify accurate localization and progression. Prognosis of IPNB is said to be better than normal bile duct cancer.

Key Words: Intraductal papillary neoplasm of the bile duct; Intraductal papillary mucinous neoplasm of the pancreas; Peroral cholangioscopy; Cholangioscopy

Core Tip: Intraductal papillary neoplasm of the bile duct (IPNB) is classified into type 1 that is similar to intraductal papillary mucinous neoplasm (IPMN) and type 2 that is not similar to IPMN. Many of IPNB spreads superficially, and diagnosis with

Manuscript source: Invited manuscript

Specialty type: Gastroenterology and hepatology

Country/Territory of origin: Japan

Peer-review report's scientific quality classification
Grade A (Excellent): 0
Grade B (Very good): B, B
Grade C (Good): 0
Grade D (Fair): 0
Grade E (Poor): 0

Received: January 17, 2021
Peer-review started: January 17, 2021
First decision: February 9, 2021
Revised: February 13, 2021
Accepted: March 24, 2021
Article in press: March 24, 2021
Published online: April 21, 2021

P-Reviewer: Karaca CA, Pan W
S-Editor: Zhang L
L-Editor: A
P-Editor: Li JH

cholangioscopy is considered mandatory to identify accurate localization and progression. Prognosis of IPNB is said to be better than normal bile duct cancer.

Citation: Sakai Y, Ohtsuka M, Sugiyama H, Mikata R, Yasui S, Ohno I, Iino Y, Kato J, Tsuyuguchi T, Kato N. Current status of diagnosis and therapy for intraductal papillary neoplasm of the bile duct. *World J Gastroenterol* 2021; 27(15): 1569-1577
URL: https://www.wjgnet.com/1007-9327/full/v27/i15/1569.htm
DOI: https://dx.doi.org/10.3748/wjg.v27.i15.1569

INTRODUCTION

Presence of intraductal tumours showing a pattern of spurring papillary neoplasm has been known since before[1-4]. Although the names of these tumours varied depending on the country and region, it is known that the tumours have a better postoperative prognosis than normal infiltrating bile duct cancer. Also known are the facts that quite a few pre-infiltrating phases can be found in these tumours; cases with a low grade dysplasia are present; and some cases have excessive mucus production. Many similarities with intraductal papillary mucinous neoplasm (IPMN) of the pancreas are also pointed out. A recommendation has been made in recent years to call these tumours intraductal papillary neoplasm of the bile duct (IPNB)[1]. Diagnosis of IPNB and the current status of its treatment are hereby reported.

HISTORY OF IPNB

Epithelial tumours demonstrating a variety of images develop in the bile duct. Of these tumours, bile duct epithelial tumours indicate papillary neoplasm in the bile duct lumen[1-4]. These tumours have better prognosis than normal bile duct cancer, and often present with distinguishing and diverse clinical pathophysiology. Yet, no specific name was given to these tumours. In the United States and Europe, these tumours are called biliary papilloma if they are solitary, and biliary papillomatosis if they are multiple[5,6]. These are slow growing, low grade tumours with potential malignancy, and some cases of infiltration and metastasis have been also reported. Separately, hepatobiliary cystadenoma and adenoma also exist, and differences among these diseases were not necessarily clear-cut.

Intrahepatic stone-related intrahepatic bile duct cancer was examined in 2001. There are quite a few bile duct epithelial tumours showing papillary growth in the bile duct, with excessive mucus production. These tumours are morphologically and characteristically similar to IPMN of the pancreas; thus, we consider these cases as neoplastic lesion and reported it as intraductal papillary neoplasm of the liver[7]. As similar tumours were also noted thereafter in the extrahepatic bile duct, the tumours were renamed IPNB[8]. This lesion was officially named IPNB in the revised World Health Organization Classification of Tumours of the Digestive System in 2010[9].

PATHOLOGICAL DIAGNOSIS OF IPNB

IPNB is epithelial tumour with intraductal papillary proliferation, and defined as having a histologically thin fibrovascular stem[1-4]. Excessive mucus production is often noted but this is not a decisive element for diagnosis of IPNB. IPNB is reported to be a lesion similar to IPMN. Specific lesions are: (1) Papillary proliferation of tumours in the bile duct lumen or in the bile duct; (2) Intestinal, gastric, pancreatobiliary, and oncocytic subtypes noted in IPMN are also common in IPNB; (3) As in IPMN, cancerous cells show intraepithelial and intramucosal progression along the intraductal wall adjacent to the primary site, and some are multiple cases with asynchronous and simultaneous tumours; (4) IRNB has better prognosis compared with normal bile duct cancer or normal pancreatic carcinoma; (5) Some IPNB cases show excessive mucus production; however, the incidence is lower than that of IPMN. In some cases, no clear excessive mucus production is noted. Patients with excessive

mucus production often show cystic expansion of the bile duct at the main site of papillary growth; and (6) In the case of infiltrating growth of IPNB, either normal tubular adenocarcinoma or bile duct mucinous adenocarcinoma may result. Similar infiltrating images are also known in IPMN.

The World Health Organization Classification of Tumours of the Digestive System in 2010 added the definition of IPNB as one of precancerous, pre-infiltrating lesions of the bile duct cancer[9]. However, studies since then have revealed that some cases with intraductal noninfiltrating papillary tumours are slightly different from those cases similar to IPMN. These different cases include biliary papillary adenocarcinoma that has been previously reported by Albores-Saavedra[10,11]. Based on these results, IPNB was classified into two types. Type 1 is IPNB similar to IPMN, and mostly classified into gastric and intestinal subtypes. Type 1 shows homogeneous tissue image, and often occurs in the intrahepatic bile duct, with excessive mucus production often experienced by patients. Many of type 1 IPNB is considered a high grade dysplasia; however, some regions often show a low grade dysplasia, and some cases have only a low grade dysplasia. Type 1 includes many of patients undergoing resection in noninfiltrating phase, and those who show cystic expansion in the bile duct with lesion. Type 2 IPNB is slightly different from IPMN; however, it is experienced as IPMN in rare cases. Type 2 IPNB includes lesions previously reported by Albores-Saavedra as bile duct papillary adenocarcinoma and papillary bile duct cancer[7,8]. Tissue images of type 2 IPNB are slightly more complicated, showing some solid sites. Almost all cases are considered a high grade dysplasia, often occurring in the extrahepatic bile duct. Many cases already show infiltrating images at the time of resection, but some cases show noninfiltration. Most of the cases are classified into intestinal and pancreatobiliary subtypes, with few cases of excessive mucus production. Examination of IRNB with macroscopic mucus production revealed that many of tumours with mucus production are noninfiltrating, similar to IPMN, and those with no mucus production tended to show infiltration[12]. IPNB classification is still far from perfect. After classifying into two types, we find it difficult to classify into type 1 IPNB and type 2 IPNB in some cases, or to differentiate progressed papillary bile duct cancer from type 2 IPNB. Further consideration is necessary.

IPNB DIAGNOSIS

Image diagnosis plays an important role in giving a diagnosis of IPNB. If clinical symptoms show abdominal pain, pyrexia, and elevation of hepatobiliary enzymes in a blood test, an image diagnosis of the abdominal region will be made. In this case, abdominal ultrasonography, contrast computed tomography (Figure 1), Magnetic resonance imaging (Figure 2), and endosonography will enable us to identify the main focus[13]. However, these modalities may not ensure an accurate diagnosis because the presence of mucus, which is characteristics of IPNB, must be verified, and superficial expansion and progression of IPNB are often to the extent beyond our expectation. This is where direct cholangiography, intraductal ultrasonography (IDUS), and cholangioscopy come in[14-16]. The presence of mucus can be identified by checking papillary dilation and emission of mucus with endoscopy, or by outlining the mucous plug with cholangiography (Figure 3). Even when cholangiography contrasts the bile duct dilated with mucus, it is difficult in some cases to identify the main focus itself owing to mucus, let alone superficial expansion and progression. Meanwhile, IDUS enables us to identify the main focus and depict mucus; it can be easily conducted at the time of ERCP by following the guide wire; and it allows us to capture a wide scope of the region for observation. The presence of mucus, however, makes it difficult to evaluate the bile duct wall in IDUS. Thus, cholangioscopy plays a central role in the diagnosis of IPNB[14-16]. Cholangioscopy enables us to observe with narrow band imaging in addition to usual white light imaging, and is considered useful for the diagnosis of benignancy and malignancy as well as progression staging[14-16]. As mentioned earlier, the main focus of papillary bulge may be captured by computed tomography and magnetic resonance imaging, but the evaluation of superficial spread and progression from the main focus is difficult. Cholangioscopy allows us to directly observe the superficial spread and progression and to perform an open biopsy, thereby enabling accurate diagnosis of the progression (Figure 4). Depending on a route of approach, percutaneous transhepatic cholangioscopy (PTCS) and peroral cholangiosccopy (POCS) are available in cholangioscopy. Generally, PTCS where percutaneous biliary drainage is performed, has a bigger channel diameter and a shorter effective length. These features make it easy to wash and superior in removing

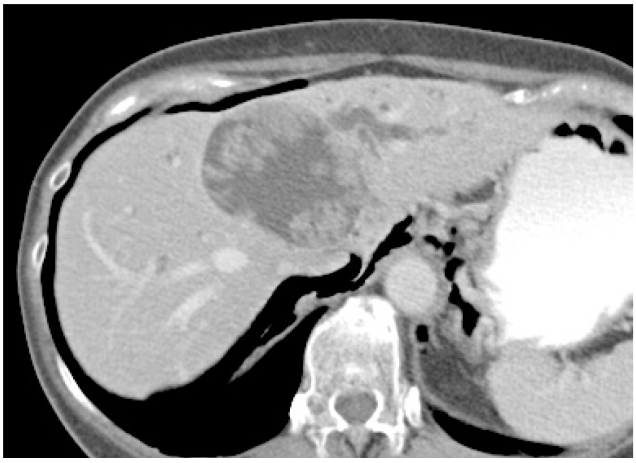

Figure 1 Contrast computed tomography revealed a 70-mm cystic lesion with a papillary bump in the lumen of left hepatic lobe.

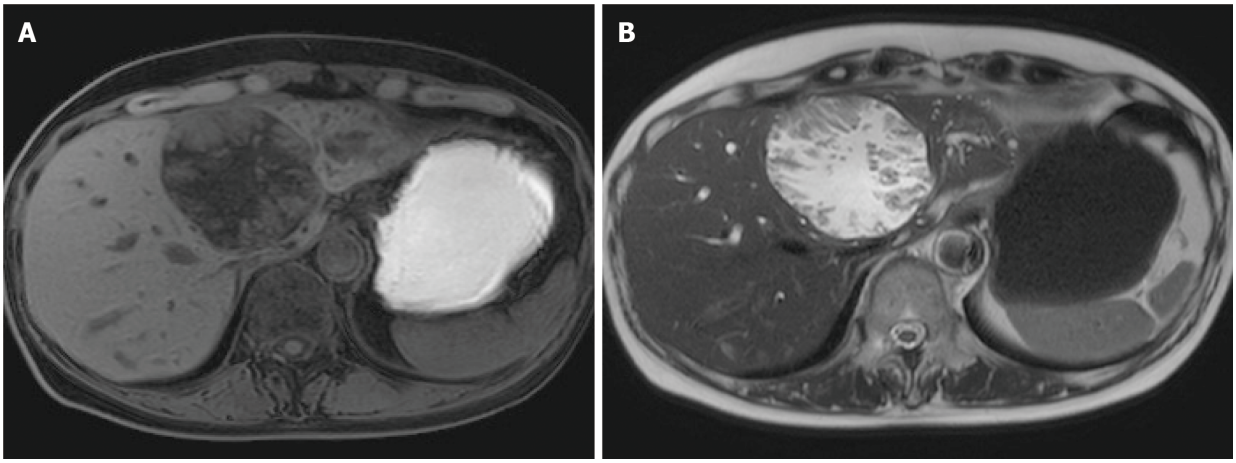

Figure 2 Magnetic resonance imaging. A: T1-weighted image; and B: T2-weighted image papillary solid lesion protuberating from cystic wall is noted and the cystic component showed the same signals as water. Transportation between the cyst and the root of left hepatic duct is noted.

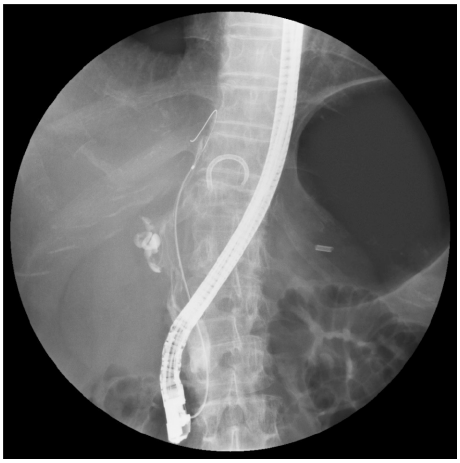

Figure 3 Translucency caused by mucus is noted from hepatic portal region to lower bile duct.

mucus. With great operability, PTCS ensures a sufficient visual field and enables a wider scope of observation and more detailed monitoring. Weak points of PTCS are that it takes time until we can observe as time to fistula formation is required, and that dissemination *via* fistula has been also reported[15]. Therefore, the current indications for PTCS are limited, and POCS is mostly performed except for the following cases:

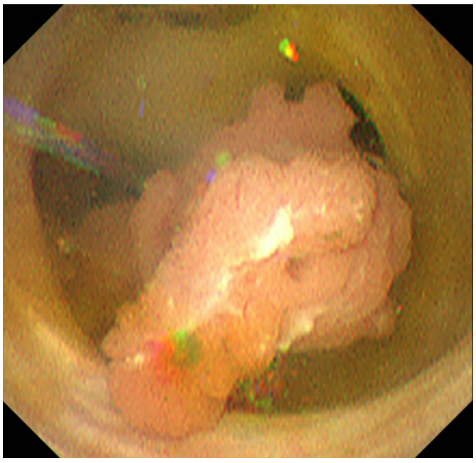

Figure 4 The lesion originates from the root of left hepatic duct, and pedunculated and elevated lesion protruded toward the extrahepatic bile duct, with no clear superficial spread.

Difficulty in biliary cannulation with ERCP; difficulty in reaching duodenal papilla after Billroth-2 method or Rou-X-en Y anastomosis; and difficulty in removing mucus with POCS. Benefits of POCS are that it does not require fistula formation, allows direct observation from the initial ERCP, and entails no risk for fistula dissemination. On the other hand, POCS may limit the scope of observation since its approach route is longer and operation is cumbersome and difficult. Nonetheless, sufficient evaluation with POCS is possible because the resection line of distal site of the tumour is important in determining the scope of resection at the time of operation on IPNB (Figures 5 and 6).

RESULTS OF SURGICAL TREATMENT OF IPNB

Treatment results in dysplasia

Kubota *et al*[17] examined 119 patients with intrahepatic IPNB, and reported the 5-year survival: 84.6% in low or intermediate-grade neoplasia group, 90.9% in high-grade neoplasia group, and 79.2% in invasive carcinoma group. When complete resection was performed, no statistical significance was noted in overall survival between the group of infiltrating cancer and the other group of noninfiltrating cancers. As further examinations of infiltrating cancer, Onoe *et al*[18] reported the ratio of infiltrating site relative to the lesion and its prognosis on 184 patients with intrahepatic and extrahepatic bile duct cancer exhibiting intraductal papillary proliferation. The 5-year survival in four groups: Noninfiltrating cancer, infiltrating site < 10%, infiltrating site = 10%-50%, and infiltrating site > 50%, were 92%, 74%, 64%, and 33%, respectively. The former three groups showed no statistical between-group differences; however, the infiltrating site > 50% group showed significantly poor prognosis, almost equivalent to the 5-year survival of 35% in 460 patients with non-papillary bile duct cancer. Onoe *et al*[18], pointed out that there still was a moot point in the disease concept of IPNB but indicated that if bile duct cancer exhibiting intraductal papillary proliferation was an infiltrating cancer, with an infiltrating site accounting for not more than 50% of the entire cancer, its good prognosis was more significant than non-papillary bile duct cancer. Rocha *et al*[19] reported that 29 of 39 IPNB patients (74%) had infiltrating cancer. Significantly poor prognostic factors were infiltration exceeding 5 mm, and infiltration beyond the bile duct wall, exceeding 10% of the entire tumour. The ratio of infiltrating cancer in IPMN is 21%-48%[19,20] , while that in IPNB is 70%-80%, slightly higher[21,22]. It is reported that prognoses of IPMN-derived infiltrating cancer and infiltrating pancreatic ductal carcinoma are almost the same[23,24], or prognosis of IPMN-derived infiltrating cancer is slightly better[25,26]. Meanwhile, better prognosis is reported in IPNB as compared with normal bile duct cancer[27]. This is due to characteristics of IPNB tumour itself, and because of relatively early diagnosis that is possible with obstructive jaundice caused by its proliferation into the intraductal lumen.

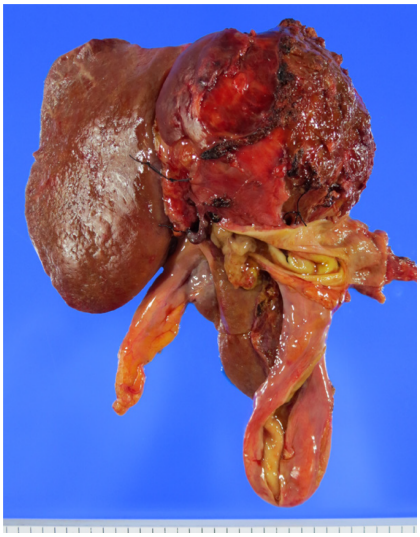

Figure 5 Resected specimen. Left lobectomy, caudal lobectomy, resection of extrahepatic bile duct, and choledochojejunostomy were performed.

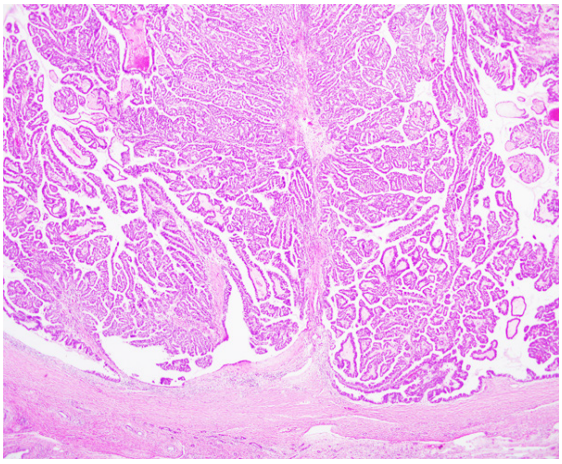

Figure 6 Pathological diagnosis is intraductal papillary neoplasm of the bile duct with an associated invasive carcinoma (Hematoxylin-Eosin Stain) with no superficial spread.

PROGNOSTIC FACTORS

Presence or absence of complete resection is an important prognostic factor, and reported in great numbers[18,19,28,29]. Luvira *et al*[28] reported that the bile duct resection stump tested positive for invasive carcinoma, and overall survival significantly decreased, while testing positive for dysplasia and carcinoma in situ did not impact prognosis. In contrast, Jung *et al*[29] reported that overall survival and recurrence-free survival of the group in which the bile duct resection stump tested positive for a low to intermediate grade dysplasia, significantly decreased to the extent similar to the overall survival of carcinoma in situ and invasive carcinoma, as compared with the group that tested negative. International consensus guidelines for the management of IPMN specifies that additional resection is indispensable if a clear high grade dysplasia or infiltrating cancer is present in the pancreatic resection stump while additional resection is not necessary even when a low grade dysplasia is present on the stump[30]. In IPNB, no guideline is available for a low grade dysplasia in the bile duct resection stump. Unlike IPMN where total pancreatectomy is therapeutic option depending on a patient, there is a resection limit for the bile duct, and thus, additional resection is performed as much as possible at each institution.

Presence or absence of metastases to lymph nodes is a major prognostic factor along with complete resection[18,28,29]. Luvira *et al*[28] reported that the 5-year survival of patients tested negative for metastases to lymph nodes was 51.2% while that of those tested positive was 11.1%, suggesting significantly poor prognosis. Of all 124 patients with IPNB, 98 patients underwent lymph node dissection. No difference in prognosis

was noted between these 98 patients and 26 patients without lymph node dissection, and thus, the results failed to support the usefulness of lymph node dissection. Patients with infiltrating cancer include those patients with lymph node dissection, and lymph node dissection may seem necessary. However, metastases to lymph node rarely occur in an intraductal growth type of intrahepatic bile duct cancer. As there are type 1 and type 2 for IPNB, more meticulous consideration may be needed to discuss the necessity of lymph node dissection in the future.

RECURRENCE OF IPNB AFTER SURGICAL TREATMENT

IPNB is known to recur in the bile duct after surgical resection. Despite that the initial resection stump of the bile duct tested negative, intraductal papillary tumour presenting with tissue image similar to the initial resection recurred. This is the characteristics similar to IPMN. IPNB recurs after more than 10 years in some cases, appearing as if it were new carcinoma. This suggests a multicentric growth of IPMN[31]. Therefore, observation of clinical course is necessary, with postoperative intraductal recurrence in mind.

CONCLUSION

IPNB is classified into type 1 that is similar to IPMN and type 2 that is not similar to IPMN. Prognosis of IPNB is said to be better than normal bile duct cancer. Cholangioscopy is useful for diagnosis of localization and progression. It is important to determine an operative method based on information obtained through cholangioscopy and to observe clinical course.

ACKNOWLEDGEMENTS

The authors thanks Masaru Miyazaki for supporting this study.

REFERENCES

1 **Bosman FT**, Camerio FC, Hurban RH. World Health Organization classification of tumours. Pathology and genetics of Tumours of the digestive system. 4th ed. IARC press, Lyon 2010
2 **Nakanuma Y**, Sudo Y. Biliary tumors with pancreatic counterparts. *Semin Diagn Pathol* 2017; **34**: 167-175 [PMID: 28109714 DOI: 10.1053/j.semdp.2016.12.013]
3 **Nakanuma Y**, Sasaki M, Ishikawa A, Tsui W, Chen TC, Huang SF. Biliary papillary neoplasm of the liver. *Histol Histopathol* 2002; **17**: 851-861 [PMID: 12168796 DOI: 10.14670/HH-17.851]
4 **Nakanuma Y**, Uesaka K, Miyayama S, Yamaguchi H, Ohtsuka M. Intraductal neoplasms of the bile duct. A new challenge to biliary tract tumor pathology. *Histol Histopathol* 2017; **32**: 1001-1015 [PMID: 28337739 DOI: 10.14670/HH-11-892]
5 **Lee SS**, Kim MH, Lee SK, Jang SJ, Song MH, Kim KP, Kim HJ, Seo DW, Song DE, Yu E, Lee SG, Min YI. Clinicopathologic review of 58 patients with biliary papillomatosis. *Cancer* 2004; **100**: 783-793 [PMID: 14770435 DOI: 10.1002/cncr.20031]
6 **Yeung YP**, AhChong K, Chung CK, Chun AY. Biliary papillomatosis: report of seven cases and review of English literature. *J Hepatobiliary Pancreat Surg* 2003; **10**: 390-395 [PMID: 14598142 DOI: 10.1007/s00534-002-0837-0]
7 **Chen TC**, Nakanuma Y, Zen Y, Chen MF, Jan YY, Yeh TS, Chiu CT, Kuo TT, Kamiya J, Oda K, Hamaguchi M, Ohno Y, Hsieh LL, Nimura Y. Intraductal papillary neoplasia of the liver associated with hepatolithiasis. *Hepatology* 2001; **34**: 651-658 [PMID: 11584359 DOI: 10.1053/jhep.2001.28199]
8 **Zen Y**, Fujii T, Itatsu K, Nakamura K, Minato H, Kasashima S, Kurumaya H, Katayanagi K, Kawashima A, Masuda S, Niwa H, Mitsui T, Asada Y, Miura S, Ohta T, Nakanuma Y. Biliary papillary tumors share pathological features with intraductal papillary mucinous neoplasm of the pancreas. *Hepatology* 2006; **44**: 1333-1343 [PMID: 17058219 DOI: 10.1002/hep.21387]
9 **Nakanuma Y**, Curado M-P, Franceschi S, Gores G, Paradis V, Sripa B. Intrahepatic cholangiocarcinoma. Bosman FT, Carneiro F, Hruban RH, Theise ND. In: World Health Organization Classification of Tumours of the Digestive System (4th). WHO 2010: 217-224
10 **Albores-Saavedra J**, Murakata L, Krueger JE, Henson DE. Noninvasive and minimally invasive papillary carcinomas of the extrahepatic bile ducts. *Cancer* 2000; **89**: 508-515 [PMID: 10931449 DOI: 10.1002/1097-0142(20000801)89:3<508::aid-cncr5>3.0.co;2-d]

11 **Hoang MP**, Murakata LA, Katabi N, Henson DE, Albores-Saavedra J. Invasive papillary carcinomas of the extrahepatic bile ducts: a clinicopathologic and immunohistochemical study of 13 cases. *Mod Pathol* 2002; **15**: 1251-1258 [PMID: 12481004 DOI: 10.1097/01.MP.0000036450.61830.8E]

12 **Ohtsuka M**, Kimura F, Shimizu H, Yoshidome H, Kato A, Yoshitomi H, Furukawa K, Takeuchi D, Takayashiki T, Suda K, Takano S, Kondo Y, Miyazaki M. Similarities and differences between intraductal papillary tumors of the bile duct with and without macroscopically visible mucin secretion. *Am J Surg Pathol* 2011; **35**: 512-521 [PMID: 21412069 DOI: 10.1097/PAS.0b013e3182103f36]

13 **Kim JE**, Lee JM, Kim SH, Baek JH, Moon SK, Yu IS, Lee JY, Han JK, Choi BI. Differentiation of intraductal growing-type cholangiocarcinomas from nodular-type cholangiocarcinomas at biliary MR imaging with MR cholangiography. *Radiology* 2010; **257**: 364-372 [PMID: 20829532 DOI: 10.1148/radiol.10092105]

14 **Sakai Y**, Tsuyuguchi T, Tsuchiya S, Fukuda Y, Miyakawa K, Sugiyama H, Asano K, Ohtsuka M, Miyazaki M, Yokosuka O. Clinical utility of peroral cholangioscopy for mucin-producing bile duct tumor. *Hepatogastroenterology* 2008; **55**: 1509-1512 [PMID: 19102332]

15 **Sakamoto E**, Hayakawa N, Kamiya J, Kondo S, Nagino M, Kanai M, Miyachi M, Uesaka K, Nimura Y. Treatment strategy for mucin-producing intrahepatic cholangiocarcinoma: value of percutaneous transhepatic biliary drainage and cholangioscopy. *World J Surg* 1999; **23**: 1038-43; discussion 1043 [PMID: 10512944 DOI: 10.1007/s002689900620]

16 **Itoi T**, Sofuni A, Itokawa F, Tsuchiya T, Kurihara T, Ishii K, Tsuji S, Moriyasu F, Gotoda T. Peroral cholangioscopic diagnosis of biliary-tract diseases by using narrow-band imaging (with videos). *Gastrointest Endosc* 2007; **66**: 730-736 [PMID: 17905015 DOI: 10.1016/j.gie.2007.02.056]

17 **Kubota K**, Nakanuma Y, Kondo F, Hachiya H, Miyazaki M, Nagino M, Yamamoto M, Isayama H, Tabata M, Kinoshita H, Kamisawa T, Inui K. Clinicopathological features and prognosis of mucin-producing bile duct tumor and mucinous cystic tumor of the liver: a multi-institutional study by the Japan Biliary Association. *J Hepatobiliary Pancreat Sci* 2014; **21**: 176-185 [PMID: 23908126 DOI: 10.1002/jhbp.23]

18 **Onoe S**, Shimoyama Y, Ebata T, Yokoyama Y, Igami T, Sugawara G, Nakamura S, Nagino M. Prognostic delineation of papillary cholangiocarcinoma based on the invasive proportion: a single-institution study with 184 patients. *Surgery* 2014; **155**: 280-291 [PMID: 24287144 DOI: 10.1016/j.surg.2013.08.011]

19 **Rocha FG**, Lee H, Katabi N, DeMatteo RP, Fong Y, D'Angelica MI, Allen PJ, Klimstra DS, Jarnagin WR. Intraductal papillary neoplasm of the bile duct: a biliary equivalent to intraductal papillary mucinous neoplasm of the pancreas? *Hepatology* 2012; **56**: 1352-1360 [PMID: 22504729 DOI: 10.1002/hep.25786]

20 **D'Angelica M**, Brennan MF, Suriawinata AA, Klimstra D, Conlon KC. Intraductal papillary mucinous neoplasms of the pancreas: an analysis of clinicopathologic features and outcome. *Ann Surg* 2004; **239**: 400-408 [PMID: 15075659 DOI: 10.1097/01.sla.0000114132.47816.dd]

21 **Nakanuma Y**, Zen Y, Harada K, Ikeda H, Sato Y, Uehara T, Sasaki M. Tumorigenesis and phenotypic characteristics of mucin-producing bile duct tumors: an immunohistochemical approach. *J Hepatobiliary Pancreat Sci* 2010; **17**: 211-222 [PMID: 19680592 DOI: 10.1007/s00534-009-0158-7]

22 **Paik KY**, Heo JS, Choi SH, Choi DW. Intraductal papillary neoplasm of the bile ducts: the clinical features and surgical outcome of 25 cases. *J Surg Oncol* 2008; **97**: 508-512 [PMID: 18314868 DOI: 10.1002/jso.20994]

23 **Wada K**, Kozarek RA, Traverso LW. Outcomes following resection of invasive and noninvasive intraductal papillary mucinous neoplasms of the pancreas. *Am J Surg* 2005; **189**: 632-6; discussion 637 [PMID: 15862510 DOI: 10.1016/j.amjsurg.2005.01.020]

24 **Schnelldorfer T**, Sarr MG, Nagorney DM, Zhang L, Smyrk TC, Qin R, Chari ST, Farnell MB. Experience with 208 resections for intraductal papillary mucinous neoplasm of the pancreas. *Arch Surg* 2008; **143**: 639-46; discussion 646 [PMID: 18645105 DOI: 10.1001/archsurg.143.7.639]

25 **Maire F**, Hammel P, Terris B, Paye F, Scoazec JY, Cellier C, Barthet M, O'Toole D, Rufat P, Partensky C, Cuillerier E, Lévy P, Belghiti J, Ruszniewski P. Prognosis of malignant intraductal papillary mucinous tumours of the pancreas after surgical resection. Comparison with pancreatic ductal adenocarcinoma. *Gut* 2002; **51**: 717-722 [PMID: 12377813 DOI: 10.1136/gut.51.5.717]

26 **Yamaguchi K**, Kanemitsu S, Hatori T, Maguchi H, Shimizu Y, Tada M, Nakagohri T, Hanada K, Osanai M, Noda Y, Nakaizumi A, Furukawa T, Ban S, Nobukawa B, Kato Y, Tanaka M. Pancreatic ductal adenocarcinoma derived from IPMN and pancreatic ductal adenocarcinoma concomitant with IPMN. *Pancreas* 2011; **40**: 571-580 [PMID: 21499212 DOI: 10.1097/MPA.0b013e318215010c]

27 **Yeh CN**, Jan YY, Yeh TS, Hwang TL, Chen MF. Hepatic resection of the intraductal papillary type of peripheral cholangiocarcinoma. *Ann Surg Oncol* 2004; **11**: 606-611 [PMID: 15172934 DOI: 10.1245/ASO.2004.04.028]

28 **Luvira V**, Pugkhem A, Bhudhisawasdi V, Pairojkul C, Sathitkarnmanee E, Luvira V, Kamsa-Ard S. Long-term outcome of surgical resection for intraductal papillary neoplasm of the bile duct. *J Gastroenterol Hepatol* 2017; **32**: 527-533 [PMID: 27356284 DOI: 10.1111/jgh.13481]

29 **Jung G**, Park KM, Lee SS, Yu E, Hong SM, Kim J. Long-term clinical outcome of the surgically resected intraductal papillary neoplasm of the bile duct. *J Hepatol* 2012; **57**: 787-793 [PMID: 22634127 DOI: 10.1016/j.jhep.2012.05.008]

30 **Tanaka M**, Fernández-Del Castillo C, Kamisawa T, Jang JY, Levy P, Ohtsuka T, Salvia R, Shimizu Y, Tada M, Wolfgang CL. Revisions of international consensus Fukuoka guidelines for the management of IPMN of the pancreas. *Pancreatology* 2017; **17**: 738-753 [PMID: 28735806 DOI:

10.1016/j.pan.2017.07.007]
31 **Nakanishi Y**, Kondo S, Hirano S, Ambo Y, Tanaka E, Morikawa T, Itoh T. Recurrence of mucosal carcinoma of the bile duct, with superficial flat spread, 12 years after operation. *J Hepatobiliary Pancreat Surg* 2006; **13**: 355-358 [PMID: 16858550 DOI: 10.1007/s00534-006-1092-6]

World Journal of Gastroenterology

Submit a Manuscript: https://www.f6publishing.com

World J Gastroenterol 2021 April 21; 27(15): 1578-1594

DOI: 10.3748/wjg.v27.i15.1578

ISSN 1007-9327 (print) ISSN 2219-2840 (online)

ORIGINAL ARTICLE

Basic Study

Leucine-rich repeat-containing G protein-coupled receptor 5 marks different cancer stem cell compartments in human Caco-2 and LoVo colon cancer lines

Samah Abdulaali Alharbi, Dmitry A Ovchinnikov, Ernst Wolvetang

ORCID number: Samah Abdulaali Alharbi 0000-0001-8989-0190; Dmitry A Ovchinnikov 0000-0001-9603-8385; Ernst Wolvetang 0000-0002-2146-6614.

Author contributions: Alharbi SA contributed investigation, methodology, formal analysis, visualization, preparation and original draft preparation; Ovchinnikov DA contributed conceptualization, methodology and supervision; Wolvetang E contributed conceptualization, supervision, funding, acquisition, project administration and resources and reviewed and edited the manuscript.

Institutional review board statement: The study was reviewed and approved by the Institutional Review Board at The University of Queensland (approval No. 2019000159).

Institutional animal care and use committee statement: All animal experiments conformed to the internationally accepted principles for the care and use of laboratory animals, The Australian Institute of Bioengineering and Nanotechnology, Brisbane; Australia (approval No.

Samah Abdulaali Alharbi, Physiology Department, College of Medicine, Umm Al-Qura University, Makkah 24231, Saudi Arabia

Samah Abdulaali Alharbi, Ernst Wolvetang, Department of Stem Cell Engineering Group, Australian Institute for Bioengineering and Nanotechnology, The University of Queensland, Brisbane 4072, QLD, Australia

Dmitry A Ovchinnikov, Australian Institute for Bioengineering and Nanotechnology, The University of Queensland, Brisbane 4072, QLD, Australia

Corresponding author: Samah Abdulaali Alharbi, PhD, Assistant Professor, Senior Scientist, Physiology Department, College of Medicine, Umm Al-Qura University, Prince Sultan bin AbdulAziz road, Makkah 24231, Saudi Arabia. saaharbi@uqu.edu.sa

Abstract

BACKGROUND

Colon cancer cell lines are widely used for research and for the screening of drugs that specifically target the stem cell compartment of colon cancers. It was reported that colon cancer carcinoma specimens contain a subset of leucine-rich repeat-containing G protein-coupled receptor 5 (LGR5)-expressing stem cells, these so-called "tumour-initiating" cells, reminiscent in their properties of the normal intestinal stem cells (ISCs), may explain the apparent heterogeneity of colon cancer cell lines. Also, colon cancer is initiated by aberrant Wnt signaling in ISCs known to express high levels of LGR5. Furthermore, *in vivo* reports demonstrate the clonal expansion of intestinal adenomas from a single LGR5-expressing cell.

AIM

To investigate whether colon cancer cell lines contain cancer stem cells and to characterize these putative cancer stem cells.

METHODS

A portable fluorescent reporter construct based on a conserved fragment of the LGR5 promoter was used to isolate the cell compartments expressing different levels of LGR5 in two widely used colon cancer cell lines (Caco-2 and LoVo). These cells were then characterized according to their proliferation capacity, gene expression signatures of ISC markers, and their tumorigenic properties *in vivo* and

AIBN/065/12/SCA/LEJEUNE/KACST).

Conflict-of-interest statement: All authors have nothing to disclose.

Data sharing statement: No additional data are available.

ARRIVE guidelines statement: The authors have read the ARRIVE Guidelines, and the manuscript was prepared and revised according to the ARRIVE Guidelines.

Manuscript source: Unsolicited manuscript

Specialty type: Gastroenterology and hepatology

Country/Territory of origin: Saudi Arabia

Peer-review report's scientific quality classification

Grade A (Excellent): A
Grade B (Very good): 0
Grade C (Good): 0
Grade D (Fair): 0
Grade E (Poor): 0

Received: December 1, 2020
Peer-review started: December 1, 2020
First decision: December 21, 2020
Revised: January 22, 2021
Accepted: February 24, 2021
Article in press: February 24, 2021
Published online: April 21, 2021

P-Reviewer: Bordonaro M
S-Editor: Gao CC
L-Editor: Filipodia

in vitro.

RESULTS

The data revealed that the LGR5 reporter can be used to identify and isolate a classical intestinal crypt stem cell-like population from the Caco-2, but not from the LoVo, cell lines, in which the cancer stem cell population is more akin to B lymphoma Moloney murine leukemia virus insertion region 1 homolog (+4 crypt) stem cells. This sub-population within Caco-2 cells exhibits an intestinal cancer stem cell gene expression signature and can both self-renew and generate differentiated LGR5 negative progeny. Our data also show that cells expressing high levels of LGR5/enhanced yellow fluorescent protein (EYFP) from this cell line exhibit tumorigenic-like properties *in vivo* and *in vitro*. In contrast, cell compartments of LoVo that are expressing high levels of LGR5/EYFP did not show these stem cell-like properties. Thus, cells that exhibit high levels of LGR5/EYFP expression represent the cancer stem cell compartment of Caco-2 colon cancer cells, but not LoVo cells.

CONCLUSION

Our findings highlight the presence of a spectrum of different ISC-like compartments in different colon cancer cell lines. Their existence is an important consideration for their screening applications and should be taken into account when interpreting drug screening data. We have generated a portable LGR5-reporter that serves as a valuable tool for the identification and isolation of different colon cancer stem cell populations in colon cancer lines.

Key Words: Colorectal cancer; Colon cancer cell lines; Intestinal stem cell; Cancer stem cell; Leucine-rich repeat-containing G protein-coupled receptor 5; Heterogenicity

Core Tip: The intestinal epithelium harbors two distinct pools of putative stem cells, the leucine-rich repeat-containing G protein-coupled receptor 5$^+$(LGR5) stem cell population and the B lymphoma Moloney murine leukemia virus insertion region 1 homolog$^+$ stem cell population. Colon cancer cell lines such as Caco-2 and LoVo are extensively used in colon cancer research, and express high levels of LGR5. Here, we aimed to investigate whether colon cancer cell lines contain cancer stem cells and characterized these cells. Using an LGR5 reporter, we characterized LGR5$^+$ cells and revealed that Caco-2 cell line contains a classical intestinal stem cell-like population (LGR5$^+$). However, in LoVo cell lines, stem cell-like population is more akin to the B lymphoma Moloney murine leukemia virus insertion region 1 homolog$^+$ stem cells.

Citation: Alharbi SA, Ovchinnikov DA, Wolvetang E. Leucine-rich repeat-containing G protein-coupled receptor 5 marks different cancer stem cell compartments in human Caco-2 and LoVo colon cancer lines. *World J Gastroenterol* 2021; 27(15): 1578-1594
URL: https://www.wjgnet.com/1007-9327/full/v27/i15/1578.htm
DOI: https://dx.doi.org/10.3748/wjg.v27.i15.1578

INTRODUCTION

Colorectal cancer (CRC) remains a leading cause of morbidity and mortality worldwide[1], highlighting the need for more effective therapeutics. It is now well established that both blood and solid cancers are initiated and propagated from a subset of rare cells, called cancer stem cells (CSCs), which are resistant to chemotherapy or radiation[2-4]. Current evidence indicates that CRC is indeed a disease of colon stem cells[2,5,6] that are resistant to current therapeutics and can rapidly proliferate to re-establish the tumor[7]. The intestinal crypt-villous structure harbors two distinct pools of putative stem cells[8]. One pool is located at the crypt base and is characterized by the expression of leucine-rich repeat-containing G protein-coupled receptor 5 (LGR5), and the other pool resides at +4 position and consists of B lymphoma Moloney murine

P-Editor: Ma YJ

leukemia virus (Mo-MLV) insertion region 1 homolog (Bmi-1) and telomerase reverse transcriptase (TERT) expressing cells[9-11]. The hierarchy of these stem cell pools in the normal crypt and their respective contributions to colon cancer and relapse following therapy is under debate. Some suggest both pools contribute equally to maintenance of the crypt, following a pattern of neutral drift[12], while others propose that Lgr5$^+$ stem cells (SCs) comprise the active population of the crypt and that Bmi-1$^+$ or TERT$^+$ cells are quiescent SCs that represent a reserve pool of SCs with the ability to replace Lgr-5$^+$ cells in case of loss or injury[8,13]. The existence of CSCs within intestinal tumors was most elegantly demonstrated by Schepers *et al*[14] using lineage re-tracing with a multicolor Cre-reporter R26R-confetti targeted to a single adenomatous polyposis coli allele in mouse intestinal stem (LGR5$^+$) cells, demonstrating that these intestinal adenomas were maintained by CSCs that exist in a cellular hierarchy. LGR5 is a receptor for R-spondins and activates potent Wnt signal enhancers such as Rnf43 and Znrf3[15]. LGR5 is present in various stem cell compartments throughout the body[16], including the intestine, and is an exquisite marker of intestinal stem cells (ISCs) capable of forming the entire intestinal mucosa[9]. LGR5$^+$ ISCs persist in adenoma and can initiate CRC through the activation of the Wnt/β-catenin signaling pathway[17].

Human colon cancer cell lines such as Caco-2 and LoVo are extensively used in drug screening and colon cancer research and express high levels of LGR5[18-20]. To establish criteria for the selection of suitable cell lines for drug discovery, several studies have investigated variability between the colon cell lines, identifying characteristic differences in gene expression signature, epigenetic and genetic make-up, migratory abilities, and proliferative capacities between different intestinal cancer and cell lines, including Caco-2 and LoVo[21,22]. However, the CSC population(s) within these cell lines remains to be fully characterized. This is important since anticancer drugs often attempt to target these CSCs[23,24].

To isolate the CSC compartment from colon cancer cell lines we constructed a reporter based on a conserved promoter fragment of the *LGR5* gene. After validating the fidelity of this LGR5 reporter, we showed that it can be used as a genetic tool to isolate LGR5-expressing CSCs from Caco-2 and LoVo human colon cancer cell lines. Surprisingly, our data revealed that these two widely used colon cancer lines possess different stem cell compartments. We conclude that this portable LGR5 reporter constitutes a valuable tool for the development of colon cancer therapeutics specifically designed to ablate these CSCs.

MATERIALS AND METHODS

Cell culture

Human colon cancer cell lines (LoVo, Caco-2, and SW480), a human fibroblast cell line (CRL-2429), a mouse fibroblast cell line (3T3), and a mouse motor neuron cell line (NSC-34) were obtained from ATCC and maintained in Dulbecco's Modified Eagle Medium (DMEM, Invitrogen, Carlsbad, CA, United States) supplemented with fetal bovine serum (FBS, Bovogen Biologicals, Keilor East, Australia) to a final concentration of 10% and passaged every 3-4 d at 80% confluency. The human neuroblastoma cell line (SH-SY5Y from ATCC) was maintained in DMEM supplemented with 20% FBS and passaged every 2-3 d. All cell lines used for experiments were at early (a maximum of 20-25) passage number.

Construction of LGR5 promoter-based reporter constructs

Conservation of the *LGR5* gene and its promoter was assessed using evolutionary conserved region browser and multiple alignments of several vertebrate genomes. The human *LGR5* gene is located on chromosome 12 and has a conserved region upstream of the main promoter. This gene segment [LGR5 promoter element (983 bp)] was amplified from RP11-59F15 bacterial artificial chromosome clones (obtained from the Australian Genome Research Facility, Ltd., Melbourne, Australia) by polymerase chain reaction (PCR) (Supplementary Figure 1A) using a set of primers (Table 1). Sequences for specific restriction sites (*Nde* I, *Nhe* I, *Sac* I, and *Xho* I) were added to allow the insertion of the amplicon into the pEYFP-N1 vector (Clontech, Mountain View, CA, United States). Subsequently, this purified deoxyribonucleic acid (DNA) fragment was A-tailed and ligated into pGEM®-T Easy Vector System I (Madison, WI, Promega). White colonies were selected and plasmid DNA isolated, purified, and sequenced. Verified plasmids containing the DNA of interest, which is also free of PCR-introduced mutations, were then digested and ligated into the pEYFP-N1 vector. A negative control clone was constructed by the deletion of the promoter insert from the

Table 1 Primer sequences

Gene	Forward primer 5'-3'	Reverse primer 5'-3'
GAPDH	TGAAGCTGGAGAAGGAGAAG	ATCGGCCTGTGTATATCCC
LGR5	CCTCTGCTGGCTTTTAGGTG	AGCAGTTTTCAGGCCTTTCA
OLFM4	ACTGTCCGAATTGACATCATGG	TTCTGAGCTTCCACCAAAACTC
ASCL2	ACCTGCGTACCTTGCTTTGG	GAAATCTGCGAGTTCCCGGT
Amplification/cloning of the *LGR5* promoter element	CATATGCTAGCTCGAGCTCACTTCGACTTCCTCACCCCGC	AAGCTTGGTGCCCGAAGTAGGGGGCCA

promoter-pEYFP-N1 clone. The original pEYFP-N1 vector (Clontech) with the CMV promoter was used as a positive control.

Transient transfection

Cell lines at 50%-60% confluence was transfected with LGR5 promoter-pEYFP-N1 DNA using FuGENE® HD Transfection Reagent (Roche, Basel, Switzerland) following the manufacturer instructions. LoVo, Caco-2, SW480, human fibroblast CRL2923, 3T3, 4T1, and EMT6 cell lines were transfected in 3:1 transfection reagent to DNA ratio in serum-free medium. For the SY5Y cell line, the ratio was 3:2. Eight to ten hours post-transfection, serum was added to the culture medium. All cultures were kept at 37 °C in a 5% CO_2 atmosphere until microscopic analyses were performed using an inverted fluorescence microscope (IX51, Nikon, Tokyo, Japan) 24-48 h post-transfection to examine enhanced yellow fluorescent protein (EYFP) expression levels.

Flow cytometry

For flow cytometry and fluorescence-activated cell sorting (FACS), cultured cells were harvested by incubation in a non-enzymatic cell dissociation buffer (Gibco® Life Technologies, Waltham, MA, United States) for 7-10 min. Next, cells were washed in phosphate buffer saline (PBS) and resuspended in 0.5 mL PBS for analysis. Flow cytometric analysis of EYFP expression of live cells was conducted using an Accuri flow cytometer (BD Biosciences, San Jose, CA, United States). FACS sorting was performed using an Influxcell sorter (BD Biosciences). Negative controls were used in every analysis to set the background fluorescence. Propidium Iodide Staining Solution (Invitrogen) was added to discriminate dead cells. Data analysis was performed on at least 10000 cells per sample as assessed by CFlow software (BD Biosciences). Fluorescence gates for positive cells were set to attain the false-positive rates of < 1%.

Colony PCR

A single colony of bacterial cells was suspended in a reaction volume of 50 µL, containing 1 µL of PCR primers (10 µmol/L each), 5 µL of 10 × PCR Buffer Minus Mg^{2+}, 1 µL of 10 mmol/L dNTP mixture, 1.5 µL of 50 mmol/L $MgCl_2$, and Milli-Q water. The cycle parameters of the reaction were as follows: Initial denaturation 95 °C for 3 min; 35 cycles of 30 s for denaturation at 95 °C, 30 s for annealing at 58 °C, and 1 min for the extension at 72 °C then final elongation at 72 °C for 2 min.

Quantitative real-time PCR

RNA extraction and complementary DNA (cDNA) synthesis: RNA was extracted from approximately 5 × 10^6 cells using RNeasy mini kit (Qiagen, Valencia, CA, United States) following the manufacturer's instructions. DNAse I treatment (on column) was performed during the extraction procedure as recommended by the kit manual. RNA quantification was performed using Nanodrop 1000. One microgram of RNA was used for cDNA synthesis using iScript™ cDNA Synthesis Kit (Bio-Rad Laboratories, Inc., Hercules, CA, United States) following the manufacturer's instructions. As a control for genomic DNA contamination, a 'no reverse transcriptase reaction' was carried out for every batch of cDNA synthesized.

Quantitative real-time PCR analysis: SsoFast™ EvaGreen® Supermix was used as the Master-mix and quantitative real-time PCR (qPCR) was carried out with a C1000™ Thermal Cycler (Bio-Rad Laboratories, Inc.). Each gene was amplified in triplicate in a reaction volume of 10 µL, containing 10 µL qPCR primers (Table 1), 5 µL of 2 × SsoFast EvaGreen Supermix, 0.2 µL cDNA, and Milli-Q water. The cycling parameters of the reaction were as follows: 95 °C for 3 min for enzyme (Sso7-fusion polymerase)

activation; 40 cycles of 10 s for denaturation at 95 °C, and 30 s for annealing and extension at 60 °C followed by a Melt Curve analysis to ensure reaction specificity. Glyceraldehyde-3-phosphate dehydrogenase was amplified in parallel and used for normalization. The amplification product was then analyzed using the 2-ΔCt method. 'No reverse transcriptase' and water controls were included in each qPCR run to exclude genomic DNA or sample cross-contamination.

Soft agar assay

To test anchorage-independent growth in soft agar, a layer of 0.6% agar (Agar Noble; Difco Laboratories, Detroit, MI, United States) in 2 × DMEM containing 20% FBS was plated in 35-mm dishes and placed in the fridge overnight. The next day, Geneticin resistant (400-500 μg/mL of Geneticin) cells were sorted for EYFP expression into high, low, and no-EYFP expressing cells using the Influxcell sorter (BD Biosciences). Cells were next washed with PBS and pelleted by centrifugation at 300 *g* for 3 min. Cells (2×10^4) were suspended in 2 mL of equal volumes of 0.6% agar (Agar Noble; Difco Laboratories) and 2 × DMEM containing 20% FBS and overlaid as a second layer. This was overlaid over a layer of 3 mL of 0.3% agar in the same medium, in 35 mm dishes. Once a week, 300 μL of medium containing 0.3% agar was added. After 21 d, plates were stained with 0.5 mL of 0.005% Crystal Violet for an hour. Colonies larger than 0.25 mm in diameter were then counted using ImageJ software.

In vivo tumorigenicity assay

Six- to eight-week-old non-obese diabetic (NOD)/severe combined immunodeficient (SCID) mice were obtained from Animal Resources Centre (Perth, Australia) and were housed in the animal house facility of the Australian Institute for Bioengineering and Nanotechnology, The University of Queensland. All procedures were approved by the University of Queensland Animal Ethics Committee (UQCCR/115/13/NHMRC) and conformed to the Animal Care and Protection Act Qld (2002) and the Australian Code of Practice for the Care and Use of Animals for Scientific Purposes (8th edition, 2013). Sorted cells were suspended in a 1:1 mixture of medium and Matrigel (BD Biosciences) and injected subcutaneously into NOD/SCID mice (2×10^5 cells per animal in a total volume of 50 μL) into the ventral side of the flank (n = 3 animals per group). Tumor growth was monitored and measured with calipers daily. Three weeks after the injection, mice were anesthetized by CO_2 inhalation, and tumors were excised, measured, weighed, and fixed in 4% paraformaldehyde for paraffin embedding. Tissue sections were stained with hematoxylin-eosin.

RESULTS

A conserved LGR5 enhancer-based promoter fragment recapitulates endogenous LGR5 expression

Due to the lack of a reliable anti-LGR5 antibody, isolation of LGR5 expressing cells *via* FACS or magnetic-ACS was not possible in our hands. We, therefore, constructed an EYFP reporter driven by a conserved LGR5 promoter fragment (Supplementary Figure 1A). To test whether the *LGR5* promoter-based construct correctly reported on LGR5 expression, we transiently transfected the LGR5-EYFP reporter as well as a negative control vector (promoter-less vector or empty-EYFP vector) and a positive control vector (CMV-EYFP) into colon cancer cell lines Caco-2, LoVo, and SW480 that display a high endogenous expression of *LGR5* and into CRL2429, 3T3, NSC-34 and SH-SY5Y cells that do not express LGR5 messenger RNA (mRNA). Transient transfection of the LGR5 reporter construct in these LGR5-expressing and LGR5-negative cell lines revealed that EYFP expression correlated well with endogenous LGR5 mRNA expression level (Supplementary Figure 1B). As expected, transfection of the promoter-less construct (empty-EYFP vector) did not result in YFP expression, whereas the CMV-driven EYFP vector showed widespread (30%-60% of cells) expression (Supplementary Figure 1B), indicating that the absence of fluorescence in LGR5 negative lines was not due to ineffective delivery of plasmid DNA.

To generate stably expressing reporter lines, Caco-2 and LoVo cell lines were transfected with a linearized LGR5 reporter vector, single-cell seeded, and maintained under Geneticin selection (400 μg/mL for LoVo cell line and 500 μg/mL for Caco-2 cell line) for 1 mo. Two single cell-derived clones from each cell line were picked, expanded, and cryopreserved. Fluorescence microscopy analysis revealed that these clonal LGR5/EYFP Caco-2 and LGR5/EYFP LoVo cultures contained a subset of cells

with a range of EYFP fluorescence, including small EYFP fluorescence bright cells (Figure 1A and B; orange arrows), which was validated using FACS (Figure 1C and D). Cells transfected with promoter-less plasmid showed no EYFP expression in any of the surviving clones, whereas the majority of CMV-promoter transfected clones homogeneously expressed EYFP, as expected. We hypothesized that cells expressing high levels of LGR5/EYFP in the colon cancer cell lines would constitute the stem cell compartment of Caco-2 and LoVo cell lines. To test this hypothesis, we sorted the cells into three populations according to their EYFP expression (EYFP^{negative}, EYFP^{low}, and EYFP^{high} cells). As anticipated, the qPCR analysis showed that LGR5 mRNA expression was 8-fold higher in EYFP high cells than in the EYFP negative fraction in both LGR5/EYFP Caco-2 and LGR5/EYFP LoVo clonal lines (Figure 1E and F, respectively).

In agreement with the idea that LGR5 marks a stem cell compartment, flow cytometric analysis of sorted EYFP^{negative}, EYFP^{low}, and EYFP^{high} cells from each of the lines revealed that over the course of several days, EYFP^{high} cells gave rise to EYFP negative "daughter" cells (Figure 1G and H). Time-lapse immunofluorescence and phase-contrast images of cultured EYFP^{high} sorted Caco-2 cells confirmed that EYFP negative cells emerged from the small EYFP^{high} cells over time (Figure 1G). No cells acquired EYFP expression amongst derivatives of FACS-sorted EYFP-negative cells (Figure 1I). LGR5-EYFP LoVo clones exhibited identical behaviors (Figure 1H and J). We interpreted these data to mean that LGR5^{high} (EYFP^{high}) cells possess stem cell-like properties, given they are capable of self-renewal and generate a distinct EYFP-negative cell population, incapable of re-acquiring expression of the LGR5 reporter.

EYFP^{high}-expressing cells of Caco-2 and LoVo CRC cell lines show an ISC gene expression signature

If LGR5/EYFP^{high} cell populations in Caco-2 and LoVo clones represent an ISC compartment, then these cells should show higher mRNA expression of typical ISC marker genes compared to LGR5/EYFP^{low} and LGR5/EYFP^{negative} fractions. Our data (Figure 2A) show that EYFP^{high} cells in the Caco-2 cell line indeed display significantly increased expression of the stem cell markers LGR5, olfactomedin 4 (OLFM4), TERT, leucine-rich repeated and immunoglobulin-like domains 1 (LRIG1), AFAP1I1, TNFRF19, organic cation transporter 1 (OCT1), and achaete-scute complex homolog 2 as compared to cells with low or no EYFP expression, but conspicuously do not express B lymphoma Moloney murine leukemia virus insertion region 1 homolog (Bmi1). Surprisingly, in the LoVo cell line (Figure 2B) EYFP^{high} cells expressing high LGR5 reporter activity possessed low levels of OLFM4, AFAP1I1, and LRIG1 compared to EYFP^{low} and EYFP^{negative} fractions. EYFP^{high} cells in the LoVo cell line instead robustly express Bmi1 as compared to EYFP^{negative} cells but exhibit lower hTERT as compared to EYFP^{negative} and EYFP^{low} fractions. These data suggest that in the LoVo cell lines LGR5 marks a different cancer cell compartment than in Caco-2 cells. Collectively, our data indicate that the LGR5/EYFP reporter faithfully marks a population of LGR5 expressing CSCs in the Caco-2 cell line but that this stem cell population is distinct from the EYFP^{high} fraction in the LoVo cell line that appears to mark a Bmi1^{high}/LGR5 TERT^{low} expressing a subset of cells.

LGR5/EYFP^{high} cells in Caco-2 colon cancer cell line exhibit increased colony-forming ability

To assess whether LGR5 expressing subsets in the Caco-2 and LoVo lines exhibit functional differences we employed the anchorage-independent tumor stem cell colony-forming assay[25]. Using this assay, we assessed the *in vitro* anchorage-independent growth of LGR5/EYFP^{high}, LGR5/EYFP^{low}, and LGR5/EYFP^{negative} cell populations of the LGR5/EYFP Caco-2 and LGR5-EYFP LoVo lines (Figure 3A and B). Our data showed that after 3-wk culture in soft agar, the number of colonies formed by the three cell populations of Caco-2 and LoVo cell lines was comparable (Figure 3C and E) but that the colony sizes of the LGR5/EYFP^{high} cell populations in Caco-2 line were considerably larger (> 0.25 mm in diameter) than those in LGR5/EYFP^{low} and LGR5/EYFP^{negative} cell populations (Figure 3D and F), suggesting LGR5^{high} cells in Caco-2 cell line exhibit increased proliferation and/or reduced cell death rates.

To assess further the tumorigenicity of the LGR5/EYFP^{high} cell compartments of Caco-2 and LoVo lines, LGR5/EYFP^{high} and EYFP^{negative} sorted cells were injected subcutaneously into the right and left flanks, respectively, of NOD-SCID mice (n = 3), and tumor growth was monitored daily before excision of tumors after 3 wk. As shown in Figure 4A, LGR5/EYFP^{high} Caco-2 cells were able to form tumors when injected into NOD-SCID mice. LGR5/EYFP^{high} formed larger tumors than the LGR5/

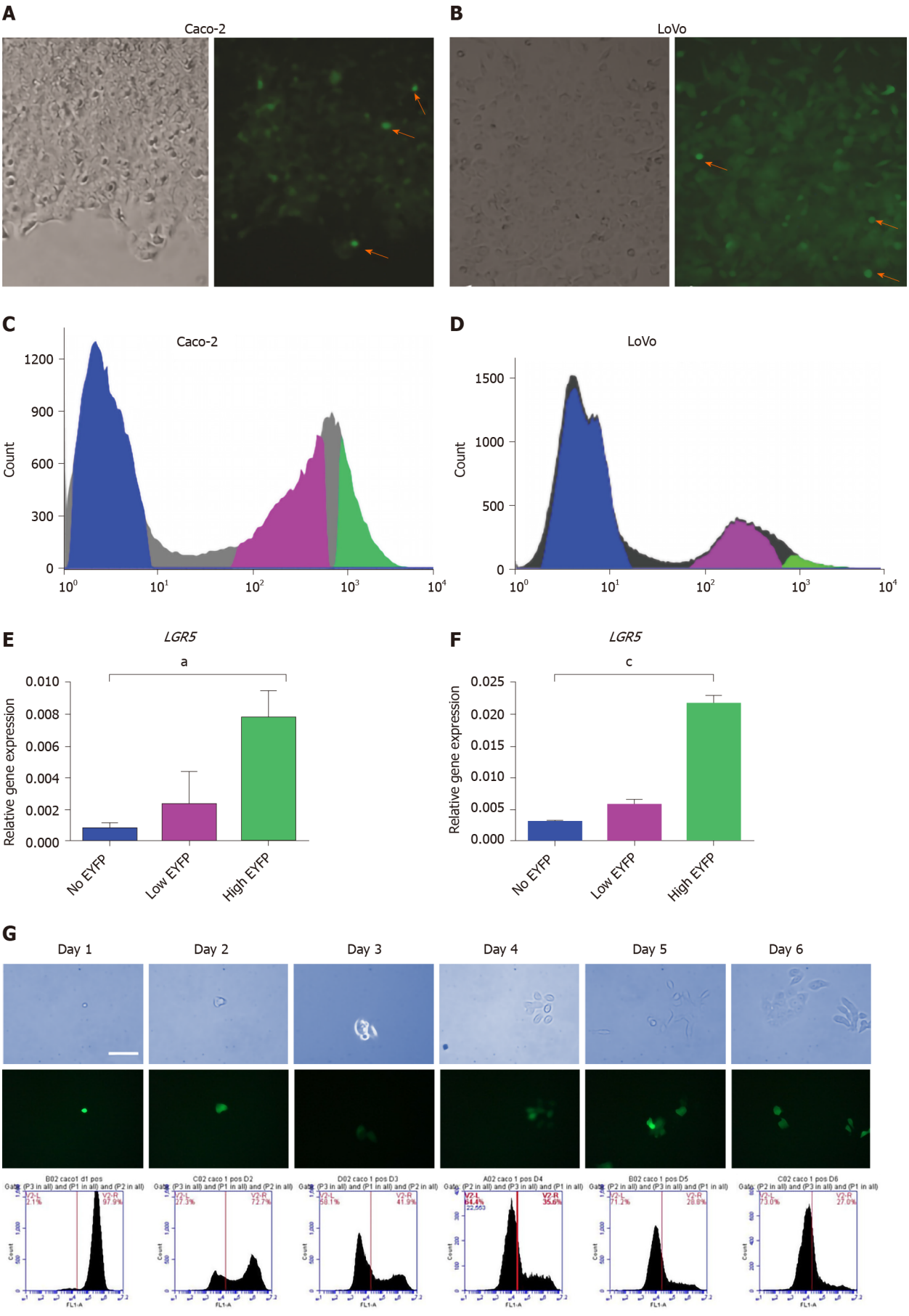
A
Caco-2
B
LoVo
C
Caco-2
Count
1200
900
600
300
0
10^0
10^1
10^2
10^3
10^4
D
LoVo
Count
1500
1000
500
0
10^0
10^1
10^2
10^3
10^4
E
LGR5
a
Relative gene expression
0.010
0.008
0.006
0.004
0.002
0.000
No EYFP
Low EYFP
High EYFP
F
LGR5
c
Relative gene expression
0.025
0.020
0.015
0.010
0.005
0.000
No EYFP
Low EYFP
High EYFP
G
Day 1
Day 2
Day 3
Day 4
Day 5
Day 6

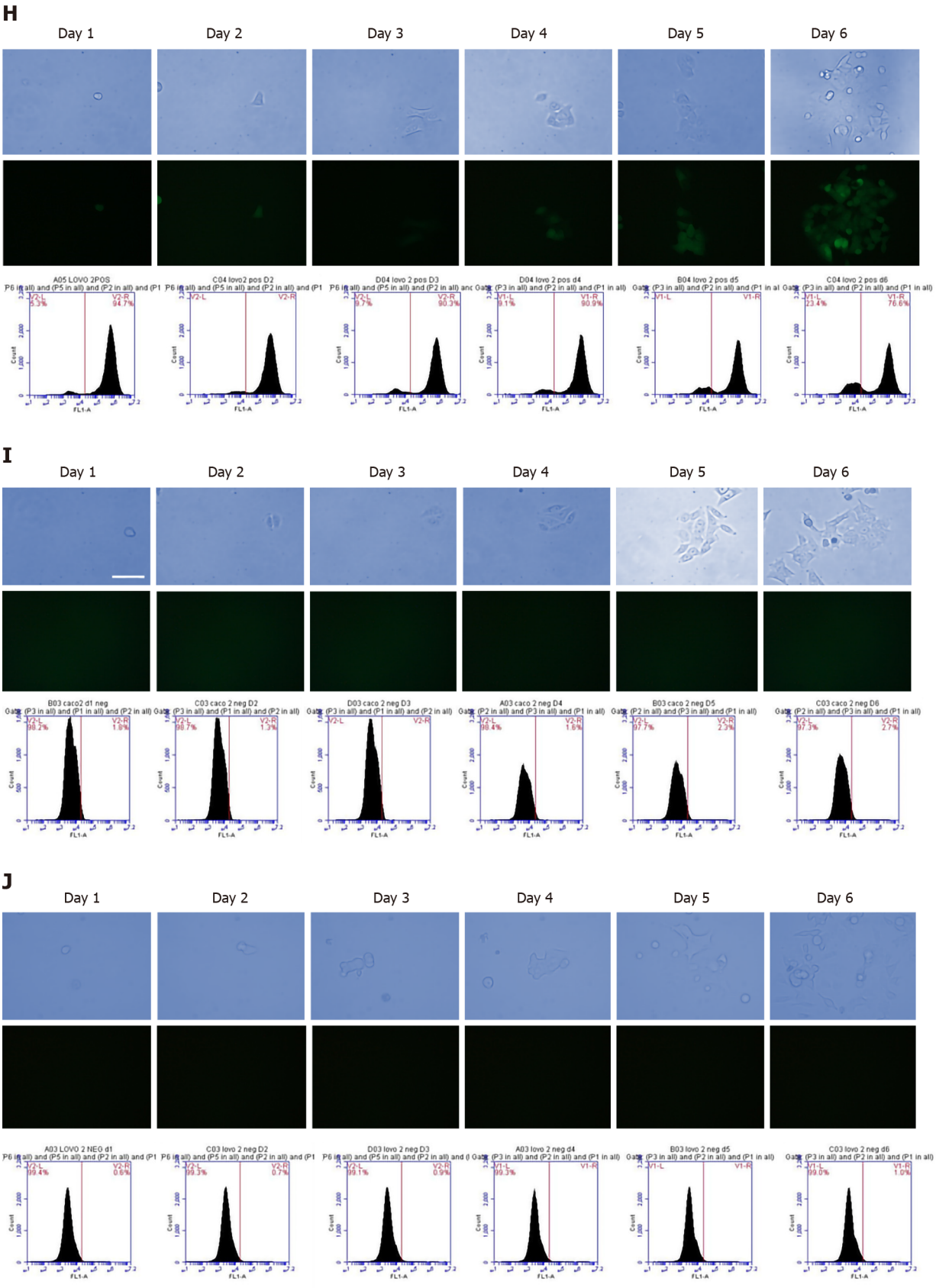

Figure 1 Proliferation and differentiation analysis of the stem cell compartment in stably transfected clones. A and B: Phase contrast and fluorescence images show colonies of stably transfected Caco-2 (A) and LoVo (B) cells expressing the enhanced yellow fluorescent protein (EYFP) reporter (red arrows show small cells expressing high level of enhanced yellow fluorescent protein, EYFP); C and E: Fluorescence-activated cell sorting (FACS) sorting of leucine-rich repeat-containing G protein-coupled receptor 5 (LGR5)/EYFP expression in Caco-2 clone (C) and LoVo clones (E) into EYFP^{high}, EYFP^{low}, and EYFP^{negative} populations; D and F: Quantitative real-time polymerase chain reaction analysis of *LGR5* messenger ribonucleic acid expression in EYFP^{high}, EYFP^{low}, and

EYFP^{negative} cells relative to glyceraldehyde-3-phosphate dehydrogenase gene in Caco-2 clones (D) and LoVo clones (F); G: Phase contrast images show proliferation of EYFP^{high} cells from LGR5/EYFP Caco-2 clone; fluorescence images show self-renewal of LGR5/EYFP stem cells and down-regulation of LGR5/EYFP in differentiated progeny in LGR5/EYFP Caco-2. Sequential FACS analysis shows EYFP expression in LGR5/EYFP Caco-2 clone over 6 d in culture; H: Phase contrast images show proliferation of EYFP^{negative} and cells from LGR5/EYFP Caco-2 clone; fluorescence images show self-renewal of LGR5 stem cells and down-regulation of LGR5 in differentiated progeny in LGR5/EYFP Caco-2. Sequential FACS analysis shows EYFP expression in LGR5/EYFP Caco-2 clone over 6 d in culture; I and J: Phase contrast images show proliferation of EYFP^{high} (I) and EYFP^{negative} (J) cells from LGR5/EYFP LoVo clone; fluorescent pictures showing self-renewal of LGR5 stem cells and down-regulation of LGR5/EYFP in differentiated progeny in LGR5/EYFP LoVo; sequential FACS analysis of EYFP expression in LGR5/EYFP LoVo clone over 6 d in culture. LGR5: Leucine-rich repeat-containing G protein-coupled receptor 5; EYFP: Enhanced yellow fluorescent protein.

EYFP^{negative} cells (Figure 4B and C).

In the LoVo cell line, on the other hand, both LGR5/EYFP^{high} cells and LGR5/EYFP^{negative} sorted cells had almost comparable tumorigenic properties (Supplementary Figure 2).

DISCUSSION

The heterogeneity of cancer cell lines has been recognized, but it was not until the 1980s that it was shown that the human DLD-1 colon cancer cell line, originally established from a single human colon carcinoma[26], contains subpopulations of cells with different morphology, karyotype, and cloning efficiency in soft agarose that produce histologically distinct tumors when injected into athymic mice. Recent studies have explained this apparent heterogeneity of colon cancer cell lines when it was discovered that colon cancer carcinoma contains a subset of stem cells expressing LGR5, termed "tumor-initiating" cells specimens[27]. This was strongly supported by lineage tracing studies[28] showing that colon cancer is initiated by aberrant Wnt signaling in ISCs, known to express high levels of LGR5. Furthermore, *in vivo* lineage tracing experiments on intestinal adenomas demonstrated the clonal expansion of these adenomas from a single LGR5-expression cell[14].

In light of this evidence, we decided to investigate whether colon cancer cell lines widely used for drug-screening[21] contain CSCs and developed a reporter that would allow their isolation and characterization. Here, we showed that a 983 bp fragment of the LGR5 promoter faithfully reports on endogenous LGR5 expression in the colon cancer cell lines LoVo and Caco-2. Interestingly, we revealed that the ISC populations in these two cell lines exhibit different gene expression and functional properties. Our data show that the Caco-2 cell line contains a population of highly proliferative cells that exhibit a classic intestinal CSC gene expression signature that is marked by a high expression of LGR5, in agreement with previous findings[28,29]. These cells can both self-renew and generate more differentiated LGR5 negative progeny and also exhibit an *in vitro* tumorigenic potential. In support of the notion that LGR5/EYFP^{high} cells within Caco-2 colon cancer cell line represent the CSC compartment, our limited gene expression analysis revealed that LGR5/EYFP^{high} cells display a transcriptional signature very similar to that of the ISC, including *LGR5*, *Olfm4*, and *Ascl2*[29-31]. Our data are also in agreement with Sato *et al*[9] who showed that only very high LGR5-expressing cells are the ISCs in normal intestinal tissue. In agreement with a study by Maddox *et al*[32], our data further show that the LGR5/EYFP^{high} fraction of the Caco-2 cell line exhibits a high expression of OCT1, a known ISC marker. The LGR5/EYFP^{high} fraction of the Caco-2 colon cancer cells also showed the highest telomerase expression (TERT), which is a characteristic of most CSCs, associated with the ability to proliferate indefinitely[33,34]. Conspicuously, the LGR5/EYFP^{high} fraction of the Caco-2 acquires Bmi1 expression upon loss of LGR5 expression, in agreement with the proposed cellular differentiation hierarchy of the intestinal crypt[10]. Collectively, these data suggest that the LGR5/EYFP^{high} fraction of the Caco-2 colon cancer cell line indeed represents a CSC-like population. These data are in close agreement with a similar study in SW480 and HT-29 human colon cancer cell lines in which LGR5 was also found to mark a CSC population[35].

In contrast to the Caco-2 cell line, in the LoVo colon cancer cell line, LGR5/EYFP^{high} cells showed the lowest expression of the ISC markers hTERT, LRIG1, AFAP1I1, and , and low expression of the CSC marker OCT1, suggesting that in LoVo cells LGR5 marks a different cell population, *i.e.* not a stem cell-like population. Indeed, our data show that in the LoVo cell line, cells with high LGR5/EYFP expression possess a gene expression signature more akin to Bmi-expressing stem cells of the crypt. In LoVo cells it is rather the LGR5^{negative} fraction that highly expresses ISC marker OCT1[32],

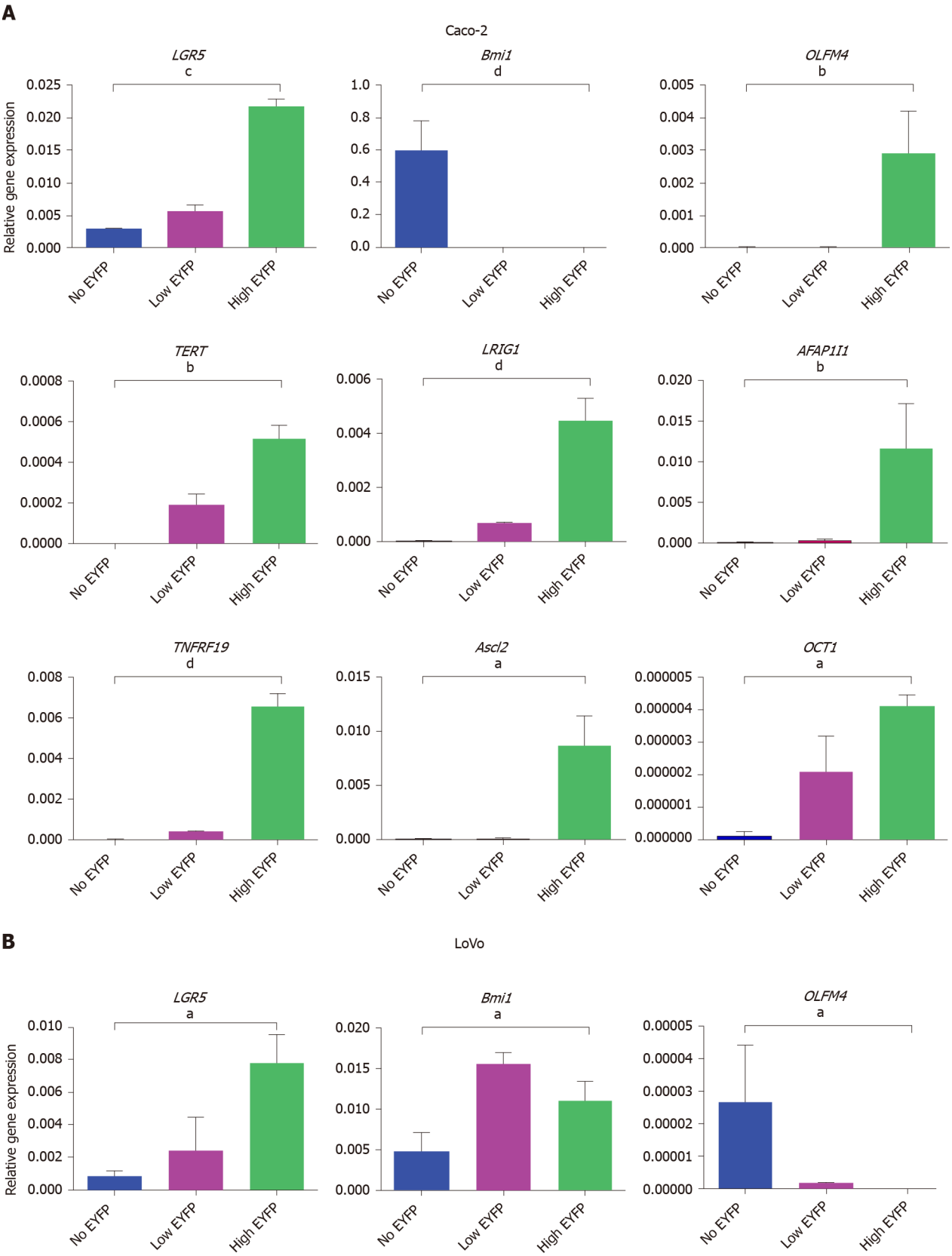
A
Caco-2
LGR5
c
Bmi1
d
OLFM4
b
TERT
b
LRIG1
d
AFAP1I1
b
TNFRF19
d
Ascl2
a
OCT1
a
Relative gene expression
No EYFP
Low EYFP
High EYFP
B
LoVo
LGR5
a
Bmi1
a
OLFM4
a

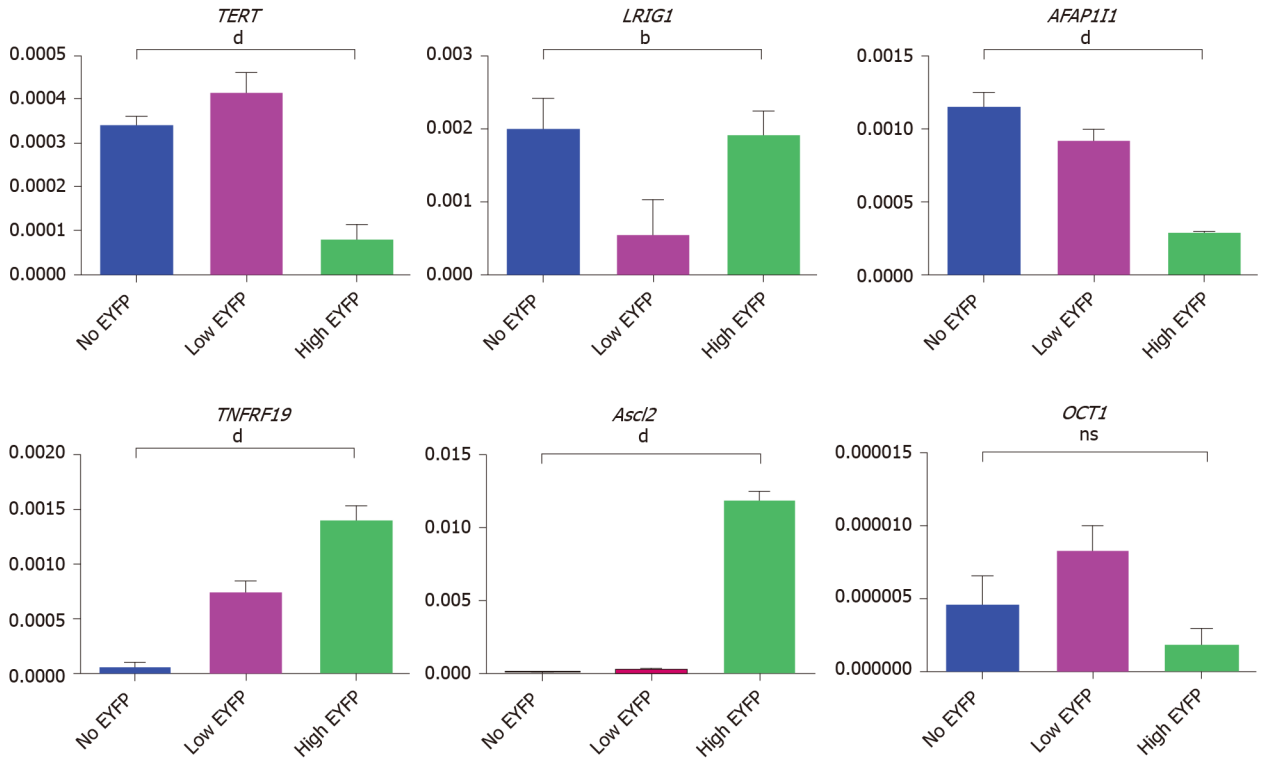

Figure 2 Quantitative polymerase chain reaction analysis. A and B: Quantitative polymerase chain reaction analysis of intestinal stem cell markers and the cancer stem cell marker organic cation transporter 1 in leucine-rich repeat-containing G protein-coupled receptor 5/enhanced yellow fluorescent protein (LGR5/EYFP)^{high}, LGR5/EYFP^{low}, and LGR5/EYFP^{negative} fractions of the Caco-2 cell line (A) and the LoVo cell line (B). The expression value of each gene was normalized to glyceraldehyde-3-phosphate dehydrogenase gene. Data were then analyzed by one-way analysis of variance. $^{a}P < 0.05$, $^{b}P < 0.01$, $^{c}P < 0.001$, $^{d}P < 0.0001$. LGR5: Leucine-rich repeat-containing G protein-coupled receptor 5; EYFP: Enhanced yellow fluorescent protein; Bmi1: B lymphoma Moloney murine leukemia virus insertion region 1 homolog; OCT1: organic cation transporter 1; TERT: Telomerase reverse transcriptase; ASCL2: Achaete-scute complex homolog 2.

OLFM4[36,37], and Bmi1[10], suggesting that this cell line originated from a CSC population other than LGR5^{+}cells. Supporting this suggestion, in a recent review on the intestinal hemostasis and plasticity in humans, the writer argued that there is a wide range of cell types in the intestinal epithelium that can revert to stem cell fate and regenerate the epithelium post-injury[38]. Moreover, Bmi1 marks a distinct pool of ISCs that mainly reside above the crypt base[39]. Lineage tracing has shown that this Bmi1^{+} stem cell pool, the so-called reserve stem cell pool, is able to regenerate intestinal epithelial tissue in the absence of LGR5^{+} ISCs[10,39] and also give rise to LGR5^{+} cells in normal and injured intestinal epithelium[40]. In support of this idea, a number of other human colon cancer cell lines (such as LIM1899, LIM1215, LIM2537, and LIM1863)[41] have previously been shown to exhibit increased anchorage-independent growth and enhanced tumorigenicity in xenograft experiments upon ablation of LGR5.

CONCLUSION

We conclude that we have generated a portable LGR5-reporter that should prove a valuable tool for the identification and isolation of different colon CSC populations in colon cancer lines. The characterization of such populations is important for drug screening and design. Since LGR5 marks adult stem cell populations in a number of tissues throughout the body[42], it will be interesting to determine whether our LGR5 promoter reporter can also be used to isolate such LGR5 expressing CSCs from other human cancer cell lines such as glioblastoma[43], esophageal adenocarcinomas[44], ovarian primary tumors[45], gastric tumors[46], and hepatomas[47-50] that are also marked by high LGR5 expression.

Our data further indicate that LGR5/EYFP^{high} expression marks two different intestinal crypt stem cell population in the Caco-2 and LoVo cell lines. Since Caco-2 and LoVo cell lines are widely used for screening of colon cancer drugs[51], our findings of different stem cell populations in these lines likely has important implications for

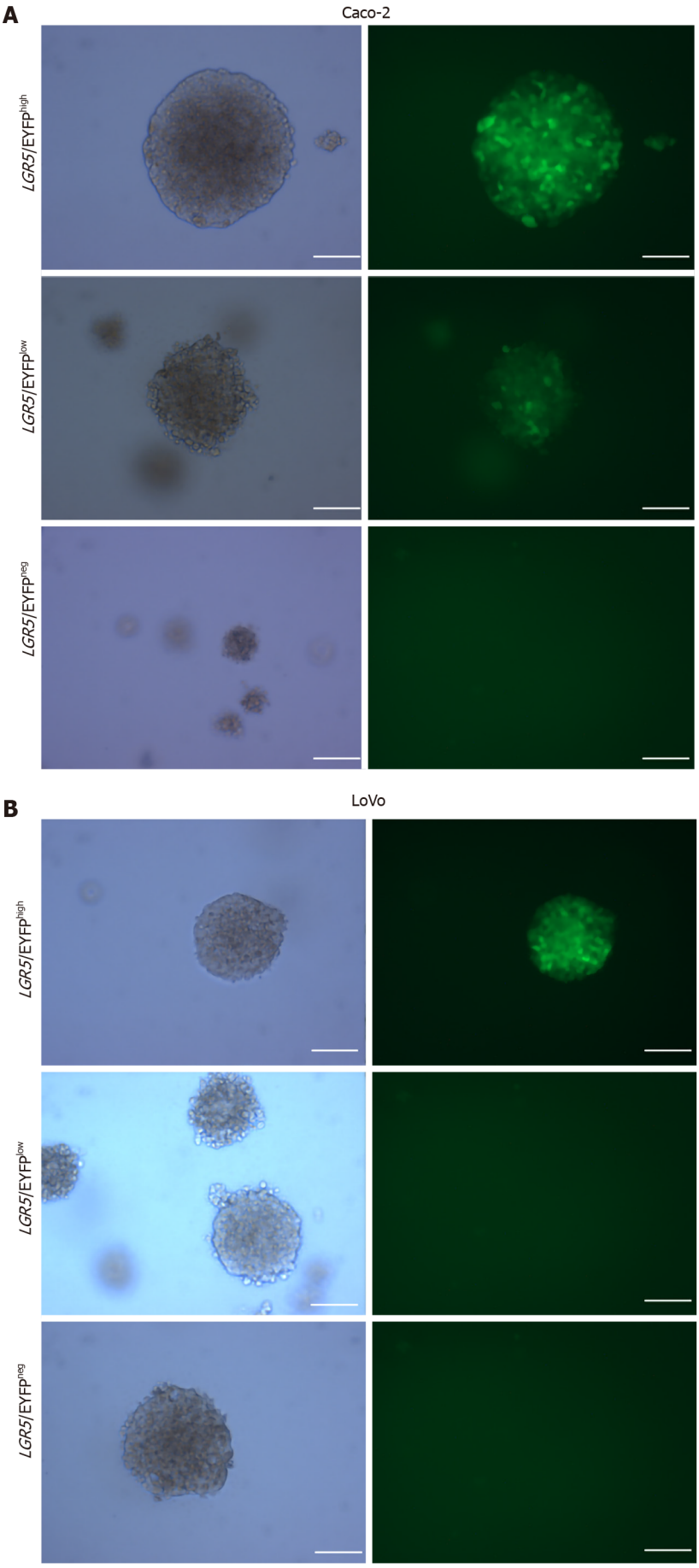
A
Caco-2
LGR5/EYFP^high
LGR5/EYFP^low
LGR5/EYFP^neg
B
LoVo
LGR5/EYFP^high
LGR5/EYFP^low
LGR5/EYFP^neg

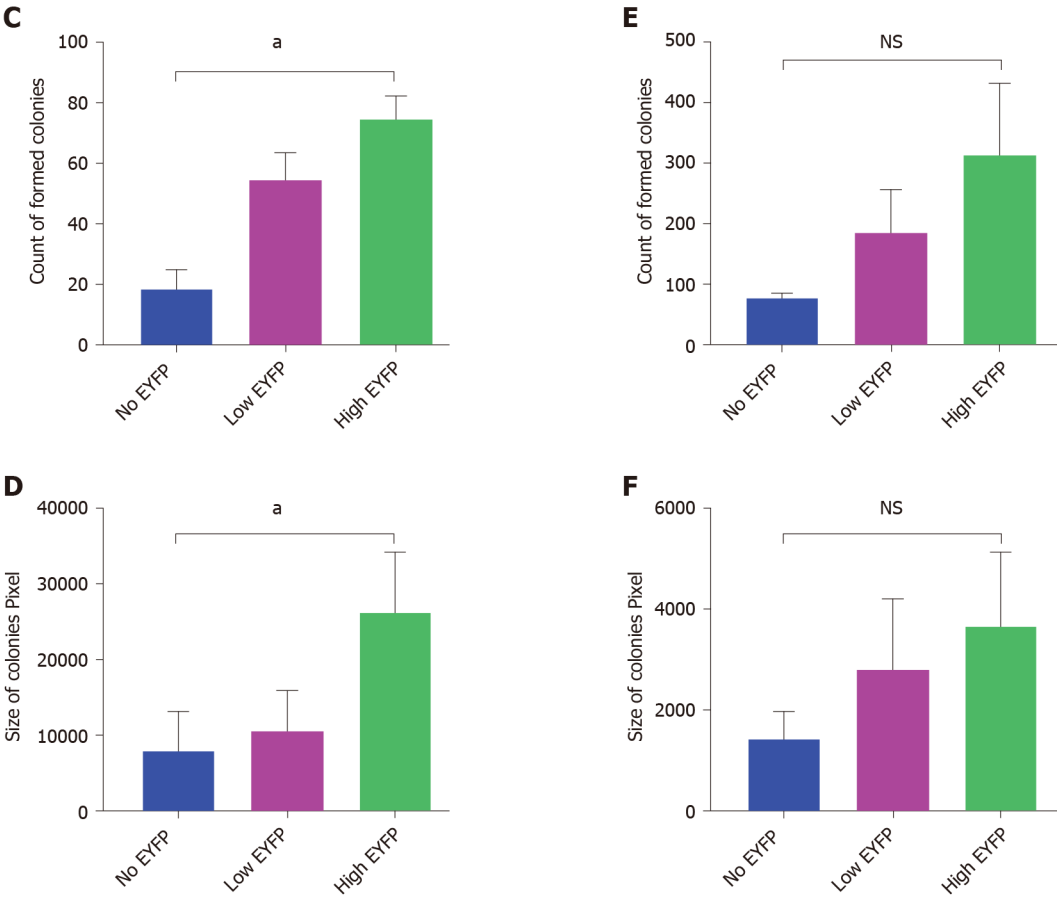

Figure 3 *In vitro* anchor independent assay of Caco-2 and LoVo colon cancer cell line. Sorted cells were cultured for 2 wk in soft agar before analysis. A-F: Representative images of colonies formed by cells with different leucine-rich repeat-containing G protein-coupled receptor 5/enhanced yellow fluorescent protein levels in Caco-2 cell line (A) and in LoVo cell line (B). Scale bar, 50 μm; the (C) and (E) number, and (D) and (F) size of colonies formed by Caco-2 and LoVo clones respectively were assessed using crystal violet staining. Colonies larger than 0.25 mm in diameter were then counted. Columns and error bars represent means ± SD of two independent experiments using duplicate measurements in each experiment. $^{a}P < 0.05$. LGR5: Leucine-rich repeat-containing G protein-coupled receptor 5; YFP: Yellow fluorescent protein; EYFP: Enhanced yellow fluorescent protein.

such drug screening programs.

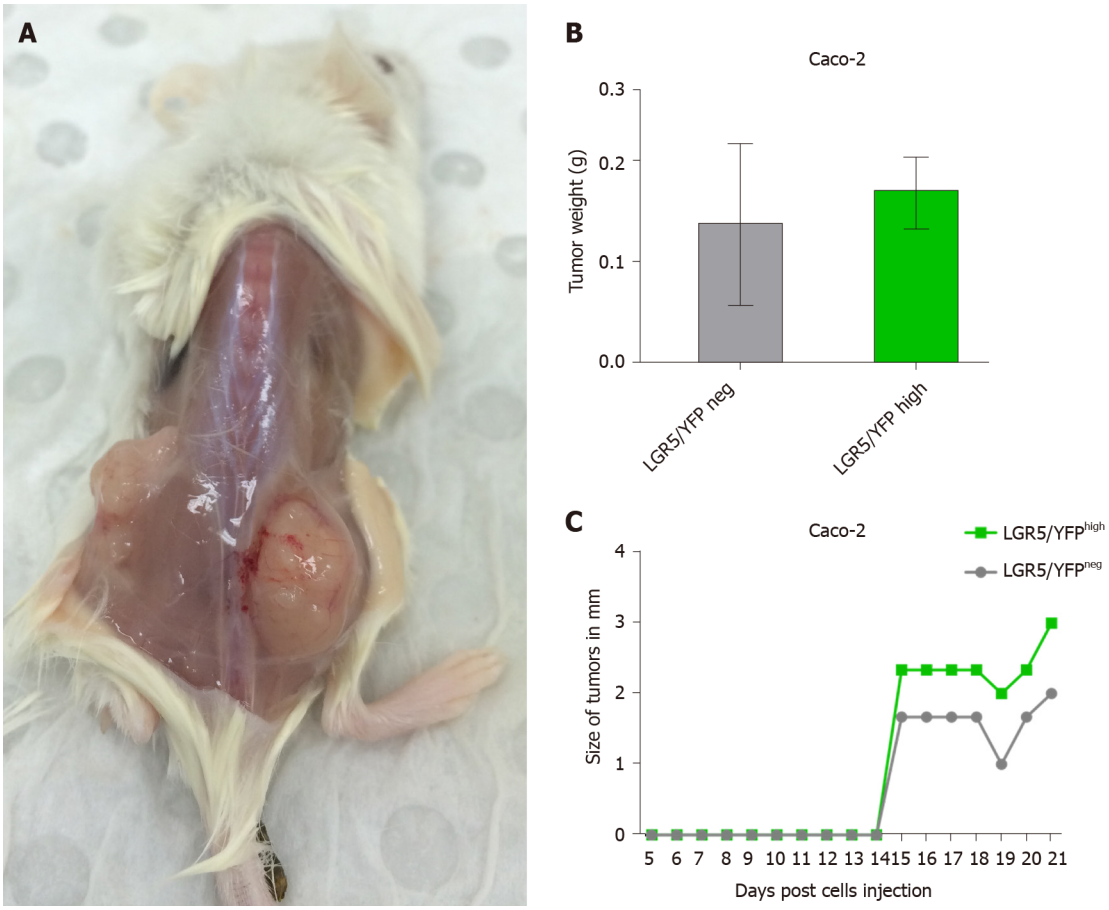

Figure 4 Stable leucine-rich repeat-containing G protein-coupled receptor 5/enhanced yellow fluorescent protein^{high} expressing Caco-2 cells line possesses stem cell-like properties *in vivo*. Sorted leucine-rich repeat-containing G protein-coupled receptor 5/enhanced yellow fluorescent protein (LGR5/EYFP)^{negative} and LGR5/EYFP^{high} cells were injected subcutaneously in left and right flanks (respectively) of non-obese diabetic- severe combined immunodeficient mice and monitored for 3 wk. A: Representative images of tumors formed by LGR5/EYFP^{high} (right flank) and LGR5/EYFP^{negative} (left flank) cells; B and C: Tumor weights (B) and size (C) resulting from LGR5/EYFP^{negative} and LGR5/EYFP^{high} sorted cells. Columns and error bars represent means ± SD of two independent experiments using duplicate measurements for each experiment. neg: Negative; LGR5: Leucine-rich repeat-containing G protein-coupled receptor 5; YFP: Yellow fluorescent protein.

ARTICLE HIGHLIGHTS

Research background

The intestinal crypt-villus structure harbors two distinct pools of putative stem cells, the active [leucine-rich repeat-containing G protein-coupled receptor 5 (LGR5)$^+$ cells] and the quiescent stem cell populations (B lymphoma Moloney murine leukemia virus insertion region 1 homolog$^+$ or telomerase reverse transcriptase$^+$ cells). Current evidence indicates that CRC is indeed a disease of colon stem cells that are resistant to current therapeutics and can rapidly proliferate to re-establish the tumor. Furthermore, it was reported that colon cancer carcinoma specimens contain a subset of LGR5-expressing stem cells. Human colon cancer cell lines, such as Caco-2 and LoVo, are extensively used in drug screening and colon cancer research and express high levels of LGR5.

Research motivation

To establish criteria for the selection of suitable cell lines for drug discovery and reveal potential variability between colon cell lines, we here identify the cancer stem cell (CSC) population(s) within colon cancer cell lines, quantify differences in gene expression signatures in these cells, and assess their proliferative and tumorgenicity capacities.

Research objectives

The present study aimed to isolate cells expressing LGR5 in Caco-2 and LoVo colon cancer cell lines and investigate whether these cells constitute the CSC compartments

in these cell lines. This was achieved through the creation of a transgenic proliferating stem cell-specific reporter construct based on the proximal promoter of *LGR5* gene.

Research methods

Using a portable fluorescent reporter construct based on a conserved fragment of the LGR5 promoter, subpopulations of cells from the colon cancer cell lines (Caco-2 and LoVo) were sorted into three cell compartments expressing different levels of LGR5 (high-, low-, and no-expression of LGR5). Next these cell compartments were characterized based on their gene expression signatures, proliferation, and tumorgenicity properties.

Research results

Cells expressing high levels of LGR5 with Caco-2 colon cancer cell line appear to represent a CSC-like population. In contrast, in the LoVo cell line, the LGR5 negative fraction possessed some features of the intestinal stem cells, *e.g.*, a specific gene expression signature, suggesting that this cell line was likely derived from a CSC population other than LGR5$^+$ cells.

Research conclusions

LGR5 marks the stem cell compartments of the Caco-2, but not LoVo, cell lines. Thus, it would appear that different colon cancer lines possess properties of different stem cell compartments. The portable LGR5 reporter outlined in this study constitutes a valuable tool for the identification and purification of LGR5-expressing cells from mixed cell populations.

Research perspectives

The portable LGR5 reporter described in this study constitutes a valuable tool for the identification and purification of LGR5-expressing cells from mixed cell populations.

ACKNOWLEDGEMENTS

We thank Professor McGuckin M (MMRI, Brisbane) for providing human colon cancer cell lines (Caco-2, LoVo, and SW480) and Dr. Rolfe B (AIBN, Brisbane) for providing mouse NSC-34 cells.

REFERENCES

1 **Favoriti P**, Carbone G, Greco M, Pirozzi F, Pirozzi RE, Corcione F. Worldwide burden of colorectal cancer: a review. *Updates Surg* 2016; **68**: 7-11 [PMID: 27067591 DOI: 10.1007/s13304-016-0359-y]
2 **Visvader JE**, Lindeman GJ. Cancer stem cells in solid tumours: accumulating evidence and unresolved questions. *Nat Rev Cancer* 2008; **8**: 755-768 [PMID: 18784658 DOI: 10.1038/nrc2499]
3 **Chen J**, Li Y, Yu TS, McKay RM, Burns DK, Kernie SG, Parada LF. A restricted cell population propagates glioblastoma growth after chemotherapy. *Nature* 2012; **488**: 522-526 [PMID: 22854781 DOI: 10.1038/nature11287]
4 **Driessens G**, Beck B, Caauwe A, Simons BD, Blanpain C. Defining the mode of tumour growth by clonal analysis. *Nature* 2012; **488**: 527-530 [PMID: 22854777 DOI: 10.1038/nature11344]
5 **Odoux C**, Fohrer H, Hoppo T, Guzik L, Stolz DB, Lewis DW, Gollin SM, Gamblin TC, Geller DA, Lagasse E. A stochastic model for cancer stem cell origin in metastatic colon cancer. *Cancer Res* 2008; **68**: 6932-6941 [PMID: 18757407 DOI: 10.1158/0008-5472.CAN-07-5779]
6 **Garza-Treviño EN**, Said-Fernández SL, Martínez-Rodríguez HG. Understanding the colon cancer stem cells and perspectives on treatment. *Cancer Cell Int* 2015; **15**: 2 [PMID: 25685060 DOI: 10.1186/s12935-015-0163-7]
7 **Liu YS**, Hsu HC, Tseng KC, Chen HC, Chen SJ. Lgr5 promotes cancer stemness and confers chemoresistance through ABCB1 in colorectal cancer. *Biomed Pharmacother* 2013; **67**: 791-799 [PMID: 24138824 DOI: 10.1016/j.biopha.2013.08.001]
8 **Yan KS**, Chia LA, Li X, Ootani A, Su J, Lee JY, Su N, Luo Y, Heilshorn SC, Amieva MR, Sangiorgi E, Capecchi MR, Kuo CJ. The intestinal stem cell markers Bmi1 and Lgr5 identify two functionally distinct populations. *Proc Natl Acad Sci USA* 2012; **109**: 466-471 [PMID: 22190486 DOI: 10.1073/pnas.1118857109]
9 **Sato T**, Vries RG, Snippert HJ, van de Wetering M, Barker N, Stange DE, van Es JH, Abo A, Kujala P, Peters PJ, Clevers H. Single Lgr5 stem cells build crypt-villus structures *in vitro* without a mesenchymal niche. *Nature* 2009; **459**: 262-265 [PMID: 19329995 DOI: 10.1038/nature07935]
10 **Tian H**, Biehs B, Warming S, Leong KG, Rangell L, Klein OD, de Sauvage FJ. A reserve stem cell

population in small intestine renders Lgr5-positive cells dispensable. *Nature* 2011; **478**: 255-259 [PMID: 21927002 DOI: 10.1038/nature10408]

11 **Vaiopoulos AG**, Kostakis ID, Koutsilieris M, Papavassiliou AG. Colorectal cancer stem cells. *Stem Cells* 2012; **30**: 363-371 [PMID: 22232074 DOI: 10.1002/stem.1031]

12 **Snippert HJ**, van der Flier LG, Sato T, van Es JH, van den Born M, Kroon-Veenboer C, Barker N, Klein AM, van Rheenen J, Simons BD, Clevers H. Intestinal crypt homeostasis results from neutral competition between symmetrically dividing Lgr5 stem cells. *Cell* 2010; **143**: 134-144 [PMID: 20887898 DOI: 10.1016/j.cell.2010.09.016]

13 **Montgomery RK**, Carlone DL, Richmond CA, Farilla L, Kranendonk ME, Henderson DE, Baffour-Awuah NY, Ambruzs DM, Fogli LK, Algra S, Breault DT. Mouse telomerase reverse transcriptase (mTert) expression marks slowly cycling intestinal stem cells. *Proc Natl Acad Sci USA* 2011; **108**: 179-184 [PMID: 21173232 DOI: 10.1073/pnas.1013004108]

14 **Schepers AG**, Snippert HJ, Stange DE, van den Born M, van Es JH, van de Wetering M, Clevers H. Lineage tracing reveals Lgr5+ stem cell activity in mouse intestinal adenomas. *Science* 2012; **337**: 730-735 [PMID: 22855427 DOI: 10.1126/science.1224676]

15 **de Lau W**, Peng WC, Gros P, Clevers H. The R-spondin/Lgr5/Rnf43 module: regulator of Wnt signal strength. *Genes Dev* 2014; **28**: 305-316 [PMID: 24532711 DOI: 10.1101/gad.235473.113]

16 **Leushacke M**, Barker N. Lgr5 and Lgr6 as markers to study adult stem cell roles in self-renewal and cancer. *Oncogene* 2012; **31**: 3009-3022 [PMID: 22002312 DOI: 10.1038/onc.2011.479]

17 **Uchida H**, Yamazaki K, Fukuma M, Yamada T, Hayashida T, Hasegawa H, Kitajima M, Kitagawa Y, Sakamoto M. Overexpression of leucine-rich repeat-containing G protein-coupled receptor 5 in colorectal cancer. *Cancer Sci* 2010; **101**: 1731-1737 [PMID: 20384634 DOI: 10.1111/j.1349-7006.2010.01571.x]

18 **Li AP**. Screening for human ADME/Tox drug properties in drug discovery. *Drug Discov Today* 2001; **6**: 357-366 [PMID: 11267922 DOI: 10.1016/s1359-6446(01)01712-3]

19 **Lieberman MM**, Patterson GM, Moore RE. In vitro bioassays for anticancer drug screening: effects of cell concentration and other assay parameters on growth inhibitory activity. *Cancer Lett* 2001; **173**: 21-29 [PMID: 11578805 DOI: 10.1016/s0304-3835(01)00681-4]

20 **Balimane PV**, Patel K, Marino A, Chong S. Utility of 96 well Caco-2 cell system for increased throughput of P-gp screening in drug discovery. *Eur J Pharm Biopharm* 2004; **58**: 99-105 [PMID: 15207543 DOI: 10.1016/j.ejpb.2004.02.014]

21 **Christensen J**, El-Gebali S, Natoli M, Sengstag T, Delorenzi M, Bentz S, Bouzourene H, Rumbo M, Felsani A, Siissalo S, Hirvonen J, Vila MR, Saletti P, Aguet M, Anderle P. Defining new criteria for selection of cell-based intestinal models using publicly available databases. *BMC Genomics* 2012; **13**: 274 [PMID: 22726358 DOI: 10.1186/1471-2164-13-274]

22 **Ahmed D**, Eide PW, Eilertsen IA, Danielsen SA, Eknæs M, Hektoen M, Lind GE, Lothe RA. Epigenetic and genetic features of 24 colon cancer cell lines. *Oncogenesis* 2013; **2**: e71 [PMID: 24042735 DOI: 10.1038/oncsis.2013.35]

23 **Tang C**, Ang BT, Pervaiz S. Cancer stem cell: target for anti-cancer therapy. *FASEB J* 2007; **21**: 3777-3785 [PMID: 17625071 DOI: 10.1096/fj.07-8560rev]

24 **Chen K**, Huang YH, Chen JL. Understanding and targeting cancer stem cells: therapeutic implications and challenges. *Acta Pharmacol Sin* 2013; **34**: 732-740 [PMID: 23685952 DOI: 10.1038/aps.2013.27]

25 **Hamburger AW**, Salmon SE. Primary bioassay of human tumor stem cells. *Science* 1977; **197**: 461-463 [PMID: 560061 DOI: 10.1126/science.560061]

26 **Dexter DL**, Spremulli EN, Fligiel Z, Barbosa JA, Vogel R, VanVoorhees A, Calabresi P. Heterogeneity of cancer cells from a single human colon carcinoma. *Am J Med* 1981; **71**: 949-956 [PMID: 7315857 DOI: 10.1016/0002-9343(81)90312-0]

27 **Vermeulen L**, Todaro M, de Sousa Mello F, Sprick MR, Kemper K, Perez Alea M, Richel DJ, Stassi G, Medema JP. Single-cell cloning of colon cancer stem cells reveals a multi-lineage differentiation capacity. *Proc Natl Acad Sci USA* 2008; **105**: 13427-13432 [PMID: 18765800 DOI: 10.1073/pnas.0805706105]

28 **Barker N**, Ridgway RA, van Es JH, van de Wetering M, Begthel H, van den Born M, Danenberg E, Clarke AR, Sansom OJ, Clevers H. Crypt stem cells as the cells-of-origin of intestinal cancer. *Nature* 2009; **457**: 608-611 [PMID: 19092804 DOI: 10.1038/nature07602]

29 **Merlos-Suárez A**, Barriga FM, Jung P, Iglesias M, Céspedes MV, Rossell D, Sevillano M, Hernando-Momblona X, da Silva-Diz V, Muñoz P, Clevers H, Sancho E, Mangues R, Batlle E. The intestinal stem cell signature identifies colorectal cancer stem cells and predicts disease relapse. *Cell Stem Cell* 2011; **8**: 511-524 [PMID: 21419747 DOI: 10.1016/j.stem.2011.02.020]

30 **Barker N**, van Es JH, Kuipers J, Kujala P, van den Born M, Cozijnsen M, Haegebarth A, Korving J, Begthel H, Peters PJ, Clevers H. Identification of stem cells in small intestine and colon by marker gene Lgr5. *Nature* 2007; **449**: 1003-1007 [PMID: 17934449 DOI: 10.1038/nature06196]

31 **Van der Flier LG**, Sabates-Bellver J, Oving I, Haegebarth A, De Palo M, Anti M, Van Gijn ME, Suijkerbuijk S, Van de Wetering M, Marra G, Clevers H. The Intestinal Wnt/TCF Signature. *Gastroenterology* 2007; **132**: 628-632 [PMID: 17320548 DOI: 10.1053/j.gastro.2006.08.039]

32 **Maddox J**, Shakya A, South S, Shelton D, Andersen JN, Chidester S, Kang J, Gligorich KM, Jones DA, Spangrude GJ, Welm BE, Tantin D. Transcription factor Oct1 is a somatic and cancer stem cell determinant. *PLoS Genet* 2012; **8**: e1003048 [PMID: 23144633 DOI: 10.1371/journal.pgen.1003048]

33 **Shay JW**, Zou Y, Hiyama E, Wright WE. Telomerase and cancer. *Hum Mol Genet* 2001; **10**: 677-685

[PMID: 11257099 DOI: 10.1093/hmg/10.7.677]
34 **Hiyama E**, Hiyama K. Telomere and telomerase in stem cells. *Br J Cancer* 2007; **96**: 1020-1024 [PMID: 17353922 DOI: 10.1038/sj.bjc.6603671]
35 **Hirsch D**, Barker N, McNeil N, Hu Y, Camps J, McKinnon K, Clevers H, Ried T, Gaiser T. LGR5 positivity defines stem-like cells in colorectal cancer. *Carcinogenesis* 2014; **35**: 849-858 [PMID: 24282287 DOI: 10.1093/carcin/bgt377]
36 **van der Flier LG**, Haegebarth A, Stange DE, van de Wetering M, Clevers H. OLFM4 is a robust marker for stem cells in human intestine and marks a subset of colorectal cancer cells. *Gastroenterology* 2009; **137**: 15-17 [PMID: 19450592 DOI: 10.1053/j.gastro.2009.05.035]
37 **Schuijers J**, van der Flier LG, van Es J, Clevers H. Robust cre-mediated recombination in small intestinal stem cells utilizing the olfm4 locus. *Stem Cell Reports* 2014; **3**: 234-241 [PMID: 25254337 DOI: 10.1016/j.stemcr.2014.05.018]
38 **Buczacki S**. Fate plasticity in the intestine: The devil is in the detail. *World J Gastroenterol* 2019; **25**: 3116-3122 [PMID: 31333305 DOI: 10.3748/wjg.v25.i25.3116]
39 **Sangiorgi E**, Capecchi MR. Bmi1 is expressed *in vivo* in intestinal stem cells. *Nat Genet* 2008; **40**: 915-920 [PMID: 18536716 DOI: 10.1038/ng.165]
40 **Buczacki SJ**, Zecchini HI, Nicholson AM, Russell R, Vermeulen L, Kemp R, Winton DJ. Intestinal label-retaining cells are secretory precursors expressing Lgr5. *Nature* 2013; **495**: 65-69 [PMID: 23446353 DOI: 10.1038/nature11965]
41 **Walker F**, Zhang HH, Odorizzi A, Burgess AW. LGR5 is a negative regulator of tumourigenicity, antagonizes Wnt signalling and regulates cell adhesion in colorectal cancer cell lines. *PLoS One* 2011; **6**: e22733 [PMID: 21829496 DOI: 10.1371/journal.pone.0022733]
42 **Haegebarth A**, Clevers H. Wnt signaling, lgr5, and stem cells in the intestine and skin. *Am J Pathol* 2009; **174**: 715-721 [PMID: 19197002 DOI: 10.2353/ajpath.2009.080758]
43 **Nakata S**, Campos B, Bageritz J, Bermejo JL, Becker N, Engel F, Acker T, Momma S, Herold-Mende C, Lichter P, Radlwimmer B, Goidts V. LGR5 is a marker of poor prognosis in glioblastoma and is required for survival of brain cancer stem-like cells. *Brain Pathol* 2013; **23**: 60-72 [PMID: 22805276 DOI: 10.1111/j.1750-3639.2012.00618.x]
44 **von Rahden BH**, Kircher S, Lazariotou M, Reiber C, Stuermer L, Otto C, Germer CT, Grimm M. LgR5 expression and cancer stem cell hypothesis: clue to define the true origin of esophageal adenocarcinomas with and without Barrett's esophagus? *J Exp Clin Cancer Res* 2011; **30**: 23 [PMID: 21345220 DOI: 10.1186/1756-9966-30-23]
45 **McClanahan T**, Koseoglu S, Smith K, Grein J, Gustafson E, Black S, Kirschmeier P, Samatar AA. Identification of overexpression of orphan G protein-coupled receptor GPR49 in human colon and ovarian primary tumors. *Cancer Biol Ther* 2006; **5**: 419-426 [PMID: 16575208 DOI: 10.4161/cbt.5.4.2521]
46 **Wu C**, Xie Y, Gao F, Wang Y, Guo Y, Tian H, Li Y, Fan W. Lgr5 expression as stem cell marker in human gastric gland and its relatedness with other putative cancer stem cell markers. *Gene* 2013; **525**: 18-25 [PMID: 23664892 DOI: 10.1016/j.gene.2013.04.067]
47 **Barker N**, Huch M, Kujala P, van de Wetering M, Snippert HJ, van Es JH, Sato T, Stange DE, Begthel H, van den Born M, Danenberg E, van den Brink S, Korving J, Abo A, Peters PJ, Wright N, Poulsom R, Clevers H. Lgr5(+ve) stem cells drive self-renewal in the stomach and build long-lived gastric units in vitro. *Cell Stem Cell* 2010; **6**: 25-36 [PMID: 20085740 DOI: 10.1016/j.stem.2009.11.013]
48 **Vries RG**, Huch M, Clevers H. Stem cells and cancer of the stomach and intestine. *Mol Oncol* 2010; **4**: 373-384 [PMID: 20598659 DOI: 10.1016/j.molonc.2010.05.001]
49 **Furuyama K**, Kawaguchi Y, Akiyama H, Horiguchi M, Kodama S, Kuhara T, Hosokawa S, Elbahrawy A, Soeda T, Koizumi M, Masui T, Kawaguchi M, Takaori K, Doi R, Nishi E, Kakinoki R, Deng JM, Behringer RR, Nakamura T, Uemoto S. Continuous cell supply from a Sox9-expressing progenitor zone in adult liver, exocrine pancreas and intestine. *Nat Genet* 2011; **43**: 34-41 [PMID: 21113154 DOI: 10.1038/ng.722]
50 **Fujii Y**, Yoshihashi K, Suzuki H, Tsutsumi S, Mutoh H, Maeda S, Yamagata Y, Seto Y, Aburatani H, Hatakeyama M. CDX1 confers intestinal phenotype on gastric epithelial cells *via* induction of stemness-associated reprogramming factors SALL4 and KLF5. *Proc Natl Acad Sci USA* 2012; **109**: 20584-20589 [PMID: 23112162 DOI: 10.1073/pnas.1208651109]
51 **Bu XD**, Li N, Tian XQ, Huang PL. Caco-2 and LS174T cell lines provide different models for studying mucin expression in colon cancer. *Tissue Cell* 2011; **43**: 201-206 [PMID: 21470648 DOI: 10.1016/j.tice.2011.03.002]

World Journal of Gastroenterology

Submit a Manuscript: https://www.f6publishing.com

World J Gastroenterol 2021 April 21; 27(15): 1595-1615

DOI: 10.3748/wjg.v27.i15.1595

ISSN 1007-9327 (print) ISSN 2219-2840 (online)

ORIGINAL ARTICLE

Basic Study

Abelson interactor 1 splice isoform-L plays an anti-oncogenic role in colorectal carcinoma through interactions with WAVE2 and full-length Abelson interactor 1

Kun Li, Yi-Fan Peng, Jing-Zhu Guo, Mei Li, Yu Zhang, Jing-Yi Chen, Ting-Ru Lin, Xin Yu, Wei-Dong Yu

ORCID number: Kun Li 0000-0002-1945-0779; Yi-Fan Peng 0000-0002-6159-6088; Jing-Zhu Guo 0000-0002-8492-0335; Mei Li 0000-0001-8010-910X; Yu Zhang 0000-0002-3461-8453; Jing-Yi Chen 0000-0002-4174-5207; Ting-Ru Lin 0000-0003-4686-3250; Xin Yu 0000-0002-5479-5019; Wei-Dong Yu 0000-0002-7573-4979.

Author contributions: Li K, Peng YF, and Guo JZ contributed equally to this work and performed the majority of experiments; Li M, Zhang Y, Chen JY, Lin TR, and Yu X performed minor experiments, provided vital reagents, and were also involved in revising the manuscript; Peng YF and Yu WD designed the study, wrote the manuscript, and provided financial support; all authors read and approved the final manuscript.

Supported by National Natural Science Foundation of China, No. 30872923 and No. 81672853; and Peking University People's Hospital Scientific Research Development Found, No. RDH2020-11.

Institutional review board statement: The study was reviewed and approved by the Peking University People's

Kun Li, Mei Li, Ting-Ru Lin, Department of Central Laboratory and Institute of Clinical Molecular Biology, Peking University People's Hospital, Beijing 100044, China

Kun Li, Yu Zhang, Jing-Yi Chen, Ting-Ru Lin, Department of Gastroenterology, Peking University People's Hospital, Peking University, Beijing 100044, China

Yi-Fan Peng, Gastrointestinal Cancer Center, Unit III, Key Laboratory of Carcinogenesis and Translational Research (Ministry of Education), Peking University Cancer Hospital and Institute, Beijing 100142, China

Jing-Zhu Guo, Department of Pediatrics, Peking University People's Hospital, Beijing 100044, China

Yu Zhang, Jing-Yi Chen, Wei-Dong Yu, Department of Central Laboratory and Institute of Clinical Molecular Biology, Peking University People's Hospital, Beijing 100044, China

Xin Yu, Department of Hepatobiliary Surgery, Peking University People's Hospital, Beijing 100044, China

Corresponding author: Wei-Dong Yu, PhD, Professor, Department of Central Laboratory and Institute of Clinical Molecular Biology, Peking University People's Hospital, No. 11 Xizhimen South Street, Xicheng District, Beijing 100044, China. weidongyu@bjmu.edu.cn

Abstract

BACKGROUND

Expression of the full-length isoform of Abelson interactor 1 (ABI1), ABI1-p65, is increased in colorectal carcinoma (CRC) and is thought to be involved in one or more steps leading to tumor progression or metastasis. The ABI1 splice isoform-L (ABI1-SiL) has conserved WAVE2-binding and SH3 domains, lacks the homeodomain homologous region, and is missing the majority of PxxP- and Pro-rich domains found in full-length ABI1-p65. Thus, ABI1-SiL domain structure suggests that the protein may regulate CRC cell morphology, adhesion, migration, and metastasis *via* interactions with the WAVE2 complex pathway.

AIM

To investigate the potential role and underlying mechanisms associated with

Hospital Institutional Review Board (No. 2020-11).

Conflict-of-interest statement: The authors declare that they have no conflicts of interest to disclose.

Data sharing statement: No additional data are available.

Manuscript source: Unsolicited manuscript

Specialty type: Gastroenterology and hepatology

Country/Territory of origin: China

Peer-review report's scientific quality classification

Grade A (Excellent): A
Grade B (Very good): B, B
Grade C (Good): 0
Grade D (Fair): 0
Grade E (Poor): 0

Received: January 21, 2021
Peer-review started: January 21, 2021
First decision: February 9, 2021
Revised: February 17, 2021
Accepted: March 13, 2021
Article in press: March 13, 2021
Published online: April 21, 2021

P-Reviewer: Schlevogt B, Schulte B, Tamori A
S-Editor: Gao CC
L-Editor: Wang TQ
P-Editor: Liu JH

ABI1-SiL-mediated regulation of CRC.

METHODS

ABI1-SiL mRNA expression in CC tissue and cell lines was measured using both qualitative reverse transcriptase-polymerase chain reaction (RT-PCR) and real-time quantitative RT-PCR. A stably ABI1-SiL overexpressing SW480 cell model was constructed using Lipofectamine 2000, and cells selected with G418. Image J software, CCK8, and transwell assays were used to investigate SW480 cell surface area, proliferation, migration, and invasion. Immunoprecipitation, Western blot, and co-localization assays were performed to explore intermolecular interactions between ABI1-SiL, WAVE2, and ABI1-p65 proteins.

RESULTS

ABI1-SiL was expressed in normal colon tissue and was significantly decreased in CRC cell lines and tissues. Overexpression of ABI1-SiL in SW480 cells significantly increased the cell surface area and inhibited the adhesive and migration properties of the cells, but did not alter their invasive capacity. Similar to ABI1-p65, ABI1-SiL still binds WAVE2, and the ABI1-p65 isoform in SW480 cells. Furthermore, co-localization assays confirmed these intermolecular interactions.

CONCLUSION

These results support a model in which ABI1-SiL plays an anti-oncogenic role by competitively binding to WAVE2 and directly interacting with phosphorylated and non-phosphorylated ABI1-p65, functioning as a dominant-negative form of ABI1-p65.

Key Words: Colon cancer; Abelson interactor 1 isoform-L; Cell adhesion; Cell migration; WAVE2

Core Tip: The purpose of this study was to investigate the role and mechanism of Abelson interactor 1 splice isoform-L (ABI1-SiL) in the metastatic behavior of colorectal carcinoma cells. Our results showed that ABI1-SiL played a key role in cell surface area, adhesion, and migration, but not in proliferation and apoptosis in SW480 cells. ABI1-SiL may have anti-oncogenic roles by competitively binding to WAVE2, and directly interacting with phosphorylated and non-phosphorylated ABI1-p65, functioning as a dominant-negative molecule towards ABI1-p65.

Citation: Li K, Peng YF, Guo JZ, Li M, Zhang Y, Chen JY, Lin TR, Yu X, Yu WD. Abelson interactor 1 splice isoform-L plays an anti-oncogenic role in colorectal carcinoma through interactions with WAVE2 and full-length Abelson interactor 1. *World J Gastroenterol* 2021; 27(15): 1595-1615
URL: https://www.wjgnet.com/1007-9327/full/v27/i15/1595.htm
DOI: https://dx.doi.org/10.3748/wjg.v27.i15.1595

INTRODUCTION

Globally, colorectal carcinoma (CRC) is the third most commonly diagnosed cancer and the fourth most common cause of cancer death[1]. Despite treatment advances for CRC over the past two decades, novel molecular therapeutic strategies are required to generate informative biomarkers and identify new targets[2,3].

Abelson interactor protein-1 (ABI1) is increased and/or phosphorylated in many malignant tumors and has been proposed as a potential tumor promoter[4-11]. By forming complexes with Eps8-Sos1[6], NWasp[12], and WAVE2[13,14], ABI1 has been shown to play critical roles in the regulation of cell proliferation, apoptosis, adhesion, and migration in breast cancer, Bcr-Abl-induced leukemia, and melanoma, both *in vitro* and *in vivo*[4-15]. Recent findings have indicated that ABI1-p65 is increased and involved in colonic tumorigenesis and that it mediates the invasive properties of

CRC[7,8]. Recently, using a CRC tissue chip, we showed that increased expression of ABI1-p65 is significantly correlated with infiltration and associated with shorter overall survival[16]. Taken together, this evidence strongly suggests that ABI1 is involved in one or more of the steps leading to tumor progression or metastasis.

Alternative splicing is one of the main engines that drive proteome diversity, and up to 94% of genes are estimated to be alternatively spliced in humans[17,18]. There are many abnormal mRNA splice isoforms specifically associated with cancer progression and metastasis, some of which exert antagonistic functions[2,19,20]. Numerous structurally distinct isoforms of ABI1 exist in mammalian cells[12,21]. The ABI1-p65 isoform is increased in CRC and is thought to be involved in one or more of the steps leading to tumor progression and metastasis. However, the specific role, if any, that other splice isoforms of ABI1, such as ABI1 splice isoform-L (ABI1-SiL), play in CRC development remains unknown. As Figure 1 shows, ABI1-SiL is a splice isoform of ABI1 resulting from the alternative splicing of exons III, IV, and VIII through X. ABI1-SIL has conserved WAVE2-binding and SH3 domains, as well as several phosphorylated sites, such as pY213, pY421/pY435, and pY506, but lacks the homeodomain homologous region (HHR) and the majority of the PxxP- and Pro-rich domain[16,21]. The domain structure of ABI1-SiL suggests that it might regulate cell morphology, adhesion, migration, and even metastasis of CRC cells, similar to the ABI1-p65 isoform, by interacting with WAVE2 or other proteins.

In this study, we generated polymerase chain reaction (PCR) primers capable of specific detection of the ABI1-SiL isoform. We demonstrated that, compared with ABI1-p65, the expression of ABI1-SiL was significantly decreased in CRC tissues and cell lines, and overexpression of ABI1-SiL repressed migration and adhesion in SW480 colon cancer cells. We showed that both ABI1-p65 and ABI1-SiL were able to interact and co-localize with WAVE2 and ABI1-p65 in SW480 cells. Taken together, this evidence is the first to demonstrate that ABI1-SiL is an antagonistic splice isoform of ABI1-p65 that functions as a potential anti-oncogene.

MATERIALS AND METHODS

Cell lines and reagents

The CRC cell lines HCT-116, HT-29, LoVo, LS174T, SW480, and SW620 (the Type Culture Collection of the Chinese Academy of Sciences, Shanghai, China.), as well as the normal colon cell line CRL-1541 (ATCC, Rockville, MD, United States), were cultured in DMEM (HyClone, Beijing, China) supplemented with 10% fetal bovine serum (FBS) (Sigma, St. Louis, MO, United States). HEK-293T cells (ClonTech, Mountain View, CA, United States) were grown in DMEM (HyClone, Beijing, China) supplemented with 10% FBS. Plasmid-mediated transfection of SW480 cells with pCMV6 and pCMV6-ABI1-GFP (green fluorescence protein) transcript variant 12 (ABI1-Tv12) was performed as previously described using Lipofectamine (Invitrogen, CA, United States)[4,22]. Both pCMV6 and the vector containing human ABI1 cDNA (NM_001178125.1, ABI1-Tv12, encoding ABI1-SiL) were purchased from OriGene Technologies, Inc. (Rockville, MD, United States). G418 (500 μg/mL) was used to select stable cell lines overexpressing ABI1-SiL.

Patient tissue collection

CRC and matched adjacent tissue samples were obtained from 24 patients. All CRC cases were diagnosed using enteroscopy, and primary carcinoma of the colon-rectum was histologically identified. All samples were anonymized prior to this study. The local ethics committee of the Peking University, People's Hospital approved the study.

Qualitative and quantitative PCR analysis

Tissue samples, as well as the cell lines described above, were analyzed for the expression of transcript variant-12 (ABl1-SiL)[21]. Total RNA was isolated from patient samples, CRC cell lines, and transfected SW480 cells using an RNeasy mini kit (QIAGEN, Valencia, CA, United States) as previously described[23]. cDNA was subsequently generated using oligo-(dT) primers and the SuperScript III First-strand Synthesis System (Invitrogen, Carlsbad, CA, United States). PCR was performed to confirm the expression of ABI1-SiL[21] using the following primers: Forward, 5'-CCTCTCAGCTTCGGAGAATGG-3' and reverse, 5'-AGGAGGATTTGT TCTCGACAGTGT-3'. A 101 bp-amplified fragment in the PCR products was shown to be ABI1-SiL (confirmed by DNA sequencing). Quantitative PCR (qPCR) was performed using either human ABI1 universal 1 (ABI1-U1) (transcript variant 1-12)

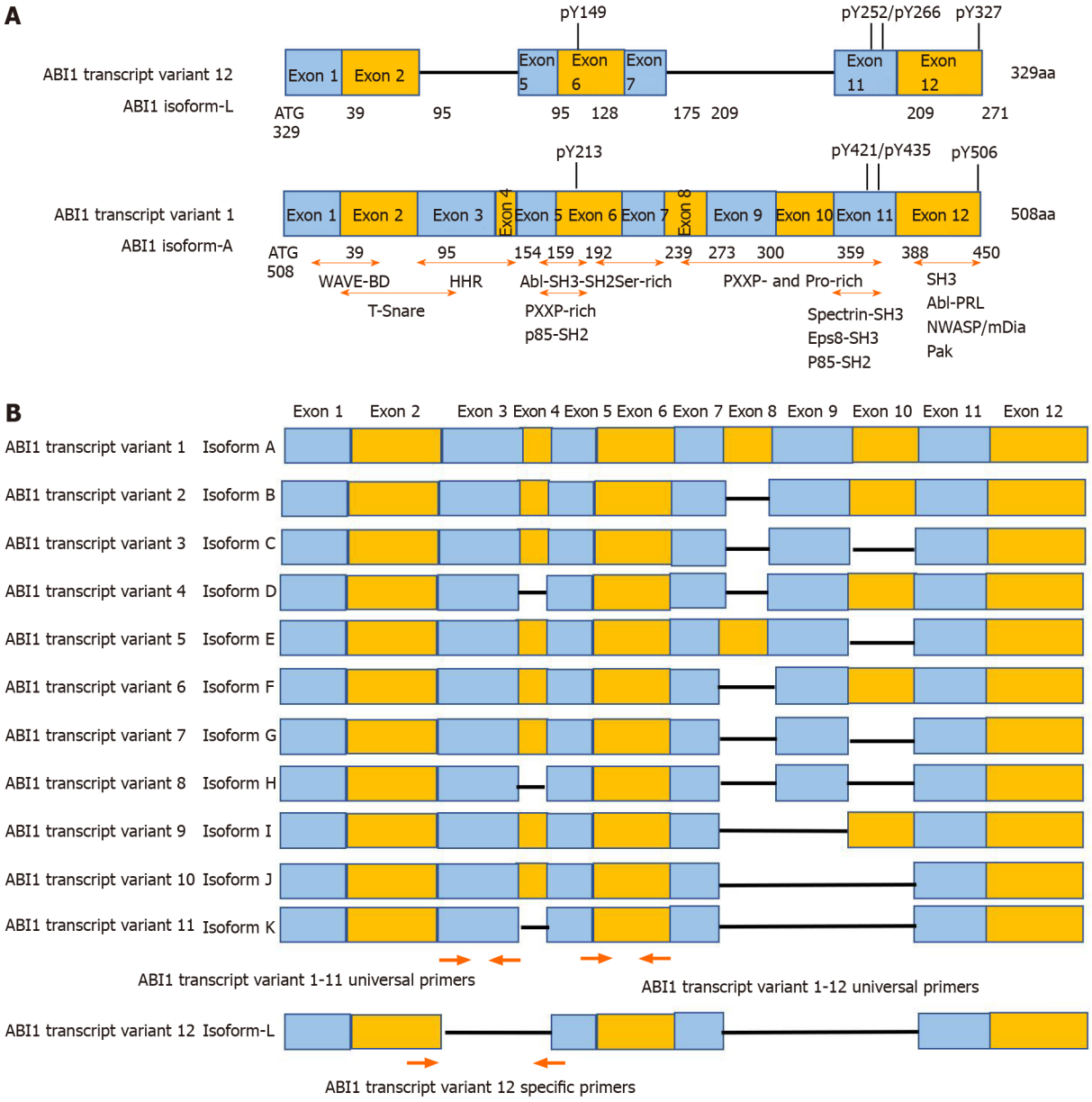

Figure 1 Diagram of Abelson interactor 1 isoforms and polymerase chain reaction primers used to measure expression levels of Abelson interactor 1. A: Schematic comparison of the exons and functional domains of two major isoforms of Abelson interactor 1 (ABL1): ABL1 splice isoform L (ABI1-SiL) and ABL1 splice isoform A (ABI1-p65). ABI1-SiL has conserved WAVE2-binding and SH3 domains, but lacks the homeo-domain homologous region and the majority of the PxxP- and Pro-rich domain; B: Schematic showing locations of ABI1 universal 1 (ABI1-U1)-, ABI1 universal 2 (ABI1-U2)-, and ABI1-SiL-specific primers. Primers were selected to target exon 3, as it represents a major structural difference between ABI1-SiL and other ABI1 variants. Three sets of primers were designed to analyze the expression of ABI1-SiL in colorectal carcinoma cells and tissues. Transcript variant 12-specific primers were used for qualitative analysis, while transcript variant 1-12 universal (ABI1-U1) and transcript variant 1-11 universal (ABI1-U2) primers were used for quantitative analysis of ABI1-SiL expression. ABI1: Abelson interactor 1; HHR: Homeo-domain homologous region.

primers (forward: 5′-ACACTGGGACGGAATACTCCTTAT-3′; reverse: 5′-CTACCACTGTTTTCTCGACTTCCA-3′) or human ABI1 universal 2 (ABI1-U2) (transcript variant 1-11) primers (forward: 5′-AGTGGCACGAAGAGAGATTGG-3′; reverse: 5′-CTGTGTAATCGATAGGTTTCCGAAT-3′) and SYBR Green Master Mix (Applied Biosystems, Foster City, CA, United States). PCR reactions began with a 10 min incubation at 95 °C for AmpliTaq Gold activation, followed by 40 cycles at 95 °C for 15 s for the denaturation step and 60 °C for 1 min for the primer annealing and extension step. qPCR was performed using the DNA Engine Option 2 System (Bio-Rad, CA, United States). Glyceraldehyde-3-phosphate dehydrogenase (GAPDH) was used as an endogenous housekeeping control for relative quantification of transcription (forward primer: 5′-AACGACCCCTTCATTGAC-3′, reverse primer: 5′-TCCACGACATACTCAGCAC-3′). The percentage of ABI1-SiL among all variants was calculated as $(1\text{-}2^{-[\text{Ct-ABI1-U2-Ct-ABI1-U1}]}) \times 100\%$.

To examine the potential roles of ABI1-SiL overexpression on differentiation and invasion of SW480 cells, a series of additional genetic markers (including POU, CD44, KRT20, MMP1-4, and WAVE2) were also analyzed by qPCR (primers sequences are not shown).

Cell culture and transfection

Lipofectamine-mediated transfection of SW480 cells was performed as previously described[4]. Cells were plated in six-well plates 24 h prior to transfection, and 2 μg of plasmid DNA was used for each transfection. To overexpress ABI1-SiL, a pCMV6 vector specifically coding for ABI1-SiL or a control pCMV6 empty vector was used for stable transfection of SW480 cells or transient transfection of 293T cells. Forty-eight hours after transfection, transfected cells were treated with G418 (500 μg/mL). Individual G418-resistant clones were picked after 3-4 wk. Clones were analyzed by qPCR and Western blot for ABI1-SiL expression, and clones with the highest ABI1-SiL expression were chosen for further studies. Clones 3 and 6 overexpressing ABI1-SiL were named SW480-ABI1-SiL3 and SW480-ABI1-SiL6, respectively. SW480 cells transfected with the empty pCMV6 vector were named SW480-V.

To analyze the subcellular localization of ABI1-SiL in SW480 cells and to test for co-localization with ABI1-p65 and/or WAVE2, a pCMV6 vector encoding a GFP-ABI1-SiL fusion protein was used for both transient and stable transfections. In transient experiments, 48 h after transfection, the 293T cells underwent subcellular localization studies by fixing the cells in 4% paraformaldehyde in phosphate buffer saline (PBS) for 10 min, followed by fluorescence microscopy analysis.

Western blot and co-immunoprecipitation

Western blot analyses were performed as previously described[4]. We used the following antibodies: GAPDH (1:2000 dilution; #CB100999, Proteintech, IL, United States), ABI1-p65 (1:1000 dilution; D147-3, BML, MA, United States), WAVE2 (1:500 dilution; 07-410, Upstate, NY, United States), GFP (1:200 dilution; 1G6; Pregene Co. Beijing, China), and NAP-1 (1:1000 dilution; #12140-1-AP, Proteintech, IL, United States) protein A/G (Sc-2003, Santa Cruz, CA, United States). The protease inhibitor cocktail was purchased from Sigma (St. Louis, MO, United States). Cells were lysed in lysis buffer (20 mmol/L HEPES, pH 7.2; 150 mmol/L NaCl; 1% Triton X-100; and 10% glycerol). Total protein lysates (150 μg each) from all tested cell lines were separated on sodium dodecyl sulfate-polyacrylamide gel electrophoresis (SDS-PAGE) gels, transferred to a nitrocellulose membrane, and immunoblotted with appropriate antibodies. Immunoprecipitation analysis was performed as described previously[4]. Briefly, SW480-V and/or SW480-ABI1-SiL6 cells were lysed as described above and incubated with appropriate antibodies bound to sepharose beads. Immunoprecipitates were resolved by SDS-PAGE, transferred to nitrocellulose, and immunoblotted with appropriate antibodies. Membranes were then washed with TBST buffer and incubated with secondary antibodies conjugated to HRP (horseradish peroxidase) (Jackson ImmunoResearch Laboratories Beijing, China). Bound antibodies were detected using the SuperSignal West Pico Trial Kit (Thermo Scientific, Rockford, IL, United States), and images were acquired using an ImageQuant 350 system (GE Healthcare, Piscataway, NJ, United States) and analyzed using ImageJ software (NIH, Bethesda, MD, United States).

Cell surface area assay

To measure the surface area, all four tested cell lines were routinely cultured and images were captured using a Cannon EOS600D camera. ImageJ was used to measure the cell surface area of 100 cells per condition. The measured values were normalized to the mean value of the SW480 parental cells.

Cell adhesion, migration, and invasion assays

For adhesion assays, 2.5×10^5 cells from each cell line were plated in a six-well plate (2.5 mL/well) coated with or without either 0.2% BSA or 0.1% gelatin, or fibronectin (5 μg/mL) (BD Biosciences, Bedford, MA, United States) and incubated at 37 °C/5% CO_2 for 6 h. Non-adherent cells were removed, and adherent cells were washed three times with 1 mL pre-warmed DMEM medium. To determine the number of adherent cells, the number of adherent cells within five randomly selected microscopic fields was counted in three independent experiments.

Cell migration assays were performed using a 24-well transwell chamber (Corning, New York, NY, United States) with 8.0-μm pore polycarbonate filter inserts, and cell invasion assays were performed using inserts of Transwell plates (8.0-μm pores,

Corning Costar Corp., Cambridge, MA, United States) coated with Matrigel (Costar, Cambridge, MA, United States)[22]. Cells (2.5×10^4 cells/well) suspended in serum-free DMEM containing 0.2% BSA were placed in the upper chamber of each transwell. In each lower chamber, 600 μL of DMEM supplemented with 10% FBS was added. The inserts were then incubated at 37 °C in a humidified atmosphere containing 5% CO_2 for 24 h (migration) and 48 h (invasion), respectively. Cells that had not penetrated the filters were removed using cotton swabs. Cells that migrated to the bottom of the insert were fixed in 4% paraformaldehyde for 10 min and stained with 0.1% crystal violet for 30 min, followed by rinsing with PBS and examination under a bright-field microscope equipped with a 100 × objective. Migratory or invasive activity was expressed as the average number of migrated cells per microscopic field over five fields in each assay from three independent experiments.

Cell proliferation and apoptosis assays

Cell proliferation assays were performed using Cell Counting Kit-8 (CCK-8; Dojindo, Rockville, MD, United States) according to the manufacturer's instructions. All tested cell lines were seeded at 2.5×10^4 cells per well of a 96-well plate and cultured in 100 μL of DMEM supplemented with 10% FBS. At the indicated time points, culture medium was exchanged for 110 μL of DMEM supplemented with CCK-8 reagent (10 μL CCK-8 and 100 μL DMEM), and cells were incubated for an additional 2 h. Absorbance was measured for each well at a wavelength of 450 nm, with the reference wavelength set at 600 nm. An increase or decrease in absorbance values at 450 nm in the experimental wells relative to the initial value was indicative of cell growth or death, respectively. Cell growth was monitored at 24 h, 48 h, 72 h, and 96 h, and was repeated in replicates of three wells per time point.

Apoptosis assays were performed immediately after selection with G418. Cells were washed twice and seeded at a density of 2×10^5 cells/mL in DMEM and 10% FBS in the presence of G418 (for SW480-V, SW480-ABI1-SiL3, and SW480-ABI1-SiL6). After 48 h of culture, apoptosis was monitored using the Annexin V-FITC Apoptosis Detection Kit (KeyGen Biotech, #KGA107, Shanghai, China). For FACS analysis, 1×10^5 cells were co-stained with Annexin V-EGFP and with the fluorescent dye propidium iodide (PI). Cells that stained negative for both PI and annexin V were considered viable cells; PI-negative and annexin V-positive stained cells were considered early apoptotic cells; PI-positive and annexin V-positive stained cells were considered to be in the later stages of apoptosis. All assays were carried out independently, in triplicate.

Immunofluorescence microscopy

Samples of 293T cells were cultured on fibronectin-coated coverslips and transiently transfected with either the ABI1-SiL-GFP plasmid or a control plasmid, as well as SW480-ABI1-SiL6. The cells were fixed in 4% paraformaldehyde in PBS for 10 min and permeabilized with 0.2% Triton X-100 in PBS for 8 min. Non-specific binding was blocked by incubation of the coverslips with 3% bovine serum albumin in PBS, followed by incubation with primary antibodies (anti-ABI1-p65 and or anti-WAVE2) in 1% bovine serum albumin/PBS. After extensive washing with PBS, cells were incubated with appropriate Alexa-conjugated secondary antibodies. Cytoskeleton was detected by Phalloidin staining. The slides were examined under a Nikon Eclipse TE2000-U fluorescence microscope, and images were captured and analyzed using Nikon NIS Elements imaging software.

Statistical analysis

SPSS version 16.0 software (SPSS Inc., Chicago, IL, United States) was used for statistical analyses. Data from all quantitative assays are expressed as the mean ± SD and were analyzed statistically using one-way analysis of variance (ANOVA) followed by Dunnett test and general linear model analysis (univariate). *P* values less than 0.05 were considered statistically significant.

RESULTS

Establishment of qualitative and quantitative real-time reverse transcriptional polymerase chain reaction assays for detection of ABI1-SiL

The *ABI1* gene encodes a member of the Abelson interactor family of adaptor proteins. At least 12 alternatively spliced transcript variants encoding multiple isoforms have been observed for this gene[21]. There are significant differences in the exons and

functional domains contained in the different isoforms of *ABI1*, which may result in structural differences in the proteins that lead to differing functions between ABI1-SiL and other transcript variants (Figure 1A). To detect the expression of ABI1-SiL, we designed a set of qualitative primers and two sets of universal quantitative primers that detect this isoform specifically, as shown in Figure 1B. Using qualitative PCR, two visible bands were amplified, and we verified through sequencing that the 101-bp band represents the transcript variant-12 specific PCR product (Figure 2A). We demonstrated that ABI1-SiL was expressed in all tested CRC cells and control CRL-1541 cells.

Next, we tested the reliability of the primers designed for quantitative analysis of ABI1-SiL expression. ABI1-SiL and 12 plasmids (single and/or mixtures), as well as the cDNA from CRL-1541 cells and HCT116 cells, were used as templates to perform qPCR. PCR amplified products were examined by 1.5% agarose gel electrophoresis (Figure 2B). Taken with the analysis of the amplification curve, the melting curve, and the sequencing data for the PCR products (data not shown), these observations indicated that we have successfully established a quantitative assay specific for detection of ABI1-SiL.

The proportion of ABI1-SiL isoform is significantly decreased, relative to other ABI1 splice isoforms, in colon cancer tissues and cell lines

In previous studies, we and other groups have shown that the full-length isoform of ABI1 (ABI1-p65) is increased in colon cancer cells and tissues and involved in the progression and development of colon cancer[7,8,22]. To analyze the potential role of ABI1-SiL in colon cancer, we examined the expression level of ABI1-SiL in CRC cells and tissues using qPCR. As Figure 2D and E shows, the ratio of the ABI1-SiL isoform to other ABI1 splice isoforms was significantly decreased in all CRC cells compared with control CRL-1541 cells and was also decreased in 16 of 24 CRC tissues compared with adjacent tissues. These observations indicated that ABI1-SiL may play an anti-oncogenic role in colorectal tissues.

Successful creation of a human colon cancer SW480 cell model stably overexpressing ABI1-SiL

To test the function of ABI1-SiL in cellular phenotypes of colon cancer, we overexpressed ABI1-SiL in SW480 colon cancer cells. The full-length cDNA of ABI1-SiL, or an empty vector control plasmid, was introduced into SW480 by Lipofectamine-mediated transfection. We confirmed ABI1-SiL expression in two stable cell lines, SW480-ABI1-SiL3 and SW480-ABI1-SiL6 (Figure 3A and B). As shown in Figure 3C, the expression of the cDNA in SW480 cells resulted in a significant increase in the proportion of the ABI1-SiL isoform relative to other isoforms by about 30%, as compared to the parental SW480 and SW480-V cell lines. We also demonstrated through Western blot that the ABI1-SiL-GFP fusion protein was expressed in SW480-ABI1-SiL3 and SW480-ABI1-SiL6 cells, but not in parental SW480 and SW480-V cells (Figure 3D). These data confirm that we successfully constructed a SW480 colon cancer cell model overexpressing ABI1-SiL.

Overexpression of ABI1-SiL increases the surface area of human colon cancer SW480 cells

We observed that the SW480-ABI1-SiL3 and SW480-ABI1-SiL6 stable cell lines were substantially larger and were more similar in morphology to epithelial cells than the parental and empty vector transfected cells (Figure 4A-D, see arrows). To quantitatively assess this difference in cellular morphology, Image J and SPSS software were used to examine the cell surface area of the transfected and control cell lines. As Figure 4E shows, the cellular surface area was significantly increased by about 40% in SW480-ABI1-SiL3 and SW480-ABI1-SIL6 cells compared with the parental and control SW480 cells ($P < 0.01$). To determine whether ABI1-SiL-induced changes in cellular morphology are due to effects on differentiation of SW480 cells, we used qPCR to analyze the expression of POUS, CD44, and KRT20, but we observed no difference in the expression of these genes, except for KRT20 in SW480-SiL3 (Figure 4E).

Overexpression of ABI1-SiL inhibits adhesion and migration, but not invasion, of SW480 human colon cancer cells

We performed adhesion, migration, and invasion assays to test whether ABI1-SiL overexpression activated these cellular mechanisms. In the adhesion assay, we discovered that ABI1-SiL overexpression significantly impaired the adhesive

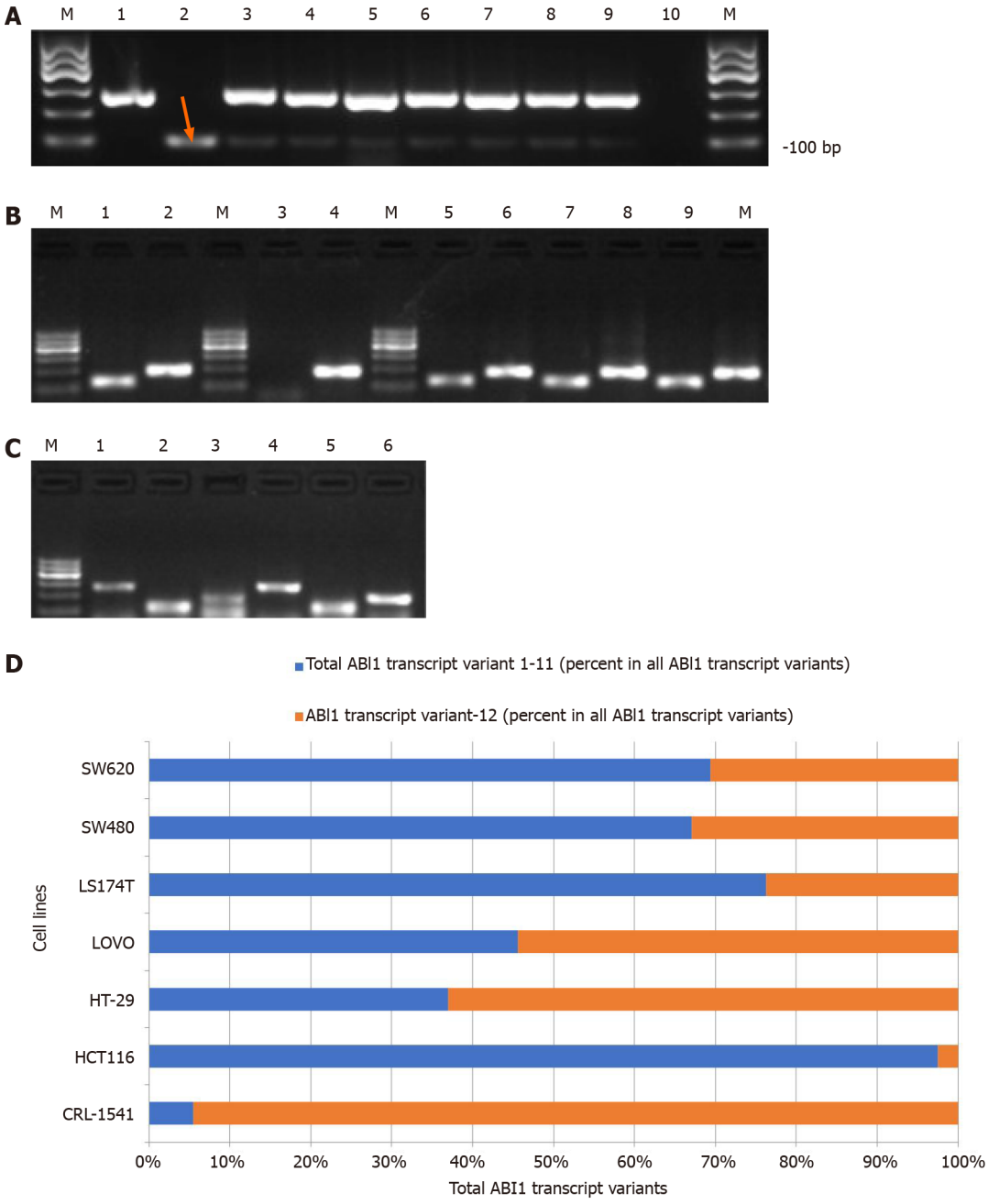
A
M 1 2 3 4 5 6 7 8 9 10 M
-100 bp
B
M 1 2 M 3 4 M 5 6 7 8 9 M
C
M 1 2 3 4 5 6
D
Total ABl1 transcript variant 1-11 (percent in all ABl1 transcript variants)
ABl1 transcript variant-12 (percent in all ABl1 transcript variants)
SW620
SW480
LS174T
LOVO
HT-29
HCT116
CRL-1541
Cell lines
0% 10% 20% 30% 40% 50% 60% 70% 80% 90% 100%
Total ABI1 transcript variants

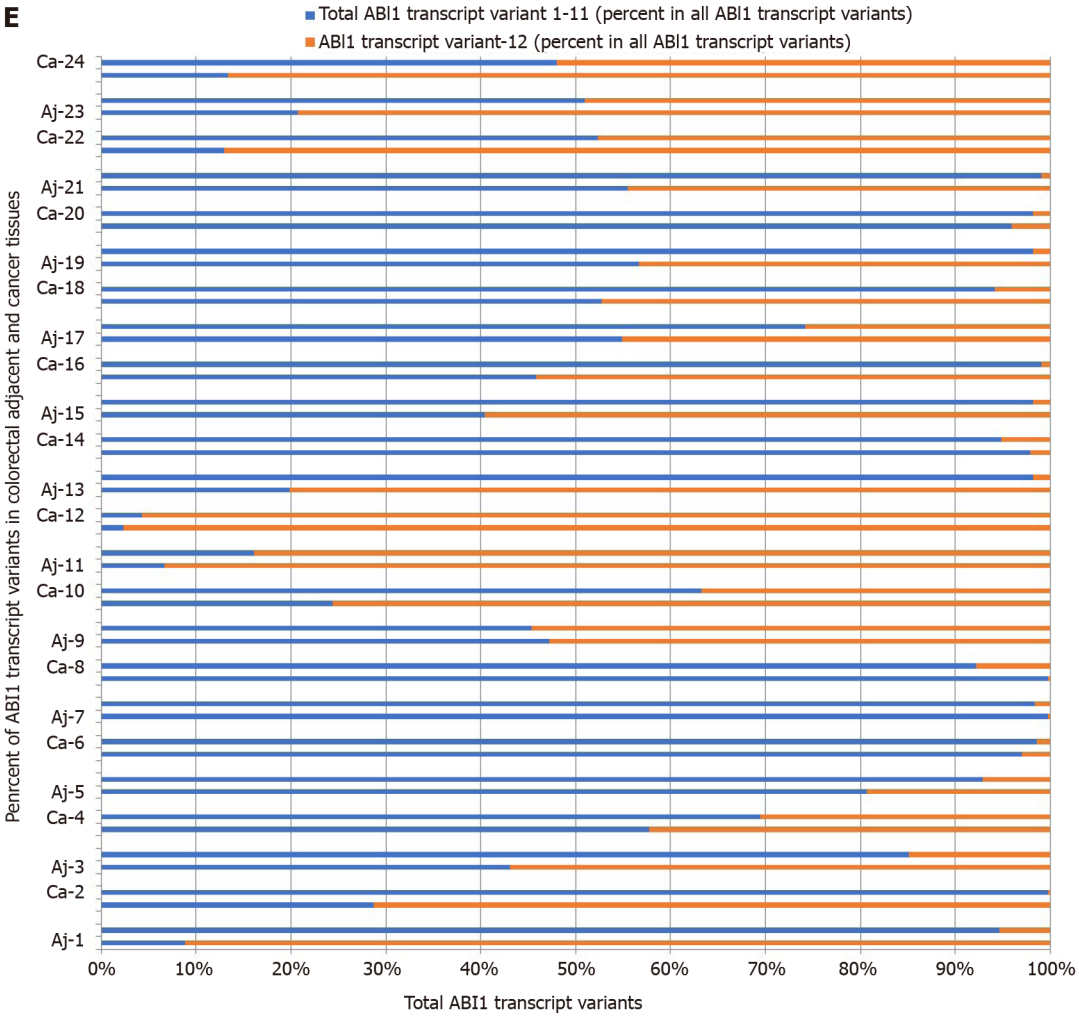

Figure 2 The proportion of Abelson interactor 1 splice isoform-L is significantly decreased in colon cancer tissues and cell lines compared to other Abelson interactor 1 splice isoforms. A: Expression of endogenous Abelson interactor 1 splice isoform-L (ABI1-SiL) in colorectal carcinoma cells. M, 100 bp DNA Marker; 1, ABI1-Tv1 positive Ctrl (278 bp); 2, ABI1-SiL positive control (101 bp, orange arrow); 3, CRL-1541; 4, HCT-116; 5, HT-29; 6, LoVo; 7, LS174T; 8, SW480; 9, SW620; 10, negative control; B: ABI1-Tv1, ABI1-SiL, or a mixture of ABI1-Tv1 and ABI1-SiL were used as templates to confirm the feasibility of the ABI1-SiL quantitative polymerase chain reaction assay using the ABI1-U2 (lanes 1, 3, 5, 7, and 9) and ABI1-U1 primers (lanes 2, 4, 6, 8, and 10); C: ABI1-U1- (lanes 2 and 5) and ABI1-U2-specific (lanes 3 and 6) polymerase chain reaction products amplified from cDNA from CRL-1541 (lanes 1-3) and HCT116 (lanes 4-6) cells. Lanes 1 and 4 contain GAPDH (glyceraldehyde-3-phosphate dehydrogenase); D: The ratio of ABI1-SiL relative to all other ABI1 isoforms was significantly decreased in colorectal carcinoma cells compared with control CRL-1541 cells; E: The ratio of ABI1-SiL relative to other ABI1 isoforms was significantly decreased in 66.7% (16/24) of all tested colorectal tissues compared with adjacent tissues. M: Maker; ABI1: Abelson interactor 1; Aj: Adjacent; Ca: Cancer.

capability in all tested conditions (0.2% BSA, gelatin, fibronectin, and no coating) (P < 0.01, Figure 5A). Among the tested coating conditions, the adhesion assay showed that ABI1-SiL had the strongest inhibitory effect on adhesion in the presence of fibronectin. In the migration assay, ABI1-SiL overexpression also greatly inhibited the migration of SW480 cells *in vitro* (P < 0.01) (Figure 5B-F). Interestingly, ABI1-SiL overexpression showed no inhibitory effect on invasion of SW480 cells (P > 0.05; Figures 5G-K). Furthermore, expression analysis using qPCR revealed that ABI1-SiL overexpression had no effect on expression of matrix metalloproteases 1, 2, 3, or 4 (Figure 5L).

Overexpression of ABI1-SiL does not alter either proliferation or apoptosis of the human colon cancer cell line SW480

It has been reported that the full-length isoform of ABI1 (ABI1-p65) promotes proliferation and inhibits apoptosis of colon cancer cells[24-26], but the action of ABI1-SiL in colon cancer cells is unknown. To further determine the effect of ABI1-SiL overexpression on the proliferation and apoptosis of SW480 cells, we performed CCK-8 cell viability and apoptosis assays. As Figure 6A and B shows, overexpression of ABI1-SiL had no effects on proliferation or apoptosis of SW480 cells. These observations confirmed that changes in migration and invasion did not result from alterations in cell proliferation and apoptosis.

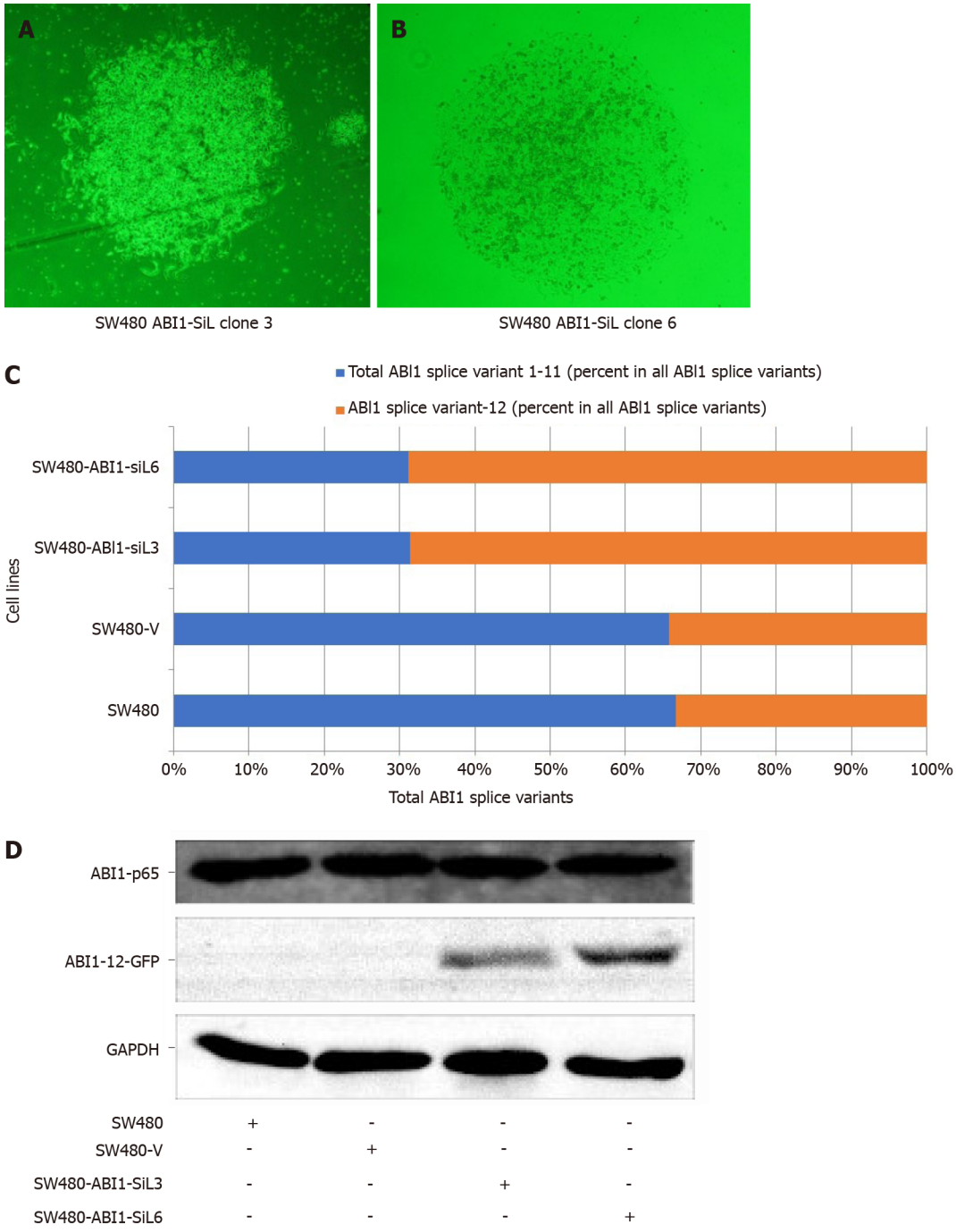

Figure 3 Construction of a human colon cancer SW480 cell model stably overexpressing Abelson interactor 1 splice isoform-L. A: SW480 clone #3 overexpressing Abelson interactor 1 splice isoform-L (ABI1-SiL); B: SW480 clone #6 overexpressing ABI1-SiL; C: The ratio of ABI1-SiL to all Abelson interactor 1 (ABI1) isoforms was determined by quantitative polymerase chain reaction using ABI1 universal 1 and ABI1 universal 2 primers; D: Western blot demonstrating efficacy of ABI1-SiL overexpression. Lysates from 1 × 10^6 cells were separated by sodium dodecyl sulfate-polyacrylamide gel electrophoresis and transferred to a nitrocellulose membrane. The membrane was probed with the indicated antibodies. ABI1-SiL: Abelson interactor 1 splice isoform-L; ABI1: Abelson interactor 1; GFP: Green fluorescence protein; GAPDH: Glyceraldehyde-3-phosphate dehydrogenase.

Potential mechanism underlying the effects of ABI1-SiL on cell morphology, adhesion, and migration of SW480 cells

It has been widely accepted that ABI1 regulates cancer cell morphology, adhesion, and migration by directly interacting with WAVE2 and forming the ABI1-WAVE2-NAP-1 complex[27-29]. We confirmed the expression of ABI1-p65, WAVE2 and NAP-1 in all tested cell lines. As Figures 3D, 7A, and 7B demonstrate, ABI1-SiL overexpression did not alter the expression of ABI-p65 and WAVE2 at either the mRNA or protein level, as well as NAP-1 at the protein level. The SW480-Vector and SW480-ABI1-SiL6 cell lines were used to analyze potential mechanisms underlying the effect of ABI1-SiL expression on cell morphology, adhesion, and migration of SW480 cells. Western blot

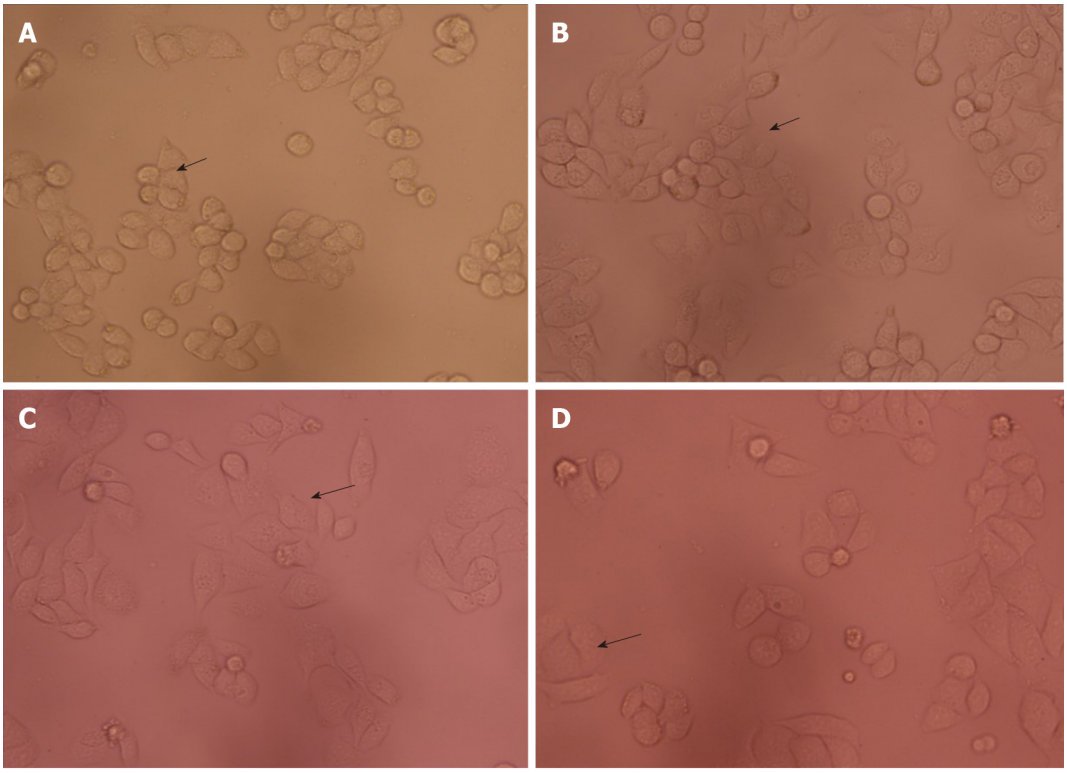

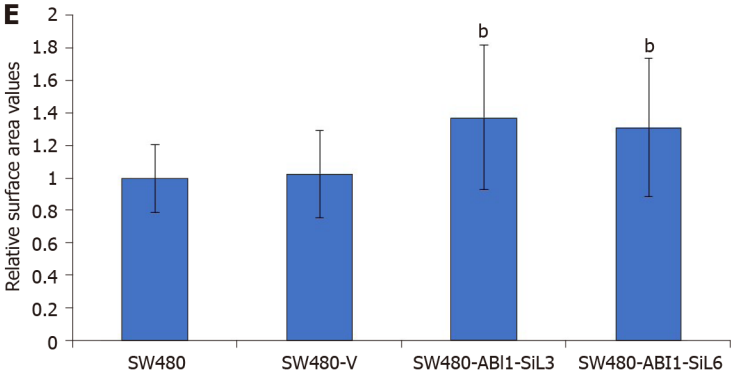

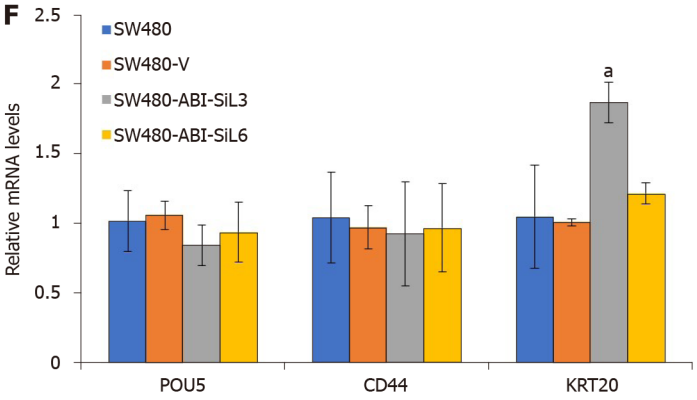

Figure 4 Alterations in cellular morphology occur with exogenous Abelson interactor 1 splice isoform-L expression in SW480 colon cancer cells. A: SW480; B: SW480-V; C: SW480-ABI1-SiL3; D: SW480-ABI1-SiL6 cells; E: Cell surface area measured using ImageJ software. The mean values are normalized to those of parental SW480 cells. Data represent the mean ± SD of triplicate experiments. SW480 cells overexpressing Abelson interactor 1 splice isoform-L (ABI1-SiL) showed a 1.4 folds increase in cell surface area, $^{b}P < 0.01$; F: Expression levels of stem-cell and cell differentiation markers determined by quantitative polymerase chain reaction using gene-specific primers. No significant differences were observed between SW480-ABI1-SiL (3 and 6) cells and parental SW480 cells or SW480-V cells ($P > 0.05$), except for KRT20 in the SW480-ABI1-SiL3 cells ($^{a}P < 0.05$).

and co-immunoprecipitation (co-IP) revealed that both ABI1-p65 and ABI1-SiL-GFP were able to interact with WAVE2 in SW480-ABI1-SiL6 cells, as determined by successful bidirectional co-IP of ABI1-p65, ABI1-SiL-GFP, and WAVE2 (Figure 7C and

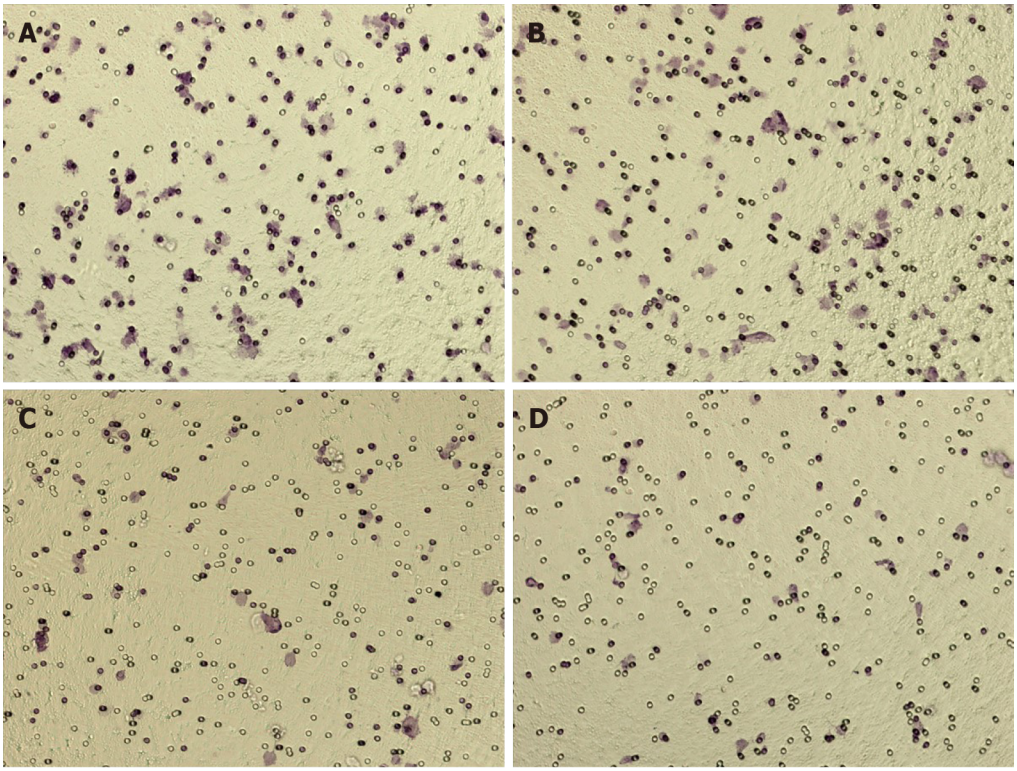
A
B
C
D

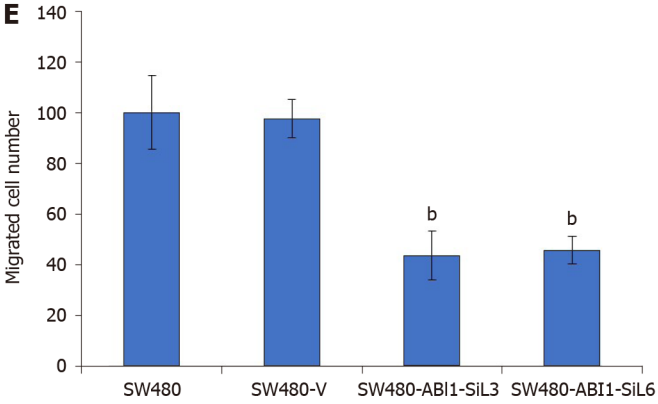
E
Migrated cell number
140
120
100
80
60
40
20
0
b
b
SW480
SW480-V
SW480-ABI1-SiL3
SW480-ABI1-SiL6

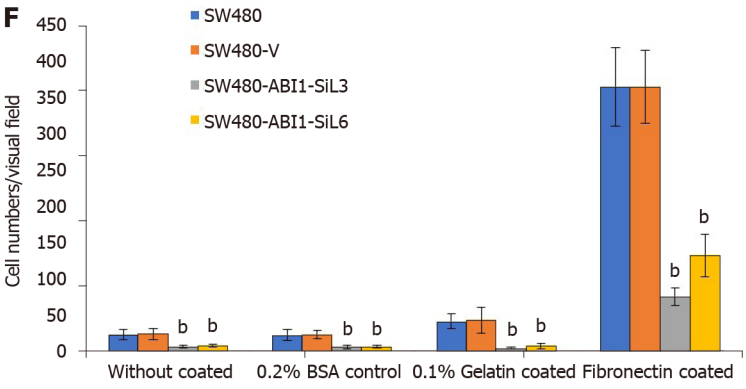
F
Cell numbers/visual field
450
400
350
300
250
200
150
100
50
0
SW480
SW480-V
SW480-ABI1-SiL3
SW480-ABI1-SiL6
b
Without coated
0.2% BSA control
0.1% Gelatin coated
Fibronectin coated

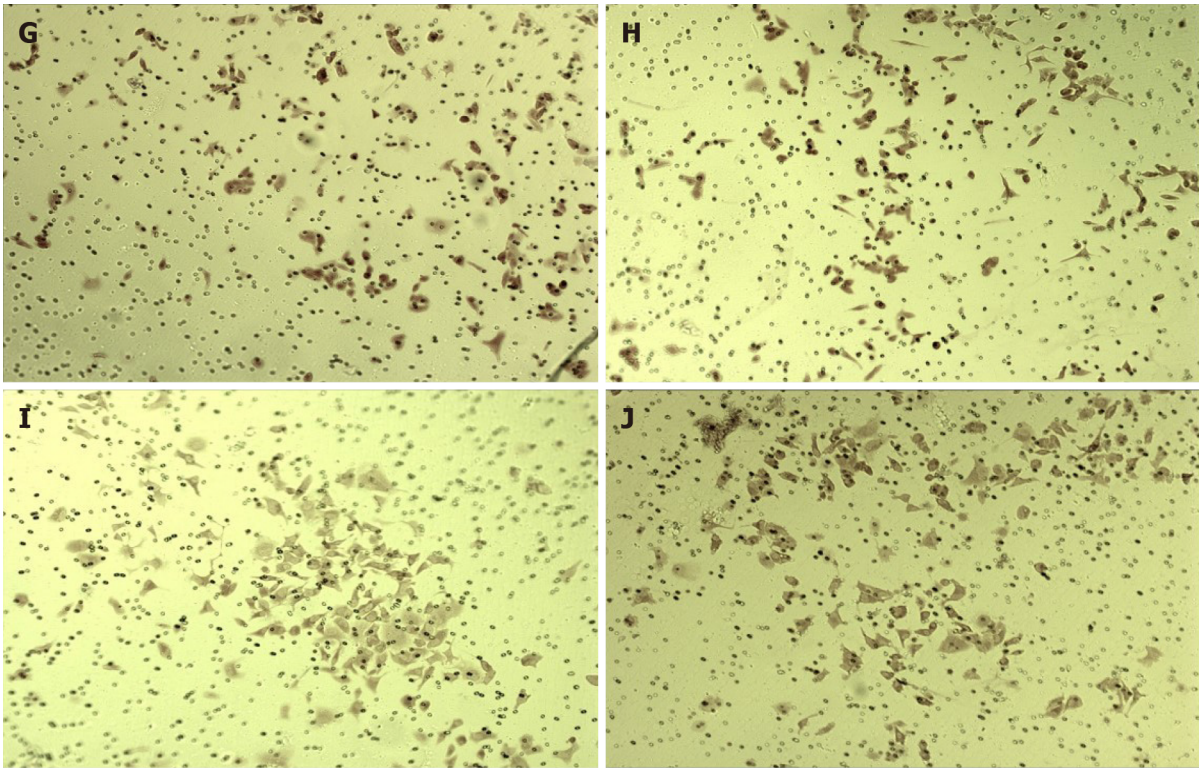

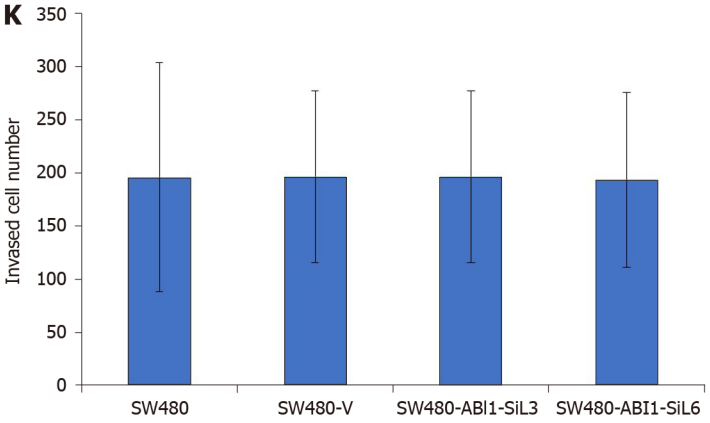

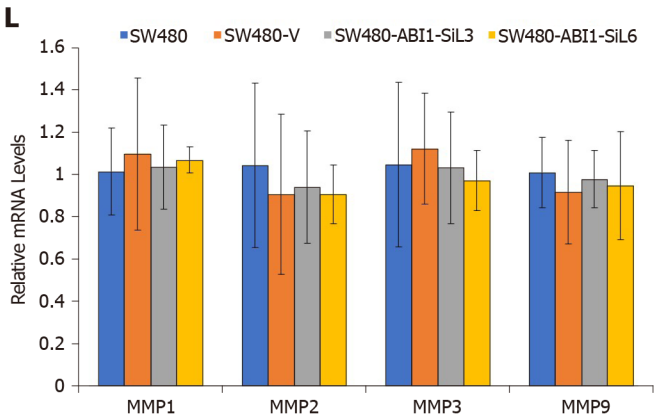

Figure 5 Overexpression of Abelson interactor 1 splice isoform-L inhibits migration and adhesion, but not invasion, of SW480 human colon cancer cells. A-F: Effect of Abelson interactor 1 splice isoform-L (ABI1-SiL) overexpression on migration of SW480 cells *in vitro*. A migration assay was conducted over 24 h with 2.5 × 10^4 cells using a transwell chamber. Cells on the lower surface of the filter were imaged. SW480 (A), SW480-V (B), SW480-ABI1-SiL3 (C), and SW480-ABI1-SiL6 (D) were used. The number of migrating cells that penetrated the transwell chamber is expressed as the mean number of cells from five random fields. Representative results from one experiment of three are shown (E). The effects of ABI1-SiL overexpression on SW480 cell adhesion on 0.2% BSA, 0.1% gelatin, or fibronectin-coated surfaces were assessed (F). All tested cell lines were cultured in 0.2% BSA, 0.1% gelatin, or 5 μg/mL fibronectin-coated six-well plates (2.5 × 10^5 cells per well) for 6 h. The total number of cells that were adherent in each condition were counted. The vertical axis shows the number of the

adherent cells per field (from five random fields) and is expressed as the mean ± SD of triplicate wells; G-L: Effect of ABI1-SiL overexpression on invasion of SW480 cells *in vitro*. An invasion assay was conducted over 48 h with 2.5 × 10 ^{4} cells using Matrigel filters. Results shown here are for one representative experiment. Cells on the lower surface of the filter were imaged. SW480 (G), SW480-V (H), SW480-ABI1-SiL3 (I), and SW480-ABI1-SiL6 (J) were used. The number of migrated cells that penetrated through Matrigel-coated filters is expressed as the mean number of cells in five random fields (K). ABI1-SiL overexpression in SW480 cells has no effect on the mRNA expression of MMPs (L). $^aP < 0.05$ and $^bP < 0.01$ indicate significant differences between SW480, SW480-V, SW480-ABI1-SiL3, and SW480-ABI1-SiL6 cells. ABI1-SiL: Abelson interactor 1 splice isoform-L.

D). Interestingly, we also observed evidence of a direct interaction between ABI1-p65, phosphorylated ABI1-p72, and ABI1-SiL-GFP (Figure 7D). Additionally, we showed that ABI1-SiL does not bind to NAP-1, but ABI1-p65 and phosphorylated ABI1-p72 do in SW480-ABI1-SiL6 cells (Figure 7E). Finally, 293T cells, transfected with ABI1-SiL-GFP and stable SW480-ABI1-SiL6, were used to examine the co-localization of ABI1-SiL-GFP and WAVE2 or ABI1-p65. As shown in Figures 8 and 9, ABI1-SiL co-localizes with both WAVE2 and ABI1-p65. These observations suggested that the ABI1-SiL isoform inhibits the adhesion and migration of SW480 cells *in vitro* by competitively interacting with WAVE2 and directly binding to ABI1-p65. These results provide a novel molecular mechanism explaining the functions of distinct ABI1 isoforms in CRC cells.

DISCUSSION

In this study, we have identified a novel function for ABl1-SiL in adhesion and migration of colon cancer SW480 cells and propose a mechanism underlying this function. Our model is based on a combination of gene expression and mechanistic studies of ABI1-SiL in colon cancer cells and tissues. We and other groups have previously shown that overexpressed non-phosphorylated ABI1-p65 functions as a pro-oncogene in development and progression of CRC[7,8,22]. Now, we wanted to address the question of whether there are other ABI1 isoforms that exist in colon tissues and cells that play additional roles in colon cancer. Identification of novel alternatively spliced isoforms with dysregulated expression in cancer could lead to the development of tumor-specific molecular targets for prognosis and therapy[30].

At present, there is no commercial antibody available that can detect the ABI1-SiL protein. Here, we report a set of PCR-based methods that can specifically measure ABI1-SiL mRNA expression. Unlike the full-length ABI1-p65 isoform, ABI1-SiL was significantly decreased in colorectal tissues and cells compared with the adjacent tissues and CRL-1541 normal colon cells (Figure 2). This observation, coupled with the structural differences between ABI1-SiL and other isoforms, especially ABI1-p65 (Figure 1A), led us to postulate that ABI1-SiL might function as an anti-oncogene.

ABI1-SiL mRNA expression was significantly decreased in SW480 cells, so we selected this cell line to investigate the effects of ABI1-SiL expression on cellular phenotypes in colon cancer cells. We successfully constructed SW480 cell lines that stably overexpress ABI1-SiL. We observed that ABI1-SiL overexpression in SW480 cells resulted in enlarged cell size and impaired adhesion and migration, but had no effect on invasion, proliferation, apoptosis, or transcriptional regulation (Figures 3-6). ABI1-SiL overexpression did not alter the mRNA expression levels of ABI1-p65, WAVE2, MMPs, POU, CD44, or KRT20. In combination with its decresion in CRC tissues and cells, these observations suggest that ABI1-SiL could function as an anti-oncogene and that the underlying mechanism needs to be explored.

It is widely accepted that an ABI1-WAVE2 complex is involved in epithelial morphogenesis[31], adhesion, migration, and invasion of cancer cells[13,28,32]. As shown in Figure 1A, the conserved WAVE2-binding and SH3 domains of ABI1-SiL provide the same sites as ABI1-p65 to competitively bind to WAVE2 and/or the proline-rich domain (PRD) of other molecules, including the PRD of ABI1-p65, but the lack of the HHR and the majority of the PxxP- and Pro-rich domain makes it likely to function as a native dominant negative that suppresses the pro-oncogenic functions of ABI1-p65. Bidirectional co-IP experiments confirmed interactions between ABI1-SiL, WAVE2, and ABI1-p65. In control SW480 cells, ABI1-p65 interacts with WAVE2, while in SW480 ABI1-SiL6 cells, both ABI1-p65 and ABI1-SiL are able to bind to WAVE2 (Figure 7C and D). These observations suggested a possible mechanism by which ABI1-SiL competitively binds to WAVE2. Increased ABI-SIL expression could inhibit ABI1-p65-WAVE2 complex formation, resulting in reduced adhesion and migration. Competitive binding of WAVE2 to ABI1 isoforms suggests the possibility of fine

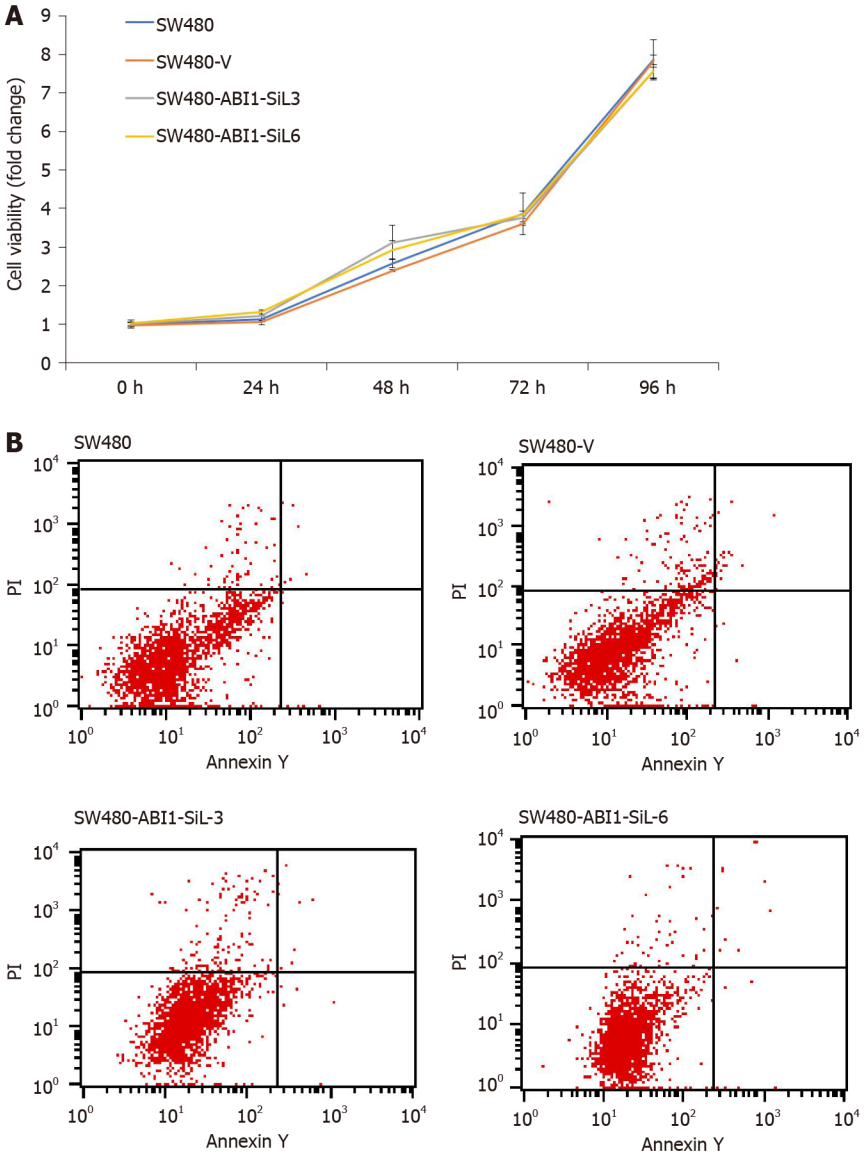

Figure 6 Overexpression of Abelson interactor 1 splice isoform-L does not alter proliferation or death of SW480 cells. Abelson interactor 1 splice isoform-L (ABI1-SiL) overexpression did not impair the proliferation of SW480 cells *in vitro*. Proliferative assay was performed with a Cell Counting Kit-8. A: Cell viability (fold change) is shown in the vertical axis as the mean ± SD of triplicate wells (n = 3). ABI1-SiL overexpression did not induce the apoptosis of SW480 cells *in vitro*; B: Cell apoptosis was assessed by Annexin-V assay. ABI1-SiL: Abelson interactor 1 splice isoform-L.

regulation of WAVE2 complex function in an ABI1 isoform-dependent manner. Interestingly, we also found that ABI1-SiL might interact directly with ABI1-p65, thus indirectly decreasing the formation of the ABI1-p65-WAVE2 complex. These intermolecular interactions were further confirmed by the co-localization of ABI1-SiL-GFP with WAVE2 and ABI1-p65 (Figures 8 and 9). WAVE2, ABI1, and NAP-1 are required for the WAVE regulatory complex (WRC) which activates the Arp2/3 complex to control branched actin polymerization in response to Rac activation[33-35]. As Figure 7E shows, the fact that ABI1-SiL (lacks a HHR domain required for binding to Nap1) does not bind to NAP-1, but ABI1-p65 and phosphorylated ABI1-p72 do in SW480-ABI1-SiL6 cells, suggests that ABI1-SiL overexpression disturbed WRC assembly and further impaired SW480 adhesion and migration. Additionally, all of the above observations were also observed in leukemia K562 and gastric cancer NCI-N87 cells (data not shown).

The present results indicate possible functions of ABI1-SiL in the regulation of SW480 morphogenesis, adhesion, and migration through interactions with WAVE2 and ABI1-p65, respectively. Although the overexpression of ABI1-SiL results in increased cell surface area and a more epithelial-like morphology, we did not find alterations in expression levels of any mRNA involved in differentiation of SW480 cells. Future studies will explore correlations between ABI1 splicing-isoform expression and *KRAS* or *BRAF* mutations or *MSI* in patients with colon cancer.

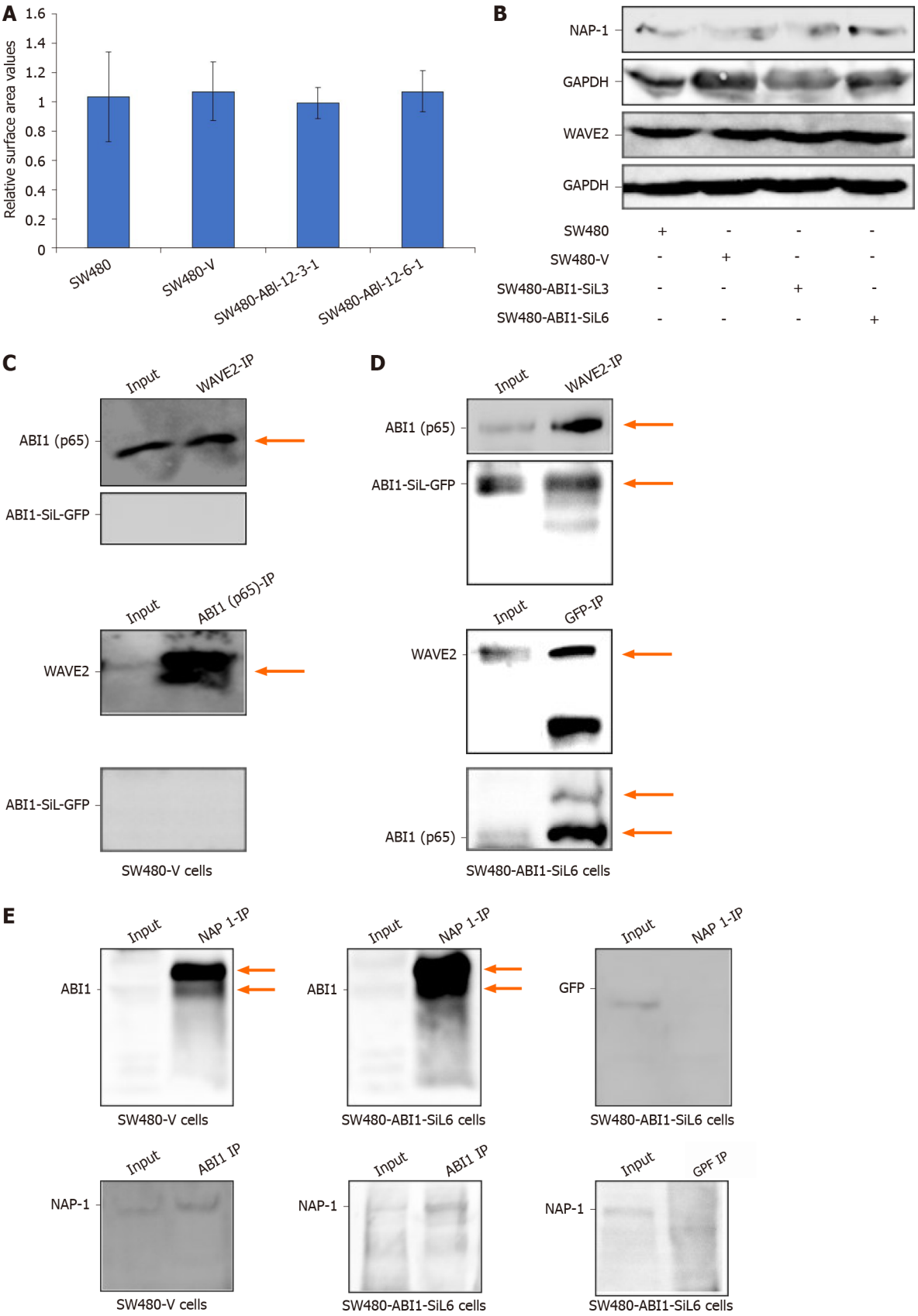

Figure 7 Abelson interactor 1 splice isoform-L interacts with WAVE2, phosphorylated or non-phosphorylated Abelson interactor 1-p65, and NAP-1 in SW480 cells. A and B: Abelson interactor 1 splice isoform-L (ABI1-SiL) overexpression does not change the mRNA (A) or protein (B) expression of WAVE2; C and D: Co-immunoprecipitates (IP) were subjected to Western blot using the indicated antibodies. Bidirectional co-IP and Western blot analysis show that both ABI1-p65 and ABI1-SiL bind to WAVE2 in SW480-V (C) and SW480-ABI1-SiL6 cells (D); E: ABI1-SiL interacts with phosphorylated and non-phosphorylated ABI1-p65 in SW480 cells (arrows). ABI1-SiL does not bind to NAP-1, but ABI1-p65 does. ABI1-SiL: Abelson interactor 1 splice isoform-L; ABI1: Abelson interactor 1; GFP: Green fluorescence protein; GAPDH: Glyceraldehyde-3-phosphate dehydrogenase.

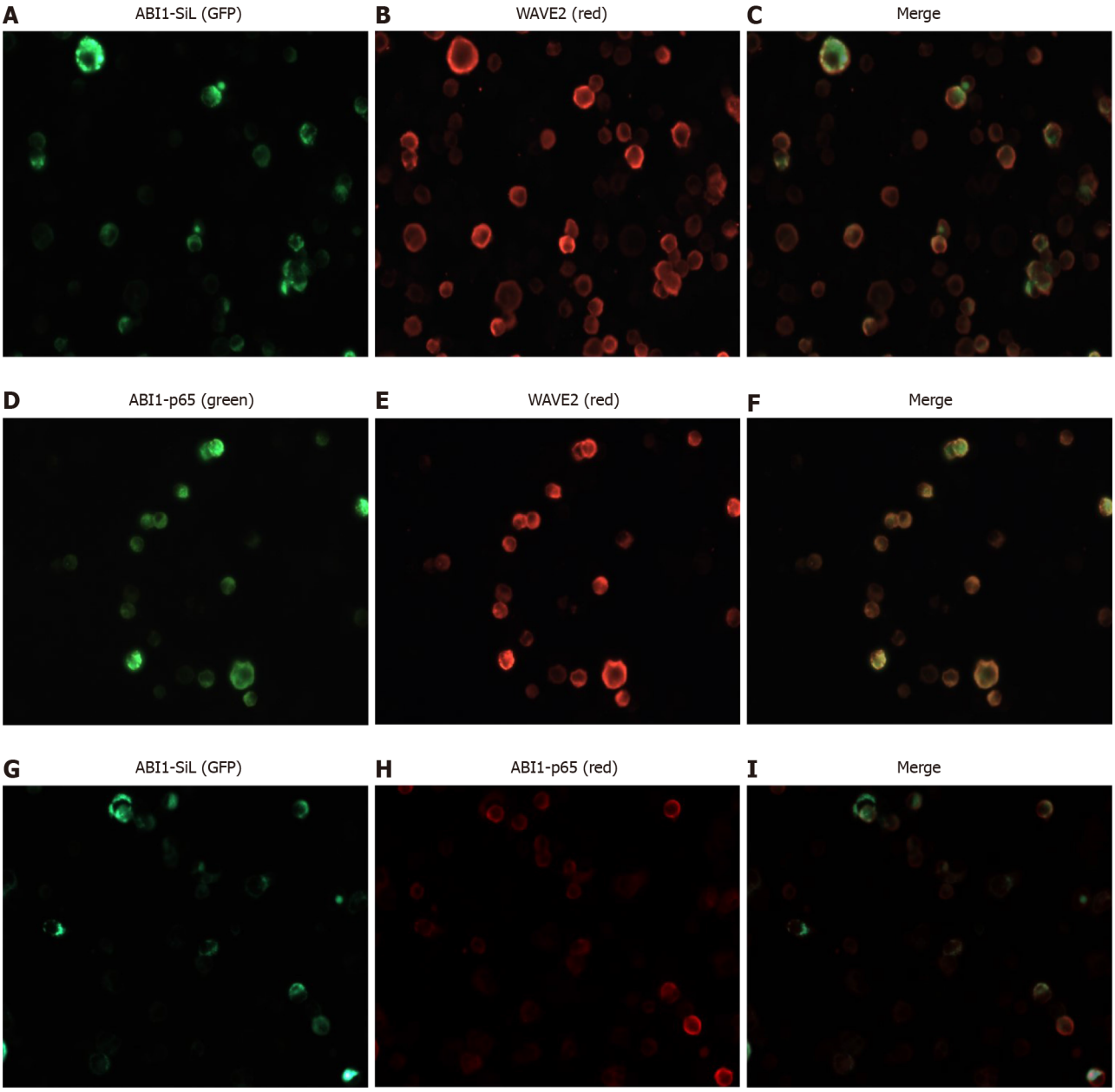

Figure 8 Abelson interactor 1 splice isoform-L co-localizes with WAVE2 and Abelson interactor 1-p65 in 293T cells. A-I: Abelson interactor 1 splice isoform-L-GFP (green fluorescence protein) co-localizes with WAVE2 and ABI1-p65. Samples of 293T cells transiently transfected with Abelson interactor 1 splice isoform-L were probed with WAVE2 (A, B, and C) and Abelson interactor 1-p65 (G, H, and I) antibodies, respectively, while 293T cells were probed for WAVE2 and Abelson interactor 1-p65 (D, E, and F). Magnification × 400. ABI1-SiL: Abelson interactor 1 splice isoform-L; ABI1: Abelson interactor 1; GFP: Green fluorescence protein.

Similarly, relationships and underlying mechanisms will be investigated to connect ABI1-SiL overexpression with mesenchymal-epithelial transition, and determine the roles of other ABI1 isoforms in the cellular and molecular phenotypes underlying colon cancer. Furthermore, ABI1 is present in several intrinsic protein complexes that regulate actin cytoskeletal remodeling, and the existence of several ABI1 isoforms raises the possibility of isoform-specific roles in other ABI1-specific functions[36]. In conclusion, we have shown for the first time herein that ABI1-SiL regulates adhesion and migration in SW480 cells *via* a mechanism involving fine regulation of WAVE2 complex activity, providing a putative biomarker and novel therapeutic target for colon cancer.

In addition, there are still some other limitations in the current study. First, we need more specific and accurate quantitative methods[37,38] to investigate the expression pattern of ABI1-SiL in a large-scale population in the future, and evaluate its potential application value as a clinical molecular diagnostic marker. Second, we need to systematically analyze the exon sequences of all ABI1 transcriptional variants, and use

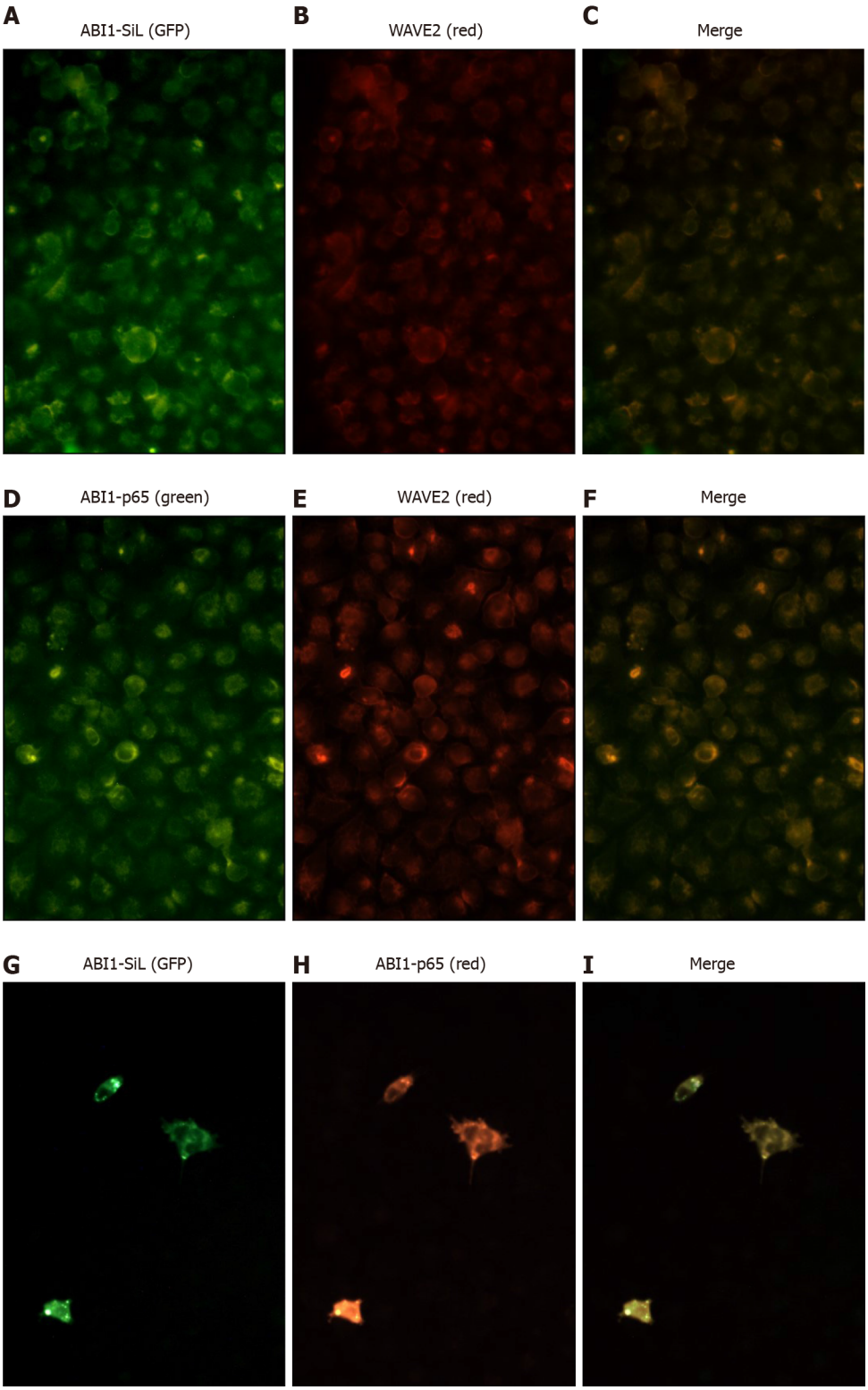

Figure 9 Abelson interactor 1 splice isoform-L co-localizes with WAVE2 and Abelson interactor 1-p65 in SW480-ABI1-SiL6 cells. A-I: Abelson interactor 1 splice isoform-L (ABI1-SiL)-GFP (green fluorescence protein) co-localizes with WAVE2 and ABI1-p65. SW480-ABI1-SiL6 cells were probed with WAVE2 (A, B, and C) and ABI1-p65 (G, H, and I) antibodies, while SW480 cells were similarly probed for WAVE2 and ABI1-p65 (D, E, and F). Magnification × 400. ABI1-SiL: Abelson interactor 1 splice isoform-L; ABI1: Abelson interactor 1; GFP: Green fluorescence protein.

splice switching oligonucleotides[39] and/or gene modification techniques[40] to explore clinical interventions targeting ABI1-SiL. Finally, we also need to rely on animal models to further verify the underlying mechanism of the anti-oncogenic role of ABI1-SiL.

CONCLUSION

These results support a model in which ABI1-SiL plays an anti-oncogenic role by competitively binding to WAVE2 and directly interacting with phosphorylated and non-phosphorylated ABI1-p65, functioning as a dominant-negative form of ABI1-p65.

ARTICLE HIGHLIGHTS

Research background

Abnormally expressed and/or phosphorylated Abelson interactor 1 (ABI1) participates in the metastasis and progression of colorectal carcinoma (CRC), but the roles of ABI1 splice isoforms (ABI1-SIs) are unknown. Exploring the roles and underlying mechanism of ABI1-SIs has important theoretical and practical significance for molecular diagnosis and targeted therapy of CRC.

Research motivation

ABI1-SIs-L (ABI1-SiL) plays an anti-oncogenic role in CRC, and it may be a potential molecular marker and therapeutic target in CRC.

Research objectives

To exploring the roles and underlying mechanism of ABI1-SiL in CRC.

Research methods

We report a set of polymerase chain reaction-based methods that can specifically measure ABI1-SiL mRNA expression and constructed an ABI-SiL overexpressing SW480 cell model. CCK8, transwell, immunoprecipitation, Western blot, and co-localization assays were used to identify the anti-oncogenic role of ABI-SiL and the underlying mechanism in CRC.

Research results

ABI-SiL had a potential anti-tumor effect in CRC. Overexpression of ABI-SiL did not affect the proliferation and invasion of SW480 cells, but can increase the surface area and migration of SW480 cells by competitively binding WAVE2 and ABI1-p65.

Research conclusions

ABI1-SiL plays an antioncogenic role in CRC cells by competitively binding WAVE2 and ABI1-p65.

Research perspectives

Targeting ABI1-SIL expression is a potential treatment for colorectal cancer metastasis.

ACKNOWLEDGEMENTS

We are very grateful to Dr. Dai ZH for his reasonable suggestions and comments on the revision of the manuscript.

REFERENCES

1 **Brenner H**, Kloor M, Pox CP. Colorectal cancer. *Lancet* 2014; **383**: 1490-1502 [PMID: 24225001 DOI: 10.1016/S0140-6736(13)61649-9]

2 **Miura K**, Fujibuchi W, Unno M. Splice isoforms as therapeutic targets for colorectal cancer. *Carcinogenesis* 2012; **33**: 2311-2319 [PMID: 23118106 DOI: 10.1093/carcin/bgs347]

3 **Yi Q**, Tang L. Alternative spliced variants as biomarkers of colorectal cancer. *Curr Drug Metab* 2011; **12**: 966-974 [PMID: 21787266 DOI: 10.2174/138920011798062355]

4 **Yu W**, Sun X, Clough N, Cobos E, Tao Y, Dai Z. Abi1 gene silencing by short hairpin RNA impairs Bcr-Abl-induced cell adhesion and migration *in vitro* and leukemogenesis in vivo. *Carcinogenesis* 2008; **29**: 1717-1724 [PMID: 18453543 DOI: 10.1093/carcin/bgn098]

5 **Maia V**, Ortiz-Rivero S, Sanz M, Gutierrez-Berzal J, Alvarez-Fernández I, Gutierrez-Herrero S, de Pereda JM, Porras A, Guerrero C. C3G forms complexes with Bcr-Abl and p38α MAPK at the focal adhesions in chronic myeloid leukemia cells: implication in the regulation of leukemic cell adhesion.

Cell Commun Signal 2013; **11**: 9 [PMID: 23343344 DOI: 10.1186/1478-811X-11-9]
6 **Taki T**, Shibuya N, Taniwaki M, Hanada R, Morishita K, Bessho F, Yanagisawa M, Hayashi Y. ABI-1, a human homolog to mouse Abl-interactor 1, fuses the MLL gene in acute myeloid leukemia with t(10;11)(p11.2;q23). *Blood* 1998; **92**: 1125-1130 [PMID: 9694699]
7 **Steinestel K**, Brüderlein S, Lennerz JK, Steinestel J, Kraft K, Pröpper C, Meineke V, Möller P. Expression and Y435-phosphorylation of Abelson interactor 1 (Abi1) promotes tumour cell adhesion, extracellular matrix degradation and invasion by colorectal carcinoma cells. *Mol Cancer* 2014; **13**: 145 [PMID: 24913355 DOI: 10.1186/1476-4598-13-145]
8 **Steinestel K**, Brüderlein S, Steinestel J, Märkl B, Schwerer MJ, Arndt A, Kraft K, Pröpper C, Möller P. Expression of Abelson interactor 1 (Abi1) correlates with inflammation, KRAS mutation and adenomatous change during colonic carcinogenesis. *PLoS One* 2012; **7**: e40671 [PMID: 22808230 DOI: 10.1371/journal.pone.0040671]
9 **Wang C**, Tran-Thanh D, Moreno JC, Cawthorn TR, Jacks LM, Wang DY, McCready DR, Done SJ. Expression of Abl interactor 1 and its prognostic significance in breast cancer: a tissue-array-based investigation. *Breast Cancer Res Treat* 2011; **129**: 373-386 [PMID: 21046228 DOI: 10.1007/s10549-010-1241-0]
10 **Sun X**, Li C, Zhuang C, Gilmore WC, Cobos E, Tao Y, Dai Z. Abl interactor 1 regulates Src-Id1-matrix metalloproteinase 9 axis and is required for invadopodia formation, extracellular matrix degradation and tumor growth of human breast cancer cells. *Carcinogenesis* 2009; **30**: 2109-2116 [PMID: 19843640 DOI: 10.1093/carcin/bgp251]
11 **Chen H**, Wu X, Pan ZK, Huang S. Integrity of SOS1/EPS8/ABI1 tri-complex determines ovarian cancer metastasis. *Cancer Res* 2010; **70**: 9979-9990 [PMID: 21118970 DOI: 10.1158/0008-5472.CAN-10-2394]
12 **Hu J**, Mukhopadhyay A, Craig AW. Transducer of Cdc42-dependent actin assembly promotes epidermal growth factor-induced cell motility and invasiveness. *J Biol Chem* 2011; **286**: 2261-2272 [PMID: 21062739 DOI: 10.1074/jbc.M110.157974]
13 **Li Y**, Clough N, Sun X, Yu W, Abbott BL, Hogan CJ, Dai Z. Bcr-Abl induces abnormal cytoskeleton remodeling, beta1 integrin clustering and increased cell adhesion to fibronectin through the Abl interactor 1 pathway. *J Cell Sci* 2007; **120**: 1436-1446 [PMID: 17389688 DOI: 10.1242/jcs.03430]
14 **Leng Y**, Zhang J, Badour K, Arpaia E, Freeman S, Cheung P, Siu M, Siminovitch K. Abelson-interactor-1 promotes WAVE2 membrane translocation and Abelson-mediated tyrosine phosphorylation required for WAVE2 activation. *Proc Natl Acad Sci USA* 2005; **102**: 1098-1103 [PMID: 15657136 DOI: 10.1073/pnas.0409120102]
15 **Watahiki A**, Waki K, Hayatsu N, Shiraki T, Kondo S, Nakamura M, Sasaki D, Arakawa T, Kawai J, Harbers M, Hayashizaki Y, Carninci P. Libraries enriched for alternatively spliced exons reveal splicing patterns in melanocytes and melanomas. *Nat Methods* 2004; **1**: 233-239 [PMID: 15782199 DOI: 10.1038/nmeth719]
16 **Li K**, Li M, Liu Y, Ma S, Yu W. [The relationship between ABI1 upregulation and the clinicopathologic features and prognosis of colon adenocarcinoma]. *Zhonghua Putong Waike Zazhi* 2015; **30**: 643-646
17 **Pan Q**, Shai O, Lee LJ, Frey BJ, Blencowe BJ. Deep surveying of alternative splicing complexity in the human transcriptome by high-throughput sequencing. *Nat Genet* 2008; **40**: 1413-1415 [PMID: 18978789 DOI: 10.1038/ng.259]
18 **Wang ET**, Sandberg R, Luo S, Khrebtukova I, Zhang L, Mayr C, Kingsmore SF, Schroth GP, Burge CB. Alternative isoform regulation in human tissue transcriptomes. *Nature* 2008; **456**: 470-476 [PMID: 18978772 DOI: 10.1038/nature07509]
19 **Lapuk AV**, Volik SV, Wang Y, Collins CC. The role of mRNA splicing in prostate cancer. *Asian J Androl* 2014; **16**: 515-521 [PMID: 24830689 DOI: 10.4103/1008-682X.127825]
20 **Oltean S**, Bates DO. Hallmarks of alternative splicing in cancer. *Oncogene* 2014; **33**: 5311-5318 [PMID: 24336324 DOI: 10.1038/onc.2013.533]
21 **National Center for Biotechnology Information**. ABI1: abl interactor 1 [Homo sapiens (human)]. [cited Jan 15, 2021]. Database: NCBI Gene [Internet]. Available from: http://www.ncbi.nlm.nih.gov/gene/10006
22 **Yu W**, Ma S, Wang L, Zuo B, Li M, Qiao Z, Pan X, Liu Y, Wang J. Upregulation of GPR34 expression affects the progression and prognosis of human gastric adenocarcinoma by PI3K/PDK1/AKT pathway. *Histol Histopathol* 2013; **28**: 1629-1638 [PMID: 23836308 DOI: 10.14670/HH-28.1629]
23 **Ikeguchi A**, Yang HY, Gao G, Goff SP. Inhibition of v-Abl transformation in 3T3 cells overexpressing different forms of the Abelson interactor protein Abi-1. *Oncogene* 2001; **20**: 4926-4934 [PMID: 11526477 DOI: 10.1038/sj.onc.1204502]
24 **Wang C**, Navab R, Iakovlev V, Leng Y, Zhang J, Tsao MS, Siminovitch K, McCready DR, Done SJ. Abelson interactor protein-1 positively regulates breast cancer cell proliferation, migration, and invasion. *Mol Cancer Res* 2007; **5**: 1031-1039 [PMID: 17951403 DOI: 10.1158/1541-7786.MCR-06-0391]
25 **Cui MH**, Yu WD, Dong JQ, Liu YL. [Effect of Abl-interacting protein 1 overexpression upon human gastric cancer cell proliferation in vitro]. *Zhonghua Yixue Zazhi* 2009; **89**: 3111-3115 [PMID: 20193272]
26 **Kotula L**. Abi1, a critical molecule coordinating actin cytoskeleton reorganization with PI-3 kinase and growth signaling. *FEBS Lett* 2012; **586**: 2790-2794 [PMID: 22617151 DOI:

10.1016/j.febslet.2012.05.015]

27 **Dubielecka PM**, Ladwein KI, Xiong X, Migeotte I, Chorzalska A, Anderson KV, Sawicki JA, Rottner K, Stradal TE, Kotula L. Essential role for Abi1 in embryonic survival and WAVE2 complex integrity. *Proc Natl Acad Sci USA* 2011; **108**: 7022-7027 [PMID: 21482783 DOI: 10.1073/pnas.1016811108]

28 **Mendoza MC**, Er EE, Zhang W, Ballif BA, Elliott HL, Danuser G, Blenis J. ERK-MAPK drives lamellipodia protrusion by activating the WAVE2 regulatory complex. *Mol Cell* 2011; **41**: 661-671 [PMID: 21419341 DOI: 10.1016/j.molcel.2011.02.031]

29 **Kheir WA**, Gevrey JC, Yamaguchi H, Isaac B, Cox D. A WAVE2-Abi1 complex mediates CSF-1-induced F-actin-rich membrane protrusions and migration in macrophages. *J Cell Sci* 2005; **118**: 5369-5379 [PMID: 16280551 DOI: 10.1242/jcs.02638]

30 **Sebestyén E**, Zawisza M, Eyras E. Detection of recurrent alternative splicing switches in tumor samples reveals novel signatures of cancer. *Nucleic Acids Res* 2015; **43**: 1345-1356 [PMID: 25578962 DOI: 10.1093/nar/gku1392]

31 **Bryce NS**, Reynolds AB, Koleske AJ, Weaver AM. WAVE2 regulates epithelial morphology and cadherin isoform switching through regulation of Twist and Abl. *PLoS One* 2013; **8**: e64533 [PMID: 23691243 DOI: 10.1371/journal.pone.0064533]

32 **Takahashi K**. WAVE2 Protein Complex Coupled to Membrane and Microtubules. *J Oncol* 2012; **2012**: 590531 [PMID: 22315597 DOI: 10.1155/2012/590531]

33 **Wu S**, Ma L, Wu Y, Zeng R, Zhu X. Nudel is crucial for the WAVE complex assembly *in vivo* by selectively promoting subcomplex stability and formation through direct interactions. *Cell Res* 2012; **22**: 1270-1284 [PMID: 22453242 DOI: 10.1038/cr.2012.47]

34 **Burianek LE**, Soderling SH. Under lock and key: spatiotemporal regulation of WASP family proteins coordinates separate dynamic cellular processes. *Semin Cell Dev Biol* 2013; **24**: 258-266 [PMID: 23291261 DOI: 10.1016/j.semcdb.2012.12.005]

35 **Ryu JR**, Echarri A, Li R, Pendergast AM. Regulation of cell-cell adhesion by Abi/Diaphanous complexes. *Mol Cell Biol* 2009; **29**: 1735-1748 [PMID: 19158278 DOI: 10.1128/MCB.01483-08]

36 **Dubielecka PM**, Cui P, Xiong X, Hossain S, Heck S, Angelov L, Kotula L. Differential regulation of macropinocytosis by Abi1/Hssh3bp1 isoforms. *PLoS One* 2010; **5**: e10430 [PMID: 20479892 DOI: 10.1371/journal.pone.0010430]

37 **Sun B**, Zheng YL. Simultaneous Quantification of Multiple Alternatively Spliced mRNA Transcripts Using Droplet Digital PCR. *Methods Mol Biol* 2018; **1768**: 387-400 [PMID: 29717455 DOI: 10.1007/978-1-4939-7778-9_22]

38 **Wang H**, Wang H, Duan X, Sun Y, Wang X, Li Z. Highly sensitive and multiplexed quantification of mRNA splice variants by the direct ligation of DNA probes at the exon junction and universal PCR amplification. *Chem Sci* 2017; **8**: 3635-3640 [PMID: 28580102 DOI: 10.1039/c7sc00094d]

39 **Wan J**. Antisense-mediated exon skipping to shift alternative splicing to treat cancer. *Methods Mol Biol* 2012; **867**: 201-208 [PMID: 22454063 DOI: 10.1007/978-1-61779-767-5_13]

40 **Maruyama R**, Yokota T. Creation of DMD Muscle Cell Model Using CRISPR-Cas9 Genome Editing to Test the Efficacy of Antisense-Mediated Exon Skipping. *Methods Mol Biol* 2018; **1828**: 165-171 [PMID: 30171541 DOI: 10.1007/978-1-4939-8651-4_10]

World Journal of Gastroenterology

Submit a Manuscript: https://www.f6publishing.com

World J Gastroenterol 2021 April 21; 27(15): 1616-1629

DOI: 10.3748/wjg.v27.i15.1616

ISSN 1007-9327 (print) ISSN 2219-2840 (online)

ORIGINAL ARTICLE

Basic Study

Effects of CXCL12 isoforms in a pancreatic pre-tumour cellular model: Microarray analysis

Monia Cecati, Matteo Giulietti, Alessandra Righetti, Berina Sabanovic, Francesco Piva

ORCID number: Monia Cecati 0000-0003-4947-5157; Matteo Giulietti 0000-0002-9871-265X; Alessandra Righetti 0000-0003-2043-0406; Berina Sabanovic 0000-0002-0883-3248; Francesco Piva 0000-0003-1850-2482.

Author contributions: Piva F designed and coordinated the study; Cecati M and Righetti A performed the experiments, acquired and analyzed data; Giulietti M and Sabanovic B analyzed and interpreted the data; Giulietti M, Sabanovic B and Cecati M wrote the manuscript; all authors approved the final version of the article.

Supported by Fondazione Cariverona, No. 2017.0570 (to Piva F).

Institutional review board statement: The authors declare that the requirement of the Institutional Review Board Approval Form or Document is not applicable, since the experiments did not involve humans.

Conflict-of-interest statement: The authors have no conflicts of interest to disclose.

Data sharing statement: Datasets available from the corresponding author at m.giulietti@univpm.it.

Monia Cecati, Matteo Giulietti, Alessandra Righetti, Berina Sabanovic, Francesco Piva, Department of Specialistic Clinical and Odontostomatological Sciences, Polytechnic University of Marche, Ancona 60126, Italy

Corresponding author: Matteo Giulietti, PhD, Academic Research, Department of Specialistic Clinical and Odontostomatological Sciences, Polytechnic University of Marche, Via Brecce Bianche, Ancona 60126, Italy. m.giulietti@univpm.it

Abstract

BACKGROUND

Pancreatic ductal adenocarcinoma (PDAC) is the fourth leading cause of death among cancers, it is characterized by poor prognosis and strong chemoresistance. In the PDAC microenvironment, stromal cells release different extracellular components, including CXCL12. The CXCL12 is a chemokine promoting the communication between tumour and stromal cells. Six different splicing isoforms of CXCL12 are known (α, β, γ, δ, ε, θ) but their role in PDAC has not yet been characterized.

AIM

To investigate the specific role of α, β, and γ CXCL12 isoforms in PDAC onset.

METHODS

We used hTERT-HPNE E6/E7/KRasG12D (Human Pancreatic Nestin-Expressing) cell line as a pancreatic pre-tumour model and exposed it to the α, β, and γ CXCL12 isoforms. The altered expression profiles were assessed by microarray analyses and confirmed by Real-Time polymerase chain reaction. The functional enrichment analyses have been performed by Enrichr tool to highlight Gene Ontology enriched terms. In addition, wound healing assays have been carried out to assess the phenotypic changes, in terms of migration ability, induced by the α, β, and γ CXCL12 isoforms.

RESULTS

Microarray analysis of hTERT-HPNE cells treated with the three different CXCL12 isoforms highlighted that the expression of only a few genes was altered. Moreover, the α and β isoforms showed an alteration in expression of different genes, whereas γ isoform affected the expression of genes also common with α and β isoforms. The β isoform altered the expression of genes mainly involved in cell cycle regulation. In addition, all isoforms affected the expression of genes

Manuscript source: Invited manuscript

Specialty type: Gastroenterology and hepatology

Country/Territory of origin: Italy

Peer-review report's scientific quality classification
Grade A (Excellent): A
Grade B (Very good): B
Grade C (Good): 0
Grade D (Fair): 0
Grade E (Poor): 0

Received: January 28, 2021
Peer-review started: January 28, 2021
First decision: February 24, 2021
Revised: March 5, 2021
Accepted: March 29, 2021
Article in press: March 29, 2021
Published online: April 21, 2021

P-Reviewer: Reshkin SJ
S-Editor: Gao CC
L-Editor: A
P-Editor: Liu JH

associated to cell migration, adhesion and cytoskeleton. In vitro cell migration assay confirmed that CXCL12 enhanced the migration ability of hTERT-HPNE cells. Among the CXCL12 splicing isoforms, the γ isoform showed higher induction of migration than α and β isoforms.

CONCLUSION
Our data suggests an involvement and different roles of CXCL12 isoforms in PDAC onset. However, more investigations are needed to confirm these preliminary observations.

Key Words: CXCL12; Splicing isoforms; Pancreatic cancer; Microarray; Migration; Wound healing assay

Core Tip: In the microenvironment of pancreatic ductal adenocarcinoma (PDAC), stromal cells release different extracellular components, including CXCL12, in order to communicate with cancer cells. Here, we investigated the specific role of α, β, and γ CXCL12 splicing isoforms in PDAC onset, by using a pre-tumour model. Microarray analysis suggested a role of CXCL12 in cell migration, and wound healing assays confirmed this hypothesis. In particular, γ isoform showed the highest promotion of migration. Our results shed light on the molecular basis of PDAC onset and progression.

Citation: Cecati M, Giulietti M, Righetti A, Sabanovic B, Piva F. Effects of CXCL12 isoforms in a pancreatic pre-tumour cellular model: Microarray analysis. *World J Gastroenterol* 2021; 27(15): 1616-1629
URL: https://www.wjgnet.com/1007-9327/full/v27/i15/1616.htm
DOI: https://dx.doi.org/10.3748/wjg.v27.i15.1616

INTRODUCTION

Pancreatic ductal adenocarcinoma (PDAC) is one of the most aggressive gastrointestinal tumours with a 5-year survival rate of 7%[1]. Due to the lack of early symptoms and specific diagnostic markers of early-stage disease, PDAC is often diagnosed at an advanced stage. At the time of diagnosis, the 90% of patients already presents advanced tumour progression and distant metastasis, therefore the surgical treatment is no longer applicable. This tumour also shows a high resistance rate to anti-tumour drugs, so chemio- and radio-therapy are not effective[2,3]. Progressive accumulation of genetic mutations, causing activation of different signalling pathways, drives tumour growth and development[4]. The earliest genetic event in the progression of the normal ductal epithelial cells to premalignant pancreatic intraepithelial neoplasia (PanIN) is the mutation of the K-Ras oncogene[5]. The activation of K-Ras protein triggers various downstream effector proteins which promote proliferation, metabolic reprogramming, anti-apoptosis, evasion of the immune response and remodelling of the microenvironment[6]. Recently, increasing interest has been focused on the PDAC microenvironment. The PDAC microenvironment is composed of a large portion of stroma surrounding cancer cells and contains cells such as cancer-associated fibroblasts (CAFs), T cells, stellate cells, macrophages, regulatory T cells, endothelial cells and others[7-9]. To maintain a favourable microenvironment for cancer cell survival, stromal cells secrete extracellular components, such as extracellular matrix (ECM), matrix metallo-proteinases, growth factors, transformation growth factor-β and cytokines.

One of the above-mentioned molecules is the chemokine CXCL12 (C-X-C motif chemokine ligand 12), a low molecular weight protein (about 12 kDa), belonging to the CXC chemokine family. In PDAC, CXCL12 is a key messenger in the intercellular communication between tumour and stromal cells[10]. In fact, CXCL12 promotes tumour proliferation, epithelial to mesenchymal transition, metastases, angiogenesis and immunosurveillance[10,11]. In PDAC setting, it acts through highly expressed

receptors namely CXCR4 and CXCR7[11]. Although six different CXCL12 splicing variants have been described (α, β, γ, δ, ε, θ), only some properties of α, β and γ isoforms are known[12]. The sequence of the isoforms differ significantly one from another, thus also the function of the isoforms which are not yet characterized could be different or even contrary[12,13]. In breast cancer the role of the isoforms α, β, γ, and to a lesser extent δ, was studied[14,15], whereas in PDAC no information is available about the specific role played by each isoform of CXCL12. Moreover, often the papers focusing on CXCL12 role in PDAC actually report the results without stating which isoform in particular is under investigation[12].

The hTERT-HPNE E6/E7/KRasG12D (Human Pancreatic Nestin-Expressing) is a pancreatic pre-tumour cell line. These cells derive from normal pancreas duct epithelial cells and harbour the classical KRas (G12D) mutation, furthermore it bears inactivated p53 and Rb tumour suppressor genes. This status mimics the cells that have acquired the cancer predisposing mutations, but are not yet fully transformed. The phenotype of this cell line is similar to the third phase of the premalignant lesions, called PanIN-3[5,6,16].

Here, we investigated the transcriptomic alterations induced by treatments with the α, β and γ CXCL12 isoforms (the only ones commercially available) in a pancreatic pre-cancerous model in order to study PDAC onset. To this aim, we treated hTERT-HPNE cells with different CXCL12 isoforms, and assessed the gene expression profiles of these cells by microarray analyses. Since microarray analyses indicated several deregulated genes involved in cell migration, we also performed wound healing assays.

MATERIALS AND METHODS

Cell culture

The human pancreatic pre-tumour cell line hTERT-HPNE E6/E7/K-RasG12D (ATCC® CRL-4038™) was purchased from American Type Culture Collection. These cells are adherent and have an epithelial-like morphology. Furthermore, they lack fundamental features of malignant pancreatic cancer cells, such as the anchorage independent growth in soft agar and the ability to engraft as tumours in athymic mice. This cell line was developed from human pancreatic duct cells by transduction of human telomerase gene (*hTERT*) in order to escape from cellular senescence. Further immortalization steps included the introduction of the human papillomavirus 16 E6 and E7 proteins, which are able to impair the function of key tumour suppressors p53 and Rb. In these cells, the KRAS *G12D* mutation is sufficient to induce formation of PanIN lesions, without inducing a fully malignant phenotype. Cells were maintained in high glucose Dulbecco's Modified Eagle's Medium (Lonza, Milan, Italy) supplemented with 10% fetal bovine serum, 1% L-Glutamine and 1% Penicillin/Streptomycin (EuroClone, Milan, Italy). Cells were maintained at 37 °C in a humidified atmosphere of 5% CO_2 in air.

Cell treatments

A total of 2 × 10^6 hTERT-HPNE cells were seeded in p100 dishes for cell treatments. Once cells reached the right confluence, they were treated for 24 h with 100 ng/mL of each of the following isoforms: Human recombinant CXCL12-α (PHC1346, Thermo Fisher Scientific, Milan, Italy), human recombinant CXCL12-β (2716-SD, R&D Systems) and human recombinant CXCL12-γ (6448-SD-025, R&D Systems, Minneapolis, MN, United States). Cells cultured similarly for 24 h have been used as control. All experiments were carried out in biological triplicates.

RNA isolation and cDNA synthesis

Total RNA was isolated from harvested cells (12 samples in total) using the RNeasy Protect Cell Mini Kit (Qiagen, Milan, Italy) according to the manufacturer's instructions. The RNA concentration in isolated samples was determined by ultraviolet absorption at 260 nm. The quality of total RNA was first assessed using an Agilent Bioanalyzer 2100 (Agilent Technologies, Palo Alto, CA, United States). Biotin-labelled cDNA targets were synthesized starting from 150 ng of total RNA. Double stranded cDNA synthesis and related cRNA was performed with GeneChip® WT Plus Kit (Affymetrix, Thermo Fisher Scientific, Milan, Italy). Same kit was used to synthesize the sense strand cDNA before fragmenting and labelling. All steps of the labelling protocol were performed as suggested by Affymetrix, starting from 5.5 μg of ssDNA.

DNA microarray hybridization and image acquisition

Hybridization was performed using the GeneChip® Hybridization, Wash and Stain Kit (Affymetrix, Thermo Fisher Scientific, Milan, Italy). In particular, fragmented and labelled sscDNA were diluted in hybridization buffer at a concentration of 23 ng/μL for a 2.3 μg total and denatured at 99 °C for 5 min, incubated at 45 °C for 5 min and centrifuged at maximum speed for 1 min prior to introduction into the GeneChip® cartridge. A single GeneChip® Human Clariom S was then hybridized with each biotin-labelled sense target (12 samples in total). Hybridizations were performed for 16 h at 45 °C in a rotisserie oven (60 rpm). GeneChip® cartridges were washed and stained with GeneChip® Hybridization, Wash and Stain Kit in the Affymetrix Fluidics Station. GeneChip arrays were scanned using an Affymetrix GeneChip® Scanner 3000 7G using default parameters. Affymetrix GeneChip® Command Console software was used to acquire GeneChip® images and generate .DAT and .CEL files, which were used for subsequent analysis.

Bioinformatics analysis of microarray data

Analyses of the raw expression data (probe-level .CEL files) were carried out within R/Bioconductor environment (version 3.6 and 3.9, respectively). In particular, we applied the background correction and quantile normalization by employing the Robust Multi-array Average method available in the *oligo* R package[17]. Then, ComBat function from *sva* R package[18] was used to remove potential batch effects. Principal component analysis was used for the data quality control, before and after batch effect correction. For differential expression analysis, *genefilter* and *limma* R packages have been used[19]. In particular, for the identification of differentially expressed genes (DEGs), we considered the Benjamini-Hochberg corrected *P* value cut-off (FDR), set at 0.05, and a $\log_2$ Fold Change $|\log_2 FC| > 0.7$.

Functional and pathway enrichment analyses

Enrichr tool (http://amp.pharm.mssm.edu/Enrichr/)[20] was used to perform functional enrichment analysis of the DEGs, *i.e.*, the identification of the most over-represented (enriched) Gene Ontology (GO) terms. In this tool, we selected the panels GO Biological Process, GO Molecular Function and GO Cellular Component. Only statistically significant results are reported ($P < 0.05$).

Real-Time polymerase chain reaction

To confirm the microarray results, we assessed the expression of some DEGs by Real-Time polymerase chain reaction (PCR). We selected six genes (CXCL8, RRP12, ADH1B, UBA7, FEM1C, and CASP1) based on the commonly used criteria, that is their fold-changes in relative expression and *P* values[21]. For this purpose, we isolated RNA from hTERT-HPNE cells as described previously for microarray analysis. Then, RNA was reverse transcribed with HyperScript First Strand Synthesis Kit (GeneAll Biotechnology, Korea) using random primers to obtain complementary DNA (cDNA). The selected genes were run in duplicate by Real-Time PCR, using SYBR Green chemistry. The primer sequences are reported in Supplementary Table 1. All samples were tested in triplicate using GAPDH (glyceraldehyde-3-phosphate dehydrogenase) as the reference gene for data normalization to correct for variations in RNA quality and quantity. Threshold cycle (C_T) values of genes of interest were normalized against C_T values of GAPDH, and a relative fold change in expression with respect to a reference sample was calculated by the $2^{-\Delta\Delta Ct}$ method.

Monolayer wound healing assay

To evaluate the cell migration capacity, hTERT-HPNE cells were seeded into a 24-well plate (2×10^4 cells/well) and allowed to attach and grow until reaching the 90%-100% confluence. Cell monolayers were scratched with a sterile 1000 μL pipette tip to make a wound. Then, wounded cell monolayers were washed with phosphate-buffered saline 1× to remove cell debris, and incubated for 24 h in DMEM with 100 ng/mL of each CXCL12 isoform. Cells were monitored under the Eclipse Ti2E microscope (Nikon, Tokyo, Japan) equipped with a camera (Hamamatsu Photonics, Japan) and photographed at 0 h, 12 h and 24 h. Each experiment was performed in triplicate and the data were presented as mean ± SD.

Statistical analysis

For Real-Time PCR and migration assays, differences in gene expression levels between the treated and untreated cells or difference in cell migration ability were determined using the *t*-test. *P* values less than 0.05 were considered statistically

significant. All statistical analyses were performed by using the Stat6 Software for Windows (Stat6 Software, San Diego, CA, United States).

RESULTS

Identification of DEGs

Gene expression alterations in pancreatic hTERT-HPNE cells treated with α, β or γ CXCL12 isoforms, compared to the untreated cells, have been assessed by microarray analyses on Affymetrix Human Clariom S Array. After data processing (*i.e.*, quality control, normalization, batch effect removal), only a few genes resulted to be differentially expressed between treated and untreated cells. Indeed, pairwise comparisons between each treatment and the controls highlighted 17, 24 and 16 DEGs for α, β and γ isoforms, respectively (Table 1). This observation suggests that treatments with CXCL12 did not dramatically alter the gene expression of hTERT-HPNE cells and that, among tested isoforms, the β isoform may induce the highest effect on the transcriptome. Among DEGs regulated by α isoform, 7 were overexpressed and 10 were underexpressed; regarding β isoform, 12 genes were upregulated and 12 were downregulated; finally, for γ isoform, 2 genes were overexpressed and 14 were underexpressed. By hierarchical clustering, the expression levels of these DEGs allow to easily highlight control samples, but homogeneous clusters of samples treated with each CXCL12 isoform are not so clearly distinguishable (Figure 1). This result suggests that, although CXCL12 treatments alter gene expression in hTERT-HPNE cells, the specific effect of each isoform is quite difficult to identify. Therefore, we compared DEGs among different treatments, revealing common and exclusive genes (Figure 2). In particular, 10, 11 and 1 (*i.e.*, LGR5) DEGs were exclusive for α, β and γ isoforms, respectively, suggesting that the effects on the transcriptome of γ isoform is intermediate between those induced by α and β isoforms. Indeed, α and β isoforms induced expression alteration in many different genes, whereas γ isoform affected the expression of genes also common with α and β isoforms (Figure 2).

Quantitative PCR validation

Real-Time PCR analysis was carried out on treated and control samples in order to validate microarray data. Among significant DEGs identified by microarray analysis, we chose 3 up-regulated (UBA7, FEM1C, CASP1) and 3 down-regulated (CXCL8, RRP12 and ADH1B) genes for Real-Time PCR validation. As reported in the Figure 3, the selected genes showed no discrepancies in their expression profiles, for each CXCL12 isoform, between microarray and Real-Time PCR. Indeed, for all isoforms, CXCL8, RRP12 and ADH1B genes resulted to be downregulated also in Real-Time PCR results. In particular, CXCL8, RRP12 and ADH1B genes showed an average fold change reduction of 2.01, 1.78 and 1.72, respectively. Regarding UBA7, FEM1C and CASP1 genes, Real-Time PCR confirmed that they were upregulated, on average, of 1.74, 1.55 and 1.60 times, respectively, after all CXCL12 isoform treatments.

Functional and pathway enrichment analyses

The three lists of DEGs (*i.e.*, for each CXCL12 isoform) have been submitted to Enrichr tool in order to provide an interpretation of the biological processes associated with these genes. This gene enrichment analysis has been performed considering GO terms, regarding GO Biological Process, GO Molecular Function and GO Cellular Component (Supplementary Table 2-4). Our analyses showed that β isoform seems to alter, more than α and γ isoforms the expression of genes involved in cell cycle regulation, DNA replication, G2/M checkpoints, p53 signalling pathway, regulation of apoptosis and senescence. In addition, enrichment analyses highlighted that, for all CXCL12 isoforms, most enriched GO terms involved cell migration and adhesion. Indeed, we often found terms such as "intermediate filament", "cytoskeleton", "microtubule", "kinesin complex", "motor activity", "tubulin binding", " positive chemotaxis", "hemidesmosome assembly", "cell-substrate junction assembly", "microtubule polymerization or depolymerisation", "regulation of cell motility", "regulation of actin filament depolymerisation" (Supplementary Tables 2-4). Since these terms seem to be uniformly distributed among the three CXCL12 isoforms, we decided to carry out *in vitro* assays to evaluate better the specific effect of each CXCL12 isoform on cell migration.

Table 1 List of differentially expressed genes upon treatment of pancreatic hTERT-HPNE cells with 3 different isoforms of CXCL12

Probe name	Log_2FC	*P* value	Adjusted *P* value	Gene name
CXCL12 α isoform *vs* control				
TC1100012755.hg.1	-1.203589	3.12×10^{-8}	0.000052	KIRREL3
TC1700010680.hg.1	-1.036293	1.56×10^{-6}	0.001479	KRT14
TC0200015894.hg.1	-1.009543	1.37×10^{-6}	0.001358	DOCK10
TC1700007330.hg.1	-0.937268	9.64×10^{-6}	0.007801	KSR1
TC0200007399.hg.1	-0.920275	1.26×10^{-5}	0.009220	PLEKHH2
TC1000011549.hg.1	-0.908378	2.40×10^{-5}	0.016397	RRP12
TC1100009990.hg.1	-0.841133	5.45×10^{-5}	0.032188	OR6A2
TC1000011923.hg.1	-0.827117	7.17×10^{-5}	0.038532	GFRA1
TC0300013528.hg.1	-0.824444	7.59×10^{-5}	0.038532	GMNC
TC1800009242.hg.1	-0.818366	1.03×10^{-4}	0.049741	SERPINB2
TC0300007393.hg.1	0.807450	1.12×10^{-4}	0.049980	UBA7
TSUnmapped00000150.hg.1	0.812168	1.05×10^{-4}	0.049741	OBP2B
TC0400008134.hg.1	0.841986	5.91×10^{-5}	0.033939	MMRN1
TC1300010008.hg.1	0.854761	4.73×10^{-5}	0.028684	GAS6-AS1
TC0100008815.hg.1	0.864724	1.12×10^{-4}	0.049980	IFI44L
TC1600010467.hg.1	0.873123	2.89×10^{-5}	0.019144	CNGB1
TC0400011618.hg.1	0.958292	5.08×10^{-6}	0.004269	NEUROG2
CXCL12 β isoform *vs* control				
TC0400007836.hg.1	-1.317647	3.40×10^{-9}	0.000008	CXCL8
TC0400011408.hg.1	-1.007967	2.72×10^{-6}	0.002057	ADH1B
TC2100006784.hg.1	-1.000559	9.12×10^{-7}	0.000839	JAM2
TSUnmapped00000478.hg.1	-0.944922	2.60×10^{-6}	0.002052	ZNF502
TC0400006661.hg.1	-0.799480	1.01×10^{-4}	0.033702	STK32B
TC0200014802.hg.1	-0.797931	7.39×10^{-5}	0.028291	SCN3A
TC1000011549.hg.1	-0.796631	8.77×10^{-5}	0.030275	RRP12
TC0200015894.hg.1	-0.792474	9.80×10^{-5}	0.033299	DOCK10
TC0X00010399.hg.1	-0.779084	1.41×10^{-4}	0.042386	BEX1
TC0600014250.hg.1	-0.776865	1.08×10^{-4}	0.034696	ZBED9
TC0300007220.hg.1	-0.767719	1.30×10^{-4}	0.040552	ZNF502
TC0400009879.hg.1	-0.764228	1.70×10^{-4}	0.049472	CYTL1
TC0600013231.hg.1	0.768484	1.61×10^{-4}	0.047319	SGK1
TC1300007248.hg.1	0.803510	8.35×10^{-5}	0.029556	CKAP2
TC1100013221.hg.1	0.818187	4.63×10^{-5}	0.019311	CASP1
TC0500012030.hg.1	0.819484	4.61×10^{-5}	0.019311	GDF9
TC0300007393.hg.1	0.838000	3.14×10^{-5}	0.014151	UBA7
TC0300012670.hg.1	0.853540	2.67×10^{-5}	0.012705	ATR
TC0100013700.hg.1	0.868308	2.28×10^{-5}	0.011426	CLSPN
TC0600007138.hg.1	0.884415	1.49×10^{-5}	0.008040	E2F3
TC0600010241.hg.1	0.895254	9.02×10^{-6}	0.005389	KIF25
TC0100008101.hg.1	0.951395	3.50×10^{-6}	0.002479	KIF2C

TC0500010150.hg.1	1.068352	1.53×10^{-7}	0.000178	DNAH5
TC0500011752.hg.1	1.070992	1.39×10^{-7}	0.000171	FEM1C
CXCL12 γ isoform *vs* control				
TC1700010680.hg.1	-1.080970	5.93×10^{-8}	0.000105	KRT14
TC0400011408.hg.1	-0.986416	1.69×10^{-5}	0.011437	ADH1B
TC0200015894.hg.1	-0.932303	1.47×10^{-6}	0.001696	DOCK10
TC0400007836.hg.1	-0.928065	6.86×10^{-6}	0.005275	CXCL8
TC0400006661.hg.1	-0.899192	5.58×10^{-6}	0.004432	STK32B
TC2100006784.hg.1	-0.897234	3.99×10^{-6}	0.003542	JAM2
TC1000011549.hg.1	-0.840455	1.83×10^{-5}	0.012077	GFRA1
TC1100012755.hg.1	-0.836071	2.44×10^{-5}	0.015179	KIRREL3
TC1200008176.hg.1	-0.818598	6.33×10^{-5}	0.032429	LGR5
TC1700007330.hg.1	-0.815796	2.93×10^{-5}	0.017802	KSR1
TSUnmapped00000478.hg.1	-0.787902	4.44×10^{-5}	0.025573	ZNF502
TC1100009990.hg.1	-0.785292	4.90×10^{-5}	0.027540	OR6A2
TC0600014250.hg.1	-0.774330	6.12×10^{-5}	0.032045	ZBED9
TC0X00010399.hg.1	-0.769031	1.00×10^{-4}	0.047072	BEX1
TC0500011752.hg.1	0.893861	4.79×10^{-6}	0.004094	FEM1C
TC1100013221.hg.1	0.922373	2.14×10^{-6}	0.002246	CASP1

Only significant differentially expressed genes are reported (adjusted *P* values < 0.05). FC: Fold change.

Monolayer wound healing assay

To assess the biological influence of each CXCL12 isoform on cell migration, hTERT-HPNE cells have been subjected to monolayer wound healing assay. Compared with untreated control, the migration ability of treated hTERT-HPNE cells significantly ($P < 0.05$) increased at 12 h and 24 h time-points after CXCL12 isoforms administration. In particular, the γ isoform increased (37% at 24 h) the hTERT-HPNE migration more than α (16% at 24 h) and β (22% at 24 h) CXCL12 isoforms (Figure 4). Our results confirmed the functional enrichment analyses on DEGs identified by microarray experiments.

DISCUSSION

The strong interaction between stroma and tumour cells is a typical characteristic of PDAC microenvironment. CAFs, representing the 50% of PDAC stroma, are involved in malignant progression, by releasing several chemokines such as CXCL12[12]. In cancer cells presenting the CXCL12 receptor (CXCR4), numerous signalling pathways are activated, which promote cell growth, proliferation, migration, invasion, metastasis and drug resistance[12]. In this study, we investigated the potential role of three different CXCL12 splicing isoforms in a pancreatic pre-tumour model. In particular, we used immortalized, epithelial-like pancreatic duct cells bearing a mutation in the KRAS gene (*G12D*), which is known to be present in 90% of low-grade PanIN-1 lesions. The *G12D* mutation triggers conformational changes that result in KRAS protein activation, which, in turn, can constitutively stimulate several effector pathways involved in tumour development. However, in pancreas, it leads only to a pre-malignant phenotype; indeed, further mutations, amplifications or inactivation of other genes are necessary for the tumour formation[5,6,16]. Therefore, this model has a great value as control in functional *in vitro* assays.

Our microarray data identified some DEGs in hTERT-HPNE cells upon treatment with different CXCL12 isoforms. The DEGs of each isoform were associated with cell migration, adhesion, and cytoskeleton. In vitro wound healing assays confirmed these gene expression results for all isoforms. Our data also showed that the treatment with

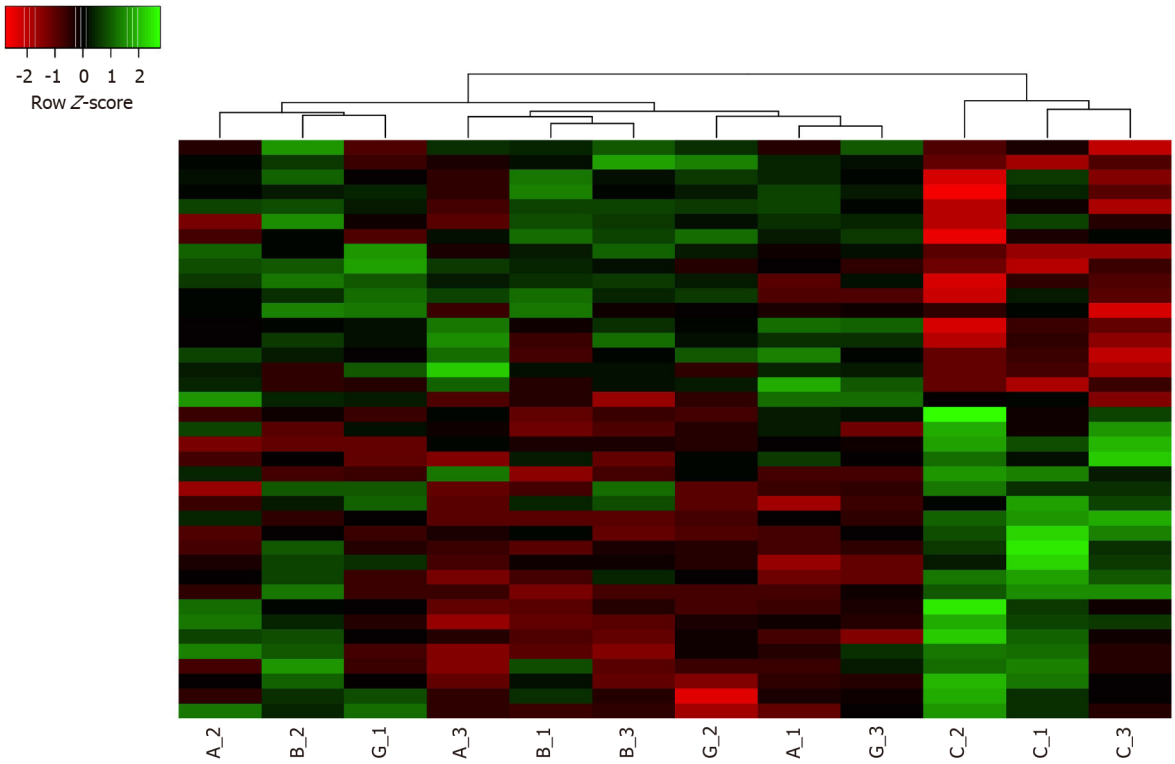

Figure 1 Hierarchical cluster heatmap of treated (α, β and γ isoforms) and control (C1, C2, C3) samples based on the obtained differentially expressed genes. Distance measurement method: Pearson; Clustering method: Average linkage.

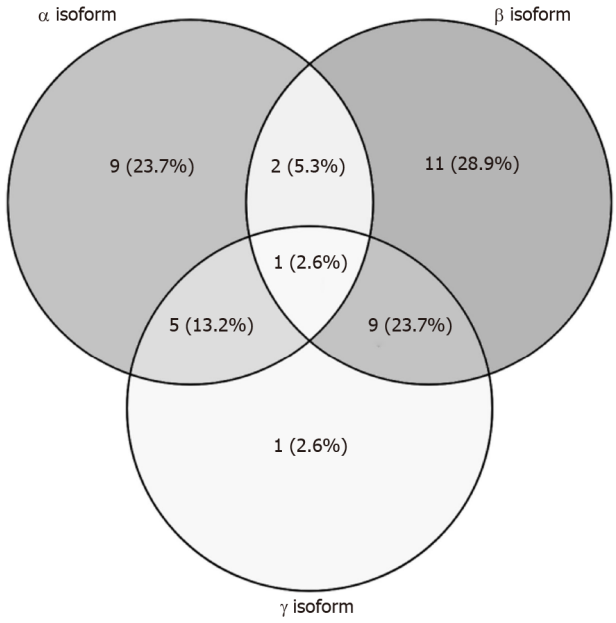

Figure 2 Comparison of the number of differentially expressed genes in all treatment conditions (α, β and γ CXCL12 isoforms) in hTERT-HPNE cells. Differentially expressed genes were detected using an FDR-corrected *P* value threshold of $P < 0.05$.

CXCL12 γ isoform on hTERT-HPNE cells caused enhanced wound healing repair than α and β isoforms.

Similar previous results are not available, since the different CXCL12 isoforms have been usually evaluated in terms of their chemoattractant abilities, that is in *in vitro* chemotaxis assays with a CXCL12 gradient. In a study of Yu *et al*[22], β isoform was more efficient than the others, while in some other studies the isoform with the highest attractant ability was α isoform[23,24]. Furthermore, there are in other studies which determined that γ isoform induced greater migration than other isoforms[25,26]. In

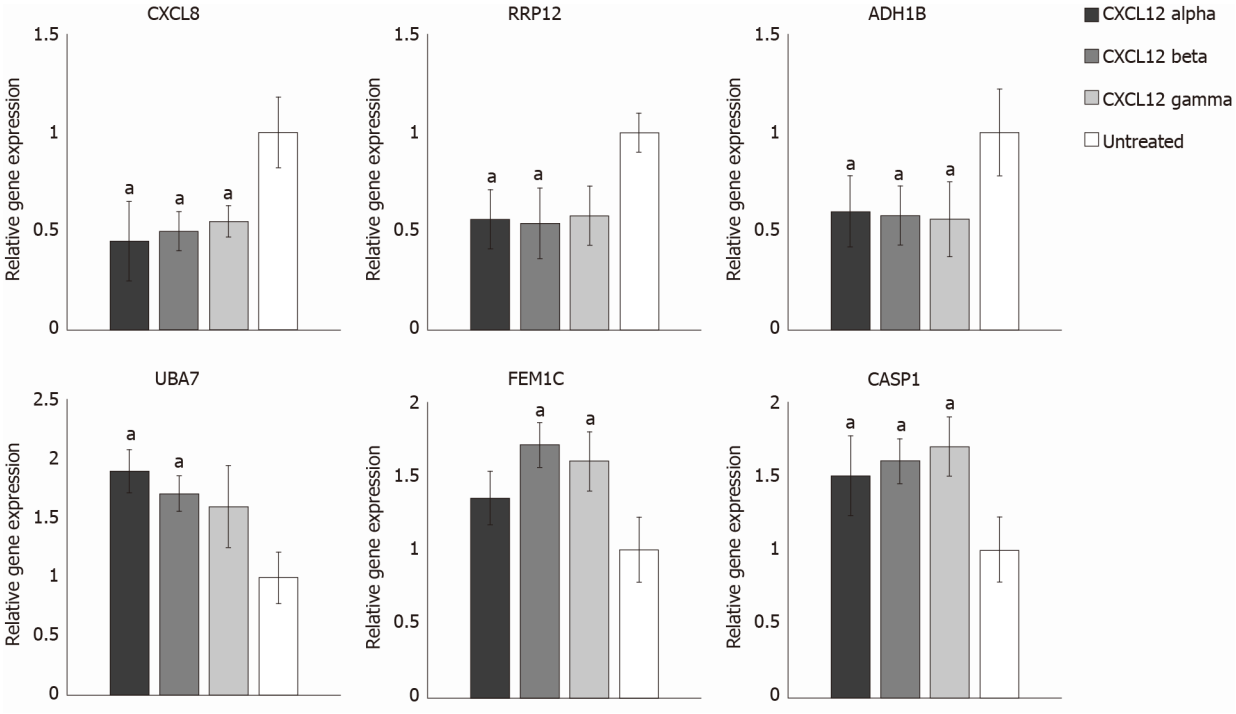

Figure 3 Real-Time polymerase chain reaction analysis of differentially expressed genes. Expression levels of CXCL8, RRP12, ADH1B, UBA7, FEM1C, and CASP1 in treated and untreated hTERT-HPNE cells. All values are expressed as the mean ± SD. Values were considered to be significantly different respect to the control at $^{a}P < 0.05$.

another *in vitro* chemotaxis assay, the use of different concentrations allowed to realize that α isoform induced greatest migration at low concentrations, whereas γ isoform at high concentrations[27]. It was also observed that the chemotactic responses of cells toward CXCL12 can be drawn as a bell-shaped curve with very low effects at both high and low concentrations of CXCL12 isoforms, maybe due the CXCR7 scavenging which alters the CXCL12 gradient to facilitate migration[25]. On the contrary, γ isoform drives chemotaxis to a much greater extent than α and β in *in vivo* studies. Indeed, γ isoform binds to the ECM components, with an extremely greater affinity than α isoform, allowing its local increase and so its activation by oligomerization[26,27].

Among genes with significantly altered expression upon treatments with the different CXCL12 isoforms, there are many genes already known to be involved in cell migration. Interestingly, this is the first study highlighting the possible genes targeted by different CXCL12 isoforms. For example, all CXCL12 isoforms were able to reduce the expression of DOCK10 gene, involved in several cellular processes, including the cellular migration. In particular, it regulates amoeboid motility[28] and it is able to induce filopodia and membrane ruffles[29]. In many tumour types, the overexpression of the receptor GFRA1 Leads to enhanced cancer cell proliferation and migration[30]. The GFRA1 downregulation caused by α and γ CXCL12 isoforms could highlight their potential anti-tumoral role. Both β and γ isoform affect the expression of the alcohol dehydrogenase gene (*ADH1B*), known to take part in several pathways promoting ovarian cancer cell infiltration[31]. Since CXCL12 β and γ isoform downregulate ADH1B gene, it suggests their possible anti-tumoral effect. Also JAM2 expression is downregulated by CXCL12 β and γ isoforms and, interestingly, JAM2 is known to affect cell invasion and migration abilities in pancreatic cancer cells[32]. GAS6-AS1 (GAS6 antisense RNA 1), overexpressed only upon treatments with the α isoform, promotes cancer cell growth, migration, and invasion ability in breast[33] and gastric cancer[34]. The CXCL12 β treatment induced overexpression of GDF9, CKAP2 and KIF2C. While GDF9 overexpression is correlated with a loss of the invasiveness, growth, and migration in human kidney cancer[35], CKAP2 overexpression increased cell proliferation, migration and invasion in HeLa cells[36]. Similarly to CKAP2, KIF2C mediates the cell migration in gastric cancer[37] and hepatocellular carcinoma[38]. Moreover, in KRas mutated cells, the knock down of KIF2C reduced the cell migration[39]. Our results showed that only CXCL12 γ isoform reduced the expression of LGR5. It is able to alter actin cytoskeleton, and in turn, reduce cell migration[40]. However, other studies demonstrated the central role of LGR5 in the tumour

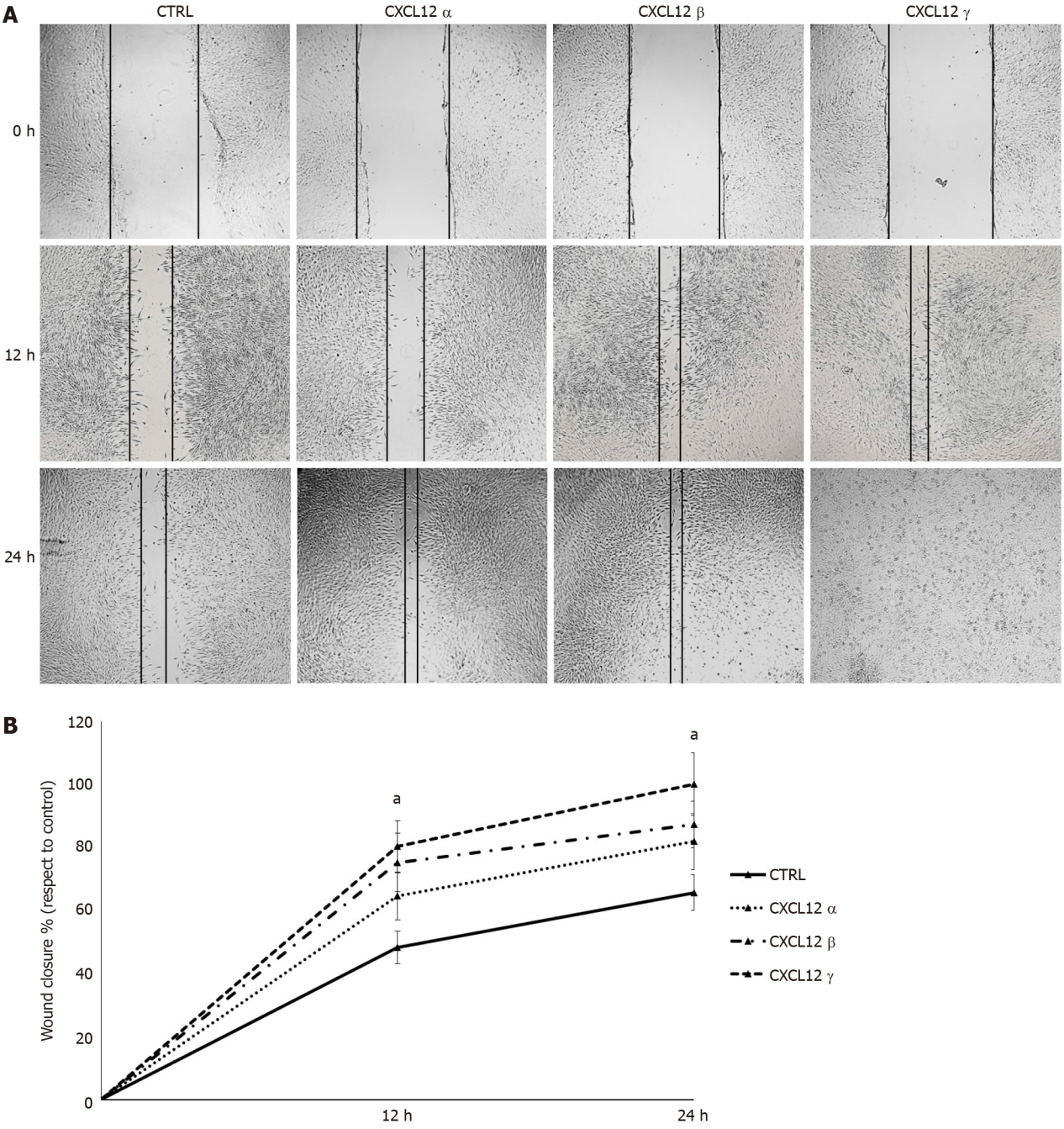

Figure 4 Migration ability of hTERT-HPNE cells. Wound healing assay was used to assess the effect of CXCL12 isoform treatments on cell migration. A: The cells were photographed immediately (0 h) after wounding by a pipette tip and at different time points (12 h and 24 h); B: The migration ability of the treated cells was evaluated by measuring their efficiency in wound repair compared with that of the control. All values are expressed as the mean ± SD. Values were considered to be significantly different respect to the control at $^{a}P < 0.05$.

physiopathology, although its utility as a marker of cancer stem cells is still controversial[41].

Besides cell migration, CXCL12 treatments affected the expression of genes involved in cell cycle regulation, genome integrity, stroma remodelling, and inflammation. For example, only the CXCL12 β treatment induced overexpression of *E2F3* and *ATR* genes. The upregulation of *E2F3* gene, involved in regulation of cell cycle, promotes proliferation and progression of pancreatic cancer cells[42]. The DNA damage sensing by the *ATR* kinases plays critical role in the resistance to chemotherapeutic drugs. Indeed, the inhibition of ATR increased pancreatic cancer cells' sensitivity to gemcitabine and radiation *in vitro*[43,44]. The *SERPINB2* gene expression is downregulated only upon treatments with α isoform. Interestingly, since *SERPINB2* mediates the remodelling of PDAC stroma, leading to the suppression of tumour growth and local invasion[45], α isoform may have a pro-tumoral activity in our hTERT-

HPNE cell model. The expression of the pro-tumour *KSR1* (Kinase suppressor of Ras-1) gene in our KRAS mutated pancreatic cells was downregulated upon treatments with CXCL12 α and γ isoforms. Interestingly, deletion of *KSR1* prevented cell signalling, leading to the block of the transformation induced by mutated KRAS[46]. The inhibition of *KSR1* gene determined a significant growth reduction of pancreatic tumours in vivo, as observed after injection of Panc-1 cells, a cellular model of KRAS-dependent PDAC, in nude mice[47]. Finally, CXCL12 β and γ isoforms downregulated the expression of the major metastasis-promoting inflammatory chemokine CXCL8 (also known as interleukin-8, IL-8). Indeed, KRAS mutation induces overexpression of CXCL8, which is necessary for cancer growth, vascularization and stromal remodelling[48]. Unlike CXCL12 β and γ isoforms, tumor necrosis factor-α, leukemia inhibitory factor, IL-1β, IL-6, and interferon-β induced the expression of CXCL8 in PDAC cells[49]. On the contrary, Matsuo *et al*[50] demonstrated that CXCL8 secretion by pancreatic cancer cell lines was significantly induced by CXCL12. However, unlike our experiments, these authors performed assays in a tumour model and without information about the involved CXCL12 isoform.

CONCLUSION

In conclusion, we showed that treatments with different CXCL12 isoforms prompt cell migration to different extents, probably due to different genes identified by our microarray analysis. Our results may facilitate the elucidation of the role of some CXCL12 isoforms in pancreatic cancer onset, and its underlying molecular mechanisms. In addition, the identified genes may represent novel candidates for diagnostic biomarkers and therapeutic targets for pancreatic cancer.

ARTICLE HIGHLIGHTS

Research background

Pancreatic ductal adenocarcinoma (PDAC) is a highly lethal cancer type, since it is usually diagnosed late, it has a very poor prognosis and strong chemoresistance. In the tumour microenvironment, cancer cells and other cell types co-exist and communicate by exchanging several molecules, including the chemokine CXCL12.

Research motivation

CXCL12 pre-mRNA can be alternatively spliced into different isoforms (α, β, γ, δ, ε, θ). However, their specific roles in PDAC have not yet been fully described.

Research objectives

Here, we aim to evaluate the specific roles of the main CXCL12 isoforms (α, β, and γ) in PDAC onset.

Research methods

We administered α, β, and γ CXCL12 isoforms to a pre-tumour model of PDAC, *i.e.*, the hTERT-HPNE E6/E7/KRasG12D cells. Then, we performed microarray analysis and Real-Time polymerase chain reaction validation in order to evaluate the global gene expression alterations. We also carried out wound healing assays in order to evaluate the effect of α, β, and γ CXCL12 isoforms on the cell migration ability.

Research results

The transcriptomic analyses showed that the expression of only few genes was affected by the treatment with the three isoforms. In particular, α and β isoforms affect different genes, whereas γ isoform altered the expression of genes already affected by the other isoforms. Since many genes affected by all isoforms are involved in cell migration and cytoskeleton remodelling, we performed cell migration assays, which confirmed the role of CXCL12 in migration, mainly caused by the γ isoform.

Research conclusions

Our results suggest that α, β and γ CXCL12 isoforms can trigger different responses in a pancreatic pre-tumour model. The γ isoform induced the highest level of cell migration.

Research perspectives

Although our data shed light on the molecular basis of PDAC onset and progression, further studies are necessary for a deeper characterization of CXCL12 isoforms.

ACKNOWLEDGEMENTS

We thank the Microarray Unit of Cogentech S.R.L. Benefit Corporation (Milan, Italy) for their assistance in the experimental microarray analyses.

REFERENCES

1 **Luchini C**, Capelli P, Scarpa A. Pancreatic Ductal Adenocarcinoma and Its Variants. *Surg Pathol Clin* 2016; **9**: 547-560 [PMID: 27926359 DOI: 10.1016/j.path.2016.05.003]
2 **Sleightholm RL**, Neilsen BK, Li J, Steele MM, Singh RK, Hollingsworth MA, Oupicky D. Emerging roles of the CXCL12/CXCR4 axis in pancreatic cancer progression and therapy. *Pharmacol Ther* 2017; **179**: 158-170 [PMID: 28549596 DOI: 10.1016/j.pharmthera.2017.05.012]
3 **Ding Y**, Du Y. Clinicopathological significance and prognostic role of chemokine receptor CXCR4 expression in pancreatic ductal adenocarcinoma, a meta-analysis and literature review. *Int J Surg* 2019; **65**: 32-38 [PMID: 30902754 DOI: 10.1016/j.ijsu.2019.03.009]
4 **Adamska A**, Domenichini A, Falasca M. Pancreatic Ductal Adenocarcinoma: Current and Evolving Therapies. *Int J Mol Sci* 2017; **18** [PMID: 28640192 DOI: 10.3390/ijms18071338]
5 **Deramaudt T**, Rustgi AK. Mutant KRAS in the initiation of pancreatic cancer. *Biochim Biophys Acta* 2005; **1756**: 97-101 [PMID: 16169155 DOI: 10.1016/j.bbcan.2005.08.003]
6 **Feldmann G**, Beaty R, Hruban RH, Maitra A. Molecular genetics of pancreatic intraepithelial neoplasia. *J Hepatobiliary Pancreat Surg* 2007; **14**: 224-232 [PMID: 17520196 DOI: 10.1007/s00534-006-1166-5]
7 **Pillarisetty VG**. The pancreatic cancer microenvironment: an immunologic battleground. *Oncoimmunology* 2014; **3**: e950171 [PMID: 25610740 DOI: 10.4161/21624011.2014.950171]
8 **Carr RM**, Fernandez-Zapico ME. Pancreatic cancer microenvironment, to target or not to target? *EMBO Mol Med* 2016; **8**: 80-82 [PMID: 26747091 DOI: 10.15252/emmm.201505948]
9 **Ren B**, Cui M, Yang G, Wang H, Feng M, You L, Zhao Y. Tumor microenvironment participates in metastasis of pancreatic cancer. *Mol Cancer* 2018; **17**: 108 [PMID: 30060755 DOI: 10.1186/s12943-018-0858-1]
10 **Pan B**, Liao Q, Niu Z, Zhou L, Zhao Y. Cancer-associated fibroblasts in pancreatic adenocarcinoma. *Future Oncol* 2015; **11**: 2603-2610 [PMID: 26284509 DOI: 10.2217/FON.15.176]
11 **Qian D**, Lu Z, Xu Q, Wu P, Tian L, Zhao L, Cai B, Yin J, Wu Y, Staveley-O'Carroll KF, Jiang K, Miao Y, Li G. Galectin-1-driven upregulation of SDF-1 in pancreatic stellate cells promotes pancreatic cancer metastasis. *Cancer Lett* 2017; **397**: 43-51 [PMID: 28336327 DOI: 10.1016/j.canlet.2017.03.024]
12 **Righetti A**, Giulietti M, Šabanović B, Occhipinti G, Principato G, Piva F. CXCL12 and Its Isoforms: Different Roles in Pancreatic Cancer? *J Oncol* 2019; **2019**: 9681698 [PMID: 31275385 DOI: 10.1155/2019/9681698]
13 **Roy I**, Zimmerman NP, Mackinnon AC, Tsai S, Evans DB, Dwinell MB. CXCL12 chemokine expression suppresses human pancreatic cancer growth and metastasis. *PLoS One* 2014; **9**: e90400 [PMID: 24594697 DOI: 10.1371/journal.pone.0090400]
14 **Zhao S**, Chang SL, Linderman JJ, Feng FY, Luker GD. A Comprehensive Analysis of CXCL12 Isoforms in Breast Cancer[1,2]. *Transl Oncol* 2014 [PMID: 24836649 DOI: 10.1016/j.tranon.2014.04.001]
15 **Ray P**, Stacer AC, Fenner J, Cavnar SP, Meguiar K, Brown M, Luker KE, Luker GD. CXCL12-γ in primary tumors drives breast cancer metastasis. *Oncogene* 2015; **34**: 2043-2051 [PMID: 24909174 DOI: 10.1038/onc.2014.157]
16 **Furukawa T**, Sunamura M, Horii A. Molecular mechanisms of pancreatic carcinogenesis. *Cancer Sci* 2006; **97**: 1-7 [PMID: 16367914 DOI: 10.1111/j.1349-7006.2005.00134.x]
17 **Carvalho BS**, Irizarry RA. A framework for oligonucleotide microarray preprocessing. *Bioinformatics* 2010; **26**: 2363-2367 [PMID: 20688976 DOI: 10.1093/bioinformatics/btq431]
18 **Leek JT**, Johnson WE, Parker HS, Jaffe AE, Storey JD. The sva package for removing batch effects and other unwanted variation in high-throughput experiments. *Bioinformatics* 2012; **28**: 882-883 [PMID: 22257669 DOI: 10.1093/bioinformatics/bts034]
19 **Ritchie ME**, Phipson B, Wu D, Hu Y, Law CW, Shi W, Smyth GK. limma powers differential expression analyses for RNA-sequencing and microarray studies. *Nucleic Acids Res* 2015; **43**: e47 [PMID: 25605792 DOI: 10.1093/nar/gkv007]
20 **Kuleshov MV**, Jones MR, Rouillard AD, Fernandez NF, Duan Q, Wang Z, Koplev S, Jenkins SL, Jagodnik KM, Lachmann A, McDermott MG, Monteiro CD, Gundersen GW, Ma'ayan A. Enrichr: a comprehensive gene set enrichment analysis web server 2016 update. *Nucleic Acids Res* 2016; **44**: W90-W97 [PMID: 27141961 DOI: 10.1093/nar/gkw377]

21 **Morey JS**, Ryan JC, Van Dolah FM. Microarray validation: factors influencing correlation between oligonucleotide microarrays and real-time PCR. *Biol Proced Online* 2006; **8**: 175-193 [PMID: 17242735 DOI: 10.1251/bpo126]

22 **Yu L**, Cecil J, Peng SB, Schrementi J, Kovacevic S, Paul D, Su EW, Wang J. Identification and expression of novel isoforms of human stromal cell-derived factor 1. *Gene* 2006; **374**: 174-179 [PMID: 16626895 DOI: 10.1016/j.gene.2006.02.001]

23 **Altenburg JD**, Broxmeyer HE, Jin Q, Cooper S, Basu S, Alkhatib G. A naturally occurring splice variant of CXCL12/stromal cell-derived factor 1 is a potent human immunodeficiency virus type 1 inhibitor with weak chemotaxis and cell survival activities. *J Virol* 2007; **81**: 8140-8148 [PMID: 17507482 DOI: 10.1128/JVI.00268-07]

24 **Altenburg JD**, Jin Q, Alkhatib B, Alkhatib G. The potent anti-HIV activity of CXCL12gamma correlates with efficient CXCR4 binding and internalization. *J Virol* 2010; **84**: 2563-2572 [PMID: 20015992 DOI: 10.1128/JVI.00342-09]

25 **Cavnar SP**, Ray P, Moudgil P, Chang SL, Luker KE, Linderman JJ, Takayama S, Luker GD. Microfluidic source-sink model reveals effects of biophysically distinct CXCL12 isoforms in breast cancer chemotaxis. *Integr Biol (Camb)* 2014; **6**: 564-576 [PMID: 24675873 DOI: 10.1039/c4ib00015c]

26 **Chang SL**, Cavnar SP, Takayama S, Luker GD, Linderman JJ. Cell, isoform, and environment factors shape gradients and modulate chemotaxis. *PLoS One* 2015; **10**: e0123450 [PMID: 25909600 DOI: 10.1371/journal.pone.0123450]

27 **Rueda P**, Balabanian K, Lagane B, Staropoli I, Chow K, Levoye A, Laguri C, Sadir R, Delaunay T, Izquierdo E, Pablos JL, Lendinez E, Caruz A, Franco D, Baleux F, Lortat-Jacob H, Arenzana-Seisdedos F. The CXCL12gamma chemokine displays unprecedented structural and functional properties that make it a paradigm of chemoattractant proteins. *PLoS One* 2008; **3**: e2543 [PMID: 18648536 DOI: 10.1371/journal.pone.0002543]

28 **Gadea G**, Sanz-Moreno V, Self A, Godi A, Marshall CJ. DOCK10-mediated Cdc42 activation is necessary for amoeboid invasion of melanoma cells. *Curr Biol* 2008; **18**: 1456-1465 [PMID: 18835169 DOI: 10.1016/j.cub.2008.08.053]

29 **Jaudon F**, Raynaud F, Wehrlé R, Bellanger JM, Doulazmi M, Vodjdani G, Gasman S, Fagni L, Dusart I, Debant A, Schmidt S. The RhoGEF DOCK10 is essential for dendritic spine morphogenesis. *Mol Biol Cell* 2015; **26**: 2112-2127 [PMID: 25851601 DOI: 10.1091/mbc.E14-08-1310]

30 **Ma WR**, Xu P, Liu ZJ, Zhou J, Gu LK, Zhang J, Deng DJ. Impact of *GFRA1* gene reactivation by DNA demethylation on prognosis of patients with metastatic colon cancer. *World J Gastroenterol* 2020; **26**: 184-198 [PMID: 31988584 DOI: 10.3748/wjg.v26.i2.184]

31 **Gharpure KM**, Lara OD, Wen Y, Pradeep S, LaFargue C, Ivan C, Rupaimoole R, Hu W, Mangala LS, Wu SY, Nagaraja AS, Baggerly K, Sood AK. ADH1B promotes mesothelial clearance and ovarian cancer infiltration. *Oncotarget* 2018; **9**: 25115-25126 [PMID: 29861857 DOI: 10.18632/oncotarget.25344]

32 **Zhang W**, He R, Chen S, Zhang L, Cao G, Yang W, Li J. The JAM-B/c-src/MMP9 pathway is associated with progression and regulates the invasion of pancreatic cancer. *J Cancer* 2020; **11**: 3246-3255 [PMID: 32231730 DOI: 10.7150/jca.40953]

33 **Li S**, Jia H, Zhang Z, Wu D. LncRNA GAS6-AS1 facilitates the progression of breast cancer by targeting the miR-324-3p/SETD1A axis to activate the PI3K/AKT pathway. *Eur J Cell Biol* 2020; **99**: 151124 [PMID: 33223203 DOI: 10.1016/j.ejcb.2020.151124]

34 **Zhang P**, Dong Q, Zhu H, Li S, Shi L, Chen X. Long non-coding antisense RNA GAS6-AS1 supports gastric cancer progression *via* increasing GAS6 expression. *Gene* 2019; **696**: 1-9 [PMID: 30735718 DOI: 10.1016/j.gene.2018.12.079]

35 **Du P**, Ye L, Li H, Ruge F, Yang Y, Jiang WG. Loss of expression of growth differentiation factor-9 (GDF9) in human kidney cancer and regulation of growth and migration of kidney cancer cells by GDF9. *Anticancer Res* 2012; **32**: 4375-4383 [PMID: 23060562]

36 **Guo QS**, Song Y, Hua KQ, Gao SJ. Involvement of FAK-ERK2 signaling pathway in CKAP2-induced proliferation and motility in cervical carcinoma cell lines. *Sci Rep* 2017; **7**: 2117 [PMID: 28522860 DOI: 10.1038/s41598-017-01832-y]

37 **Nakamura Y**, Tanaka F, Haraguchi N, Mimori K, Matsumoto T, Inoue H, Yanaga K, Mori M. Clinicopathological and biological significance of mitotic centromere-associated kinesin overexpression in human gastric cancer. *Br J Cancer* 2007; **97**: 543-549 [PMID: 17653072 DOI: 10.1038/sj.bjc.6603905]

38 **Wei S**, Dai M, Zhang C, Teng K, Wang F, Li H, Sun W, Feng Z, Kang T, Guan X, Xu R, Cai M, Xie D. KIF2C: a novel link between Wnt/β-catenin and mTORC1 signaling in the pathogenesis of hepatocellular carcinoma. *Protein Cell* 2020 [PMID: 32748349 DOI: 10.1007/s13238-020-00766-y]

39 **Zaganjor E**, Osborne JK, Weil LM, Diaz-Martinez LA, Gonzales JX, Singel SM, Larsen JE, Girard L, Minna JD, Cobb MH. Ras regulates kinesin 13 family members to control cell migration pathways in transformed human bronchial epithelial cells. *Oncogene* 2014; **33**: 5457-5466 [PMID: 24240690 DOI: 10.1038/onc.2013.486]

40 **Carmon KS**, Gong X, Yi J, Wu L, Thomas A, Moore CM, Masuho I, Timson DJ, Martemyanov KA, Liu QJ. LGR5 receptor promotes cell-cell adhesion in stem cells and colon cancer cells *via* the IQGAP1-Rac1 pathway. *J Biol Chem* 2017; **292**: 14989-15001 [PMID: 28739799 DOI: 10.1074/jbc.M117.786798]

41 **Andrikou K**, Santoni M, Piva F, Bittoni A, Lanese A, Pellei C, Conti A, Loretelli C, Mandolesi A,

Giulietti M, Scarpelli M, Principato G, Falconi M, Cascinu S. Lgr5 expression, cancer stem cells and pancreatic cancer: results from biological and computational analyses. *Future Oncol* 2015; **11**: 1037-1045 [PMID: 25804119 DOI: 10.2217/fon.15.27]

42 **Sun FB**, Lin Y, Li SJ, Gao J, Han B, Zhang CS. MiR-210 knockdown promotes the development of pancreatic cancer *via* upregulating E2F3 expression. *Eur Rev Med Pharmacol Sci* 2018; **22**: 8640-8648 [PMID: 30575904 DOI: 10.26355/eurrev_201812_16628]

43 **Prevo R**, Fokas E, Reaper PM, Charlton PA, Pollard JR, McKenna WG, Muschel RJ, Brunner TB. The novel ATR inhibitor VE-821 increases sensitivity of pancreatic cancer cells to radiation and chemotherapy. *Cancer Biol Ther* 2012; **13**: 1072-1081 [PMID: 22825331 DOI: 10.4161/cbt.21093]

44 **Liu S**, Ge Y, Wang T, Edwards H, Ren Q, Jiang Y, Quan C, Wang G. Inhibition of ATR potentiates the cytotoxic effect of gemcitabine on pancreatic cancer cells through enhancement of DNA damage and abrogation of ribonucleotide reductase induction by gemcitabine. *Oncol Rep* 2017; **37**: 3377-3386 [PMID: 28440428 DOI: 10.3892/or.2017.5580]

45 **Harris NLE**, Vennin C, Conway JRW, Vine KL, Pinese M, Cowley MJ, Shearer RF, Lucas MC, Herrmann D, Allam AH, Pajic M, Morton JP; Australian Pancreatic Cancer Genome Initiative, Biankin AV, Ranson M, Timpson P, Saunders DN. SerpinB2 regulates stromal remodelling and local invasion in pancreatic cancer. *Oncogene* 2017; **36**: 4288-4298 [PMID: 28346421 DOI: 10.1038/onc.2017.63]

46 **Kortum RL**, Lewis RE. The molecular scaffold KSR1 regulates the proliferative and oncogenic potential of cells. *Mol Cell Biol* 2004; **24**: 4407-4416 [PMID: 15121859 DOI: 10.1128/mcb.24.10.4407-4416.2004]

47 **Xing HR**, Cordon-Cardo C, Deng X, Tong W, Campodonico L, Fuks Z, Kolesnick R. Pharmacologic inactivation of kinase suppressor of ras-1 abrogates Ras-mediated pancreatic cancer. *Nat Med* 2003; **9**: 1266-1268 [PMID: 12960962 DOI: 10.1038/nm927]

48 **Sparmann A**, Bar-Sagi D. Ras-induced interleukin-8 expression plays a critical role in tumor growth and angiogenesis. *Cancer Cell* 2004; **6**: 447-458 [PMID: 15542429 DOI: 10.1016/j.ccr.2004.09.028]

49 **Kamohara H**, Takahashi M, Ishiko T, Ogawa M, Baba H. Induction of interleukin-8 (CXCL-8) by tumor necrosis factor-alpha and leukemia inhibitory factor in pancreatic carcinoma cells: Impact of CXCL-8 as an autocrine growth factor. *Int J Oncol* 2007; **31**: 627-632 [PMID: 17671691 DOI: 10.3892/ijo.31.3.627]

50 **Matsuo Y**, Ochi N, Sawai H, Yasuda A, Takahashi H, Funahashi H, Takeyama H, Tong Z, Guha S. CXCL8/IL-8 and CXCL12/SDF-1alpha co-operatively promote invasiveness and angiogenesis in pancreatic cancer. *Int J Cancer* 2009; **124**: 853-861 [PMID: 19035451 DOI: 10.1002/ijc.24040]

World Journal of Gastroenterology

Submit a Manuscript: https://www.f6publishing.com

World J Gastroenterol 2021 April 21; 27(15): 1630-1642

DOI: 10.3748/wjg.v27.i15.1630

ISSN 1007-9327 (print) ISSN 2219-2840 (online)

ORIGINAL ARTICLE

Retrospective Cohort Study

Resection of pancreatic cystic neoplasms in recurrent acute pancreatitis prevents recurrent pancreatitis but does not identify more malignancies

Thiruvengadam Muniraj, Harry R Aslanian, Loren Laine, Priya A Jamidar, James F Farrell, Kisha A Mitchell, Ronald R Salem

ORCID number: Thiruvengadam Muniraj 0000-0002-4904-2645; Harry R Aslanian 0000-0000-0001-0001; Loren Laine 0000-0000-0002-0002; Priya A Jamidar 0000-0000-0003-0003; James F Farrell 0000-0003-0004-5693; Kisha A Mitchell 0000-0000-0006-0006; Ronald R Salem 0000-0000-0007-0007.

Author contributions: Muniraj T, Aslanian HR, Laine L and Salem RR performed the study design; Muniraj T, Aslanian HR, and Salem RR performed the data acquisition; Muniraj T performed the statistical analysis; Muniraj T, Aslanian HR, and Laine L drafting of the manuscript; all authors performed data interpretation, review of manuscript for important intellectual content, final approval of the manuscript, and access to the data and a role in writing the manuscript.

Institutional review board statement: The study was reviewed and approved by the Yale University Institutional Review Board, USA, No. 2000029508.

Informed consent statement: The signed informed consent forms have been waived by the Yale

Thiruvengadam Muniraj, Harry R Aslanian, Loren Laine, Priya A Jamidar, James F Farrell, Section of Digestive Diseases, Department of Medicine, Yale University School of Medicine, New Haven, CT 06510, United States

Kisha A Mitchell, Department of Pathology, Yale University School of Medicine, New Haven, CT 06510, United States

Ronald R Salem, Department of Surgery, Yale University School of Medicine, New Haven, CT 06510, United States

Corresponding author: Thiruvengadam Muniraj, MD, Assistant Professor, Department of Digestive Diseases, Yale University School of Medicine, 15 York Street, New Haven, CT 06510, United States. thiruvengadam.muniraj@yale.edu

Abstract

BACKGROUND

Recurrent acute pancreatitis (RAP) may be a presenting feature of and an indication for resection of pancreatic cysts, including intra-ductal papillary mucinous neoplasm (IPMN). Few data are available regarding the prevalence of malignancy and post-operative RAP in this population.

AIM

To study the role of resection to help prevent RAP and analyze if presentation as RAP would be a predictor for malignancy.

METHODS

This retrospective study assessed 172 patients who underwent surgical resection of pancreatic cystic neoplasms at a university hospital between 2002 and 2016. The prevalence of preoperative high-risk cyst features, and of neoplasia was compared between patients with and without RAP. To identify the cause of pancreatitis, all the patients had a detailed history of alcohol, smoking, medications obtained, and had cross-sectional imaging (contrast-enhanced computed tomography/magnetic resonance imaging) and endoscopic ultrasound to look for gallstone etiology and other structural causes for pancreatitis. The incidence of RAP post-resection was the primary outcome.

University Institutional Review Board.

Conflict-of-interest statement: They authors declare that they have no conflict of interest.

Data sharing statement: No additional data are available.

STROBE statement: The authors have read the STROBE Statement—checklist of items, and the manuscript was prepared and revised according to the STROBE Statement—checklist of items.

Manuscript source: Invited manuscript

Specialty type: Gastroenterology and hepatology

Country/Territory of origin: United States

Peer-review report's scientific quality classification

Grade A (Excellent): 0
Grade B (Very good): B, B
Grade C (Good): C, C, C
Grade D (Fair): D
Grade E (Poor): 0

Received: December 21, 2020
Peer-review started: December 21, 2020
First decision: January 10, 2021
Revised: January 24, 2021
Accepted: March 22, 2021
Article in press: March 22, 2021
Published online: April 21, 2021

P-Reviewer: Faias S, Gupta V, Inchingolo R, Sato H

RESULTS

IPMN accounted for 101 cases (58.7%) {[branch duct (BD) 59 (34.3%), main duct (MD) 42] (24.4%)}. Twenty-nine (16.9%) presented with RAP (mean 2.2 episodes): 15 had BD-IPMN, 8 MD-IPMN, 5 mucinous cystic neoplasm and 1 serous cystic neoplasm. Malignancy was similar among those with *vs* without RAP for all patients [6/29 (20.7%) *vs* 24/143 (16.8%)] and IPMN patients [6/23 (26.1%) *vs* 23/78 (29.5%)], although tended to be higher with RAP in BD-IPMN, [5/15 (33.3%) *vs* 3/44 (6.8%), $P = 0.04$]. At mean follow-up of 7.2 years, 1 (3.4%) RAP patient had post-resection RAP. The mean episodes of acute pancreatitis before *vs* after surgery were 3.4 *vs* 0.02 ($P < 0.0001$).

CONCLUSION

Malignancy was not increased in patients with pancreatic cystic neoplasms who have RAP compared to those without RAP. In addition, specific cyst characteristics were not clearly associated with RAP. The incidence of RAP was markedly decreased in almost all patients following cyst resection.

Key Words: Pancreatic cyst; Pancreatic neoplasm; Pancreatitis; Malignancies

Core Tip: Our findings from this original study support international consensus guidelines recommendations for surgical resection of pancreatic cystic neoplasms presenting with acute pancreatitis but more for the effective treatment of recurrent acute pancreatitis (RAP) rather than for the identification of malignancy. The objective of this research was to study the role of resection to help prevent RAP and analyze if presentation as RAP would be a predictor for malignancy.

Citation: Muniraj T, Aslanian HR, Laine L, Jamidar PA, Farrell JF, Mitchell KA, Salem RR. Resection of pancreatic cystic neoplasms in recurrent acute pancreatitis prevents recurrent pancreatitis but does not identify more malignancies. *World J Gastroenterol* 2021; 27(15): 1630-1642
URL: https://www.wjgnet.com/1007-9327/full/v27/i15/1630.htm
DOI: https://dx.doi.org/10.3748/wjg.v27.i15.1630

INTRODUCTION

Acute pancreatitis is among the most frequent gastrointestinal causes of hospital admission in the United States with nearly 280000 hospitalizations annually[1]. While pancreatic cysts in the setting of pancreatitis are frequently assumed to be pseudocysts, neoplastic pancreatic cysts are recognized as a cause of acute pancreatitis. Intra-ductal papillary mucinous neoplasms (IPMN) are the most common cystic pancreatic neoplasms. They arise within the main pancreatic duct or side-branches and are characterized by production of thick mucinous fluid. Additional pancreas cystic neoplasms include mucinous cystic neoplasm and serous cystic neoplasm. Pancreatic cysts may cause acute pancreatitis by compression of the pancreatic duct or by obstruction of the pancreatic duct with mucus. The reported rate of acute pancreatitis among patients with IPMN varies between 7% and 67%[2-5]. A careful clinical history could help to differentiate such neoplastic cysts from a mature, encapsulated fluid collection without necrosis (pseudocyst) or with necrosis (walled-off necrosis, WON) that may occur as a cystic lesion after 4 wk from the onset of acute pancreatitis[6]. The presence of a pancreatic cyst in imaging at diagnosis of index pancreatitis is probably a neoplastic cyst, while the detection of a cyst in the follow-up of pancreatitis with a normal first imaging exam likely a post inflammatory pseudocyst or WON.

The diagnosis of acute pancreatitis is based on the presence of two of the following three features: (1) Abdominal pain consistent with acute pancreatitis (acute onset of a persistent, severe, epigastric pain often radiating to the back); (2) Serum lipase activity (or amylase activity) at least three times greater than the upper limit of normal; And (3) Characteristic findings of acute pancreatitis on contrast-enhanced computed

S-Editor: Fan JR
L-Editor: A
P-Editor: Ma YJ

tomography (CECT) or magnetic resonance imaging (MRI) or transabdominal ultrasonography[6]. Recurrent acute pancreatitis (RAP), defined as two or more definite episodes of acute pancreatitis, occurs in approximately 17% to 29% of patients who present with a first episode of acute pancreatitis[5,7-9]. Approximately 80% of RAP is related to alcohol and gallstones. Other etiologies include medications, pancreas divisum, sphincter of Oddi dysfunction, pancreatic cancer, hypertriglyceridemia, hypercalcemia, infections, and genetic predisposition[10,11].

Few data are available regarding the prevalence of malignancy and on the course of RAP associated with pancreatic cystic neoplasms, such as IPMN, and the potential benefit of surgical resection in patients with acute pancreatitis due to pancreatic cysts. We, therefore, performed a retrospective study to assess the characteristics of patients with pancreatic cystic neoplasms who present with unexplained RAP and the effect of surgical resection on the natural history.

MATERIALS AND METHODS

We conducted a retrospective cohort study at the Yale-New Haven Hospital to identify patients who underwent surgical resection of pancreatic cystic neoplasms between January 1, 2002 and December 1, 2016. Those who had RAP, defined as 2 or more episodes of acute pancreatitis without an identifiable cause prior to resection[12], and imaging [computed tomography, magnetic resonance imaging, and/or endoscopic ultrasound (EUS)] documenting the cyst pre-operatively were defined as the RAP cohort. To identify the cause of pancreatitis, all the patients had detailed history of alcohol, smoking, medications obtained and had cross-sectional imaging (CECT/MRI) and EUS to look for gallstone etiology and other structural causes for pancreatitis. The diagnosis was double-checked. Patients with resection who did not have prior RAP served as the control cohort. Patient follow-up extended until September 2018. The study was approved by the institutional review board at Yale University.

Preoperative classification was based on preoperative imaging and results of fine-needle aspiration, if performed. Cysts were classified as IPMNs and non-IPMNs. The IPMNs were sub-classified as main-duct (MD) and branch-duct (BD). Mixed-type IPMNs were included in the MD group. Preoperative diagnosis of IPMNs were based on clinical findings from the images obtained. Histopathology from post-surgical resection specimens was used as the gold standard to ascertain the final diagnosis. The pathological classification and pre-surgical classification were made on the basis of World Health Organization criteria and current literature[13-16]. Performing metastatic urothelial cancer (MUC) staining or gene sequencing

Malignancy was defined as the presence of invasive carcinoma or high-grade dysplasia on final surgical pathology. Patients with no follow-up data post-operatively, known pseudocysts and predominantly solid pancreatic masses were excluded. Patient demographic, clinical, radiographic, and pathologic data were extracted from the medical record. In patients with multiple cysts, the features of the largest cyst or the cyst with the most concerning high-risk features (*e.g.*, mural nodules) were the characteristics recorded for the patient. Patient data post-resection were also extracted, with the primary goal of identifying episodes of acute pancreatitis. On surgically resected specimens, MUC staining, histologic examination and gene sequencing were used for pathologic subclassification[17,18].

Statistical analysis

The primary analysis involved a comparison of the number of episodes of acute pancreatitis pre- and post-resection of pancreas cyst in patients who had RAP. We also compared baseline patient and cyst characteristics between patients with RAP and those without RAP. Comparisons between the RAP cohort and control (non-RAP) cohort and between the preoperative and post-operative time period were performed with the Mantel-Haenszel risk difference calculation for continuous variables and Mantel-Haenszel risk ratio for proportions. Statistical analysis was performed by using the statistical algorithms in Cochrane Review Manager Software 5.3.

RESULTS

A total of 172 patients with pancreatic cysts underwent surgery between 2002 and

2016. The indication for surgery was RAP along with cyst characteristics in 11 patients and among all other patients, the indication for surgery was based on the cyst morphology. IPMNs accounted for 101 (58.7%) of these 172 cases {BD-IPMN [59 (34.3%)] and MD-IPMN [42 (24.4%)]} (Table 1 and Figure 1). The next most common types of lesions were mucinous cystic neoplasms [32/172 (18.6%)] and serous cystic neoplasms [16/172 (9.3%)] (Table 1). Since preoperative diagnosis on cysts were made using radiologic findings, the final diagnosis might have varied based on surgical findings. Twenty-nine (16.9%) patients had RAP without other identifiable cause prior to resection, while the remaining 143 (83.1%) patients had no episodes of acute pancreatitis prior to resection. No patient had evidence of chronic pancreatitis. Among the 29 patients with RAP with cystic neoplasms, the surgical procedure performed was pancreaticoduodenectomy (n = 18) or distal pancreatectomy (n = 11) with surgical mortality 0%, morbidity 3/29 (10%) (one patient had mesenteric bleeding requiring immediate exploratory laparotomy, one had afferent limb syndrome 2 wk later required exploratory laparotomy for adhesion lysis, and other with a delayed abscess in left upper quadrant managed with external drainage.

Comparison of pre-resection and post-resection period in the RAP cohort

The mean number of pancreatitis episodes *per* patient prior to resection in the RAP cohort was 2.2 (range 2-32 episodes). The median elapsed time between the first episode of acupuncture (AP) and surgery was 17 mo (range 1.5 mo to 7 years). The mean follow-up after surgery was 7.2 years (range 1.9-13.8 years).

Only 1 (3%) of 29 RAP patients (with BD-IPMN) had acute pancreatitis documented post-resection. The mean number of recurrent episodes of acute pancreatitis *per* patient-year before *vs* after surgery was 3.40 *vs* 0.02 (absolute difference = 3.38, 95%CI 1.76 to 5.00; $P < 0.0001$)). All the episodes were mild acute pancreatitis and none of the patients in this cohort had severe acute pancreatitis[3]. A marked decrease was seen in all types of cysts (Table 2). The one patient with recurrent pancreatitis after resection had BD-IPMN; he had 8 episodes before resection and 32 after resection and progressed to chronic pancreatitis with ductal calcification at 6 years after resection. No patient without prior RAP developed acute pancreatitis after resection.

Comparison of RAP and control cohort

Selected characteristics of the RAP and control cohorts are shown in Table 3. Median age and proportion who were male were comparable. No clear differences were identified between the cohorts in characteristics of the cystic lesions, including in size, or proportion with malignancy except for location in the tail of pancreas where most cyst patients were without RAP. IPMNs tended to be more common among patients with RAP than in those without RAP (79.3% *vs* 54.5%; risk difference = 0.25; 95%CI: 0.08, 0.41, $P = 0.004$) with most of the difference seen in the BD-IPMN patients.

Table 4 shows the results for the RAP and control cohorts in all patients with IPMN. Patients with RAP were more likely to have intestinal and less likely to the gastric IPMN cysts (intestinal: 34.8% *vs* 12.8%; risk difference: 0.22 (95%CI: 0.01, 0.43); $P = 0.04$; gastric: 13% *vs* 53.9%; risk difference: -0.41 (95%CI: -0.58, -0.23); $P < 0.0001$). The pathological subtypes of 21.8% of RAP patients and 10.3% of non-RAP patients was unknown.

Table 5 is restricted to patients with BD-IPMN. Again, no clear differences were seen between cohorts in patient or cyst characteristics with the possible exception of a tendency to a higher prevalence of malignancy in the RAP group *vs* non-RAP group with BD-IPMNs {33.3% *vs* 6.8%, [risk difference = 0.27 (95%CI: 0.02, 0.52); $P = 0.04$]} although the numbers in each cohort were small. A similar difference in pathological subtypes were noted. Patients with RAP were more likely to have BD-IPMN of an intestinal subtype and less likely to have a gastric subtype *vs* the control cohort [intestinal: 46.7% *vs* 9.1%; risk difference = 0.38 (95%CI: 0.11, 0.64); $P = 0.006$; gastric: 0% *vs* 68.2%; risk difference = -0.68 (95%CI: -0.84, -0.52); $P < 0.001$]. However, it should be noted that the pathological subtype of 26.7% of BD-IPMNs was not recorded. Based on the significant results from Univariate analysis, multivariable analysis logistic regression performed, however, the results did not vary in any significance (Tables 6-8).

DISCUSSION

Surgical resection has been recommended for patients with pancreatic cystic neoplasms who present with acute pancreatitis[16], regardless of cyst type. Reasons for

Table 1 Types of pancreatic cysts

IPMN cysts (total)	101
BD-IPMN	59
MD-IPMN	42
Non-IPMN cysts (total)	71
Mucinous cystic neoplasm	32
Serous cystic neoplasm	16
Pancreatic neuroendocrine tumor	11
Solid pseudopapillary epithelial neoplasm	6
Squamoid	3
Benign	2
Cystic degeneration	1

IPMN: Intra-ductal papillary mucinous neoplasm; MD-IPMN: Main duct-IPMN; BD-IPMN: Branch duct-IPMN.

Table 2 Incidence of recurrent acute pancreatitis episodes in recurrent acute pancreatitis patients

	Episodes *per* patient-year (mean + SD)		Mean difference [95%CI]	*P* value
	Pre-resection	Post-resection		
All cysts (n = 29)	3.40 (4.46)	0.02 (0.08)	3.38 [1.76, 5.00]	< 0.0001
IPMN (n = 23)	2.32 (1.69)	0.03 (0.09)	2.29 [1.60, 2.98]	< 0.0001
BD-IPMN (n = 15)	2.06 (1.85)	0.04 (0.11)	2.02 [1.08, 2.96]	< 0.0001
MD-IPMN (n = 8)	2.81 (1.32)	0 (0)[1]	2.81 [1.83, 3.79]	< 0.0001
Non-IPMN (n = 6)	7.52 (8.53)	0 (0)[1]	7.52 [0.69, 14.35]	0.03

[1]In order to calculate mean differences and risk ratios, a standard deviation of 0.0001 was substituted for zero. IPMN: Intra-ductal papillary mucinous neoplasm; MD-IPMN: Main duct-IPMN; BD-IPMN: Branch duct-IPMN; SD: Standard deviation; CI: Confidence interval.

resection include identification and removal of underlying malignancy, prevention of the development of malignancy, and prevention of additional attacks of pancreatitis[16]. The characteristics of cystic neoplasms associated with acute pancreatitis and the impact of surgical resection on the prevention of malignancy and future episodes of RAP, however, have not been well defined. We found that cyst characteristics, such as location, size, the proportion with solid component, and prevalence of malignancy were not clearly different between patients with *vs* without RAP. IPMN was the most common cystic neoplasm among patients with a history of RAP undergoing surgical resection. Although a prior report found MD/combined type IPMN to be more frequently associated with RAP (%)[3] and another study found no difference[5], we found that among patients with IPMN, RAP was more often associated with BD-IPMN (65%) than MD-IPMN (35%). Our results are different from Jang *et al*[3] where MD/combined IPMN resulting more RAP was thought to be due to mechanical obstruction of the main pancreatic duct by thick mucin, resulting in ductal hypertension, thereby premature activation and release of pancreatic enzymes[3]. However, BD-IPMN leading to AP/RAP is assumed primarily due to the obstruction of the main pancreatic duct by the migration of mucin from the BD or may not be related to mucin but just to the viscosity of cyst fluid[3]. Patients with RAP also were more likely to have intestinal histological subtype *vs* the control cohort, although histologic subtype was unknown in a third of patients.

Malignancy was present in approximately one-fifth of patients undergoing surgical resection of pancreatic cysts, with similar proportions in those with and without RAP. Malignancy tended to be more common in BD-IPMN patients with RAP (33.3% *vs* 6.8% without RAP), although given relatively small numbers and multiple comparisons, this finding must be viewed as hypothesis-generating. Prior studies vary

Table 3 Characteristics of all patients (*n* = 172)

	With RAP (*n* = 29) *n* (%)	Without RAP (*n* = 143) *n* (%)	Risk difference [95%CI]	*P* value
Median age	61 (IQR 18)	65 (IQR 15)	NA	0.65
Sex (M)	13 (44.8)	58 (40.6)	NA	0.67
Location of cyst				
Head	16 (55.2)	65 (45.5)	0.10 [-0.10, 0.30]	0.34
Neck	2 (6.9)	7 (4.9)	0.02 [-0.08, 0.12]	0.69
Body	8 (27.6)	32 (22.4)	0.05 [-0.12, 0.23]	0.56
Tail	3 (10.3)	37 (25.9)	-0.16 [-0.29, -0.02]	0.02
Diffuse	0 (0)	2 (1.4)	-0.01 [-0.06, 0.04]	0.59
Main pancreas duct > 10	4 (13.8)	10 (7.0)	0.07 [-0.06, 0.20]	0.31
Cyst size > 3	6 (20.7)	36 (25.2)	-0.04 [-0.21, 0.12]	0.59
Solid component	7 (24.1)	46 (32.2)	-0.08 [-0.25, 0.09]	0.36
Malignancy	6 (20.7)	24 (16.8)	0.04 [-0.12, 0.20]	0.63
Pathological subtype				
Intestinal	10 (34.5)	11 (7.7)	0.27 [0.09, 0.45]	0.003
Gastric	3 (10.3)	43 (30.1)	-0.20 [-0.33, -0.06]	0.004
Pancreatobiliary	7 (24.1)	15 (10.5)	0.14 [-0.03, 0.30]	0.10
Oncocytic	0 (0)	3 (2.1)	-0.02 [-0.07, 0.03]	0.43
Unknown	9 (31.0)	71 (49.7)	-0.19 [-0.37, 0.001]	0.05
Cyst type				
IPMN total	23 (79.3)	78 (54.5)	0.25 [0.08, 0.41]	0.004
BD-IPMN	15 (51.7)	44 (30.8)	0.21 [0.01, 0.41]	0.04
MD-IPMN	8 (27.6)	34 (23.8)	0.04 [-0.14, 0.22]	0.67
Non-IPMN	6 (20.7)	65 (45.5)	-0.25 [-0.42, -0.08]	0.004

RAP: Recurrent acute pancreatitis; IPMN: Intra-ductal papillary mucinous neoplasm; MD-IPMN: Main duct-IPMN; BD-IPMN: Branch duct-IPMN; IQR: Interquartile range; CI: Confidence interval.

in the reported association of malignancy within pancreatic cysts in patients presenting with acute pancreatitis[19]. Some report no increased risk[20-22]. However, a recent study identified IPMN presenting with acute pancreatitis to be associated with an increased risk of malignancy as compared to IPMN without pancreatitis on multivariable analysis[23]. Morales-Oyarvide *et al*[23] also identified a significant association of AP with IPMN of intestinal subtype (OR = 4.7, 2.5-8.8)[23]. The intestinal phenotype of IPMN has a propensity for mucin hypersecretion, which may promote AP due to ductal obstruction[24-27]. In addition, the intestinal phenotype has been associated with an increased risk of malignancy and with colloid carcinoma[25].

Among the 15 BD-IPMN patients with RAP who had surgical resection in our study, pre-operatively only 1 (6.7%) demonstrated all 3 high-risk features for malignancy (dilated main pancreatic duct > 10 mm, size > 3 cm, solid component)[28] and 3 (20%) had 2 high-risk features. One-third, however, had malignancy identified on surgical pathology. Based on the presence of high-risk stigmata/worrisome features alone, *per* international revised consensus guidelines of 2017[16,29] or European guidelines[30], resection would not have been indicated in 14 of the 15 BD-IPMN patients if they had not presented with acute pancreatitis. And based on American Gastroenterological Association guidelines, if these patients did not have RAP, only 3 of 15 would have had EUS based on the requirement for at least 2 high-risk features[28]. American College of Gastroenterology guidelines recommends EUS or referral to a multidisciplinary team for pancreatic cystic lesions in the presence of pancreatitis regardless of high-risk

Table 4 Characteristics of patients with intra-ductal papillary mucinous neoplasm with and without recurrent acute pancreatitis

	With RAP (*n* = 23) *n* (%)	Without RAP (*n* = 78) *n* (%)	Risk difference [95%CI]	*P* value
Median age	64 (IQR 17)	67 (IQR 12)	NA	0.64
Sex (M)	13 (56.5)	38 (48.7)	NA	0.51
Location of cyst				
Head	16 (69.6)	46 (59)	0.11 [-0.11, 0.32]	0.34
Body/Tail	7 (30.4)	32 (41)	-0.11 [-0.32, 0.11]	0.34
Main pancreas duct > 10	4 (17.4)	10 (12.8)	0.05 [-0.13, 0.22]	0.60
Cyst size > 3 cm	6 (26)	36 (46.2)	-0.20 [-0.41, 0.01]	0.06
Solid component	5 (21.7)	20 (25.6)	-0.04 [-0.23, 0.16]	0.69
Malignancy	6 (26.1)	23 (29.5)	-0.03 [-0.24, 0.17]	0.75
Pathological subtype				
Intestinal	8 (34.8)	10 (12.8)	0.22 [0.01, 0.43]	0.04
Gastric	3 (13)	42 (53.9)	-0.41 [-0.58, -0.23]	< 0.0001
Pancreatobiliary	7 (30.4)	15 (19.2)	0.11 [-0.10, 0.32]	0.29
Oncocytic	0 (0%)	3 (3.8)	-0.04 [-0.11, 0.03]	0.30
Unknown	5 (21.8)	8 (10.3)	0.11 [-0.07, 0.30]	0.22

RAP: Recurrent acute pancreatitis; IQR: Interquartile range; CI: Confidence interval.

features[31]. While observational studies have suggested an increased risk of pancreatic cancer in all patients presenting with acute pancreatitis[19,32], further studies are needed to evaluate whether acute pancreatitis may be an independent predictor of malignancy within pancreatic cysts.

The primary goal of our study was to determine the post-resection course of patients with RAP associated with pancreatic cystic neoplasms. We found that episodes of RAP are rare following surgical resection of pancreatic cystic neoplasms, suggesting that the pancreatic cystic neoplasms were indeed the cause of RAP in almost all cases. Only 1 (3%) of 29 patients presenting with RAP had RAP after resection, and the rate of acute pancreatitis *per* patient-year decreased from 3.4 to 0.02 ($P < 0.0001$), with marked reductions in all types of pancreatic cystic lesions. It is also important to note that as the pancreatic exocrine function decreases after pancreas resection, the mere resection itself may reduce the frequency of RAP[33]. Pancreatic surgery for an indication of RAP alone is a very invasive procedure and therefore, risk/benefits should be considered while making the decision. In such cases, since the pancreatic ductal occlusion at the site of the papilla has been postulated to be the main reason for RAP in IPMN, performing an endoscopic pancreatic sphincterotomy with or without stenting may be effective in preventing pancreatitis recurrence[34].

We recognize several limitations to this study, including the retrospective review of data. In addition, this cohort is limited to patients who have undergone surgical resection of pancreas cystic neoplasms, which makes it a selected population not representative of the overall group of patients with pancreatic cystic neoplasms. For example, most patients with BD-IPMN or serous cystic neoplasms do not undergo resection. Patient cases were reviewed to exclude other identifiable causes of acute pancreatitis; however, given the study's retrospective nature, the evaluation was not standardized. All of the patients in our surgical cohort had RAP, with 2 or more episodes. This is reflective of clinical practice for BD-IPMN, as resection in the absence of multiple high-risk features is typically not pursued following a single episode of idiopathic pancreatitis. Although, this study clearly shows the risk reduction of RAP after the pancreatic resection, further investigation with large population prospective study is needed to prove causal relationship between the cause of RAP and pancreatic resection.

Table 5 Characteristics of patients with branch-duct intra-ductal papillary mucinous neoplasm with and without recurrent acute pancreatitis

	With RAP (*n* = 15) *n* (%)	Without RAP (*n* = 44) *n* (%)	Risk difference [95%CI]	*P* value
Median age	60 (IQR 23)	65 (IQR 12.5)	NA	0.50
Sex (M)	8 (53.3)	24 (54.6)	NA	0.94
Location of cyst				
Head	11 (73)	28 (64)	0.10 [-0.17, 0.36]	0.47
Body/Tail	4 (9.1)	16 (36)	-0.10 [-0.36, 0.17]	0.47
Main pancreas duct > 10	2 (13.3)	2 (4.6)	0.09 [-0.10, 0.27]	0.35
Cyst size > 3 cm	6 (40)	21 (47.7)	-0.08 [-0.37, 0.21]	0.60
Solid component	2 (13.3)	4 (9.1)	0.04 [-0.15, 0.23]	0.66
Malignancy	5 (33.3)	3 (6.8)	0.27 [0.02, 0.52]	0.04
Pathological subtype				
Intestinal	7 (46.7)	4 (9.1)	0.38 [0.11, 0.64]	0.006
Gastric	0	30 (68.2)	-0.68 [-0.84, -0.52]	< 0.001
Pancreatobiliary	4 (26.7)	7 (16)	0.11 [-0.14, 0.36]	0.4
Oncocytic	0	0	NA	NA
Unknown	4 (26.7)	3 (6.8)	0.20 [-0.04, 0.43]	0.10

RAP: Recurrent acute pancreatitis; IQR: Interquartile range; NA: Not available; CI: Confidence interval.

CONCLUSION

In conclusion, we found that malignancy is not increased in patients with pancreatic cystic neoplasms who have RAP compared to those without RAP. In addition, specific cyst characteristics were not clearly associated with RAP, although intestinal histological subtype appeared to be more common in patients with RAP. Most importantly, episodes of RAP were markedly reduced after cyst resection, with only one of 29 patients having recurrent episodes. Our findings support international consensus guidelines recommendations for surgical resection of pancreatic cystic neoplasms presenting with acute pancreatitis but more for the effective treatment of RAP rather than for the identification of malignancy[16].

Table 6 Multivariable analysis of all patients (*n* = 172)

	With RAP (*n* = 29)	Without RAP (*n* = 143)	*P* value
	Odds ratio	95%CI	
Location of cyst			
Head	-		
Neck	1.240013	[0.19933, 7.713993]	0.818
Body	1.736854	[0.570778, 5.285173]	0.331
Tail	0.686678	[0.155679, 3.028833]	0.62
Diffuse	-		
Pathological subtype			
Intestinal			
Gastric	0.059886	[0.013402, 0.267608]	< 0.001
Pancreatobiliary	0.454606	[0.122387, 1.688636]	0.239
Oncocytic	-		
Unknown	0.355592	[0.088518, 1.428472]	0.145
Cyst type			
IPMN total	3.462462	[0.782586, 15.31927]	0.102
BD-IPMN	1.660612	[0.558816, 4.934779]	0.361
MD-IPMN	-		

RAP: Recurrent acute pancreatitis; IPMN: Intra-ductal papillary mucinous neoplasm; MD-IPMN: Main duct-IPMN; BD-IPMN: Branch duct-IPMN; CI: Confidence interval.

Table 7 Multivariable analysis of patients with intra-ductal papillary mucinous neoplasm with and without recurrent acute pancreatitis

	With RAP (*n* = 29)	Without RAP (*n* = 143)	*P* value
	Odds ratio	95%CI	
Location of cyst			
Head	-	-	
Neck	1.265446	[0.169046, 9.472912]	0.819
Body	0.506621	[0.111835, 2.295024]	0.378
Tail	0.572817	[0.090659, 3.619267]	0.554
Diffuse	-	-	
Pathological subtype			
Intestinal	-	-	
Gastric	0.096091	[0.020977, 0.440165]	0.003
Pancreatobiliary	0.773074	[0.199147, 3.001027]	0.71
Oncocytic	-		
Unknown	1.034683	[0.214488, 4.991279]	0.966
Cyst type			
IPMN total			
BD-IPMN	1.571892	[0.530571, 4.65695]	0.414
MD-IPMN	-		

RAP: Recurrent acute pancreatitis; IPMN: Intra-ductal papillary mucinous neoplasm; MD-IPMN: Main duct-IPMN; BD-IPMN: Branch duct-IPMN; CI: Confidence interval.

Table 8 Multivariable analysis patients with branch-duct intra-ductal papillary mucinous neoplasm with and without recurrent acute pancreatitis

	With RAP (*n* = 29)	Without RAP (*n* = 143)	*P* value
	Odds ratio	95%CI	
Location of cyst			
Head	-	-	
Neck	-	-	
Body	0.61173	[0.059835, 6.254136]	0.679
Tail	0.537057	[0.050552, 5.705601]	0.606
Diffuse	-	-	
Pathological subtype			
Intestinal	-	-	
Gastric	-	-	
Pancreatobiliary	0.461648	[0.063565, 3.352753]	0.445
Oncocytic	-	-	
Unknown	1.458186	[0.15039, 14.13861]	0.745

RAP: Recurrent acute pancreatitis; CI: Confidence interval.

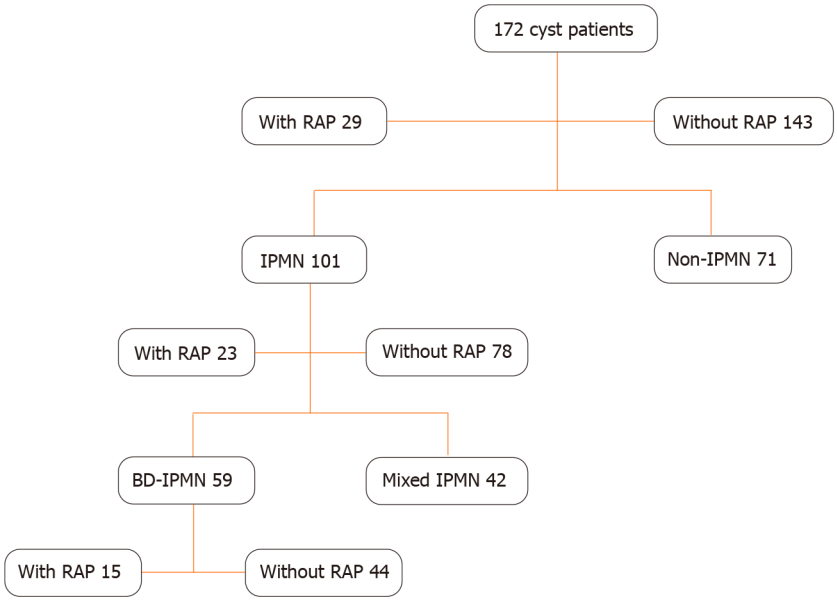

Figure 1 Flow chart of patient population with cyst resection. RAP: Recurrent acute pancreatitis; IPMN: Intra-ductal papillary mucinous neoplasm; BD-IPMN: Branch duct--IPMN.

ARTICLE HIGHLIGHTS

Research background

Pancreatic cystic neoplasms may present recurrent acute pancreatitis (RAP). Little is known on the role of resection for preventing RAP and if any correlation of higher prevalence of malignancy is seen among these patients.

Research motivation

Predicting malignancy among the pancreatic cystic neoplasms and management of RAP is challenging.

Research objectives

The objective of this research was to study the role of resection to help prevent RAP and analyze if presentation as RAP would be a predictor for malignancy.

Research methods

We adopted a retrospective cohort study model, enrolling all the patients with pancreatic cystic neoplasms who underwent surgical resection and compare between those who presented with RAP and without RAP. Incidence of RAP after resection and prevalence of malignancy among those who presented with RAP were the primary outcomes.

Research results

Malignancy was similar among those with *vs* without RAP for all patients 20.7% *vs* 16.8%. The mean episodes of acute pancreatitis before *vs* after surgery were 3.4 *vs* 0.02 ($P < 0.0001$). These findings clearly contribute much to this area of science. Although, this study clearly shows the risk reduction of RAP after the pancreatic resection, further investigation with large population prospective study is needed to prove a causal relationship between the cause of RAP and pancreatic resection.

Research conclusions

When patients with RAP are noted to have pancreatic cysts, it should be emphasized to differentiate if those cysts are the cause or the effect of RAP, *i.e.*, if cystic neoplasms are causing the RAP or if cysts are pseudocysts as a result of RAP. Larger data is needed to see if there exists a causal relationship. Similar to the presentation of jaundice as a predictor for malignancy among pancreas cystic neoplasms, RAP may have a role as a predictor of high-risk cysts.

Research perspectives

Future research to be focused on a larger prospective cohort to answer the above two questions.

REFERENCES

1 **Peery AF**, Crockett SD, Murphy CC, Lund JL, Dellon ES, Williams JL, Jensen ET, Shaheen NJ, Barritt AS, Lieber SR, Kochar B, Barnes EL, Fan YC, Pate V, Galanko J, Baron TH, Sandler RS. Burden and Cost of Gastrointestinal, Liver, and Pancreatic Diseases in the United States: Update 2018. *Gastroenterology* 2019; **156**: 254-272. e11 [PMID: 30315778 DOI: 10.1053/j.gastro.2018.08.063]

2 **Venkatesh PG**, Navaneethan U, Vege SS. Intraductal papillary mucinous neoplasm and acute pancreatitis. *J Clin Gastroenterol* 2011; **45**: 755-758 [PMID: 21602701 DOI: 10.1097/MCG.0b013e31821b1081]

3 **Jang JW**, Kim MH, Jeong SU, Kim J, Park DH, Lee SS, Seo DW, Lee SK, Kim JH. Clinical characteristics of intraductal papillary mucinous neoplasm manifesting as acute pancreatitis or acute recurrent pancreatitis. *J Gastroenterol Hepatol* 2013; **28**: 731-738 [PMID: 23301513 DOI: 10.1111/jgh.12121]

4 **Tibayan F**, Vierra M, Mindelzun B, Tsang D, McClenathan J, Young H, Trueblood HW. Clinical presentation of mucin-secreting tumors of the pancreas. *Am J Surg* 2000; **179**: 349-351 [PMID: 10930477 DOI: 10.1016/s0002-9610(00)00376-7]

5 **Crippa S**, Fernández-Del Castillo C, Salvia R, Finkelstein D, Bassi C, Domínguez I, Muzikansky A, Thayer SP, Falconi M, Mino-Kenudson M, Capelli P, Lauwers GY, Partelli S, Pederzoli P, Warshaw AL. Mucin-producing neoplasms of the pancreas: an analysis of distinguishing clinical and epidemiologic characteristics. *Clin Gastroenterol Hepatol* 2010; **8**: 213-219 [PMID: 19835989 DOI: 10.1016/j.cgh.2009.10.001]

6 **Banks PA**, Bollen TL, Dervenis C, Gooszen HG, Johnson CD, Sarr MG, Tsiotos GG, Vege SS; Acute Pancreatitis Classification Working Group. Classification of acute pancreatitis--2012: revision of the Atlanta classification and definitions by international consensus. *Gut* 2013; **62**: 102-111 [PMID: 23100216 DOI: 10.1136/gutjnl-2012-302779]

7 **Ahmed Ali U**, Issa Y, Hagenaars JC, Bakker OJ, van Goor H, Nieuwenhuijs VB, Bollen TL, van Ramshorst B, Witteman BJ, Brink MA, Schaapherder AF, Dejong CH, Spanier BW, Heisterkamp J, van der Harst E, van Eijck CH, Besselink MG, Gooszen HG, van Santvoort HC, Boermeester MA. Risk of Recurrent Pancreatitis and Progression to Chronic Pancreatitis After a First Episode of Acute Pancreatitis. *Clin Gastroenterol Hepatol* 2016; **14**: 738-746 [PMID: 26772149 DOI: 10.1016/j.cgh.2015.12.040]

8 **Yadav D**, O'Connell M, Papachristou GI. Natural history following the first attack of acute pancreatitis. *Am J Gastroenterol* 2012; **107**: 1096-1103 [PMID: 22613906 DOI: 10.1038/ajg.2012.126]

9 **Sankaran SJ**, Xiao AY, Wu LM, Windsor JA, Forsmark CE, Petrov MS. Frequency of progression from acute to chronic pancreatitis and risk factors: a meta-analysis. *Gastroenterology* 2015; **149**: 1490-1500. e1 [PMID: 26299411 DOI: 10.1053/j.gastro.2015.07.066]

10 **Coyle WJ**, Pineau BC, Tarnasky PR, Knapple WL, Aabakken L, Hoffman BJ, Cunningham JT, Hawes RH, Cotton PB. Evaluation of unexplained acute and acute recurrent pancreatitis using endoscopic retrograde cholangiopancreatography, sphincter of Oddi manometry and endoscopic ultrasound. *Endoscopy* 2002; **34**: 617-623 [PMID: 12173081 DOI: 10.1055/s-2002-33245]

11 **Sajith KG**, Chacko A, Dutta AK. Recurrent acute pancreatitis: clinical profile and an approach to diagnosis. *Dig Dis Sci* 2010; **55**: 3610-3616 [PMID: 20232145 DOI: 10.1007/s10620-010-1175-8]

12 **Testoni PA**. Acute recurrent pancreatitis: Etiopathogenesis, diagnosis and treatment. *World J Gastroenterol* 2014; **20**: 16891-16901 [PMID: 25493002 DOI: 10.3748/wjg.v20.i45.16891]

13 **Hruban RPM**, Klimstra DS. Tumors of the Pancreas. Washington, DC: American Registry of Pathology, 2007

14 **Adsay NV**, Fukushima N. Bosman FT, Carneiro F, Hruban RH, Theise ND. Intraductal neoplasms of the pancreas, WHO Classification of Tumors. 4th ed. Lyon, France: WHO Press, 2010

15 **Ma GK**, Goldberg DS, Thiruvengadam N, Chandrasekhara V, Kochman ML, Ginsberg GG, Vollmer CM, Ahmad NA. Comparing American Gastroenterological Association Pancreatic Cyst Management Guidelines with Fukuoka Consensus Guidelines as Predictors of Advanced Neoplasia in Patients with Suspected Pancreatic Cystic Neoplasms. *J Am Coll Surg* 2016; **223**: 729-737. e1 [PMID: 27497827 DOI: 10.1016/j.jamcollsurg.2016.07.011]

16 **Tanaka M**, Fernández-del Castillo C, Adsay V, Chari S, Falconi M, Jang JY, Kimura W, Levy P, Pitman MB, Schmidt CM, Shimizu M, Wolfgang CL, Yamaguchi K, Yamao K; International Association of Pancreatology. International consensus guidelines 2012 for the management of IPMN and MCN of the pancreas. *Pancreatology* 2012; **12**: 183-197 [PMID: 22687371 DOI: 10.1016/j.pan.2012.04.004]

17 **Patra KC**, Bardeesy N, Mizukami Y. Diversity of Precursor Lesions For Pancreatic Cancer: The Genetics and Biology of Intraductal Papillary Mucinous Neoplasm. *Clin Transl Gastroenterol* 2017; **8**: e86 [PMID: 28383565 DOI: 10.1038/ctg.2017.3]

18 **Furukawa T**, Hatori T, Fujita I, Yamamoto M, Kobayashi M, Ohike N, Morohoshi T, Egawa S, Unno M, Takao S, Osako M, Yonezawa S, Mino-Kenudson M, Lauwers GY, Yamaguchi H, Ban S, Shimizu M. Prognostic relevance of morphological types of intraductal papillary mucinous neoplasms of the pancreas. *Gut* 2011; **60**: 509-516 [PMID: 21193453 DOI: 10.1136/gut.2010.210567]

19 **Goh BK**, Tan YM, Cheow PC, Chung YF, Chow PK, Wong WK, Ooi LL. Cystic lesions of the pancreas: an appraisal of an aggressive resectional policy adopted at a single institution during 15 years. *Am J Surg* 2006; **192**: 148-154 [PMID: 16860621 DOI: 10.1016/j.amjsurg.2006.02.020]

20 **Kitagawa Y**, Unger TA, Taylor S, Kozarek RA, Traverso LW. Mucus is a predictor of better prognosis and survival in patients with intraductal papillary mucinous tumor of the pancreas. *J Gastrointest Surg* 2003; **7**: 12-19 [PMID: 12559180 DOI: 10.1016/S1091-255X(02)00152-X]

21 **Sugiyama M**, Izumisato Y, Abe N, Masaki T, Mori T, Atomi Y. Predictive factors for malignancy in intraductal papillary-mucinous tumours of the pancreas. *Br J Surg* 2003; **90**: 1244-1249 [PMID: 14515294 DOI: 10.1002/bjs.4265]

22 **Pelletier AL**, Hammel P, Rebours V, Couvelard A, Vullierme MP, Maire F, Hentic O, Aubert A, Sauvanet A, Lévy P, Ruszniewski P. Acute pancreatitis in patients operated on for intraductal papillary mucinous neoplasms of the pancreas: frequency, severity, and clinicopathologic correlations. *Pancreas* 2010; **39**: 658-661 [PMID: 20173669 DOI: 10.1097/MPA.0b013e3181c81b74]

23 **Morales-Oyarvide V**, Mino-Kenudson M, Ferrone CR, Gonzalez-Gonzalez LA, Warshaw AL, Lillemoe KD, Fernández-del Castillo C. Acute pancreatitis in intraductal papillary mucinous neoplasms: A common predictor of malignant intestinal subtype. *Surgery* 2015; **158**: 1219-1225 [PMID: 26077509 DOI: 10.1016/j.surg.2015.04.029]

24 **Aso T**, Ohtsuka T, Ideno N, Kono H, Nagayoshi Y, Mori Y, Ohuchida K, Ueda J, Takahata S, Morimatsu K, Aishima S, Igarashi H, Ito T, Ishigami K, Mizumoto K, Tanaka M. Diagnostic significance of a dilated orifice of the duodenal papilla in intraductal papillary mucinous neoplasm of the pancreas. *Gastrointest Endosc* 2012; **76**: 313-320 [PMID: 22658387 DOI: 10.1016/j.gie.2012.03.682]

25 **Adsay NV**, Merati K, Basturk O, Iacobuzio-Donahue C, Levi E, Cheng JD, Sarkar FH, Hruban RH, Klimstra DS. Pathologically and biologically distinct types of epithelium in intraductal papillary mucinous neoplasms: delineation of an "intestinal" pathway of carcinogenesis in the pancreas. *Am J Surg Pathol* 2004; **28**: 839-848 [PMID: 15223952 DOI: 10.1097/00000478-200407000-00001]

26 **Adsay NV**, Merati K, Andea A, Sarkar F, Hruban RH, Wilentz RE, Goggins M, Iocobuzio-Donahue C, Longnecker DS, Klimstra DS. The dichotomy in the preinvasive neoplasia to invasive carcinoma sequence in the pancreas: differential expression of MUC1 and MUC2 supports the existence of two separate pathways of carcinogenesis. *Mod Pathol* 2002; **15**: 1087-1095 [PMID: 12379756 DOI: 10.1097/01.mp.0000028647.98725.8b]

27 **Hata T**, Sakata N, Okada T, Aoki T, Motoi F, Katayose Y, Egawa S, Unno M. Dilated papilla with mucin extrusion is a potential predictor of acute pancreatitis associated with intraductal papillary mucinous neoplasms of pancreas. *Pancreatology* 2013; **13**: 615-620 [PMID: 24280579 DOI: 10.1016/j.pan.2013.09.003]

28 **Vege SS**, Ziring B, Jain R, Moayyedi P; Clinical Guidelines Committee; American Gastroenterology Association. American gastroenterological association institute guideline on the diagnosis and management of asymptomatic neoplastic pancreatic cysts. *Gastroenterology* 2015; **148**: 819-22; quize12 [PMID: 25805375 DOI: 10.1053/j.gastro.2015.01.015]

29 **Tanaka M**, Fernández-Del Castillo C, Kamisawa T, Jang JY, Levy P, Ohtsuka T, Salvia R, Shimizu Y, Tada M, Wolfgang CL. Revisions of international consensus Fukuoka guidelines for the management of IPMN of the pancreas. *Pancreatology* 2017; **17**: 738-753 [PMID: 28735806 DOI: 10.1016/j.pan.2017.07.007]

30 **European Study Group on Cystic Tumours of the Pancreas**. European evidence-based guidelines on pancreatic cystic neoplasms. *Gut* 2018; **67**: 789-804 [PMID: 29574408 DOI: 10.1136/gutjnl-2018-316027]

31 **Elta GH**, Enestvedt BK, Sauer BG, Lennon AM. ACG Clinical Guideline: Diagnosis and Management of Pancreatic Cysts. *Am J Gastroenterol* 2018; **113**: 464-479 [PMID: 29485131 DOI: 10.1038/ajg.2018.14]

32 **Kirkegård J**, Cronin-Fenton D, Heide-Jørgensen U, Mortensen FV. Acute Pancreatitis and Pancreatic Cancer Risk: A Nationwide Matched-Cohort Study in Denmark. *Gastroenterology* 2018; **154**: 1729-1736 [PMID: 29432727 DOI: 10.1053/j.gastro.2018.02.011]

33 **Moore JV**, Tom S, Scoggins CR, Philips P, Egger ME, Martin RCG 2nd. Exocrine Pancreatic Insufficiency After Pancreatectomy for Malignancy: Systematic Review and Optimal Management Recommendations. *J Gastrointest Surg* 2021 [PMID: 33483914 DOI: 10.1007/s11605-020-04883-1]

34 **Bernardoni L**, Crinò SF, De Conti G, Conti Bellocchi MC, De Pretis N, Amodio A, Frulloni L, Gabbrielli A. Preliminary experience with pancreatic sphincterotomy as treatment for intraductal papillary mucinous neoplasm-associated recurrent pancreatitis. *Endosc Int Open* 2017; **5**: E1144-E1150 [PMID: 29124124 DOI: 10.1055/s-0043-119753]

World Journal of Gastroenterology

Submit a Manuscript: https://www.f6publishing.com

World J Gastroenterol 2021 April 21; 27(15): 1643-1654

DOI: 10.3748/wjg.v27.i15.1643

ISSN 1007-9327 (print) ISSN 2219-2840 (online)

ORIGINAL ARTICLE

Retrospective Study

Intestinal bacterial overgrowth in the early stage of severe acute pancreatitis is associated with acute respiratory distress syndrome

Xue-Ying Liang, Tian-Xu Jia, Mei Zhang

ORCID number: Xue-Ying Liang 0000-0002-8815-6493; Tian-Xu Jia 0000-0001-5375-9625; Mei Zhang 0000-0002-8596-1868.

Author contributions: Liang XY made substantial contributions to the conception and design of the study, acquisition, analysis, and interpretation of data, and drafting the article; Jia TX made substantial contributions to the acquisition and analysis of data; Zhang M made substantial contributions to the conception, design and guide of the study; all authors read and approved the final manuscript.

Supported by Beijing Municipal Education Commission Science and Technology Plan General Project, No. KM201310025015.

Institutional review board statement: The study was reviewed and approved by the Department of Gastroenterology of Xuanwu Hospital, Capital Medical University.

Informed consent statement: All study participants, or their legal guardian, provided informed written consent prior to study enrollment.

Conflict-of-interest statement: The authors declare the absence of conflicts of interest.

Xue-Ying Liang, Tian-Xu Jia, Mei Zhang, Department of Gastroenterology, Xuanwu Hospital, Capital Medical University, Beijing 100053, China

Corresponding author: Mei Zhang, PhD, Chief Physician, Doctor, Professor, Department of Gastroenterology, Xuanwu Hospital, Capital Medical University, No. 45 Changchun Street, Xuanwu District, Beijing 100053, China. zhang2955@sina.com

Abstract

BACKGROUND

In the early stage of acute pancreatitis (AP), a large number of cytokines induced by local pancreatic inflammation seriously damage the intestinal barrier function, and intestinal bacteria and endotoxins enter the blood, causing inflammatory storm, resulting in multiple organ failure, infectious complications, and other disorders, eventually leading to death. Intestinal failure occurs early in the course of AP, accelerating its development. As an alternative method to detect small intestinal bacterial overgrowth, the hydrogen breath test is safe, noninvasive, and convenient, reflecting the number of intestinal bacteria in AP indirectly. This study aimed to investigate the changes in intestinal bacteria measured using the hydrogen breath test in the early stage of AP to clarify the relationship between intestinal bacteria and acute lung injury (ALI)/acute respiratory distress syndrome (ARDS). Early clinical intervention and maintenance of intestinal barrier function would be highly beneficial in controlling the development of severe acute pancreatitis (SAP).

AIM

To analyze the relationship between intestinal bacteria change and ALI/ARDS in the early stage of SAP.

METHODS

A total of 149 patients with AP admitted to the intensive care unit of the Digestive Department, Xuanwu Hospital, Capital Medical University from 2016 to 2019 were finally enrolled, following compliance with the inclusion and exclusion criteria. The results of the hydrogen breath test within 1 wk of admission were collected, and the hydrogen production rates at admission, 72 h, and 96 h were calculated. The higher the hydrogen production rates the more bacteria in the small intestine. First, according to the improved Marshall scoring system in the 2012 Atlanta Consensus on New Standards for Classification of Acute

Data sharing statement: No additional data are available.

Manuscript source: Unsolicited manuscript

Specialty type: Gastroenterology and hepatology

Country/Territory of origin: China

Peer-review report's scientific quality classification

Grade A (Excellent): A
Grade B (Very good): B, B
Grade C (Good): 0
Grade D (Fair): 0
Grade E (Poor): 0

Received: December 22, 2020
Peer-review started: December 22, 2020
First decision: January 27, 2021
Revised: February 4, 2021
Accepted: March 10, 2021
Article in press: March 10, 2021
Published online: April 21, 2021

P-Reviewer: Kumar N, Lens S, Levick C
S-Editor: Gao CC
L-Editor: Webster JR
P-Editor: Ma YJ

Pancreatitis, 66 patients with a PaO_2/FiO_2 score ≤ 1 were included in the mild AP (MAP) group, 18 patients with a PaO_2/FiO_2 score ≥ 2 and duration < 48 h were included in the moderately SAP (MSAP) group, and 65 patients with a PaO_2/FiO_2 score ≥ 2 and duration > 48 h were included in the SAP group, to analyze the correlation between intestinal bacterial overgrowth and organ failure in AP. Second, ALI (PaO_2/FiO_2 = 2) and ARDS (PaO_2/FiO_2 > 2) were defined according to the simplified diagnostic criteria proposed by the 1994 European Union Conference. The MSAP group was divided into two groups according to the PaO_2/FiO_2 score: 15 patients with PaO_2/FiO_2 score = 2 were included in group A, and three patients with score > 2 were included in group B. Similarly, the SAP group was divided into two groups: 28 patients with score = 2 were included in group C, and 37 patients with score > 2 were included in group D, to analyze the correlation between intestinal bacterial overgrowth and ALI/ARDS in AP.

RESULTS

A total of 149 patients were included: 66 patients in the MAP group, of whom 53 patients were male (80.3%) and 13 patients were female (19.7%); 18 patients in the MSAP group, of whom 13 patients were male (72.2%) and 5 patients were female (27.8%); 65 patients in the SAP group, of whom 48 patients were male (73.8%) and 17 patients were female (26.2%). There was no significant difference in interleukin-6 and procalcitonin among the MAP, MSAP, and SAP groups (P = 0.445 and P = 0.399, respectively). There was no significant difference in the growth of intestinal bacteria among the MAP, MSAP, and SAP groups (P = 0.649). There was no significant difference in the growth of small intestinal bacteria between group A and group B (P = 0.353). There was a significant difference in the growth of small intestinal bacteria between group C and group D (P = 0.038).

CONCLUSION

Intestinal bacterial overgrowth in the early stage of SAP is correlated with ARDS.

Key Words: Acute respiratory distress syndrome; Hydrogen breath test; Intestinal bacterial overgrowth; Severe acute pancreatitis; Interleukin-6; Acute lung injury

Core Tip: Our retrospective study included 149 patients with acute pancreatic disease. The changes in intestinal flora were detected by the hydrogen breath test. We found that the change in intestinal flora in patients with severe acute pancreatitis was related to acute respiratory distress syndrome, which can aggravate the disease. The results of the hydrogen breath test can be used as a warning signal for severe acute pancreatitis.

Citation: Liang XY, Jia TX, Zhang M. Intestinal bacterial overgrowth in the early stage of severe acute pancreatitis is associated with acute respiratory distress syndrome. *World J Gastroenterol* 2021; 27(15): 1643-1654
URL: https://www.wjgnet.com/1007-9327/full/v27/i15/1643.htm
DOI: https://dx.doi.org/10.3748/wjg.v27.i15.1643

INTRODUCTION

Acute pancreatitis (AP) is a common form of acute abdomen. The mortality rate of severe AP (SAP) with early organ failure can be as high as 36%-50%[1]. The earliest SAP-related organ dysfunction occurs in the respiratory system with the main symptoms of acute lung injury (ALI) and acute respiratory distress syndrome (ARDS)[2,3]. In the early stage of AP, a large number of cytokines is induced by local pancreatitis to enter the bloodstream, causing systemic inflammatory response syndrome (SIRS) through the cytokine cascade reaction; the large number of released cytokines can seriously damage the intestinal barrier function and increase intestinal wall permeability, intestinal microbial flora imbalance, intestinal bacterial overgrowth, and intestinal bacterial translocation. When intestinal bacteria and endotoxins enter

the blood, leading to multiple organ failure (multiple organ dysfunction syndrome), the end result is death[4].

The results of animal experiments have shown that when intestinal ischemia occurs in SAP, the mechanical barrier of the intestinal tract is damaged, the permeability of small intestine and colon mucosa is increased, and damage in the small intestine becomes more obvious; at that time, small intestine peristalsis decreases or even disappears, and the number of bacteria in the small intestine and colon rapidly increases, leading to small intestinal bacterial overgrowth (SIBO)[5]. Cen *et al*[4] established a model of intestinal motility disorder in AP rats, indicating that gastrointestinal motility disorder is the early cause of SIBO. Intestinal motility disorder is caused by neurohormone-mediated intestinal motility reduction induced by AP[6]. *Escherichia coli* and other bacteria grow excessively due to stagnation of substances in the cavity.

The gold standard for SIBO evaluation is quantitative culture of duodenal or jejunal aspiration under aerobic and anaerobic conditions, and a study found colony formation higher than 10^3 CFU/mL (colony-forming unit/mL)[7]. Because of the high cost and invasive nature of small intestinal fluid aspiration culture, the hydrogen breath test, as an alternative method for SIBO testing, has been suggested as an inexpensive, safe, and noninvasive alternative. It is widely used in the clinic as an important method to diagnose SIBO. However, the sensitivity range of the hydrogen breath test is 20%-90%, possibly because of the lack of uniform diagnostic criteria, which has been resolved by the recently published North American breath test consensus[8].

The lactose hydrogen respiration test is a noninvasive semi-qualitative test, originally designed to measure the oral-cecum passage time; it is currently used for many diseases of the digestive system, such as lactose intolerance, irritable bowel syndrome, dyspepsia, and non-alcoholic fatty liver[9,10]. The premise of the hydrogen breath test to detect SIBO is that the human metabolism does not produce hydrogen or methane. Methanogens are not bacteria, but belong to the category of archaea, mainly present in the colon, accounting for 10% of all anaerobic organisms[7]. Since the production of methane requires hydrogen metabolism, the hydrogen and methane concentrations can be simultaneously detected with the carbohydrate breath test. The lactulose hydrogen respiration test involves oral lactulose (non-absorbent sugar) to the cecum, fermentation with coliform bacteria to produce hydrogen and methane, absorption into the systemic circulation, and then exhalation to detect the concentration of hydrogen/methane in the breath; when the concentration of hydrogen/methane in the breath exceeds the baseline, a SIBO diagnosis can be reached[11].

This study aimed to examine the change in intestinal bacteria measured using the hydrogen breath test in the early stage of AP to elucidate the relationship between intestinal bacteria and ALI/ARDS. Early clinical intervention and maintenance of intestinal barrier function will be very beneficial in controlling the development of SAP.

MATERIALS AND METHODS

Research object and grouping

We retrospectively analyzed the data of 456 patients with AP who met the diagnostic criteria of the 2012 "Consensus on New Atlanta Classification Standards for Acute Pancreatitis" and who were admitted to the intensive care unit (ICU) of the Department of Digestive Department, Xuanwu Hospital of Capital Medical University from 2016 to 2019. A total of 152 patients were admitted with SIRS or organ failure and could cooperate with the hydrogen breath test within 1 wk of admission. According to the 2012 "Consensus on New Atlanta Classification Standards for Acute Pancreatitis" improved Marshall scoring standard[1], 1 patient had circulatory failure, 2 patients had renal failure, 66 patients had no organ failure, and 83 patients had respiratory failure. One patient with circulatory failure and 2 patients with renal failure were excluded. A total of 149 patients were finally included. General data including age, sex, body mass index (BMI), Acute Physiology and Chronic Health Evaluation (APACHE)-II score, and mediators of inflammation were collected.

Inclusion criteria: (1) admission within 48 h after onset; (2) admission to the hospital with SIRS; (3) organ failure within 1 wk after admission; (4) age older than 18 years; and (5) clear mind, understanding ability normal, ability to communicate with the

physician.

Exclusion criteria: (1) chronic pancreatitis; (2) history of immune-related diseases, immune deficiency, and AIDS; (3) malignant tumors; (4) inability to cooperate and complete the hydrogen breath test; (5) incomplete case data; or (6) circulatory failure or renal failure.

Grouping

According to the improved Marshall score standard in the 2012 "Consensus on New Atlanta Classification Standards for Acute Pancreatitis"[1]: $PaO_2/FiO_2 \geq 301$ mmHg was scored as 1 point, 201 mmHg ≤ $PaO_2/FiO_2 \leq 300$ mmHg was scored as 2 points, 101 mmHg ≤ $PaO_2/FiO_2 \leq 200$ mmHg was scored as 3 points, and $PaO_2/FiO_2 \leq 101$ mmHg was scored as 4 points.

Methods: 66 patients with a PaO_2/FiO_2 score ≤ 1 were included in the mild AP (MAP) group, 18 patients with a PaO_2/FiO_2 score ≥ 2 and duration < 48 h were included in the moderately SAP (MSAP) group, and 65 patients with a PaO_2/FiO_2 score ≥ 2 and duration > 48 h were included in the SAP group (Figure 1).

ALI and ARDS: ALI and ARDS were defined according to the European Union Conference[12]. The simplified criteria recommended by the meeting included defining arterial hypoxia $PaO_2/FiO_2 < 300$ mmHg as ALI and $PaO_2/FiO_2 < 200$ mmHg as ARDS, excluding cardiogenic pulmonary edema. In this study, a PaO_2/FiO_2 score = 2 was used to define ALI, and a PaO_2/FiO_2 score > 2 was used to define ARDS.

Methods: The MSAP group was divided into two groups according to the PaO_2/FiO_2 score: 15 patients with PaO_2/FiO_2 score = 2 were included in group A, and 3 patients with score > 2 were included in group B. Similarly, the SAP group was divided into two groups: 28 patients with score = 2 were included in group C, and 37 patients with score > 2 were included in group D (Figure 1).

Treatment

MAP: (1) abrosia, gastrointestinal decompression, saline enema; (2) fluid resuscitation, water maintenance, electrolyte and acid-base balance; and (3) lactulose to improve intestinal function, proton pump inhibitors for gastric acid secretion, ulinastatin and/or gabexate to improve pancreatic microcirculation.

MSAP/SAP: (1) abrosia, gastrointestinal decompression, saline enema; (2) fluid resuscitation, water maintenance, electrolyte and acid-base balance; and (3) lactulose to improve intestinal function, proton pump inhibitors for gastric acid secretion, ulinastatin and/or gabexate to improve pancreatic microcirculation; octreotide to inhibit pancreatic exocrine function, and parenteral nutrition support.

When ARDS appeared it was treated with a mechanical ventilator. When renal failure appeared it was treated with CRRT (continuous renal replacement therapy). Vasoactive drugs were used to increase blood pressure when circulatory failure could not be corrected. Peri-pancreatic and extra-pancreatic infections were treated with anti-infection therapy.

Outcome: After treatment, when there was no abdominal pain, abdominal distension, or fever, and when there were active bowel sounds, spontaneous defecation, and the abdominal computed tomography re-examination showed marked improvement, the patient could be discharged from the ICU (Figure 2).

Hydrogen breath test

Test methods: The patient remained awake and quiet during the examination and did not exercise vigorously. For the detection process, the fasting breath was collected twice, and the highest value was used as the basic exhaled hydrogen concentration (H_0). The subjects were asked to quickly consume a lactulose solution including 10 g of lactulose in 100 mL of room-temperature pure water. Subjects then exhaled every 20 min 9 times (H_1-H_9). The hydrogen concentration in the exhalation was measured and recorded at each time point.

Data processing: Hydrogen production at admission, 72 h and 96 h was measured. The average hydrogen production rate was calculated as follows: $[H_n\text{-}H_{(n-1)}]/H_0$, ($0< n \leq 9$).

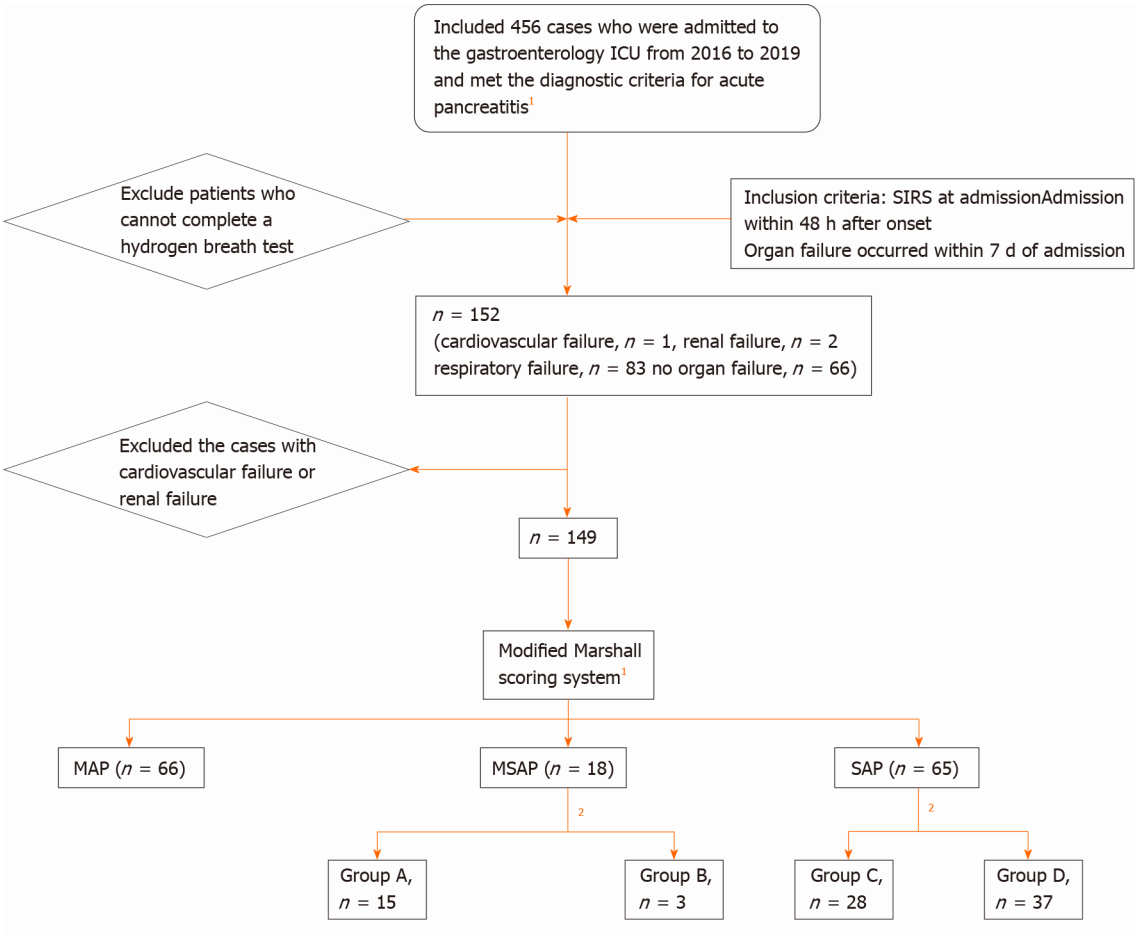

Figure 1 Research sample screening and grouping process. [1]Classification of acute pancreatitis 2012: revision of the Atlanta classification and definitions by international consensus. [2]Report of the American-European Consensus conference on acute respiratory distress syndrome in 1994. Simplified standard: PaO_2/FiO_2 < 300 mmHg is defined as acute lung injury and PaO_2/FiO_2 < 200 mmHg is defined as acute respiratory distress syndrome, and excludes cardiogenic pulmonary edema. Group A: PaO_2/FiO_2 = 2; Group B: PaO_2/FiO_2 > 2; Group C: PaO_2/FiO_2 = 2; Group D: PaO_2/FiO_2 > 2; ICU: Intensive care unit; SIRS: Systemic inflammatory response syndrome; MAP: Mild acute pancreatitis; MSAP: Moderately severe acute pancreatitis; SAP: Severe acute pancreatitis.

Statistical analysis

SPSS 25.0 (IBM Corp., Armonk, NY, United States) was used for data analysis, $P < 0.05$ was considered statistically significant. Age, BMI, APACHE-II score, and mediators of inflammation were measured, and the data are expressed as mean ± SD; and one-way analysis of variance (ANOVA) was used to compare the two groups. The hydrogen breath test data are expressed as the average hydrogen production rate ± SD, and the repeated-measures ANOVA was used in the comparison between the two groups. The number and percentage of counting data were expressed, and the chi-square test was used for comparison between the groups.

RESULTS

Clinical characteristics

A total of 149 patients were included: 66 patients in the MAP group, of whom, 53 patients were male (80.3%) and 13 patients were female (19.7%); 18 patients in the MSAP group, of whom 13 patients were male (72.2%) and 5 patients were female (27.8%); 65 patients in the SAP group, of whom 48 patients were male (73.8%) and 17 patients were female (26.2%) (Table 1). There was a significant difference in age, sex, and APACHE-II score among the MAP, MSAP, and SAP groups (both, $P < 0.001$) (Table 1).

Correlation between inflammation indicators and ALI/ARDS

There was no significant difference in interleukin (IL)-6 and procalcitonin among the MAP, MSAP, and SAP groups ($P = 0.445$ and $P = 0.399$, respectively) (Table 2). There

Table 1 Clinical characteristics

Variable	Total	MAP group	MSAP group	SAP group
Number of patients	149	66	18	65
Age, yr, (mean ± SD)	42.26 ± 12.95	36.62 ± 9.74	47.17 ± 15.17	43.00 ± 13.95
Sex (male/female)	114/35	53/13	13/5	48/17
BMI (kg/m^2)	28.21 ± 3.85	27.19 ± 3.77	27.98 ± 4.60	29.47 ± 3.77
APACHE-II score	5.92 ± 3.02	4.00 ± 3.23	6.50 ± 4.75	7.26 ± 4.07
Mortality (%)	0	0	0	0

MAP: Mild acute pancreatitis; MSAP: Moderately severe acute pancreatitis; SAP: Severe acute pancreatitis; BMI: Body mass index; APACHE: Acute Physiology and Chronic Health Evaluation.

Table 2 Correlation between inflammation indicators and acute lung injury/acute respiratory distress syndrome

Variable	Time	MAP group	MSAP group	SAP group	*P* value
IL-6	On admission	118.62 ± 137.66	98.36 ± 106.36	143.74 ± 174.40	0.445
PCT	On admission	0.46 ± 1.29	0.46 ± 0.74	0.67 ± 1.01	0.399
	72 h	0.35 ± 0.57	0.39 ± 0.49	0.66 ± 0.83	
	96 h	0.54 ± 2.51	0.19 ± 0.12	0.51 ± 0.64	

MAP: Mild acute pancreatitis; MSAP: Moderately severe acute pancreatitis; SAP: Severe acute pancreatitis; IL: Interleukin; PCT: Procalcitonin.

was no significant difference in IL-6 and procalcitonin among the MAP and MSAP groups (P = 0.306 and P = 0.683, respectively) (Table 3). There was no significant difference in IL-6 and procalcitonin among the MAP and SAP groups (P = 0.879 and P = 0.311, respectively) (Table 4). There was no significant difference in IL-6 and procalcitonin among the MSAP and SAP groups (P = 0.455 and P = 0.150, respectively) (Table 5).

Correlation between changes in the intestinal bacteria and ALI/ARDS

There was no significant difference in the number of intestinal bacteria among the MAP, MSAP, and SAP groups (P = 0.649) (Table 6). There was no significant difference in the number of intestinal bacteria among the MAP and MSAP groups (P = 0.196) (Table 7). There was no significant difference in the number of intestinal bacteria among the MAP and SAP groups (P = 0.494) (Table 8). There was no significant difference in the number of intestinal bacteria among the MSAP and SAP groups (P = 0.784) (Table 9). There was no significance difference in the number of intestinal bacteria and ALI/ARDS between group A and group B (P = 0.353) (Table 10). There was a significant difference in the number of intestinal bacteria and ALI/ARDS between group C and group D (P = 0.038) (Table 11, Figure 3). The changes in intestinal bacteria in the early stage of SAP were correlated with ARDS.

DISCUSSION

In this study, we used the hydrogen breath test to detect changes in intestinal bacteria in the early stage of AP and demonstrated that there was a correlation between ARDS and SIBO in the early stage of SAP.

This study also had some limitations. The results of the hydrogen breath test are easily affected by the number of aerogenes and the enzymatic activity of fructase. The number of gas-producing bacteria in the intestinal tract is affected by individual factors, including the environment and dietary habits, resulting in varying numbers of gas-producing bacteria among individuals. Abrosia and the use of antibiotics[13] also affect the number of gas-producing bacteria. The higher the enzymatic activity of fructase, the more gas is produced[11]. Routine lactulose treatment can improve the intestinal acid-base environment, reduce intestinal bacteria, and inhibitory activity[14];

Table 3 Correlation between the mild acute pancreatitis and moderately severe acute pancreatitis groups inflammation indicators and acute lung injury/acute respiratory distress syndrome

Variable	Time	MAP group	MSAP group	*P* value
IL-6	On admission	118.62 ± 137.66	98.36 ± 106.36	0.306
PCT	On admission	0.46 ± 1.29	0.46 ± 0.74	0.683
	72 h	0.35 ± 0.57	0.39 ± 0.49	
	96 h	0.54 ± 2.51	0.19 ± 0.12	

MAP: Mild acute pancreatitis; MSAP: Moderately severe acute pancreatitis; IL: Interleukin; PCT: Procalcitonin.

Table 4 Correlation between the mild acute pancreatitis and severe acute pancreatitis groups inflammation indicators and acute lung injury/acute respiratory distress syndrome

Variable	Time	MAP group	SAP group	*P* value
IL-6	On admission	118.62 ± 137.66	143.74 ± 174.40	0.879
PCT	On admission	0.46 ± 1.29	0.67 ± 1.01	0.311
	72 h	0.35 ± 0.57	0.66 ± 0.83	
	96 h	0.54 ± 2.51	0.51 ± 0.64	

MAP: Mild acute pancreatitis; SAP: Severe acute pancreatitis; IL: Interleukin; PCT: Procalcitonin.

Table 5 Correlation between the moderately severe acute pancreatitis and severe acute pancreatitis groups inflammation indicators and acute lung injury/acute respiratory distress syndrome

Variable	Time	MSAP group	SAP group	*P* value
IL-6	On admission	98.36 ± 106.36	143.74 ± 174.40	0.455
PCT	On admission	0.46 ± 0.74	0.67 ± 1.01	0.150
	72 h	0.39 ± 0.49	0.66 ± 0.83	
	96 h	0.19 ± 0.12	0.51 ± 0.64	

MSAP: Moderately severe acute pancreatitis; SAP: Severe acute pancreatitis; IL: Interleukin; PCT: Procalcitonin.

Table 6 Correlation between changes in intestinal bacteria and acute lung injury/acute respiratory distress syndrome

Hydrogen breath test	MAP group	MSAP group	SAP group	*P* value
On admission	1.63 ± 1.28	2.35 ± 2.14	1.68 ± 1.85	0.649
72 h	1.58 ± 1.29	1.83 ± 2.58	2.13 ± 3.27	
96 h	1.60 ± 1.22	1.58 ± 0.93	1.54 ± 1.35	

MAP: Mild acute pancreatitis; MSAP: Moderately severe acute pancreatitis; SAP: Severe acute pancreatitis.

there is also the catharsis effect of reduced intestinal bacteria; long-term lactulose treatment is equivalent to increasing the dose of lactulose in the hydrogen breath test, resulting in higher or lower results. In this study, quantitative analysis and the growth ratio were used to neutralize the influence of the basic value on the qualitative results.

As early as 2017, Zhang *et al*[15] and others were using the qualitative standard of the hydrogen breath test to examine the relationship between SAP and SIBO. The results showed that damage of intestinal barrier function is already present in the early stage of SAP; the positive SIBO rate was higher in patients with SAP, and SIBO mainly occurred within 72 h from onset. Finally, we found that there was a correlation

Table 7 Correlation between changes in intestinal bacteria and acute lung injury/acute respiratory distress syndrome

Hydrogen breath test	MAP group	MSAP group	*P* value
On admission	1.63 ± 1.28	2.35 ± 2.14	0.196
72 h	1.58 ± 1.29	1.83 ± 2.58	
96 h	1.60 ± 1.22	1.58 ± 0.93	

MAP: Mild acute pancreatitis; MSAP: Moderately severe acute pancreatitis.

Table 8 Correlation between changes in intestinal bacteria and acute lung injury/acute respiratory distress syndrome

Hydrogen breath test	MAP group	SAP group	*P* value
On admission	1.63 ± 1.28	1.68 ± 1.85	0.494
72 h	1.58 ± 1.29	2.13 ± 3.27	
96 h	1.60 ± 1.22	1.54 ± 1.35	

MAP: Mild acute pancreatitis; SAP: Severe acute pancreatitis.

Table 9 Correlation between changes in intestinal bacteria and acute lung injury/acute respiratory distress syndrome

Hydrogen breath test	MSAP group	SAP group	*P* value
On admission	2.35 ± 2.14	1.68 ± 1.85	0.784
72 h	1.83 ± 2.58	2.13 ± 3.27	
96 h	1.58 ± 0.93	1.54 ± 1.35	

MSAP: Moderately severe acute pancreatitis; SAP: Severe acute pancreatitis.

Table 10 Correlation between changes in intestinal bacteria and acute lung injury/acute respiratory distress syndrome in the moderately severe acute pancreatitis group

Hydrogen breath test	*P* value	MSAP group (*n* = 18)	
		Group A (*n* = 15)	Group B (*n* = 3)
On admission	0.353	2.59 ± 2.28	1.12 ± 0.04
72 h		1.97 ± 2.81	1.08 ± 0.43
96 h		1.54 ± 0.95	1.82 ± 0.95

MSAP: Moderately severe acute pancreatitis; Group A: $PaO_2/FiO_2 = 2$; Group B: $PaO_2/FiO_2 > 2$.

between ARDS and SIBO in the early stage of SAP ($P < 0.05$) in line with the results of previous studies. ALI/ARDS are the earliest organ-dysfunction symptoms in SAP. In this study, it was concluded that the occurrence of ARDS was related to SIBO within 72 h of admission. Studies have shown that SAP intestinal failure appears early, consistent with the results of our study. SAP-induced ALI/ARDS is mainly due to lung injury mediated by inflammatory factors[16]. Both infectious and non-infectious factors can lead to a large number of inflammatory factors. In the early stage of AP, inflammatory factors produced by pancreatic digestion damage intestinal barrier function, leading to persistent SIRS and SIBO, with SIBO leading to harmful metabolite accumulation in the intestinal tract, especially endotoxins and pathogenic intestinal bacteria[17]; subsequently, a large number of endotoxins and bacteria enter the bloodstream, flow through the pulmonary capillaries, activate neutrophils, damage the pulmonary vascular endothelium, leading to diffuse alveolar injury and type I alveolar necrosis, and eventually to ALI/ARDS[18,19]. Zhang *et al*[20] found that serum endotoxins

Table 11 Correlation between changes in intestinal bacteria and acute lung injury/acute respiratory distress syndrome in the severe acute pancreatitis group

Hydrogen breath test	*P* value	SAP group (*n* = 65)	
		Group C (*n* = 28)	Group D (*n* = 37)
On admission	0.038	2.39 ± 2.61	1.15 ± 0.58
72 h		1.68 ± 1.85	2.85 ± 4.79
96 h		1.84 ± 1.86	1.31 ± 0.71

SAP: Severe acute pancreatitis; Group C: $PaO_2/FiO_2 = 2$; Group D: $PaO_2/FiO_2 > 2$.

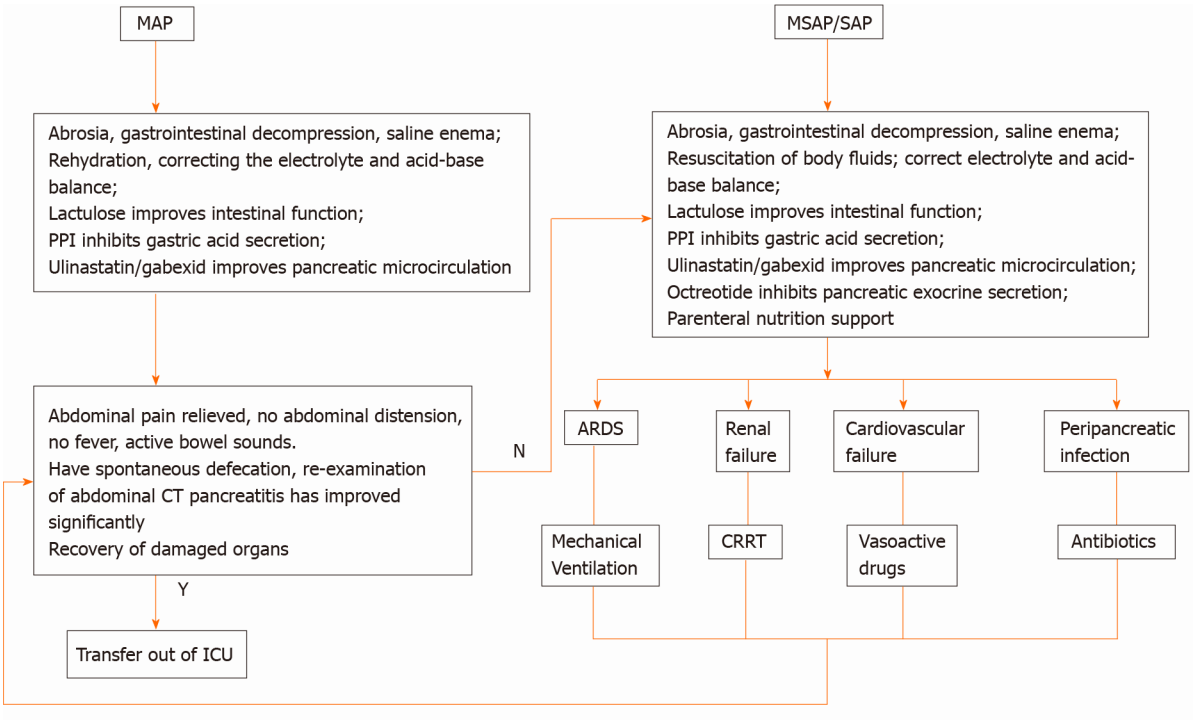

Figure 2 Treatment process. MAP: Mild acute pancreatitis; MSAP: Moderately severe acute pancreatitis; SAP: Severe acute pancreatitis; PPI: Proton pump inhibitor; CT: Computed tomography; ICU: Intensive care unit; ARDS: Acute respiratory distress syndrome; CRRT: Continuous renal replacement therapy; Y: Yes; N: No.

and intestinal mucosal permeability in patients with SAP were higher than in normal controls. Wang *et al*[3] found that lung bacteria were rich in intestine-related bacteria in mice with AP, sepsis, and ARDS. This study only showed the translocation of intestinal bacteria when sepsis and ARDS occurred simultaneously but did not explain the relationship between intestinal bacteria and ARDS when only ARDS occurred. Unfortunately, we could not locate animal experimental data on the correlation between ARDS and intestinal bacteria in the early stage of AP. The results of this clinical study showed that ARDS was correlated with intestinal bacteria, which should be further explored using animal models. However, although animal test support is lacking, in a clinical study on the relationship between the onset time and treatment time window of AP[21], the researchers concluded that the key time window for AP treatment is within 1 wk after the onset of AP; otherwise, the disease will worsen, the clinical course will be prolonged, and the mortality rate will increase; in terms of time, this study completely agrees with the previous research results. Therefore, the results of this study are of high guiding significance for clinicians who manage patients with AP. Early attention to the changes in intestinal bacteria can prevent the occurrence of SAP and high mortality.

This study also explored the correlation between IL-6 and ALI/ARDS. At present, the research results show that IL-6 is related to SAP. IL-6 can be used as an early predictor of complications[22]. The specificity of serum IL-6 > 160 pg/mL in the

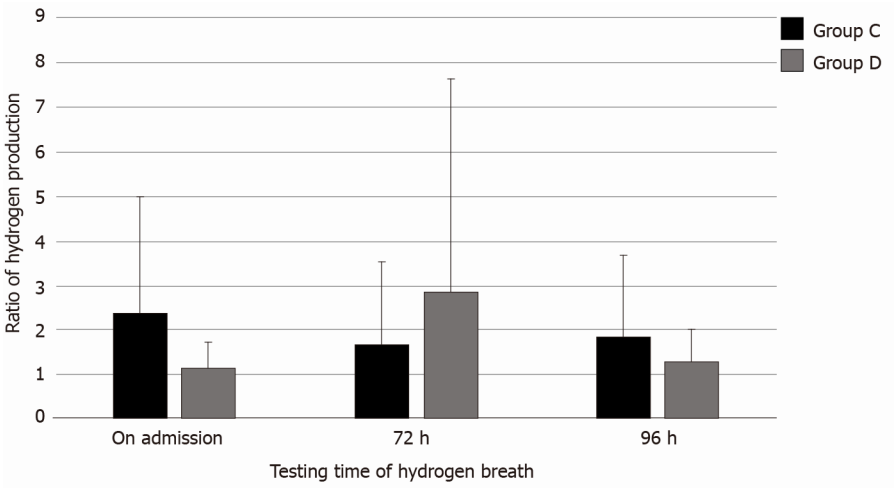

Figure 3 The correlation between changes in intestinal bacteria and acute lung injury/acute respiratory distress syndrome in the severe acute pancreatitis group. Group C: $PaO_2/FiO_2 = 2$; Group D: $PaO_2/FiO_2 > 2$.

diagnosis of SAP was 95%[23]. Relevant animal experiments have shown that when pancreatic injury occurs, IL-6 is rapidly synthesized to play an anti-inflammatory and protective role. When IL-6 continues to be synthesized and accumulates in large quantities, it mainly plays a pro-inflammatory role, leading to the occurrence and development of SAP[22]. In a clinical study conducted by Rezaie *et al*[13], it was found that the content of IL-6 in the blood was positively correlated with the abundance of *Enterobacteriaceae* and *Enterococci*, but negatively correlated with the abundance of *Bifidobacteria*. That study also compared the characteristics of intestinal bacteria between patients with AP and healthy controls. The results showed that the intestinal bacteria of patients with AP and healthy controls differed, and the abundance of *Enterobacteriaceae* and *Enterococci* and other potentially pathogenic bacteria differed from the abundance of beneficial bacteria such as *Bifidobacteria*, which decreased significantly. Although the final results of this study did not show a correlation between IL-6 and SAP, it is considered that this may be related to the treatments administered after admission.

CONCLUSION

Early organ failure in SAP was found to be closely related to the intestinal bacteria. Importantly, this study also determined the timing of SIBO, which is of great guiding significance for the clinical treatment of AP.

ARTICLE HIGHLIGHTS

Research background

In the early stage of acute pancreatitis (AP), a large number of cytokines induced by local pancreatic inflammation seriously destroy the intestinal barrier function, resulting in intestinal bacteria and endotoxins in the blood, causing inflammatory storms, and leading to multiple organ failure. Hydrogen breath testing is currently used for many diseases of the digestive system, such as lactose intolerance, irritable bowel syndrome, dyspepsia, and non-alcoholic fatty liver. This test, as an alternative method to detect small intestinal bacterial overgrowth (SIBO), was used to indirectly reflect the number of intestinal bacteria in AP. This study aimed to examine the change in intestinal bacteria measured using the hydrogen breath test in the early stage of AP to elucidate the relationship between intestinal bacteria and acute lung injury (ALI)/acute respiratory distress syndrome (ARDS). Early clinical intervention and maintenance of intestinal barrier function will be very beneficial in controlling the development of severe AP (SAP).

Research motivation

Clinical trials showed that intestinal bacteria in AP patients were different to those in healthy people and the abundance of potential pathogenic bacteria such as *Enterobacteriaceae* and *Enterococcus* increased significantly while the abundance of beneficial bacteria such as *Bifidobacterium* decreased significantly. Animal experiments showed that not only the changes in intestinal bacteria in patients with AP were verified, but also there was a correlation between the changes in intestinal bacteria and organ failure. However, neither of them showed a relationship between intestinal bacteria and organ failure in the early stage of AP. If we can understand the change in intestinal bacteria using the hydrogen breath test in the early stage of AP, in order to understand the relationship between intestinal bacteria and ALI/ARDS, we can intervene and maintain the stability of intestinal barrier function as soon as possible, which will be very beneficial in controlling the development of SAP.

Research objectives

Maintaining intestinal barrier function and reducing and preventing intestinal bacteria translocation have become the key to controlling the occurrence and development of SAP. This reduces complications in the early stage of the disease. We performed the present study to investigate the changes in organ function and intestinal bacteria in AP, and to explore the correlation between SIBO and AP organ function.

Research methods

Principle of the hydrogen breath test: after taking lactulose (nonabsorbable sugar), it reaches the cecum and is fermented with coliform bacteria to produce hydrogen and methane, which are absorbed into the systemic circulation and exhaled through the lung. When the hydrogen concentration in the exhaled breath exceeds the baseline, it is diagnosed as SIBO. In this study, a portable hydrogen expiratory detector was used to detect the patients' expired hydrogen concentration to diagnose SIBO. The change in exhaled hydrogen concentration can reflect the number of bacteria in the small intestine.

Research results

The results showed that in 37 SAP patients with ARDS, the average hydrogen production rate at admission was 1.15 ± 0.58, at 72 h was 2.85 ± 4.79 and at 96 h was 1.31 ± 0.71. In 28 SAP patients without ARDS, the average hydrogen production rate at admission was 2.39 ± 2.61, at 72 h was 1.68 ± 1.85, and at 96 h was 1.84 ± 1.86. The increase in intestinal bacteria in patients with SAP within 72 h after admission was related to the occurrence of ARDS. How to effectively maintain the stability of intestinal barrier function in the early stage of the disease and prevent the overgrowth of intestinal bacteria is a problem to be solved.

Research conclusions

In this study, intestinal bacterial overgrowth in the early stage of SAP was associated with ARDS. Moreover, the occurrence of ARDS was related to SIBO within 72 h of admission. It is of guiding significance to maintain the stability of intestinal barrier function in the early stage in order to reduce the complications of early organ failure and late infection.

Research perspectives

How to effectively maintain the stability of intestinal barrier function and prevent the excessive growth of intestinal bacteria in the early stage of disease, in order to reduce the occurrence and development of SAP, is the future research direction.

ACKNOWLEDGEMENTS

We thank Sun F, Professor of Medical Statistics, for advice on statistical methods and comments on the manuscript.

REFERENCES

1 **Banks PA**, Bollen TL, Dervenis C, Gooszen HG, Johnson CD, Sarr MG, Tsiotos GG, Vege SS; Acute Pancreatitis Classification Working Group. Classification of acute pancreatitis--2012: revision

of the Atlanta classification and definitions by international consensus. *Gut* 2013; **62**: 102-111 [PMID: 23100216 DOI: 10.1136/gutjnl-2012-302779]

2 **Wang H**, Li C, Jiang Y, Li H, Zhang D. Effects of Bacterial Translocation and Autophagy on Acute Lung Injury Induced by Severe Acute Pancreatitis. *Gastroenterol Res Pract* 2020; **2020**: 8953453 [PMID: 32104173 DOI: 10.1155/2020/8953453]

3 **Wang C**, Li Q, Ren J. Microbiota-Immune Interaction in the Pathogenesis of Gut-Derived Infection. *Front Immunol* 2019; **10**: 1873 [PMID: 31456801 DOI: 10.3389/fimmu.2019.01873]

4 **Cen ME**, Wang F, Su Y, Zhang WJ, Sun B, Wang G. Gastrointestinal microecology: a crucial and potential target in acute pancreatitis. *Apoptosis* 2018; **23**: 377-387 [PMID: 29926313 DOI: 10.1007/s10495-018-1464-9]

5 **Li XY**, He C, Zhu Y, Lu NH. Role of gut microbiota on intestinal barrier function in acute pancreatitis. *World J Gastroenterol* 2020; **26**: 2187-2193 [PMID: 32476785 DOI: 10.3748/wjg.v26.i18.2187]

6 **Yuan BS**, Zhu RM, Braddock M, Zhang XH, Shi W, Zheng MH. Interleukin-18: a pro-inflammatory cytokine that plays an important role in acute pancreatitis. *Expert Opin Ther Targets* 2007; **11**: 1261-1271 [PMID: 17907957 DOI: 10.1517/14728222.11.10.1261]

7 **Massey BT**, Wald A. Small Intestinal Bacterial Overgrowth Syndrome: A Guide for the Appropriate Use of Breath Testing. *Dig Dis Sci* 2021; **66**: 338-347 [PMID: 33037967 DOI: 10.1007/s10620-020-06623-6]

8 **Cangemi DJ**, Lacy BE, Wise J. Diagnosing Small Intestinal Bacterial Overgrowth: A Comparison of Lactulose Breath Tests to Small Bowel Aspirates. *Dig Dis Sci* 2020 [PMID: 32681227 DOI: 10.1007/s10620-020-06484-z]

9 **Yao CK**, Tuck CJ. The clinical value of breath hydrogen testing. *J Gastroenterol Hepatol* 2017; **32** Suppl 1: 20-22 [PMID: 28244675 DOI: 10.1111/jgh.13689]

10 **Takakura W**, Pimentel M. Small Intestinal Bacterial Overgrowth and Irritable Bowel Syndrome - An Update. *Front Psychiatry* 2020; **11**: 664 [PMID: 32754068 DOI: 10.3389/fpsyt.2020.00664]

11 **Pawłowska K**, Seredyński R, Umławska W, Iwańczak B. Hydrogen excretion in pediatric lactose malabsorbers: relation to symptoms and the dose of lactose. *Arch Med Sci* 2018; **14**: 88-93 [PMID: 29379537 DOI: 10.5114/aoms.2016.57884]

12 **Bernard GR**, Artigas A, Brigham KL, Carlet J, Falke K, Hudson L, Lamy M, Legall JR, Morris A, Spragg R. The American-European Consensus Conference on ARDS. Definitions, mechanisms, relevant outcomes, and clinical trial coordination. *Am J Respir Crit Care Med* 1994; **149**: 818-824 [PMID: 7509706 DOI: 10.1164/ajrccm.149.3.7509706]

13 **Rezaie A**, Buresi M, Lembo A, Lin H, McCallum R, Rao S, Schmulson M, Valdovinos M, Zakko S, Pimentel M. Hydrogen and Methane-Based Breath Testing in Gastrointestinal Disorders: The North American Consensus. *Am J Gastroenterol* 2017; **112**: 775-784 [PMID: 28323273 DOI: 10.1038/ajg.2017.46]

14 **He T**, Venema K, Priebe MG, Welling GW, Brummer RJ, Vonk RJ. The role of colonic metabolism in lactose intolerance. *Eur J Clin Invest* 2008; **38**: 541-547 [PMID: 18573099 DOI: 10.1111/j.1365-2362.2008.01966.x]

15 **Zhang M**, Zhu HM, He F, Li BY, Li XC. Association between acute pancreatitis and small intestinal bacterial overgrowth assessed by hydrogen breath test. *World J Gastroenterol* 2017; **23**: 8591-8596 [PMID: 29358867 DOI: 10.3748/wjg.v23.i48.8591]

16 **Murr MM**, Yang J, Fier A, Kaylor P, Mastorides S, Norman JG. Pancreatic elastase induces liver injury by activating cytokine production within Kupffer cells *via* nuclear factor-Kappa B. *J Gastrointest Surg* 2002; **6**: 474-480 [PMID: 12023002 DOI: 10.1016/s1091-255x(01)00071-3]

17 **Wig JD**, Kochhar R, Ray JD, Krishna Rao DV, Gupta NM, Ganguly NK. Endotoxemia predicts outcome in acute pancreatitis. *J Clin Gastroenterol* 1998; **26**: 121-124 [PMID: 9563923 DOI: 10.1097/00004836-199803000-00007]

18 **Gea-Sorlí S**, Closa D. Role of macrophages in the progression of acute pancreatitis. *World J Gastrointest Pharmacol Ther* 2010; **1**: 107-111 [PMID: 21577304 DOI: 10.4292/wjgpt.v1.i5.107]

19 **Gloor B**, Blinman TA, Rigberg DA, Todd KE, Lane JS, Hines OJ, Reber HA. Kupffer cell blockade reduces hepatic and systemic cytokine levels and lung injury in hemorrhagic pancreatitis in rats. *Pancreas* 2000; **21**: 414-420 [PMID: 11075997 DOI: 10.1097/00006676-200011000-00013]

20 **Zhang J**, Yuan C, Hua G, Tong R, Luo X, Ying Z. Early gut barrier dysfunction in patients with severe acute pancreatitis: attenuated by continuous blood purification treatment. *Int J Artif Organs* 2010; **33**: 706-715 [PMID: 21077043]

21 **Thandassery RB**, Yadav TD, Dutta U, Appasani S, Singh K, Kochhar R. Dynamic nature of organ failure in severe acute pancreatitis: the impact of persistent and deteriorating organ failure. *HPB (Oxford)* 2013; **15**: 523-528 [PMID: 23750495 DOI: 10.1111/j.1477-2574.2012.00613.x]

22 **Liu J**, Huang L, Luo M, Xia X. Bacterial translocation in acute pancreatitis. *Crit Rev Microbiol* 2019; **45**: 539-547 [PMID: 31851854 DOI: 10.1080/1040841X.2019.1621795]

23 **Garg PK**, Singh VP. Organ Failure Due to Systemic Injury in Acute Pancreatitis. *Gastroenterology* 2019; **156**: 2008-2023 [PMID: 30768987 DOI: 10.1053/j.gastro.2018.12.041]

World Journal of Gastroenterology

Submit a Manuscript: https://www.f6publishing.com

World J Gastroenterol 2021 April 21; 27(15): 1655-1663

DOI: 10.3748/wjg.v27.i15.1655

ISSN 1007-9327 (print) ISSN 2219-2840 (online)

CASE REPORT

Gastrointestinal cytomegalovirus disease secondary to measles in an immunocompetent infant: A case report

Qing-Hua Yang, Xiao-Peng Ma, Dong-Ling Dai, Da-Ming Bai, Yu Zou, Si-Xi Liu, Jian-Ming Song

ORCID number: Qing-Hua Yang 0000-0001-8259-7557; Xiao-Peng Ma 0000-0003-0115-3298; Dong-Ling Dai 0000-0002-3002-4631; Da-Ming Bai 0000-0001-8250-8518; Yu Zou 0000-0003-4808-3418; Si-Xi Liu 0000-0003-1674-2685; Jian-Ming Song 0000-0002-4982-9843.

Author contributions: Yang QH drafted the manuscript and analyzed the data; Liu SX, Bai DM, and Zou Y were involved in patient management and follow-up; Dai DL and Ma XP designed and supervised the study; Song JM contributed to data acquisition, analysis, and interpretation; Dai DL and Ma XP contributed equally to this manuscript; all of the authors approved the submission of this manuscript.

Supported by Shenzhen Innovation and Technology Committee, No. JCYJ20180228175150018.

Informed consent statement: Consent was obtained from the parents of the patient for publication of the case report and any accompanying images.

Conflict-of-interest statement: The authors who took part in this study declare that they do not have anything to disclose regarding funding or a conflict of interest with respect to this manuscript.

Qing-Hua Yang, Xiao-Peng Ma, Dong-Ling Dai, Da-Ming Bai, Yu Zou, Si-Xi Liu, Endoscopy Center and Gastroenterology Department, Shenzhen Children's Hospital, Shenzhen 518036, Guangdong Province, China

Jian-Ming Song, Department of Pathology, Shenzhen Children's Hospital, Shenzhen 518036, Guangdong Province, China

Corresponding author: Dong-Ling Dai, MD, PhD, Chief Doctor, Professor, Endoscopy Center and Gastroenterology Department, Shenzhen Children's Hospital, No. 7019 Yitian Road, Futian District, Shenzhen 518036, Guangdong Province, China. daidong3529@sina.com

Abstract

BACKGROUND

Gastrointestinal cytomegalovirus (CMV) disease occurs commonly in immunocompromised/immunodeficient patients with advanced human immunodeficiency virus infection, neoplasm, solid organ transplantation, hematopoietic stem cell transplantation, or treatment with immunosuppressants, but is rarely reported in association with measles infection.

CASE SUMMARY

We describe a case of extensive gastrointestinal CMV disease secondary to measles infection in a 9-mo-old boy who presented with persistent fever and bloody diarrhea. His condition was improved after ganciclovir treatment. Serological analysis of CMV showed negative immunoglobulin (Ig) M and positive IgG. Blood CMV-DNA was 9.26×10^3 copies/mL. The diagnosis of gastrointestinal CMV disease was confirmed by histopathological findings of intranuclear and intracytoplasmic inclusions and Owl's eye inclusion. This case highlights the differential diagnosis and histopathological characteristics of gastrointestinal CMV infection and laboratory tests.

CONCLUSION

Extensive gastrointestinal CMV lesions can be induced by the immune suppression secondary to measles infection. Rational, fast, and effective laboratory examinations are essential for suspected patients.

Key Words: Cytomegalovirus; Diarrhea; Gastrointestinal; Infant; Measles; Case report

CARE Checklist (2016) statement: The authors have read the CARE Checklist (2016), and the manuscript was prepared and revised according to the CARE Checklist (2016).

Manuscript source: Unsolicited manuscript

Specialty type: Gastroenterology and hepatology

Country/Territory of origin: China

Peer-review report's scientific quality classification

Grade A (Excellent): 0
Grade B (Very good): B, B
Grade C (Good): C
Grade D (Fair): 0
Grade E (Poor): 0

Received: January 14, 2021
Peer-review started: January 14, 2021
First decision: February 10, 2021
Revised: February 19, 2021
Accepted: March 25, 2021
Article in press: March 25, 2021
Published online: April 21, 2021

P-Reviewer: Ilic K, Komatsu H, Liatsos GD
S-Editor: Gao CC
L-Editor: Wang TQ
P-Editor: Ma YJ

Core Tip: We report a case of gastrointestinal cytomegalovirus (CMV) disease secondary to measles infection in a 9-mo-old Chinese boy who had extensive gastrointestinal lesions; the diagnosis was confirmed by histopathological analysis. His condition was improved by ganciclovir treatment. This case highlights the differential diagnosis and histopathological characteristics of gastrointestinal CMV infection and laboratory tests and sheds light on the difficulty in diagnosing gastrointestinal CMV disease due to its nonspecific clinical presentation and the weak diagnostic value of serologic antibody detection.

Citation: Yang QH, Ma XP, Dai DL, Bai DM, Zou Y, Liu SX, Song JM. Gastrointestinal cytomegalovirus disease secondary to measles in an immunocompetent infant: A case report. *World J Gastroenterol* 2021; 27(15): 1655-1663
URL: https://www.wjgnet.com/1007-9327/full/v27/i15/1655.htm
DOI: https://dx.doi.org/10.3748/wjg.v27.i15.1655

INTRODUCTION

Cytomegalovirus (CMV) is an intracellular virus, and CMV infection of the gastrointestinal tract is commonly documented in immunocompromised/immunodeficient patients. Measles infection induces immune suppression and is associated with an increased susceptibility to secondary infections[1], and this effect has typically been thought to last from a few weeks to a few months[2]. The Th2 response during convalescence of measles might inhibit Th1 responses, increasing susceptibility to other infections in children with measles[3]. The morbidity from diarrhea, one of the most common complications of measles, is reported to increase in the acute phase of measles[4]; however, gastrointestinal CMV infection is rarely reported as a causative etiology of persistent diarrhea secondary to measles infection.

CMV disease of the gastrointestinal tract is associated with significant mortality, mostly resulting from considerable bleeding and perforation when the patient is in an immunodepressed status[5]. However, it is not so common for the lesions to be very large. Limitations of the serologic assay of CMV and nonspecific clinical manifestations that mimic many other infectious diseases present a significant challenge to early and accurate diagnosis in clinical practice. Clinicians should consider CMV infection as a differential diagnosis even in immunocompetent patients with common alimentary symptoms, particularly intractable diarrhea, hematochezia, or vomiting in conjunction with fever. Here, we describe a case of gastrointestinal CMV disease secondary to measles infection that involved vast lesions, and we review the differential diagnosis, histopathological diagnosis, and treatment of gastrointes-tinal CMV infection.

CASE PRESENTATION

Chief complaints

A 9-mo-old Chinese boy was admitted to Shenzhen Children's hospital because of a persistent high fever and diarrhea that lasted for 17 d.

History of present illness

After 3 d of fever, he had a rash extending from his face to his trunk and limbs, and 5 d later, he suffered watery and bloody diarrhea. Positive immunoglobulin (Ig) M on the 10th day of fever confirmed a diagnosis of measles. Peripheral white blood cells, neutrophils, and C-reactive protein were elevated. Many leukocytes were found in his stool. Cefoperazone-sulbactam was administered intravenously for 4 d before admission, but the frequency of diarrhea increased, along with abdominal distension.

History of past illness

The patient had two episodes of pneumonia 40 d before this admission.

Personal and family history

The patient was born by cesarean section after full-term gestation, without complications during gestation or delivery. He had met physical and developmental milestones. Routine childhood immunizations were administered except for the measles vaccine.

Physical examination

On admission, the patient was weak but alert with a dehydrated appearance and typical measles skin (pigmentation and desquamation all over his body). The abdomen was soft and distended, with no tenderness or masses. The remainder of the physical examination was normal. Rapid intravenous rehydration was applied before further evaluation.

Laboratory examinations

Serological analysis for CMV showed negative IgM and positive IgG. PCR blood assay showed an elevation of CMV-DNA. The other laboratory results are shown in Tables 1 and 2.

Imaging examinations

Abdominal radiography (Figure 1) revealed upper gastrointestinal obstruction, while abdominal ultrasonography showed no obvious dilatation of the intestine or free effusion. Enhanced computed tomography demonstrated obstruction in the horizontal duodenum.

Further diagnostic work-up

On the 23rd day, gastroscopy (EG-99WR; Fujinon, Tokyo, Japan) and colonoscopy (GIF-XQ240; Olympus, Tokyo, Japan) were performed. Gastroscopy (Figure 2) revealed gastroduodenal mucosal edema and hyperemia, lymphoid hyperplasia, focal ulceration, pseudotumor formation, and stenosis in the horizontal duodenum. Incomplete colonoscopy (Figure 3) displayed diffuse mucosal edema and roughness, stiffness, friability, and white membranoid substances in the descending colon, sigmoid colon, and rectum. The histopathological examination revealed characteristic inclusions suggestive of CMV.

FINAL DIAGNOSIS

The final diagnosis of the presented case was gastrointestinal CMV disease.

TREATMENT

After admission to the hospital, suspected bacterial infection was treated with intravenous vancomycin and meropenem without improvement. On hospital day 12, diarrhea was aggravated with persistent high fever and episodes of vomiting and abdominal distension. Fasting and gastrointestinal decompression did not improve his condition. After the diagnosis of gastrointestinal CMV disease was made, intravenous ganciclovir was administered at 5 mg/kg every 12 h on the 30th hospital day for 2 wk and then reduced to 5 mg/kg each day for 1 wk.

OUTCOME AND FOLLOW-UP

The patient's condition improved after treatment with IV ganciclovir and he was discharged on the 54th hospital day. He was followed regularly to 4.5 years old, and he is doing well.

DISCUSSION

This 9-mo-old Chinese boy had persistent fever and diarrhea after measles infection; ensuing vomiting, abdominal distension, and hematochezia presented at a later stage.

Table 1 Laboratory results (international system of units)

Parameter	Reference range	5 d before admission	1 d before admission	On admission	Day 6	Day 12	Day 23	Day 37
Hemoglobin (g/L)	110-160	120	115	79	91	73	126	69
Erythrocytes (× 10^{12}/L)	3.5-5.5	4.70	4.56	2.93	3.21	2.50	3.93	2.34
Leucocytes (× 10^{9}/L)	5-12	14.96	9.36	17.87	8.37	20.42	38.68	10.35
Neutrophils (%)	50-70	54.9	32.6	55.1	62.7	61.6	80.4	59.9
Lymphocytes (%)	20-40	36.9	56.7	27	29.3	28.3	15.4	33.4
Atypical lymphocytes (%)	0-2			9	7	0	0	0
Eosinophils (%)	0.02-0.5	1.3	1.4	0.9	0.4	0	0	0
Platelets (× 10^{9}/L)	100-300	234	226	769	200	276	165	110
Sedimentation rate (mm/h)	0-15			78		1		
C-reactive protein (mg/L)	0-10	39.7		176	80	114	3.7	4.7
Procalcitonin (ng/L)	0-0.5			31.87	0.77		0.31	
Sodium (mmol/L)	135-146			116.3	138.4	131.2	139.4	135
Potassium (mmol/L)	3.5-5.5			6.15	4.53	3.9	4.2	3.61
Chloride (mmol/L)	101-111			91.1	102.7	97.8	116.9	110.5
Calcium (mmol/L)	2.25-2.75			1.79	2.46	1.87	2.04	1.66
Magnesium (mmol/L)	0.7-1.15			0.96	0.61	0.53	0.35	0.38
Albumin (g/L)	35-55			25.8	37.3	25.9	15.5	20.6
Globulin (g/L)	20-30			28.1	17.6	19.3	13.2	5.9
Aspartate amino transferase (IU/L)	0-40			70	28	48	85	22
Alanine amino transferase (IU/L)	0-40			61	12	41	53	6
Prothrombin time (s)	9.3-12.9			17.4	19.6	12.5	11.4	16.2
Activated partial thromboplastin time (s)	26.1-40.7			34.5	57.8	38	39.5	55.2
Fecal occult blood test	-			-	+	+	+	+
Fecal white blood cell	-	++	-	-	++	++++	++	-

All of these symptoms are indicative of digestive system diseases. Fever and diarrhea are common signs of different diagnoses in infants and children, including gastrointestinal infectious and noninfectious causes. In complicated cases with a prolonged course, there are difficulties in distinguishing pathogens; thus, detailed clinical data, exposure history, and pertinent laboratory tests can provide valuable assessment information.

Bacteria are reported as predominant pathogens of measles associated with diarrhea. However, this patient failed to respond to various antibiotics. Some distinct pathogens were considered. Enteroaggregative *Escherichia coli* (*E. coli*) and enteropatho -genic *E. coli* are the most commonly implicated bacterial pathogens in persistent infections in developing countries, especially among children[6]. The patient was a breastfed infant who had no ingestion of contaminated food, water, or unpasteurized milk, no exposure to sick contacts, no contact with infected pets or fowl, no travel history, and a negative result from stool culture, all of which indicated a low possibility of *shigella, salmonella, campylobacter* or other enteric infections[7].

While asymptomatic colonization of *Clostridium difficile* (*C. difficile*) is prevalent in infants, for patients with recent exposure to hospitals and antibiotics, microbiological evaluation should focus on the diagnosis of *C. difficile* infection[8]; however, *C. difficile* should be sensitive to vancomycin, together with repeated negative bacterial separation and culture and enzyme immunoassay tests for toxins A and B and glutamate dehydrogenase. There was no support for the diagnosis of *C. difficile* infection in this patient.

The patient lives in China, a country that ranks 3rd in the world for high tuberculosis

Table 2 Microbiology results

	Peripheral blood	Feces
Day 1	HBsAg (-); HBsAb (+); HBeAg (-); HBeAb (-); HBcAb (-); TP antibody (-); HIV antibody (-); HCV antibody (-); EBNA IgG (+); EBV-CA IgG (+); EBV-CA IgM (±); EBV-EA IgM (-); EBV DNA < 5.00×10^2 copies/mL (LD)	Norovirus (-); Rotavirus (-); Astrovirus (-); Enteral adenovirus (-); Shigella NA (-); Salmonella NA (-); Widal's test (-)
Day 6	G test (-); EBV DNA < 5.00×10^2 copies/mL (LD)	Norovirus (-); Rotavirus (-); Astrovirus (-); Enteral adenovirus (-)
Day 12	G test (-); Interferon-γ release assay of tuberculosis (-)	Clostridium difficile GDH (-); Clostridium difficile toxin A/B (-)
Day 16	CMV-IgM 11.5 U/mL (ref 0-22); CMV-IgG 18.3 U/mL (ref 0-14); CMV DNA quantitation 9.26×10^3 copies/mL	Clostridium difficile GDH (-); Clostridium difficile toxin A/B (-)
Day 36	CMV DNA quantitation < 5.00×10^2 copies/mL (LD); CMV-IgG 82.2 U/mL (ref 0-14)	

HBsAg: Hepatitis B virus surface antigen; HBsAb: Hepatitis B virus surface antibody; HBcAg: Hepatitis B virus core antigen; HBcAb: Hepatitis B virus core antibody; HBeAg: Hepatitis B virus e antigen; TP: Treponemal; HIV: Human immunodeficiency virus; HCV: Hepatitis C virus; EBV-CA: Epstein-Barr virus capsid antigen; EBNA: Epstein-Barr nuclear antigen; EBV-EA: Epstein-Barr virus early antigen; MV: Measles virus; RV: Rubella virus; GDH: Glutamic acid dehydrogenase; LD: Limit of detection; NA: Nucleic acid.

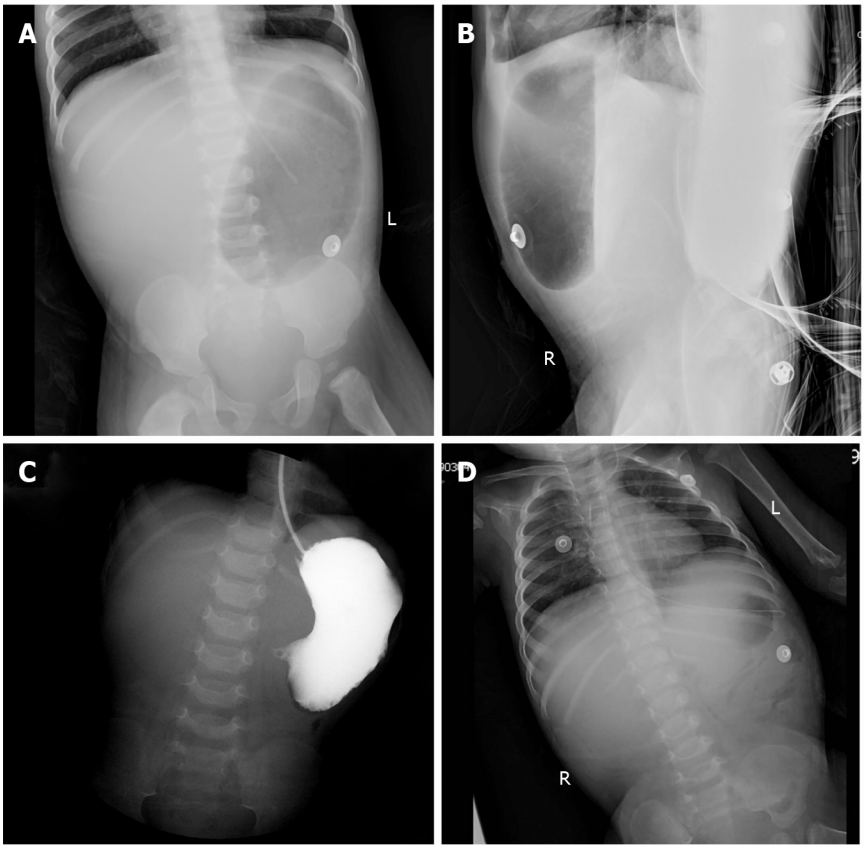

Figure 1 Abdominal plain. A and B: Supine (A) and lateral (B) abdominal plain films showed a large stomach, and no free gas was found in the small intestine, colon, or rectum. A nasogastric tube was coiled in the stomach; C: The iopromide administered by gastric tube did not enter the duodenum; D: Re-examination of abdominal film revealed decreased gas in the stomach and a few inflatable intestines.

(TB) morbidity; thus, intestinal TB (ITB) should be considered even though it is more likely to cause miliary TB in infants. ITB is characterized by low-grade fever, abdominal pain, loss of weight, altered bowel habits, and night sweats[9]. The absence of exposure to *Mycobacterium tuberculosis* and negative chest X-ray and interferon-γ release assay for TB revealed no direct evidence of TB in this patient.

As a noninfectious disease, inflammatory bowel disease (IBD) should be included in the differential diagnosis when lacking evidence of clear pathogenic microorganism infection[7]. The typical clinical presentations of infantile-onset IBD are intermittent fever and bloody diarrhea[10]; some cases are also associated with oral ulcers and

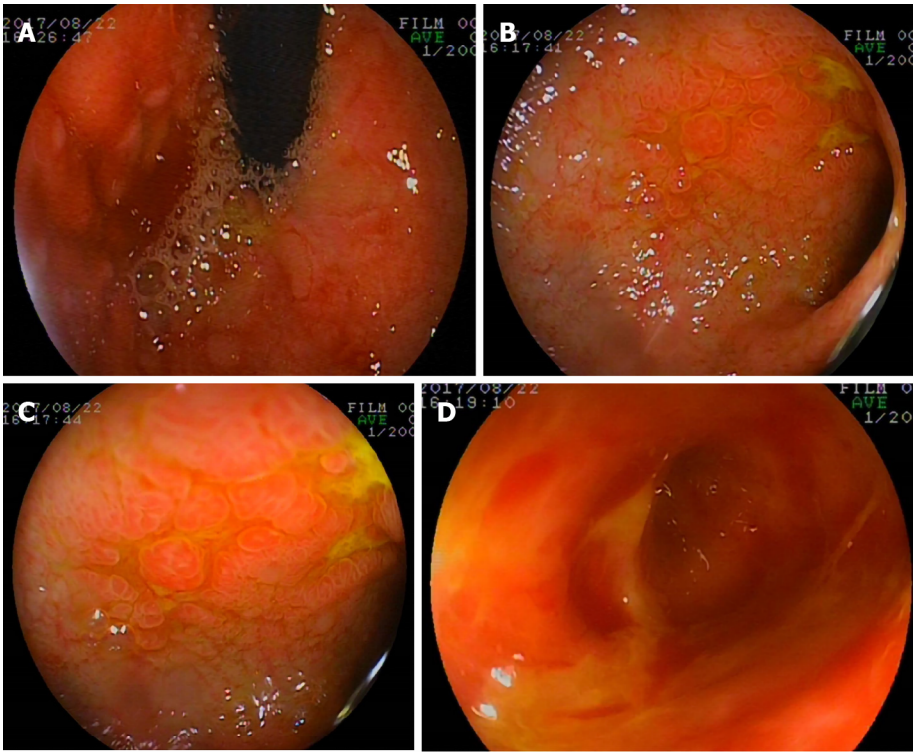

Figure 2 Gastroscopic findings. A gastroscope was inserted into the horizontal part of the duodenum. Hyperemia, edema, lymphoid hyperplasia, focal ulceration, and pseudotumor formation were seen in the stomach and duodenum. A: Gastric fundus; B and C: Duodenal bulb; D: Dilatation of proximal duodenum.

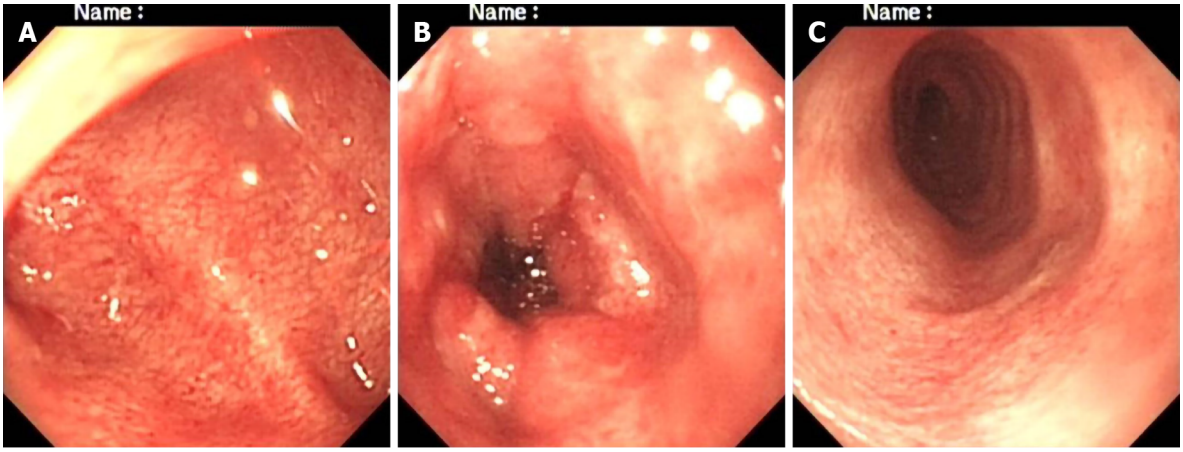

Figure 3 Colonoscopic findings. A colonoscope reached the splenic flexure of the colon. It showed hyperemia, roughness, stiffness, friability, and easy bleeding of the mucosa. A: Rectum; B: Sigmoid colon; C: Descending colon.

perianal abscess and fistula. The diagnosis relies on endoscopic evaluation and histopathological findings of mucosal biopsy other than on clinical characteristics and history. Macroscopic features revealed no contiguous or skip linear ulceration, aphtha ulceration, cobblestoning, fistula, abscesses, or other changes, and microscopic features showed no crypt architectural changes or noncaseating granuloma, so the evidence supporting IBD was insufficient[11]. Granting that very-early onset IBD may have heterogeneous or atypical symptoms and signs, endoscopy and mucosal biopsy were of great benefit to exclude IBD in this patient. There was no evidence of indigestion, malabsorption, autoimmune enteropathy, hemolytic uremic syndrome, allergic or neoplastic disorders, drug- or poison-induced diarrhea, structural diseases, or functional enteropathy in this case (Table 3).

Multiple factors may contribute to several weeks of measles-induced immune suppression[1]. There is an epidemiologically detectable long-term increase in susceptibility to infectious diseases in those who survive measles[12]. Measles infection contributes to transient lymphopenia with decreased numbers of T cells and B cells in

Table 3 Some noninfectious factors in diarrhea

Gastrointestinal diseases	Digestion and absorption disorder
(1) Inflammatory bowel disease; (2) Gastroenteric tumor; (3) Intussusception; (4) Enteric cyst; (5) Duplication of digestive tract; (6) Diverticulosis; (7) Polyposis coli; and (8) Ischemic enteropathy	(1) Short bowel syndrome; (2) Exocrine pancreatic insufficiency; (3) Bile acid-losing syndrome; and (4) Lactose intolerance
Systemic disease: (1) Anaphylactoid purpura; (2) Hyperthyroidism; and (3) Primary chronic adrenocortical hypofunction	Neoplastic diseases: (1) Gastrin adenoma; (2) Carcinoid syndrome; (3) Vasoactive intestinal peptide tumor; and (4) Pheochromocytoma
Allergic diarrhea: (1) Food protein-induced enterocolitis syndrome; (2) food protein-induced proctocolitis; and (3) eosinophilic gastroenteritis	Primary immunodeficiency diseases: (1) Chronic granulomatous disease; (2) Common variable immunodeficiency; and (3) X linked agammaglobulinemia
	Secondary immunodeficiency diseases
	Functional diarrhea
	Drugs/toxicants factor

circulation during the acute phase of infection. As viral RNA persists, suppression of lymphocyte proliferation is induced. During recovery, the later Th 2 CD4+ T-cell response may suppress macrophage activation and Th 1 responses to new infections. Moreover, measles-infected dendritic cells induce lymphocyte unresponsiveness. The suppression of interleukin (IL)-12 production, lymphocyte expression of CD30, and elevation of IL-4, IL-10, and IL-13 might contribute to immune suppression. Deficiencies of both innate and adaptive immune responses can render individuals with measles more susceptible to secondary bacterial and viral infections[13]. The susceptibility to CMV is considered to be due to impaired cell-mediated immunity and a reduction in the levels of IgM[14].

Any part of the alimentary tract can be impacted by CMV infection but the typical CMV lesions are limited to either the upper or the lower gastrointestinal tract, while both the upper and the lower gastrointestinal tracts are rarely involved simultaneously[15]. Gastrointestinal CMV disease with complex and diverse but nonspecific symptoms is a remediable disease with a high mortality; delayed diagnosis, misdiagnosis, and missed diagnosis greatly increase fatality. To the best of our knowledge, in both immunocompetent and immunodeficient patients, intractable diarrhea and fever seem to be the most common presentations of gastrointestinal CMV disease, so differentiating CMV infection from infectious diarrhea as early as possible is vital in clinical practice.

In addition to broad clinical presentations and signs, confirmation of the virus *via* laboratory methods is indispensable in diagnosing CMV disease. In this patient, CMV-IgM was negative, and the absence of evidence of active infection led to an uncertain causal relationship between CMV infection and various symptoms, which demanded histopathology detection for further verification. Nonetheless, the positive CMV-IgG titre was more than 4-fold in 2 wk, and elevated CMV DNA copies provided clues for diagnosis. Nevertheless, false negative IgM results can be obtained in immunocompromised patients and infants. Positive measles IgM was detected in this patient because the immune status was not affected by measles infection at the early stage. However, due to an immunocompromised status secondary to measles infection later, the negative IgM significantly limits its clinical application in the early diagnosis of CMV infection, which may delay diagnosis and treatment[16].

Negative results of CMV PCR do not rule out CMV disease[17]. As a marker of early diagnosis, CMV pp65 antigen is not able to differentiate between latent infection and active disease. Viral culture is the diagnostic gold standard, but its poor sensitivity and slow turn-around time limit its clinical utility, while histopathology assays can provide confirmatory information for invasive disease which is highly specific[18] (Figure 4). Therefore, when gastrointestinal CMV infection is suspected, endoscopy and biopsy must be performed to obtain positive evidence for diagnosis.

The macroscopic features of gastrointestinal CMV disease vary from normal mucosa, focal erythematous, erosion, and pseudotumor formation to deep ulceration, lacking specificity[19]. Based on the patchy distributions and diverse endoscopic findings, biopsy location and number are important to assess CMV[20]. Gastroduodenoscopy and incomplete colonoscopy were performed in this patient due to the risk of intestinal perforation and massive hemorrhage. The outcome of the histopathology assay confirmed invasive CMV disease.

CMV disease requires evidence of parenchymal organ damage before it can be diagnosed and treated with antiviral therapy. Anti-CMV treatment in immunocom-

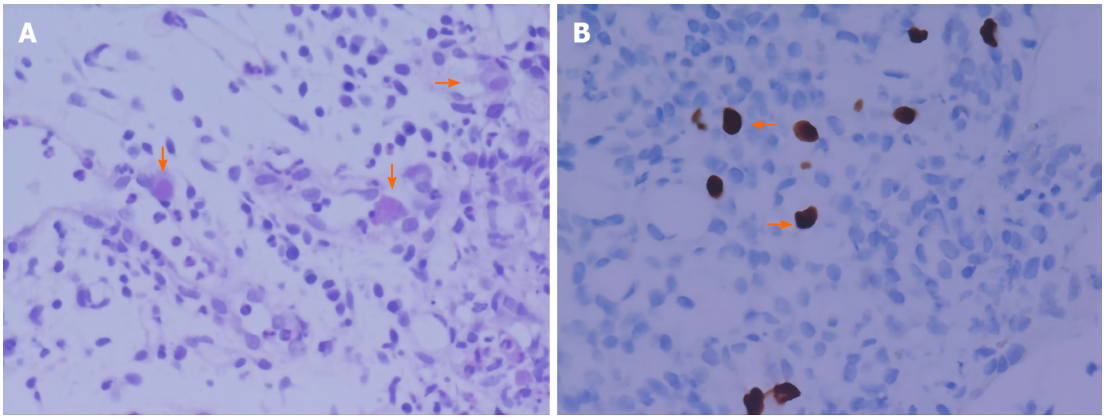

Figure 4 Gastrointestinal histopathologic findings. Histopathologic photomicrographs of gastric, duodenal, descending colony-like, sigmoid colony-like, and rectal specimens. A: Inflammatory cell infiltration and characterized cytomegalic cells (arrows) containing eosinophilic intranuclear inclusions (hematoxylin and eosin: × 400); B: Owl's eye inclusions (arrows) in cytomegalovirus-infected cells (immunohistochemical staining: × 400).

promised patients is of vital importance to improve prognosis. Ganciclovir is recommended as the first-line pharmacological treatment for CMV infection, which comprises induction and maintenance. The initial dose must be adjusted for renal function and it is commonly advised to be 5 mg/kg every 12 h for at least 2 wk to 3 wk in the induction stage[21]. The course of treatment varies with therapeutic reactions, including symptoms, quantitative detection of viral load, whole blood counts, hepatic function and renal function. When patients cannot tolerate side effects or diseases worsen with the use of ganciclovir, foscarnet is generally used as a substitution drug, whereas which can result in renal toxicity and electrolyte disturbances[22]. After the diagnosis of CMV disease, the auditory, ophthalmic, and neurodevelopmental assessments of the patient were normal. His temperature decreased, vomiting disappeared, and the bowls recovered after intravenous ganciclovir administration. Inflammation biomarkers and CMV DNA copies decreased. An obvious improvement in imaging was shown on re-examination (Figure 1). The amelioration after antiviral therapy helped exclude IBD completely. Undoubtedly, this patient was fortunate. For immunocompromised patients with severe CMV infection, surgical treatment is required when medical treatment is ineffective.

In conclusion, we sought to review the differential diagnosis for similar clinical outcomes in a young child with diarrhea, hematochezia, and fevers, and to clarify endoscopic and histopathological findings as well as outline treatment options for CMV colitis. We highlighted the diagnostic challenges of gastrointestinal CMV disease due to its nonspecific clinical presentation and the weak diagnostic value of serologic antibody detection. We hope to help clinicians improve the understanding of the importance of considering this disease in immunocompromised patients, as well as to consider it in otherwise healthy patients with a prolonged course characterized by fever, diarrhea, and hematochezia who may become immunocompromised due to measles infection.

CONCLUSION

This is the first case of gastrointestinal CMV infection due to transient immunosuppression secondary to measles infection in a presumably immunocompetent child. Gastrointestinal CMV disease should be taken into considera-tion in patients with persistent fever and diarrhea followed by measles infection. Rational, fast, and effective laboratory examinations are essential for a timely diagnosis, avoiding inappropriate treatment and reducing mortality in suspected patients.

ACKNOWLEDGEMENTS

We thank the patient's family for providing background information and allowing us to publish this manuscript. We wish to thank Dr. Cao WG and Gan YG (MD, Radiologist, Radiology Department of Shenzhen Children's Hospital) for their imaging

technical assistance.

REFERENCES

1 **Griffin DE**. Measles virus-induced suppression of immune responses. *Immunol Rev* 2010; **236**: 176-189 [PMID: 20636817 DOI: 10.1111/j.1600-065X.2010.00925.x]
2 **Bester JC**. Measles and Measles Vaccination: A Review. *JAMA Pediatr* 2016; **170**: 1209-1215 [PMID: 27695849 DOI: 10.1001/jamapediatrics.2016.1787]
3 **Moss WJ**, Griffin DE. Measles. *Lancet* 2012; **379**: 153-164 [PMID: 21855993 DOI: 10.1016/S0140-6736(10)62352-5]
4 **Jackson BD**, Black RE. Available studies fail to provide strong evidence of increased risk of diarrhea mortality due to measles in the period 4-26 weeks after measles rash onset. *BMC Public Health* 2017; **17**: 783 [PMID: 29143685 DOI: 10.1186/s12889-017-4745-2]
5 **Arnold M**, Itzikowitz R, Young B, Machoki SM, Hsiao NY, Pillay K, Alexander A. Surgical manifestations of gastrointestinal cytomegalovirus infection in children: Clinical audit and literature review. *J Pediatr Surg* 2015; **50**: 1874-1879 [PMID: 26265193 DOI: 10.1016/j.jpedsurg.2015.06.018]
6 **Pawlowski SW**, Warren CA, Guerrant R. Diagnosis and treatment of acute or persistent diarrhea. *Gastroenterology* 2009; **136**: 1874-1886 [PMID: 19457416 DOI: 10.1053/j.gastro.2009.02.072]
7 **DuPont HL**. Persistent Diarrhea: A Clinical Review. *JAMA* 2016; **315**: 2712-2723 [PMID: 27357241 DOI: 10.1001/jama.2016.7833]
8 **McDonald LC**, Gerding DN, Johnson S, Bakken JS, Carroll KC, Coffin SE, Dubberke ER, Garey KW, Gould CV, Kelly C, Loo V, Shaklee Sammons J, Sandora TJ, Wilcox MH. Clinical Practice Guidelines for Clostridium difficile Infection in Adults and Children: 2017 Update by the Infectious Diseases Society of America (IDSA) and Society for Healthcare Epidemiology of America (SHEA). *Clin Infect Dis* 2018; **66**: 987-994 [PMID: 29562266 DOI: 10.1093/cid/ciy149]
9 **Donoghue HD**, Holton J. Intestinal tuberculosis. *Curr Opin Infect Dis* 2009; **22**: 490-496 [PMID: 19623062 DOI: 10.1097/QCO.0b013e3283306712]
10 **Ye Z**, Zhou Y, Huang Y, Wang Y, Lu J, Tang Z, Miao S, Dong K, Jiang Z. Phenotype and Management of Infantile-onset Inflammatory Bowel Disease: Experience from a Tertiary Care Center in China. *Inflamm Bowel Dis* 2017; **23**: 2154-2164 [PMID: 29140941 DOI: 10.1097/MIB.0000000000001269]
11 **Levine A**, Koletzko S, Turner D, Escher JC, Cucchiara S, de Ridder L, Kolho KL, Veres G, Russell RK, Paerregaard A, Buderus S, Greer ML, Dias JA, Veereman-Wauters G, Lionetti P, Sladek M, Martin de Carpi J, Staiano A, Ruemmele FM, Wilson DC; European Society of Pediatric Gastroenterology, Hepatology, and Nutrition. ESPGHAN revised porto criteria for the diagnosis of inflammatory bowel disease in children and adolescents. *J Pediatr Gastroenterol Nutr* 2014; **58**: 795-806 [PMID: 24231644 DOI: 10.1097/MPG.0000000000000239]
12 **Griffin DE**. Measles immunity and immunosuppression. *Curr Opin Virol* 2021; **46**: 9-14 [PMID: 32891958 DOI: 10.1016/j.coviro.2020.08.002]
13 **Moss WJ**. Measles. *Lancet* 2017; **390**: 2490-2502 [PMID: 28673424 DOI: 10.1016/S0140-6736(17)31463-0]
14 **Baumgartner JD**, Glauser MP, Burgo-Black AL, Black RD, Pyndiah N, Chiolero R. Severe cytomegalovirus infection in multiply transfused, splenectomized, trauma patients. *Lancet* 1982; **2**: 63-66 [PMID: 6123807 DOI: 10.1016/s0140-6736(82)91688-9]
15 **de Andrade LG**, Rodrigues MA, Romeiro FG, Carvalho MF. Gastrointestinal cytomegalovirus disease in renal transplant recipients: a case series. *Clin Transplant* 2012; **26**: 345-350 [PMID: 22017269 DOI: 10.1111/j.1399-0012.2011.01514.x]
16 **Razonable RR**, Paya CV, Smith TF. Role of the laboratory in diagnosis and management of cytomegalovirus infection in hematopoietic stem cell and solid-organ transplant recipients. *J Clin Microbiol* 2002; **40**: 746-752 [PMID: 11880387 DOI: 10.1128/jcm.40.3.746-752.2002]
17 **Ruell J**, Barnes C, Mutton K, Foulkes B, Chang J, Cavet J, Guiver M, Menasce L, Dougal M, Chopra R. Active CMV disease does not always correlate with viral load detection. *Bone Marrow Transplant* 2007; **40**: 55-61 [PMID: 17468776 DOI: 10.1038/sj.bmt.1705671]
18 **Pillet S**, Pozzetto B, Roblin X. Cytomegalovirus and ulcerative colitis: Place of antiviral therapy. *World J Gastroenterol* 2016; **22**: 2030-2045 [PMID: 26877608 DOI: 10.3748/wjg.v22.i6.2030]
19 **Goodgame RW**. Gastrointestinal cytomegalovirus disease. *Ann Intern Med* 1993; **119**: 924-935 [PMID: 8215005 DOI: 10.7326/0003-4819-119-9-199311010-00010]
20 **Juric-Sekhar G**, Upton MP, Swanson PE, Westerhoff M. Cytomegalovirus (CMV) in gastrointestinal mucosal biopsies: should a pathologist perform CMV immunohistochemistry if the clinician requests it? *Hum Pathol* 2017; **60**: 11-15 [PMID: 27666768 DOI: 10.1016/j.humpath.2016.09.009]
21 **You DM**, Johnson MD. Cytomegalovirus infection and the gastrointestinal tract. *Curr Gastroenterol Rep* 2012; **14**: 334-342 [PMID: 22588614 DOI: 10.1007/s11894-012-0266-4]
22 **Kotton CN**, Kumar D, Caliendo AM, Huprikar S, Chou S, Danziger-Isakov L, Humar A; The Transplantation Society International CMV Consensus Group. The Third International Consensus Guidelines on the Management of Cytomegalovirus in Solid-organ Transplantation. *Transplantation* 2018; **102**: 900-931 [PMID: 29596116 DOI: 10.1097/TP.0000000000002191]

Published by **Baishideng Publishing Group Inc**
7041 Koll Center Parkway, Suite 160, Pleasanton, CA 94566, USA
Telephone: +1-925-3991568
E-mail: bpgoffice@wjgnet.com
Help Desk: https://www.f6publishing.com/helpdesk
https://www.wjgnet.com